Salinity, Sanitation and Sustainability:
A Study in Environmental Biotechnology and Integrated Wastewater Beneficiation in South Africa

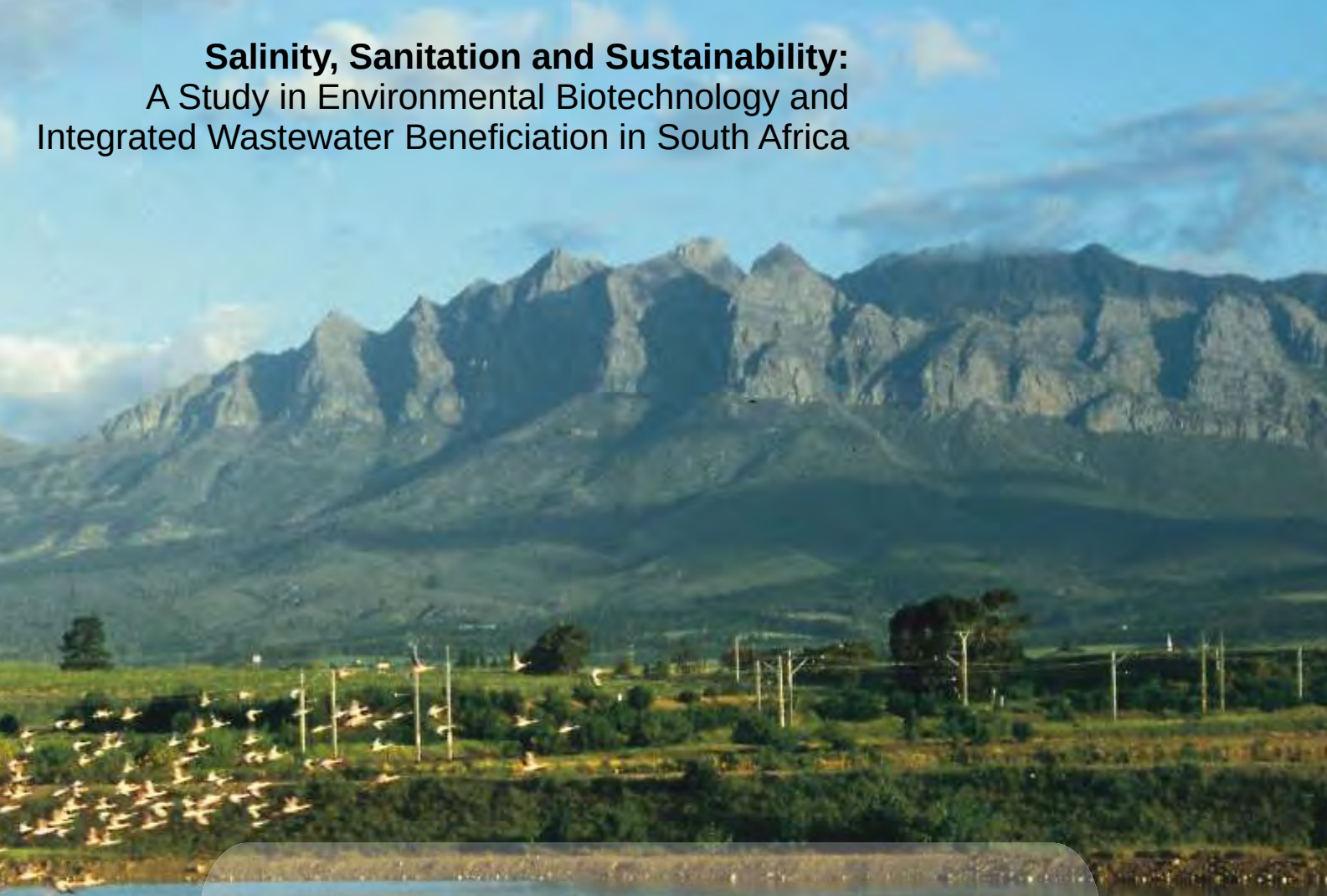

Volume 4

The Rhodes BioSURE Process

Part 3: Sulphur Removal Unit Operations

JB Molwantwa, M Bowker, J Gilfillan, N Rein,
R Dorrington, OO Hart and PD Rose

WRC Report No TT 411/09

11

Water Research Commission

Salinity, Sanitation and Sustainability:
A Study in Environmental Biotechnology and
Integrated Wastewater Beneficiation in South Africa

Volume 4

THE RHODES BioSURE PROCESS®

Part 3: Sulphur Removal Unit Operations

INVESTIGATION AND DEVELOPMENT OF THE BIOTECHNOLOGY OF SULPHUR BIOFILMS IN THE BENEFICIATION AND TREATMENT OF WASTEWATER

Report to the Water Research Commission

by

JB Molwantwa[1], M Bowker[1], J Gilfillan[1], N Rein[1], R Dorrington[2]
OO Hart[1] and PD Rose[1]

1. Environmental Biotechnology Research Unit, Rhodes University
2. Department of Biochemistry, Microbiology and Biotechnology, Rhodes University

WRC REPORT NO. TT 411/09

AUGUST 2009

Obtainable from:

Water Research Commission
Private bag X03
Gezina
0031

The studies reported here were undertaken as components of the following Water Research Commission projects: K5/1078, ‘Development and piloting of the integrated biodesalination process for sulphate removal from mine drainage water incorporating co-disposal of industrial and domestic effluents’; K5/1336, ‘Scale-up development of the Rhodes BioSURE Process for sewage sludge solubilisation and disposal’; K5/1545, ‘Investigation and development of the biotechnology of sulphur biofilms in the beneficiation and treatment of wastewaters’; and aspects of Projects K5/1456, ‘The biotechnology of saline and sewage wastewater co-treatment’, and K5/1349, ‘Development and refinement of the floating sulphur biofilm reactor for sulphide oxidation for the use in integrated passive treatment systems and the Rhodes BioSURE Process’.

ISBN 978-1-77005-872-9
Set No. 1 86845 853 9

Printed in the Republic of South Africa

EXECUTIVE SUMMARY

BACKGROUND

Mine wastewaters generated during active production operations, and decanting streams following mine closure, have major environmental impacts and volumes requiring treatment are expected to increase substantially as the South African mining industry matures (Scott, 1995). Biological treatment of minewaters has been the subject of increasing interest, especially in the provision of technological options that are sustainable over the long-term. These, however, are the subject of a number of constraints including, importantly, the process capability to remove reduced sulphates from the treated stream and thus linearise the removal of sulphur from the system, in one or other of its oxidation states. In this regard, considerable attention has been directed at biological sulphide oxidation and its possible use in process operations for producing elemental sulphur. Little progress has been reported for this approach in passive minewater treatment systems (Rose, 2002).

This study reports an investigation of floating sulphur biofilms (FSB), a phenomenon which had been previously reported on sulphidic organic wastewaters (Dunn, 1998), and the potential use of the system in the development of a novel sulphide oxidation process unit operation linked to minewater treatment. This report follows on preliminary studies undertaken in an Innovation Fund project, and also in WRC Projects K5/1349 and K5/1456.

AIMS

The aims of the current WRC study were identified as follows:

Operate laboratory- and pilot scale model systems in which the formation and productivity of sulphur biofilms may be studied;
Undertake investigations to describe the microbial ecology, chemistry and biochemistry of sulphur biofilms;
Evaluate appropriate configurations and performance of the Sulphide Oxidising Biofilm Reactor;
Support knowledge input and recovery aspects of past studies and concurrent industrial-scale applications of the Sulphide Oxidising Bioreactor;
Develop a descriptive and explanatory model for the development and productivity of sulphur biofilms.

RESULTS

Reactor Development

A Linear Flow Channel Reactor (LFCR) was developed to enable the FSB structures observed in nature to be studied under controlled laboratory conditions (Figure 1).

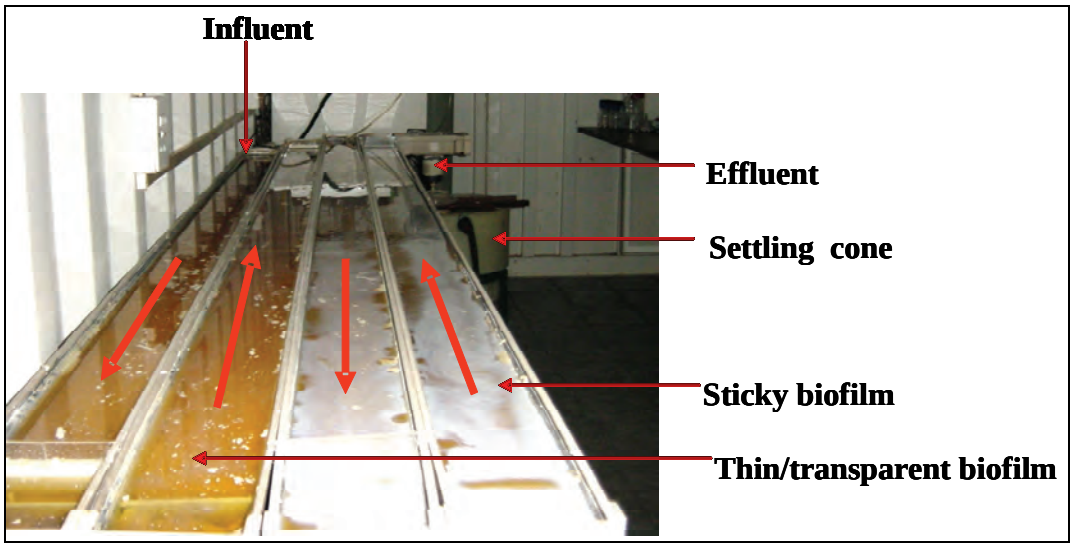

Figure 1. Four-Channel Linear Flow Channel Reactor set up in the controlled environment room operating at 25 ^{o}C.

Structure

The structure of the FSB is largely unknown and light- and scanning electron microscopy (SEM) studies showed that it was a differentiated structure composed, at least in part, of large numbers of bacteria (Figure 2). The presence of putative sulphur crystal-like structures appearing on the underside surface of the biofilm was shown, and these were confirmed to be sulphur by X-Ray fluorescence (XRF) spectroscopy and scanning electron microscopy-energy dispersive X-Ray (SEM-EDX) studies (Figure 3). The growth of the crystals within the biofilm occurs within a complex matrix of bacterial exopolymeric substance (EPS).

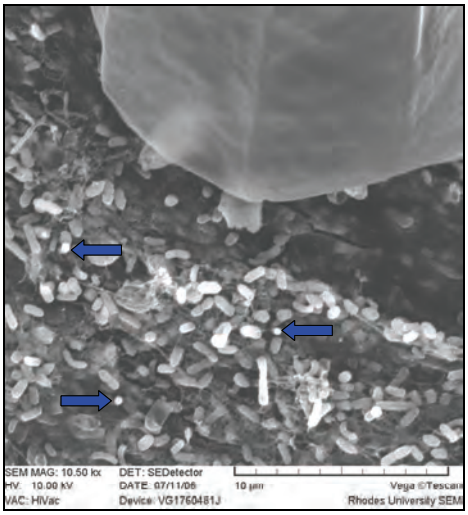

Figure 2. Scanning electron microscopy micrograph of the Brittle biofilm showing a number of external globules (indicated with blue arrows) visible in close proximity to the large crystal.

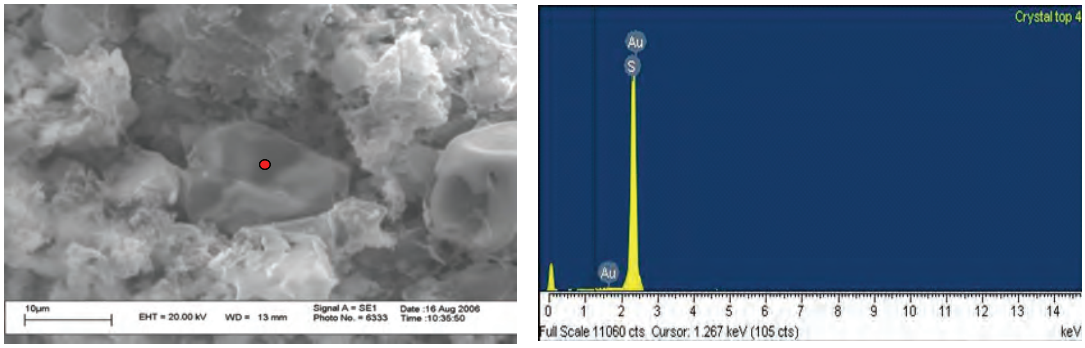

Figure 3. Scanning electron microscopy micrograph and energy dispersive X-ray spectrum of a crystal from the Brittle floating sulphur biofilm (spot area indicated in red). (S=100%).

Microbial Ecology

The formation of sulphur within the film suggested the presence of steep physico-chemical and physiological gradients established across the FSB. Given the small thickness of the film, the Gradient Tube experimental system was developed to enable the location and possible function of the various components of the population to be examined (Figure 4). Total genome DNA extracts for the whole biofilm were thus compared with the location of individual populations within the sulphide/Redox gradients established in the Gradient Tube system.

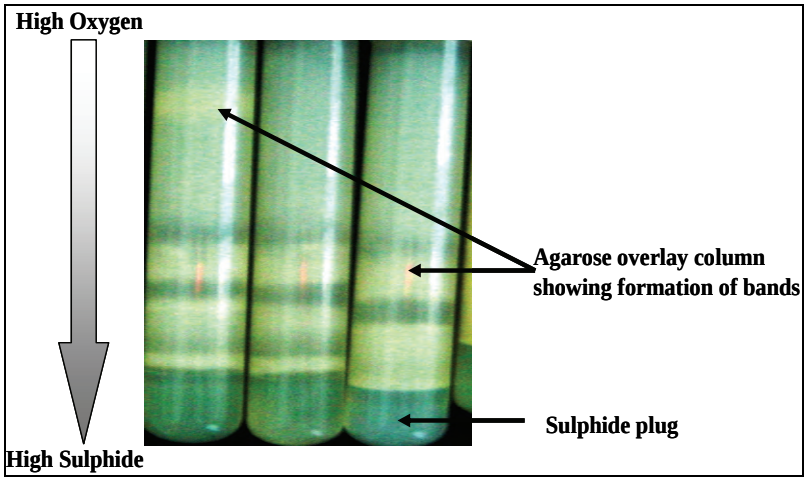

Figure 4. Gradient tubes showing the emergence of clearly defined bands indicating the presence of microbial growth within the oxygen/sulphide gradient established in the agar column. This served to expand the physiological niches occurring in the biofilm from 200-300 μm to 5 cm.

Comparison of the whole biofilm and the gradient tube analysis is reported in Table 1 and confirmed the complex nature of the biofilm and that it is composed of a number of groups occupying physiologically defined niches. The formation of the different bands and location of species at different levels in the Gradient Tubes, suggests a spatial distribution of the different bacterial species across the FSB. The demonstration of differentiation and structural/functional relationships in the FSB further confirmed that it is indeed a true biofilm

Table 1. A comparison of populations identified at the various zones in the Gradient Tubes and the total biofilm samples.

Distribution	Gradient Tube	Biofilm
Top (aerobic)	*Azoarcus* *AcidoThiobacillus*	*Thiobacillus* *HaloThiobacillus* *Thiothrix* *Thiovirga* *Sulfurimonas*
Middle (anoxic to anaerobic)	*Chryseobacterium* *Bacteroides* *Planococcus*	*Chryseobacterium* *Bacteroides* *Planococcus*
Bottom (anaerobic)	*Brevundimonas*	Uncultured anaerobe

These findings may present a first report that floating biofilms are structured as complex systems comparable to fixed biofilm systems. It appears to be a first report confirming the differentiation of structural relationships in FSBs. Having established the presence of some level of structural and physiological differentiation in the FSB system, it was then necessary to acquire more detailed insight into its physico-chemical environment in order to be able to comment on a structural/functional model accounting for the system.

Structure and Function

Micro-sensors were used to measure sulphide, Redox and pH gradients across the biofilm in increments of 5 μm (Figure 5).

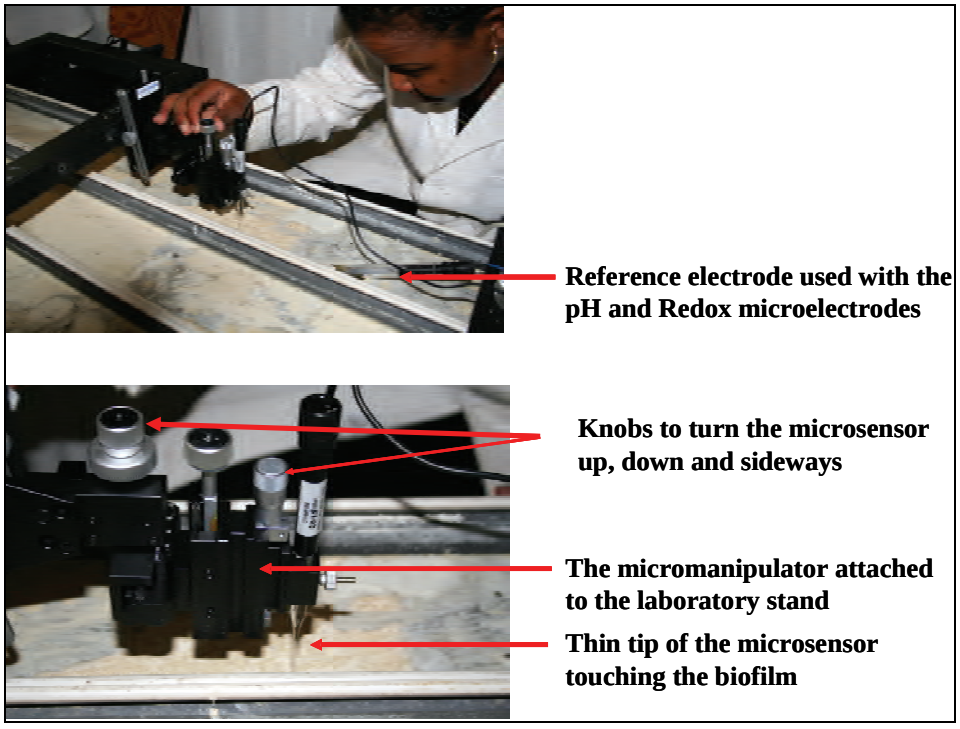

Figure 5. A closer view of the micromanipulator and microsensor set up above the Linear Flow Channel Reactor while acquiring measurements across the depth of the floating sulphur biofilm**.**

Microsensors were used for the first time in the measurement of the characteristics of FSBs and showed that steep physico-chemical gradients are established across the system. An inverse relationship was observed between pH and Redox potential which correlates with sulphide removal in the biofilm. While comparable, the effect is more pronounced in the Brittle biofilm where sulphur production is also greater.

Based on the above data a descriptive structural/functional model was constructed to account for the processes occurring in the FSB system. This is summarized in Figure 6.

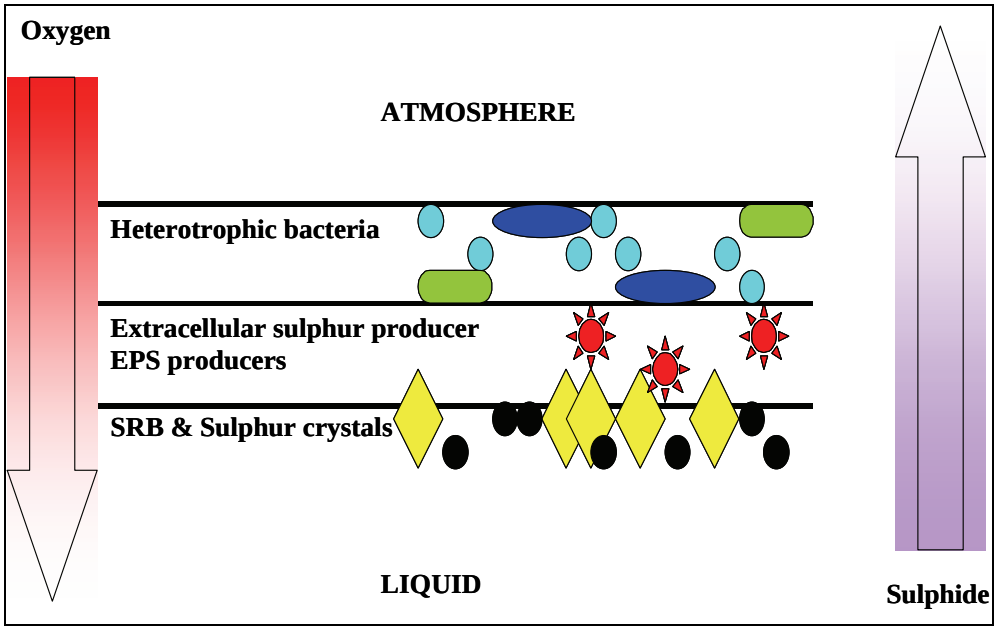

Figure 6. Summary illustration of the descriptive model integrating the various processes occurring in the floating sulphur biofilm. These occur against falling DO and Redox potential gradients and sulphide migrating upwards into the biofilm. Aerobic heterotrophic bacteria establish at the air/liquid interface and, in consuming oxygen diffusing into the strongly anaerobic system, establish steep DO and Redox gradients at the surface. Below this layer, anaerobic exopolymeric substance producers generate a copious slime layer which constitutes the matrix of the biofilm. Within the correctly poised redox window, both biological and inorganic sulphur formation occurs and gives rise to large sulphur granules which characterise the Thick film stage of the biofilm.

Development of the LFCR

A particular focus of the project was to use the basic investigations as a foundation to proceed to process development studies. The LFCR was scaled up to a Four- and an Eight-channel reactor. In these studies the LFCR showed potential as a basic unit operation for sulphide removal from treated AMD wastewaters and indicated that an all year round operation of the unit would be possible. The optimum operating temperature was found to be 20^{o}C. An average sulphide removal of 88%, and sulphur recovery of 66% was obtained for the Eight-Channel LFCR. This was an improvement on the performance of the Four-Channel LFCR and indicates the surface area dependence of the process at the 20^{o}C operating temperature. Although complete oxidation of sulphide to sulphate was observed, it was found to be significantly lower in the Eight- compared to the Four-Channel LFCR under the same operating conditions.

Development of the Floating Sulphur Biofilm Reactor

Studies were undertaken to scale-up the laboratory LFCR system and led to the development of the Floating Sulphur Biofilm Reactor shown in Figure 7.

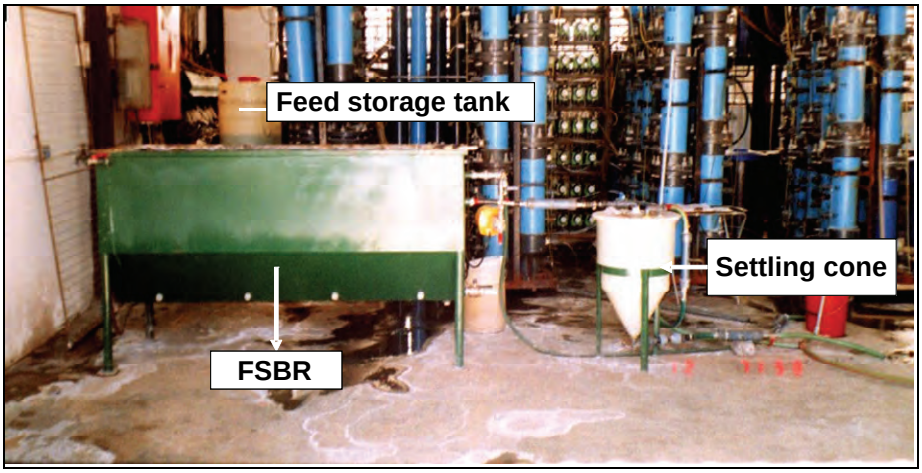

Figure 7. Floating Sulphur Biofilm Reactor as initially set up at Pulles Howard and De Lange laboratories in Johannesburg.

The object of this design was to provide a substantial sump for biofilm accumulation and also to investigate surface skimming as a possible improvement over biofilm settling as the sulphur recovery harvesting mechanism.

Over a 400 day operating study, it was shown that although an average sulphide removal of 65% and a sulphur recovery of 56% were achieved, it was lower than the LFCR where the inter-harvest recovery period was reduced from three to four days to six to 12 hours. It is probable that substantial process performance improvement could be achieved with further optimization studies.

Future Work

While the studies reported here represent a first detailed report on the structure and function of the floating sulphur biofilm, and its possible development as the basis of a bioprocess application in the treatment of sulphidic wastewaters, this may be considered as a point of departure and considerable work is required both at the fundamental and applied levels. Important items that need to be addressed include:

- Confirmation of the crystalline structure of the elemental sulphur that is produced in the biofilm. X-ray crystallographic studies should be considered here. Having established this, the sulphur balance between the various sulphur species should confirm the mechanism by which sulphur is formed in these systems. This information would have potentially important implications in sulphide removal bioprocess optimisation studies;
- Variability in the formation of the biofilm and the factors influencing changes observed should be characterized and possibly related to the structural/functional model accounting for the performance of the system. In this regard, ongoing fundamental studies would feed into bioprocess development undertaking;
- While the system is clearly complex and difficult to manipulate by a simple reductive approach, it is evident that further progress in process development will be dependent on deriving accurate kinetic values for the operations involved;

- Preliminary development of the LFCR laboratory system, and the FSBR as a bioprocess reactor prototype, has shown potential for the application of the system in the treatment of sulphidic wastewaters. However, substantial room for innovation and improvement exists here and should be the focus of future innovation.

Recommendations

The removal of sulphide from AMD treatment operations, that require a reduction in sulphate salinity, remains a major bottleneck in the development of wastewater treatment technology. Although these may be considered to be provisional and first order indication, the studies reported here provide sufficient indication that the floating sulphur biofilm system may provide a useful basis for future process technology development.

Thus, based on the above observations relating to the future potential of the system, the following recommendations are made regarding actions to be considered by the WRC:

- Reactor development and process optimisation studies be undertaken at laboratory scale to provide the basis for further innovation and technology development;
- Although still clearly a work in progress, the existing LFCR/FSBR system should be scaled up to a reactor surface of several m^2 in order to derive experience in its operation in a passive AMD treatment system application;
- Basic studies into the nature of the floating sulphur biofilm should be continued since an improved understanding of the performance of, and constraints on, the system would feed into the development of the bioprocess unit operation.

TABLE OF CONTENTS

LIST OF FIGURES

LIST OF TABLES

LIST OF ABBREVIATIONS

ALD	Anoxic limestone drains
AMD	Acid Mine Drainage
AO	Acridine orange
APS	Alkalinity producing systems
CLSM	Confocal laser scanning microscope
CO_2	Carbon dioxide
DGGE	Denaturing gradient gel electrophoresis
DNA	Deoxyribonucleic acid
DPBR	Degrading packed bed reactor
EBRU	Environmental Biotechnology Research Unit
EDX-SEM	Energy dispersive X-ray – Scanning electron microscopy
Eh	Redox potential
EM	Electron microscopy
EPS	Exopolymeric substance
FISH	Fluorescence *in situ* hybridisation
FSB	Floating sulphur biofilm
FSBR	Floating Sulphur Biofilm Reactor
G+C	Guanine + Cytosine content
HDS	High density sludge
HPLC	High pressure liquid chromatography
IMPI™	Integrated Managed Passive treatment system
LFCR	Linear Flow Channel Reactor
MPB	Methane-producing bacteria
PCR	Polymerase chain reaction
PFA	Pulverised Fuel Ash
PHD	Pulles Howard and De Lange
RAPS	Reducing alkalinity producing system
RNA	Ribonucleic acid
rRNA	Ribosomal RNA
$S_2O_3^-$	Thiosulphate
SAPS	Successive alkalinity producing system

SEM	Scanning electron microscopy
Sn^{2-}	Polysulphides
S^o	Elemental sulphur
$-SO_3-Sn-SO_3-$	Polythionates
SOB	Sulphide oxidizing bacteria
SPARRO	Slurry precipitation and recycle reverse osmosis
SRB	Sulphate reducing bacteria
STR	Stirred tank reactor
TDIS	Total dissolved inorganic solids
VCC	Vryheid Coronation Colliery
XANES	X-ray absorption near edge spectroscopy
XRF	X-ray fluorescence

ACKNOWLEDGEMENTS

The research in this report emanated from projects funded by the Water Research Commission entitled:

K5/1545, 'Investigation and development of the biotechnology of sulphur biofilms in the beneficiation and treatment of wastewaters' (WRC Project No K5/1545) and 'Development and refinement of the floating sulphur biofilm reactor for sulphide oxidation for the use in integrated passive treatment systems and the Rhodes BioSURE Process' (WRC Project No K5/1349).

The Reference Groups responsible for this project consisted of the following persons:

Mr HM du Plessis	Water Research Commission (Chairperson)
Mr G Steenveld	Water Research Commission
Prof M Wentzel	University of Cape Town
Prof E Chirwa	University of Pretoria
Mr A Wurster	Golder Associates
Dr H Greben	CSIR
Mr N Dooge	Xstrata Coal
Ms L K Chauke	Chamber of Mines
Mr W Pulles	Pulles Howard & De Lange Inc.

The financing of the project by the Water Research Commission and the contribution of the members of the Reference Groups is gratefully acknowledged.

1 LITERATURE REVIEW

1.1 ACID MINE DRAINAGE

The salinisation of the public water system has been a subject of increasing concern in South Africa. Acidic mine drainage (AMD) wastewaters have contributed substantially to this problem (Barnes and Romberg, 1986; Pulles *et al.*, 1995; Scott, 1995; Gazea *et al.*, 1996; Rose *et al.*, 1998; Younger, 2001; Johnson *et al.*, 2002; Rose, 2002). Considerable research effort has been directed at process development for the remediation and treatment of these wastewaters and biological systems have been the subject of particular interest given the need for sustainability over the long periods of time AMD flows are anticipated to require treatment (Rose *et al.*, 1998; Chang *et al.*, 2000; Johnson *et al.*, 2002; Younger, 2002; Johnson and Hallberg, 2005). Both active (Rose, 2002) and passive (Pulles *et al.*, 1995; Younger *et al.*, 1997; Younger, 1998) treatment systems have been developed for the removal of sulphate salinity and heavy metal contamination, and for neutralization of the acidic stream.

The biological sulphur cycle, and specifically sulphate reduction is the central operation of the various biological AMD treatment processes (Johnson and Hallberg, 2003). The sulphide produced in this way thus needs to be removed from the system, to prevent its reoxidation to sulphate, and thus achieving a linearisation of the biodesalinisation and prevention of recycling of the sulphur species in a treatment operation (Rose, 2002).

1.2. SULPHIDE REMOVAL

Sulphide is a toxic, corrosive and odorous compound and its removal from wastewater treatment effluent in one way or another is thus also mandatory. Strategies that have been used include precipitation as metal sulphide (Davidson *et al.*, 1989; Johnson, 1995; Boshoff *et al.*, 1996, Van Hille and Duncan., 1996; Molipane 1999; Dvorak *et al.*, 2004), oxidation to elemental sulphur (Habets and De Vegt *et al.*, 1991; Buisman *et al.*, 1996; Rein, 2002), and solvent extraction (Hammond, 1986; Steudel, 1996; Johnson, 2000).

The development of reliable technology for the oxidation of sulphide to form elemental sulphur would increase the potential of treatment technologies where waste carbon sources are used for biological sulphate reduction to produce sulphide (Bowker, 2002; Rein 2002; Son and Lee, 2004. A process that can produce elemental sulphur from sulphide under heterotrophic conditions would contribute significantly to the development of an integrated biological sulphate removal process to treat the large volumes of AMD that are predicted to occur in South Africa (Scott, 1995; Jansen *et al.*, 1999; Rein, 2002; Rose, 2002).

1.2.1 Sulphide Oxidation

H_2S is a weak acid that dissociates into HS^- (pKa_1= 7.04) and S_2^- (pKa_2). The pKa_2 has been reported to be >12 (Weast, 1981; O'Flaherty *et al.*, 1999, O'Flaherty and Colleran, 2000) and for practical purposes is disregarded. The term sulphide is commonly used for any of the reduced species that may be present. The two most important biologically relevant oxidation reactions which sulphide may undergo are shown in Equations 1 and 2 (Kuenen, 1975; Janssen *et al*., 1999):

$$2HS^- + O_2 \rightarrow 2S^o + 2OH^- \quad (1)$$

$$2HS^- + 4O_2 \rightarrow 2SO_4^{2-} + 2H^+ \quad (2)$$

These are overall equations for the oxidation of sulphide. Other possible products of oxidation include thiosulphate (S_2O^{3-}) and polythionates ($-SO_3^-$-S_n-SO_3^-) In addition to this, polysulphides (S_n^{2-}, n = 2 to 5) have been identified as important intermediates in the oxidation of sulphide (Chen and Morris, 1972; Yao and Millero, 1996; Steudel, 1996; Janssen *et al.*, 1999). An indication of the thermodynamic forces acting on a chemical system can be obtained from the Pourbaix diagram (Figure 1.1), which represents the equilibrium distribution of the domains of dominance of various chemical species at specific pH and Eh (Redox) values (Stumm and Morgan, 1995; Middelburg, 2000; Steudel, 2000).

Compared to the other oxidized forms of sulphur, elemental sulphur is formed in a narrow band of Redox potential and pH conditions (Stumm and Morgan, 1995). Lewis *et al.*, (2000) suggested that for a biological process, equilibrium

thermodynamics have less of an influence on the major product of sulphide oxidation than kinetic considerations do. It is also possible that conditions in the bulk phase (those which are measured for chemical reaction process control purposes) are quite different from the intracellular conditions in living systems (Lewis *et al.*, 2000).

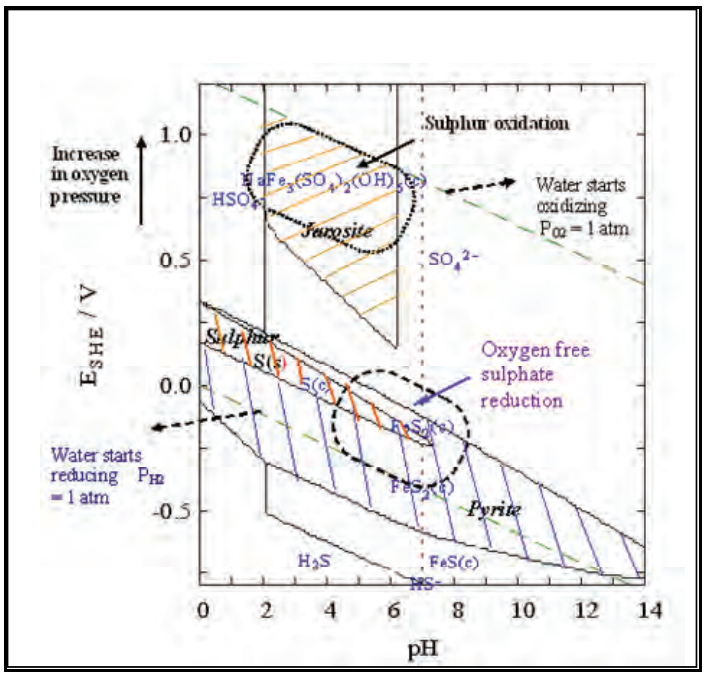

Figure 1.1. A Pourbaix diagram showing the different sulphur species at specific pH and Eh (Redox potential) values (Middelburg, 2000).

Sulphide can be converted to sulphur and sulphate during oxidation processes which can be either chemically or biologically driven.

1.2.1.1 Chemical sulphide oxidation

The removal of sulphide from solutions has been tackled in a number of ways. Physico-chemical processes include chemical oxidation reactions (Sublette, 1992; Reinhoudt and Moulijn, 2000), and chemical precipitation (Buisman *et al.*, 1989; Lens *et al.*, 2000) usually resulting in the production of metal sulphide sludges which must be disposed of. Oxidative reactions involve the contact of sulphide ions with oxygen under constrained pH and Redox potential conditions to produce S^o (elemental sulphur) and hydroxide ions (Equation 1). The elemental sulphur formed has an oxidation state of zero and consists mainly of cyclic S_8 molecules which aggregate

into larger crystals which can be separated from solution either by floatation or separation techniques (Steudel, 1996; Steudel, 2000).

Industrial sulphide physico-chemical sulphide removal processes include the Stredford Process (Hammond, 1986; Lens *et al.*, 2000; Steudel, 2000) in which sulphide is converted to elemental sulphur in the presence of a vanadium catalyst, and the Clause process (Janssen *et al.*, 1999; Steudel, 2000) used in the petrochemical industry to strip sulphide into an amine or glycol solution at high pressure and then catalytically convert it to sulphur (Guoqiang *et al.*, 1994; Gilfillan 2000; Rein, 2002). The high cost implications of such treatment options are considered in general to be inappropriate for the treatment of large volumes of sulphate-containing wastewaters.

1.2.1.2 Biological sulphide oxidation

Sulphide oxidizing bacteria (SOB) use sulphide as a source of electron donors and produce sulphur particles in the submicron range (Bruser *et al.*, 2000). These are composed of a core of elemental sulphur covered by a layer of naturally charged polymers comparable to those of the La-Mer sulphur sol, which renders the particles hydrophilic (Steudel, 1996; Jansen *et al.*, 1999; Bruser *et al.*, 2000). A range of genera capable of sulphide oxidation and sulphur formation include *Thiomicrospira, Thiobacillus, Thiothrix, Acidophilum, Leptospirillum, Thiovulum, Chromatium* and *Chlorobium* (Lane *et al.*, 1992; Okabe *et al.*, 1999; Cytryn *et al.*, 2005). These species are widely spread across the archae- and eubacteria, illustrating that traditional physiological groupings based on metabolic criteria, are often not representative of phylogenetic relationship and produce overlapping groupings for many unrelated bacterial species. The three groups of bacteria involved in sulphide oxidation are:

- Photosynthetic sulphur bacteria,
- Colourless sulphur bacteria,
- Certain heterotrophic bacterial groups which have sulphide oxidising capabilities, although they are not as well documented as the colourless sulphide oxidising bacteria.

1.2.1.3 Photosynthetic sulphur bacteria

Photosynthetic sulphur bacteria, including both green and purple sulphur bacteria forms, use sulphide as an electron donor for photosynthesis, with carbon dioxide (CO_2) as a carbon source in a reaction powered by light, as illustrated in Equation 3.

$$CO_2 + H_2S \rightarrow CH_2O + H_2O + 2S \quad (3)$$

The sulphur produced from sulphide oxidation may be located intracellularly (e.g. *Chromatium* sp.) or as extracellular sulphur globules (e.g. *Chlorobium* sp.). Alternately, sulphide may also be fully oxidised to sulphate under certain conditions. The photosynthetic sulphide oxidisers play an important role in anaerobic shallow waters, where they provide one of the few means to oxidise reduced sulphur compounds, (Campbell, 1983; Johnson, 2000) growth in stratified lakes (< 15 m) is dependent on light penetration and wavelength. The genera commonly found in these environments are *Chromatium, Chlorobium, Rhodobacter* and *Thiospirillum* (Widdel, 1988).

The sulphide oxidising potential of photosynthetic sulphur bacteria such as *Chlorobium limicola* have been used in sulphide oxidising bioreactors (Cork *et al.*, 1986; Kim *et al.,* 1990) and reportedly can transform up to 90% of inlet hydrogen sulphide to sulphur (Kim *et al.,* 1990; Johnson, 2000). Photosynthetic sulphur bacteria are not, however, the first choice in biotechnological sulphide removal processes because of the light requirement which complicates reactor design and more importantly because sulphide oxidation is strictly coupled to growth. Photosynthetic sulphide oxidising bacteria use carbon dioxide as a terminal electron acceptor with 1-2 g of sulphur being produced per 1 g of cells (Kuenen and Robertson, 1992; Johnson, 2000).

1.2.1.4 Colourless sulphur bacteria

The colourless sulphur bacteria are a diverse group of sulphide oxidisers which includes both archae- and eubacteria (Robertson and Kuenen, 1991; Johnson, 2000). Colourless sulphur bacteria inherit their name from the lack of photo-pigments,

although in dense cultures, they could appear pink or brown due to the presence of large amounts of cytochrome (Robertson and Kuenen, 1991; Johnson, 2000). The wide range of include *Thiobacillus, Thiomicrospira, Thiospaera, Sulfolobus, Leptospirillum, Acidianus, Thermothrix, Thiovulum, Beggiatoa, Thiothrix, Thioploca, Thiodendron, Thiobacterium, Macromonas, Achromatium* and *Thiospira*. The members of these genera have differing pH and thermal requirements for growth and some are capable of denitrification while others are not (Jorgensen and Revsbech, 1985; Widdel, 1988; Robertson and Kuenen, 1991; Janssen, 1997; Gardner, 1998; Nielson *et al.,* 2000; Ito *et al.*, 2004).

The *Thiobacilli* are the most well documented group of colourless sulphide oxidising bacteria. They mainly obtain energy from the chemolithotrophic oxidation of inorganic sulphur compounds, which is used to support autotrophic growth using CO_2 as the carbon source (Kelly, 1985). Thiobacilli are Gram-negative, rod-shaped eubacteria, with very high diversity amongst members of the genus. The six obligate chemolithotrophic species have a variation in G+C content from 51-68%, have pH optima from pH 2 to 7 and grow at optimal temperatures ranging from 20-30^{o}C (Kelly, 1985). The wide variation in the genus has made it a challenging task to elucidate the enzymatic pathway involved in sulphur metabolism (Kelly, 1985).

Colourless sulphur bacteria may be either aerobic or anaerobic, the latter using alternative electron acceptors such as hydrogen and ferrous iron. *T. denitrificans* has been characterised as an anaerobe, although Sublette *et al.* (1987) found that aerobic cultures can reduce the sulphide content of gas to a very low level. Under anaerobic conditions, nitrate is used by *T. denitrificans* as a terminal electron acceptor, while producing nitrogen, as described by Equation 4.

$$5H_2S + 8KNO_3 \rightarrow 4K_2SO_4 + H_2SO_4 + 4N_2 + 4H_2O \qquad (4)$$

The colourless sulphur bacteria are present wherever reduced sulphur compounds, usually sulphides or sulphur, are found including hydrothermal vents, hot springs and wastewater treatment plants (Dart and Stretton, 1980; Robertson and Kuenen, 1991; Weller *et al.*, 1991; Voordouw *et al.*, 1996; Berbee and Taylor *et al.*, 1999). Basu *et al.* (1995) reported a symbiotic relationship between sulphate reducing bacteria and

the micro-aerophilic sulphide oxidising *Beggiatoa sp*. in a micro-aerophilic sulphate reducing bioreactor. The healthy population of *Beggiatoa*, observed in sludge granules converted sulphide produced by the SRBs to sulphate, or to intracellular sulphur, while the SRB population was involved in anaerobic sulphate reduction using organic acids as a carbon and energy source (Basu *et al.*, 1995). Williams and Unz (1985) also found filamentous sulphide oxidising bacteria (*Thiothrix* and *Beggiatoa*) in activated sludge (Bruser *et al.*, 2000; *Ito et al.*, 2002).

Well known biological sulphide removal systems include the Shell-Paques process operated at the Budelco zinc refinery in the Netherlands, an example of the use of sulphide oxidising bacteria's natural role in the sulphur cycle in a biotechnological application (Scheerem *et al.*, 1993; Janssen *et al.*, 2000). This process involves collection of sulphide from the wastewater in a scrubber followed by feeding it to sulphide oxidising bacteria able to convert the sulphide into elemental sulphur. The sulphur is collected by a titled plate settler, resulting in a 99.5% removal of H_2S from the gas stream (Janssen *et al.*, 1999). There are currently two of these plants in India and one in Germany. However, the high process costs of this type of approach make it unsuitable for high volume flow and passive treatment systems (Pulles, 1995; Younger *et al.*, 1997; Rose, 2002; Coetser *et al.*, 2006).

Guoqiang *et al.* (1994) developed a desulphurisation process using *Thiobacillus ferrooxidans*, with an iron sulphate feed being converted into sulphur. The bacteria catalysed the conversion of ferrous sulphate to ferric sulphate, which oxidised hydrogen sulphide to elemental sulphur while reducing the ferric sulphate to ferrous sulphate. This reduced solution was then recycled.

1.3 FLOATING SULPHUR BIOFILMS

A possible area for the development of the sulphur bacterial system applications in wastewater has been the more recent observation and investigation of floating sulphur biofilms (FSB). The appearance of white films on sulphate reducing systems has been the subject of previous content (Jorgensen and Revsbech., 1985; Janssen, 1996; Rose, 1996; Dunn 1998) but little if any detailed study has been reported on their occurrence in natural environments.

Researchers of the Environmental Biotechnology Research Unit (EBRU) at Rhodes University had observed the appearance of white floating films on the surface of highly sulphidic tannery wastewater ponds (Figure 1.2) had initiated preliminary investigations into their nature and function (Rose *et al.*, 1996; Dunn, 1998). Early reports by Gilfillan (2000) confirmed that these were clearly differentiated structures which were mainly populated by a diverse mix of morphological types. They were provisionally identified as floating biofilms. Bowker (2002) then showed that SOB were indeed present in these structures and made preliminary reports on how the populations may be arranged within them. Rein (2002) initiated bioprocess studies on the application of these films and noted the importance and extreme sensitivity of the system to Redox poising across the narrow Eh range.

Figure 1.2. Occurrence of sulphur biofilms observed on high-organic load sulphidic tannery wastewater ponds.

Although these studies provided important indications that these systems might operate as true biofilms, even though they occurred at the air/water interface instead of attached to a solid surface, many questions remained unanswered. Potential for bioprocess development has been suggested but this would depend largely on understanding the structural/function relationships within the system and how this will affect performance in sulphide oxidation. Further progress in this area would seem to depend in some measure on understanding their structure within the context of existing knowledge about their structure and function in general.

1.4. THE STUDY OF BIOFILMS

Biofilms occur ubiquitously in aquatic environments and have been the subject of substantial attention in the last decade (Carpetier and Cerf, 1993; Costerton *et al.*, 1994; Vroom *et al.*, 1999; Davey and O' Toole, 2000; Wuertz, 2003; Okubo *et al.*, 2006). In the water treatment industry, biofilms are problematic due to adverse effects on water quality, pipeline corrosion, and disinfectant consumption (Ramesh *et al.*, 2006). The study of these structures has been limited by the constraints of traditional microbial culture-dependent techniques, which do not allow exact localization of the bacteria. Furthermore, these techniques often detect only a minor portion of the naturally occurring populations with spatial heterogeneity and aggregation increasing the uncertainty of enumeration (Okabe *et al.*, 1999). The completely mixed stirred tank reactor (STR) has generally predominated in the basic studies of biofilms and to some extent, has simplified the investigation of the microbial physiology and genetics of component organisms (Wuertz, 2003). However, pure culture planktonic growth is rarely how bacteria exist in nature and commonly, occurrence is as attached or aggregated forms in structured ecosystems (Davy and O' Toole, 2000, Johnson and Hallberg, 2005).

Carpentier and Cerf (1993) described biofilms simply as "a matrix, adhering to a surface". Costerton (1995) has provided a more comprehensive definition as "a structured community of bacterial cells enclosed in a self-produced polymeric matrix, adherent to an inert or living surface". Elder *et al.*, (1995) described biofilms in cooperative terms as "a functional consortium of microorganisms organised within an extensive exopolymeric substance (EPS) matrix". Dunne (2002) has commented that this description of biofilms is an oversimplification of a fairly complex process that does not take into account the type of microorganisms, composition of the surface, or the influence of environmental factors. However, what can be said is that there are three basic criteria underlying each of these definitions: microorganisms, glycocalyx or EPS matrix and surface (Costerton *et al.*, 1994; Elder *et al.*, 1995; Dunne, 2002).

It is important to note that a degree of functional organization and cooperation exists within the biofilm to allow interaction with the environment without compromising cell survival or exhausting available resources (Dunne, 2002). Zhang and Bishop

(1994) have noted the spatially heterogeneous structure of these systems with complex groupings of cells ranged along physical and nutrient gradients. Pores and channels occur within the biofilm allowing mass transfer into the internal structure from the outer surface and the bulk fluid surrounding the biofilm. While the initial colonizers of the surface will be mostly found within the biofilm closer to the attachment surface, the later colonizers and EPS production is mostly found at the bulk fluid/surface interface. Different species in the system could be either complementing or competing with each other for available nutrients, and later colonizers could utilise secondary metabolites produced by the initial colonisers and vice versa (Hermanowics, 2003; Wuertz, 2003).

The life of a biofilm is different from the planktonic form in that bacterial communities develop internal heterogeneity (Zhang and Bishop, 1994; Wu and Janssen, 1996) and structural and functional relationships which are in response to environmental changes (Christensen *et al.*, 1999). The advantages of biofilm life forms include the higher availability of nutrients and the long-term positioning of microbial communities in relation to other communities (Nivens *et al.*, 1995; Watnick and Kolter, 2000).

Biofilms possess a general characteristic of being substantially more resistant than their planktonic counterparts to antimicrobial stressors such as antibiotics and host-defence responses (Gilbert *et al.*, 1997; Gilbert *et al.*, 2002; Parsek and Fuqua, 2004). This characteristic is enhanced by the reduced penetrability of the EPS matrix, commonly referred to as the slime layer or glycocalyx (Carpentier and Cerf, 1993). This EPS matrix varies in composition depending upon the organisms present, and the type of environment, and is primarily produced by the microorganisms themselves (Davy and O' Toole, 2000; Dunne, 2002; Parsek and Fuqua, 2004). In most biofilms, the matrix is predominantly anionic and creates an efficient scavenging system for trapping and concentrating essential minerals and nutrients from the surrounding environment (Carpentier and Cerf, 1993; Dunne, 2002).

A white film adhering to the glass walls of a sulphide rich reactor at the gas-liquid interface has been reported by Gadre (1989). These biofilms were thought to include sulphide oxidising bacterial communities involved in the conversion of sulphide to

elemental sulphur and their use as a means of final removal of sulphate in wastewater treatment has been suggested. Rapid cycling of sulphur through both its oxidised and reduced forms within attached biofilms grown on domestic wastewaters has been documented by numerous authors (Kühl and Jørgensen, 1992; De Beer *et al.*, 1994; Goebel and Stackebrandt, 1994; Kolmert *et al.*, 1997; Okabe *et al.*, 1998; Yu and Bishop, 1998; Okabe *et al.*, 1999). This cycling could play an important role in the overall reduction of the organic load in these systems. However, most work has focused on systems attached to solid substrate and the study of floating biofilms has not been described in any great detail as they form rather at the interface between water and air.

Bacteria initiate biofilm development in response to specific environmental cues such as nutrient availability and the formation may require coordination within, interactions of, and communication between multiple bacterial species (O' Toole *et al.*, 2000); indicating a symbiotic or possible competition between the different species (Wuertz, 2003; Parsek and Fuqua, 2004). The key element in bacterial adaptability is their ability to position themselves in a niche where they can propagate (Dunne, 2002). Numerous methods of positioning have been described including flagella motility and different methods of surface translocation including twitching, darting and gliding (Davey and O' Toole, 2000). Some species are able to affect their position by synthesizing cellulose, thereby forming a fibrous pellicle that places cells near the air-water interface, and cellulose synthesis aids in attachment to surfaces such as plant cells (Ross *et al.*, 1991).

Another positioning mechanism is aggregation or attachment, which enhances cell to cell interaction and the sedimentation rate of cells (Davey and O'Toole, 2000). Through attachment, bacteria can form communities and obtain the additional benefit of the phenotypic versatility of their neighbours (Hermanowicz, 2003). Where the different species can be symbiotically involved in attachment and EPS production, other species can easily aggregate around them. Other species could produce by-products that provide nutrient source for other members of the structure (Hermanowicz, 2003).

Wuertz (2003) noted that some films without an obvious attachment surface can also form in extreme environments such as AMD where they may contribute to sulphur cycling. Cyanobacterial mat biofilms have been studied in thermal hot springs (Ward *et al.*, 1998) and marine environments (Paerl and Pinckney, 1996).

The occurrence of these structures although observed on the surface of sulphidic wastewater has not been described in any detail. It is therefore imperative to investigate their structure, gain understanding into their nature and physiological aspects from which their function could be derived. This could lead to possibilities for manipulating these systems in wastewater beneficiation.

1.4.1 Biofilm Structure and Architecture

The characterisation of biofilm morphology is fundamental to an understanding of the interactions with the surrounding environment and the description of biofilm ecological structure is crucial for assessment of biofilm function (Hermanowicz, 2003). In this context, morphology refers to the geometric, physical form of the biofilm, whereas structure includes morphological features and also spatial distribution of different biofilm elements including various microbial populations, EPS and abiotic components (Hermanowicz, 2003; Wuertz, 2003). The dynamics of biofilm development, and the resulting structure, are dependent on the processes of attachment (deposition), growth, death and detachment (Wuertz, 2003). The rates of these processes and their importance may vary spatially and temporally (Hermanowicz, 2003).

1.4.2 Biofilm Diversity

Substantial phenotypic diversification occurs within biofilm communities (Parsek and Fuqua, 2004), this reflects the adaptation to micro-environments found within a biofilm. The biofilm phenotype is loosely defined as the patterns of protein and gene expression associated with biofilm cultures in comparison to those associated with the planktonic culture (Parsek and Fuqua, 2004). Different gradients result in micro-niches and selective pressures, which produce variants with biofilm-specific phenotypes (Parsek and Fuqua, 2004). The resulting type of biofilm is determined by

stage of development or maturity (Parsek and Fuqua, 2004). One of the variants, called the “Wrinkly “ or “Sticky” variant is formed as small rough colonies on solid growth medium, and displayed as a hyper-biofilm-forming phenotype on abiotic surfaces (De Beer and Schramm, 1999; Parsek and Fuqua, 2004). Examples of these have been reported in the literature for a number of species including *Salmonella enterica* (Parsek and Fuqua, 2004), and they exhibit heightened resistance to antibiotics and biocide bleach compared to biofilms formed by the wild-type parental strain (Parsek and Fuqua, 2004).

Different types of bacteria can leave a biofilm in a process that has been termed dispersion or dissolution, presumably achieved by coordinating the breakdown of the surrounding EPS matrix through the action of secreted or cell surface-associated enzymes, with the activation of motility functions. This activity is thought to represent a final step in biofilm development, in which cells revert back to their planktonic state (Sauer *et al.*, 2002).

Taking into account the complexity of biofilm structure and function, their study has been heavily dependent on the development of appropriate techniques and as a result this has become something of an interdisciplinary field of enquiry.

1.5. TECHNIQUES USED IN THE STUDY OF BIOFILMS

1.5.1 Microscopy and Culture Techniques

Classical microscopic analyses relied on standard light microscopy using Gram- and other staining methods for identifying microorganisms based on morphology. This has severe limitations. The use of isolates in selective media and determining physiological parameters or chemotaxonomic markers has offered more progress (Wagner *et al.*, 1994). However, it has become apparent that only a limited number of microorganisms present can be isolated from complex microbial populations such as biofilms by standard methods including enrichment and plating techniques (Wagner *et al.*,, 1994; Lawrence *et al.*, 1994; Davey and O’Toole, 2000). Results from classical microscopy and culture techniques have thus offered a biased and incomplete view of the microorganisms present in such systems.

The application of confocal laser scanning microscopy (CLSM) to biofilm research has made a substantial impact on existing perceptions of biofilm structure and function. Prior to CLSM, electron microscopy (EM) was the method used to examine biofilms under high resolution, however, sample preparation for EM results in dehydration of samples, biofilm collapses, and a deceptively simplistic view of biofilm structures (Stewart *et al.*, 1995). CLSM has allowed the visualization of the three dimensional structure of fully hydrated biofilms, and has been used to monitor dynamic biofilm development in flow cells (Lewandowski, 1995). CLSM studies have shown that *in vitro* biofilms formed by single species exhibit similar overall structural features to those produced in nature by mixed species consortia (Stewart *et al.*, 1995). This includes a level of heterogeneity where aggregates are interspersed throughout an EPS matrix of various density, creating open zones where water channels are formed (Danese *et al.*, 2000).

The identification and quantification of members of a particular microbial community and a clearer understanding of the functional relationship between members is required to fully appreciate and possibly manage the complex processes that these communities perform. Examination of biofilm communities is complicated by the difficulty of identifying constituent biofilm members *in situ*, in quantifying physical, chemical and spatial aspects of biofilms and in linking processes and activity with specific biofilm bacteria (Korber *et al.*, 1999; Bowker, 2002). Molecular diagnostic tools have contributed substantially to this task (Amann *et al.*, 1995; Head *et al.*, 1998; Santegoeds *et al.*, 1998; Davey and O' Toole, 2000).

1.5.2 Molecular Biology

Techniques based on the analysis of bacterial DNA and RNA may complement the conventional microbiological approach and now are routinely used to determine the presence and distribution of individual bacterial species in complex communities such as bacterial biofilms (Amann *et al.*, 1990; Ramsing, 1998; Raskin *et al.*, 1996; Santegoeds *et al.*, 1998; Chauke, 2000; Gilfillan, 2000; Bowker, 2002). Earlier molecular methods relied on the direct extraction, purification and sequencing of 5S ribosomal RNA (rRNA) from environmental samples. However, the limited length of the 5S rRNA molecule (120bp) did not allow for high resolution analysis (Head *et al.*,

1998). The use of 16S and 23S rRNA consisting of ~1500 and ~3000bp respectively, contains sufficient information for a reliable phylogenic analysis of more complex communities (Amann *et al.*, 1995; Head *et al.*, 1998; Hugenholtz *et al.*, 1998).

Techniques used include polymerase chain reaction (PCR), degrading gradient gel electrophoresis (DGGE), hybridisation and sequencing.

1.5.2.1 Polymerase chain reaction

PCR relies on the use of oligonucleotide primers and DNA polymerase to amplify a targeted DNA sequence using temperature-controlled cycles which result in strand separation, primer annealing and primer extension, followed by viewing on an agarose gel (Head *et al.*, 1988; Amann *et al*., 1995; Santegoeds *et al.*, 1998; Bowker, 2002). However, when used to selectively amplify a target in a mixed DNA samples PCR can be biased as it is not quantitative. There is a possibility of preferential amplification of certain templates, rendering the representative assessment of natural abundance of the product genes inaccurate (Amann *et al.*, 1995; Santegoeds *et al.*, 1998). Selectivity in PCR amplification of rRNA genes is a source of bias that can affect the results of molecular biological measures of diversity, where small differences in the sequence of universally conserved regions may result in selective amplification of some sequences particularly if primer annealing is at high stringency (Head *et al.*, 1988). The other concern could be that less abundant sequences and high percentage G+C templates could be discriminated against (Head *et al.*, 1988).

1.5.2.2 Denaturing gradient gel electrophoresis

DGGE technique is frequently applied to microbial ecology for comparison of the complex structure of microbial communities and to study their dynamics (Heuer *et al.*, 1999b). This technique employs separation of DNA fragments of the same length, but different base-pair sequences, where the partially denatured and melted DNA is separated according to the decreased electrophoretic mobility on a polyacrylamide gel (Muyzer *et al.*, 1993; Muyzer and Ramsing, 1995; Heuer *et al.*, 1999b).

1.5.2.3 Hybridization

Hybridization techniques use rRNA-targeted oligonucleotide probes to quantitatively determine the composition of complex microbial communities (Hugenholtz, 1998). Ready to use species-specific probes are available for the identification of specific target organisms within mixed samples in their natural habitat (Amann *et al.*, 1995; Hugenholtz *et al.*, 1998). In cases where microorganisms are unknown, specific probes are designed using the cloned sequences obtained with the 16S rDNA approach.

Application of these probes in the dot blot or *in situ* techniques enables the detection and quantification of corresponding microorganisms present in a sample (Amann and Kuhl, 1998). These include the dot blot (Raskin *et al.*, 1994; Lin and Stahl, 1995) and fluorescent in situ hybridisation (FISH) techniques (Wagner *et al.*, 1993; Amann *et al.*, 1995; Daims *et al.*, 2001; Okabe *et al.*, 1999).

Amann *et al.*, (1995) investigated the micro-diversity in municipal activated sludge samples using rRNA-targeted probes. There was a concern that the method would provide misleading results since cultivation-independent comparative rRNA analysis relies on the PCR amplification of rRNA from nucleic acid extracts from environmental samples. This meant that at each step of the investigation, there would be several factors that could result in artificial sequence diversity in rRNA gene libraries. By using *in situ* probes and CLSM, the researchers were able to investigate the potential for high micro-diversity in a natural microbial community without the selective bias of cultivation, extraction, or amplification (Amann *et al.*, 1995). Evidence for high micro-diversity was shown, indicating that high diversity within a relatively narrow phylogenic group was present in that environment.

1.5.3 Advances in Molecular Biology

Recent technological advances in the use of rRNA-based phylogenetic analysis has, provided a means of developing tools with which to investigate microbial communities (Amman *et al.*, 1992; O' Toole, *et al.*, 2000). This includes the use of fluorescently labeled rRNA-targeted oligonucleotides, a variety of micro-sensors,

real-time image analysis and CLSM which allow researchers to investigate biofilms *in situ* (Davey and O'Toole, 2000). One key advance has been the development of tools for cultivating communities which, includes chemostats, continuous flow slide cultures, microstats and colonization tracks (Davey and O'Toole, 2000).

In a study by Raskin *et al.*, (1996) the metabolically competitive methane-producing bacteria (MPB) and SRB in a biofilm reactor, and their relative response to sulphate availability was investigated. In this study the generally accepted notion that SRB and MPB were mutually exclusive in their natural habitats was questioned. It was found that the relation of the two communities was more complex than previously suggested and that SRB were selected for under high sulphate concentration whilst MPB were selected for in sulphate depleted environments. The quantification of specific 16S rRNA compared to total 16S rRNA was used to monitor the two communities. In addition, sulphide and methane production were also assayed. It was found that in the absence of sulphate, certain SRB types were present in high numbers (possibly due to the ability of certain SRB to function as fermenters or proton-reducing acetogens as previously reported by Hansen and Blackburn (1995). Upon sulphate addition, SRB levels increased and MPB and methane production levels decreased. These experiments illustrate how the rRNA-based approach can be combined with functional assays to monitor population dynamics in conjunction with metabolic changes in a biofilm community (Davey and O'Toole, 2000).

1.6 MICRO-ELECTRODES AND MICRO-SENSORS

The use of micro-electrodes has provided a breakthrough in the direct examination of the biofilm micro-zones *in situ*. These needle-shaped devices have a tip measuring from less than one to 100 µm, which is sensitive for specific compounds (De Beer and Muyzer, 1995; De Beer *et al.*, 1997; Santegoeds *et al.*, 1998; De Beer and Schramm, 1999; De Beer and Stoodley, 2006). Due to their small size, micro-sensor measurements cause minimal disturbance to the system and allows the examination of micro-environments and the measurement of micro-gradients (Santegoeds *et al.*, 1998; Lewandowski and Beyenal, 2003; De Beer and Stoodley, 2006). The measured gradients are a function of local transport processes (usually diffusion) and if known,

the spatial distribution of microbial activity can be derived from the substrate profiles (Santegoeds *et al.*, 1998; De Beer *et al.*, 1997; De Beer and Stoodley, 2006).

An advantage of micro-sensors is the opportunity presented to unravel closed cycles such as sulphate reduction coupled with sulphide oxidation within a biofilm (Kuhl and Jorgensen, 1992) With micro-sensors, the measurement of net substrate consumption or product excretion can be performed, which can otherwise lead to considerable underestimation of the actual processes within these biofilms (Kuhl and Jorgensen, 1992; De Beer *et al.*, 1997; Santegoeds *et al.*, 1998; De Beer and Stoodley, 2006).

The use of micro-sensors coupled with conventional molecular techniques has been employed to follow how closely species composition reflected activity in a biofilm with gradually changing micro-environments (Santegoeds *et al.*, 1998; Okabe *et al.*, 1999; Santegoeds *et al.*, 1999; Schramm *et al.*, 2002). Micro-sensors with spatial resolution ~0.5 mm were used to measure oxygen and hydrogen sulphide profiles and to infer aerobic respiration and sulphate reducing activities (Okabe *et al.*, 1999; Wuertz, 2003). Molecular techniques included the use of DGGE analysis of PCR amplified 16S rDNA fragments to determine the complexity of the microbial community in the biofilm and to monitor its behaviour over time (Muyzer *et al.*, 1993 and 1995; Heuer *et al.*, 1999a; Santegoeds *et al.*, 1998; Okabe *et al.*, 1999).

Studies combining the use of FISH with micro-electrode analysis for determining pH, oxygen and sulphide profiles have been reported to evaluate the distribution of different populations in relation to chemical profiles (Ramsing *et al.*, 1993; Schramm *et al.*, 1997; Okabe *et al.*, 1999). FISH was used in a study to localise organisms belonging to a microbial domain and various types of MPB in sludge granules (Harmsen *et al.*, 1996). It was shown that the outer layers of the granules were populated with a variety of bacterial colonies most likely involved in the hydrolysis of complex organic carbon, while the interior of the granule contained methanogenic micro-colonies (Harmsen *et al.*, 1996). These experiments provided convincing evidence of layered microbial architecture in sludge granules where the bacteria on the surface of the granule hydrolyze complex organic matter, providing the anaerobic bacteria in the interior of the biofilm with an energy source.

In a comprehensive study by Schramm *et al.* (1999), the use of micro-sensors (to measure oxygen, nitrite and sulphide concentration), CLSM (to determine a three-dimensional structure of the flocs), FISH and PCR specific primers for the dissimilatory sulphate reductase gene (to monitor the SRB population) were used to investigate the occurrence of anaerobic processes such as denitrification and sulphate reduction in well-aerated activated sludge samples. It was discovered that anoxic micro-niches of SRB and denitrification activity could occur in well-aerated activated sludge, but this could be detrimental to the degradation of contaminants as a result of hydrogen sulphide production (Schramm *et al.*, 1999).

With the use of fluorescent probe hybridisation, or staining cells with acridine orange (AO), researchers have been able to evaluate growth rates by determining cellular rRNA content (Davey and O'Toole, 2000). Therefore, using FISH combined with digital microscopy, cellular content of rRNA can be quantified and, thereby, the growth rate of cells can be estimated. Using this technique, Poulsen *et al.* (1993), discovered that in a young biofilm cells have a doubling time of 33 hours while in a mature biofilm the doubling time was increased to at least 70h. Rigler (1966) used AO staining to determine the RNA-DNA ratio. The need for isolation was eliminated as the AO-nucleic acid complex emits red-fluorescence when it is attached to a single stranded template and green-fluorescence if the nucleic acids are double stranded (Davey and O'Toole, 2000).

By combining FISH and specific enzyme activity probes to assign function to certain phylogenetic groups, Kloeke (1999) was able to determine that the Cytophaga-flavobacteria group was involved in the release of inorganic phosphate during wastewater treatment contrary to the belief that these bacteria were not involved in phosphate removal (Bond *et al.*, 1995). In a study by Schramm *et al.*, (1997), the use of CLSM, FISH and rRNA-targeted oligonucleotide probes provided a powerful tool to demonstrate micro-environments within a biofilm. It was possible to study the microbial interactions between ammonia and nitrite oxidizers, whose growth occurred in aggregates in close proximity to each other.

Although application of molecular techniques in microbial ecology has revolutionized the analysis of environmental samples and revealed remarkable results, there are still

limitations in their use. These include the reproducibility and therefore reliability of results obtained for biofilm samples. The selectivity of a particular species for PCR amplification is problematic when working with multi-species samples such as biofilms, where there could be inhibitors resulting in the preferential amplification of target DNA of some organisms rather than others (Liesack *et al.*, 1991; Reysenbach *et al.*, 1992). A specific limitation of the DGGE approach is that separation of PCR products obtained from a very complex mixture of microorganisms is problematic (Muyzer and Ramsing 1995).

Speciation, identification and characterisation of the chemical states of elements in the environment or unknown samples, is indispensable in determining the environmental behaviour, bioavailability, influence of elements on the quality of the environment and the determination of composition of elements (Takahashi, 2004).

1.7. APPLICATION OF THE FLOATING SULPHUR BIOFILM REACTOR

The Water Research Commission (WRC) has made a substantial investment in sulphur systems biotechnology for the treatment of mine drainage (both active and passive systems) and industrial wastewaters. Biodesalination of these wastewaters requires that the sulphur-derived TDS be finally removed from the treated stream and, where this may be recovered as elemental sulphur, a basis for waste beneficiation may be established.

Effective sulphur removal remains a technological bottleneck in the widespread application of sulphur systems biotechnology (Younger, 2002; Coetser, 2004). Initial development of biological processes for oxidation of sulphide to elemental sulphur have been undertaken based on preliminary observations of sulphur biofilm potential made in previous studies undertaken by EBRU for the Innovation Fund and the WRC (Project No.: 1349). A preliminary study on microbial mechanisms underpinning sulphide oxidation in floating sulphur biofilms has also been undertaken in the WRC solicited programme on saline sewage wastewaters (WRC Project No.: 1456).

In a one year study funded by the WRC and in collaboration with Pulles Howard and De Lange (PHD), a 1 m^3 reactor was set up to investigate the potential sulphide

oxidation to elemental sulphur. The findings of this study showed a high potential for floating sulphur biofilm reactor system to be used as a post treatment of sulphate reduction effluent in the treatment of AMD wastewater. The results of this study are reported in WRC Report No.1349.

While these application developments have been on-going it has become apparent that little is known about the mechanisms involved in the formation of sulphur biofilm systems. A shallow knowledge base underpins the SOBR development and optimisation initiatives, and competent mathematical modeling and up-scale engineering of the process, will depend on developing a descriptive model accounting for the microbiological, chemical and biochemical determinants of the system.

1.8. AIMS

Based on this background the aims of the study were identified as follows:

1. Operate laboratory- and pilot-scale model systems in which the formation and productivity of sulphur biofilms may be studied;
2. Undertake investigations to describe the microbial ecology, chemistry and biochemistry of sulphur biofilms;
3. Evaluate appropriate configurations and performance of the Sulphide Oxidising Biofilm Reactor;
4. Support knowledge input and recovery aspects of past studies and concurrent industrial-scale applications of the Sulphide Oxidising Bioreactor
5. Develop a descriptive and explanatory model for the development and productivity of sulphur biofilms.

The aims of the study were carried out by firstly replicating the natural environment in which the floating biofilm were seen to occur on the surface of tannery ponds. For this purpose reactor was set up and fed with effluent from a sulphate reducing reactor to provide the sulphide rich water into the shallow reactor. The depth of the reactor was shallow in order to allow the diffusion of air through the reactor to oxidize the sulphide present in the feed reactor.

Once successful and the biofilm could form repetitively on the surface, microscopy studies were undertaken to investigate the composition of the fating biofilm where crystal-like structures and bacteria were observed. The main element present in the dried biofilm was fond to be sulphur according to X-Ray fluorescence analysis. With a hexadecane: water partitioning test confirming the presence of both organic and biological sulphur species in the dried sulphur samples.

The scanning electron pie – energy dispersive X-Ray technique confirmed the presence of sulphur crystals, of orthorhombic shape and enable further insight into the possible development of these crystals.

The molecular microbiological analyses were undertaken on biofilm samples to identify the different microorganisms present in the biofilm through its development stage from thin through Sticky to Brittle stages of development.

Microsensor studies were used to unravel the microenvironments within the biofilm in relation to the bulk solution and Redox, potential, sulphide and pH gradient in the microenvironment could be measured.

The molecular microbial ecology, structural analysis and the understanding of the microenvironment resulted in the development of a descriptive model for the development of the floating sulphur biofilm inking the microbial activity to function in the floating sulphur biofilm development.

The performance of the channel reactor developed for the production of the floating sulphur biofilm was undertaken under controlled environments at different flow and temperature settings. This was also scaled-up from the initial two-channel to the eight-channel reactor. The biofilm development and sulphide removal efficiency were finally studied on a 1 m^3 floating sulphur biofilm reactor.

The different studies, finding and conclusions are reported in the chapters to follow in this report.

2. THE STRUCTURE OF FLOATING SULPHUR BIOFILMS

2.1 INTRODUCTION

Microorganisms and in particular bacteria have been studied in the laboratory using methods of isolation, culturing in artificial media and enumeration resulting in the discrimination of species that do not respond to the selected culturing media (Hermanowics, 2003). Once isolated the first point of departure has been microscopy involving various staining and plating techniques which, has often created a bias in terms of the representation of populations being investigated (De Beer *et al.*, 1994). As in nature most microorganisms have been found to exist in clusters, aggregates or as a consortium of various species which sometimes complement or compete with each other for survival (Hermanowics, 2003; Bishop, 2003). Biofilms as these aggregates are known have been investigated and reported on as attached to solid surfaces and resulting in corrosion of pipes in AMD treatment plants (Costerton *et al.*, 1995; Hermanowics, 2003). They have been described as systems comprising of heterogeneous bacteria, EPS, pores and channels with mass transport of nutrients and waste taking place in the bulk liquid (Zhang and Bishop, 1994; Santegoeds *et al.*, 1998; De Beer and Schramm, 1999; Bishop, 2003).

Floating biofilms have been observed (Rose, 1996; Dunn, 1998; Jorgensen *et al.*, 1998) and described as formations on an air/liquid interface and ascribed to the presence of the steep Redox gradients found in the air/water interface on the surface of tannery ponds containing sulphidic wastewater (Rose, 1996; Dunn, 1998) without any great detail on their nature and physiological aspects been addressed. Thus, their role is not well defined and also they have not yet been described even in the literature as biofilms.

The observations made by EBRU researchers created an interest in the FSB which enabled preliminary investigations into the possible role these structures could play in wastewater beneficiation. Gilfillan (2000) reported possible structural differentiation while Bowker (2002) revealed the presence of bacterial consortium and Rein (2002) investigated possible process design applications for wastewater beneficiation.

Thus a need arose for further investigation into the structure of the FSB employing different microscopic, spectroscopic and chemical techniques which would provide the initial understanding of the nature and physiological structure of the floating biofilm. This research would also lay a foundation for further studies into the microbial ecology of the floating biofilm and to identify the different bacterial species found to exist within these structures as well to relate them to function and thus investigate possible manipulation and arrive at a process design for wastewater beneficiation.

The objective of the study addressed in this chapter was to study the structure of the FSB with the key aim of determining whether the biofilm was indeed a true biofilm, which is structurally differentiated, as well as to describe the components that comprised this structure.

2.2 MATERIALS AND METHODS

2.2.1 Reactor Development

Reproduction of the FSB under controlled conditions in the laboratory presents challenges particularly relating to the replication of conditions prevailing in the natural environment in which these structures are observed. A process of reactor development was undertaken where a 2 channel reactor (Figure 2.1) was set up outside the laboratory in an attempt to replicate the natural environment where these structures were first observed.

This reactor comprised of two channels with a total surface area of 0.55 m^2 and a total volume of 0.022 m^3 (2.5 m X 0.11 m X 0.04 m) and was fed with lignocellulose-based effluent from the degrading packed bed reactor (DPBR).
The loading rates of 1 309 and 2 618 $L.m^{-2}.d^{-1}$ were used for the feed; these were selected after a series of experiments where the reactor was fed at different flow rates and biofilm formation and inter-harvest recovery periods were monitored.

The first channel was packed with dolorite stones to limit the downward flow of the feed while the second channel was not packed with stones (Figure 2.1). However, a

number of factors including contamination by insects and rain inhibited the successful operation of this reactor and it was taken inside and operated in a controlled environment (CE) room.

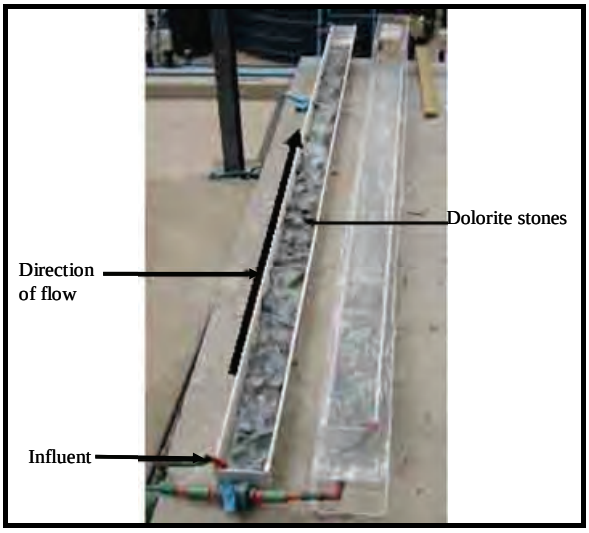

Figure 2. 1. Two-channel reactor operated outside the laboratory in Grahamstown.

Reactor development took place in the CE room and included the evaluation of conventional laboratory flask and STR systems. It was found that a number of factors require careful replication especially the maintenance of a constant Redox and sulphide gradient at the air/water interface. As these conditions could not be reliably reproduced in existing laboratory systems, a number of alternatives were considered of which the Linear Flow Channel Reactor (LFCR) proved effective (Figure 2.2). The LFCR comprised of two channels interconnected to each other and fitted with baffles (spaced at 0.5 meter intervals in the channel). These baffles controlled the flow of the water and prevented rapid mixing which interfered with the maintenance of a constant Redox potential in the channel (Figure 2.3).

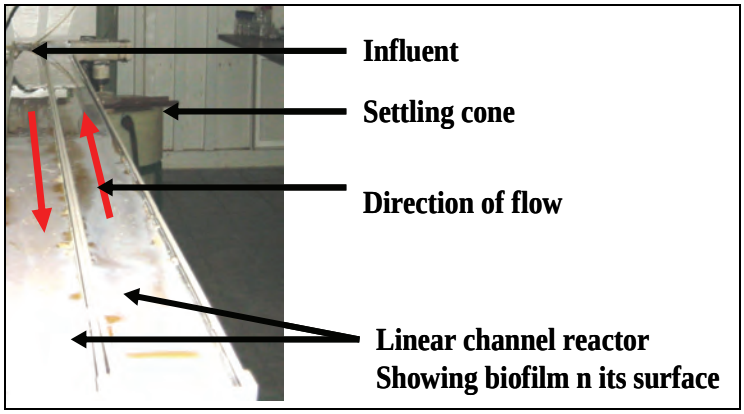

Figure 2. 2. Laminar flow channel reactor operating in the controlled environment room showing the development of a Sticky floating sulphur biofilm on its surface.

The baffles were spaced 0.5 m apart in the channels and were arranged so that the water flowed alternatively over and under the baffles (Fig 2.3).

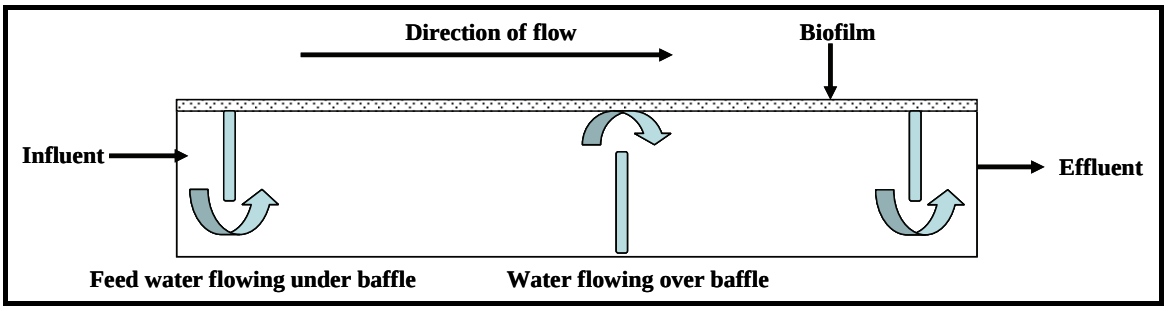

Figure 2. 3. A longitudinal section illustration of the Linear Flow Channel Reactor showing the presence of baffles and the flow of water through the length of the channel.

The feed for the LFCR was drawn from a lignocellulose degrading packed bed reactor (DPBR) as shown in Figure 2.4 and illustrated in Figure 2.5, was fed through the channel reactor at 1 309 and 2 618 $L.m^{-2}.d^{-1}$.

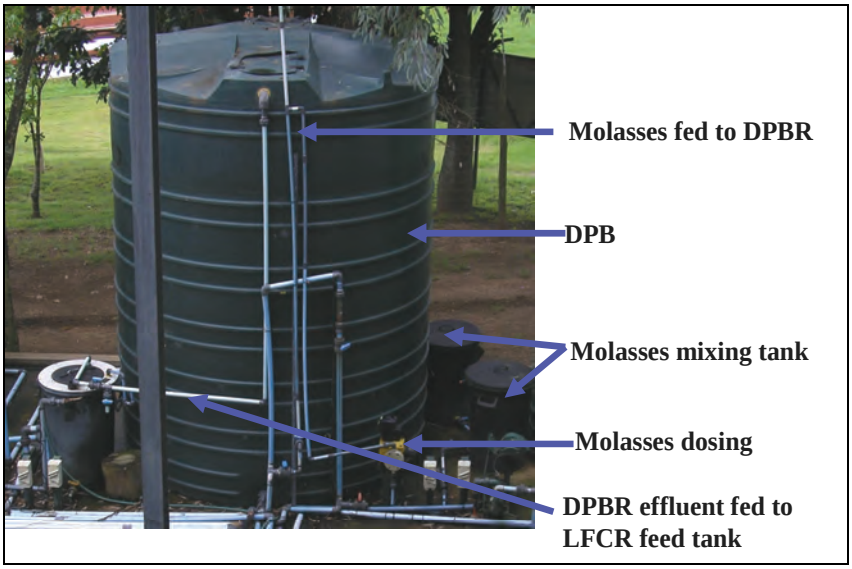

Figure 2. 4. A lignocellulose degrading packed bed reactor used as a generator of sulphide containing feed for the laminar flow channel reactor

The DBPR (Figure 2.4) was packed with various carbon sources including grass cuttings and wood chips which were layered in a sandwich formation as illustrated in Figure 2.5 The bottom of the DPBR was packed with a layer of gravel stone to act as a distribution manifold while preventing the sedimentation of material at the bottom which would result in clogging of the inlet pipe.

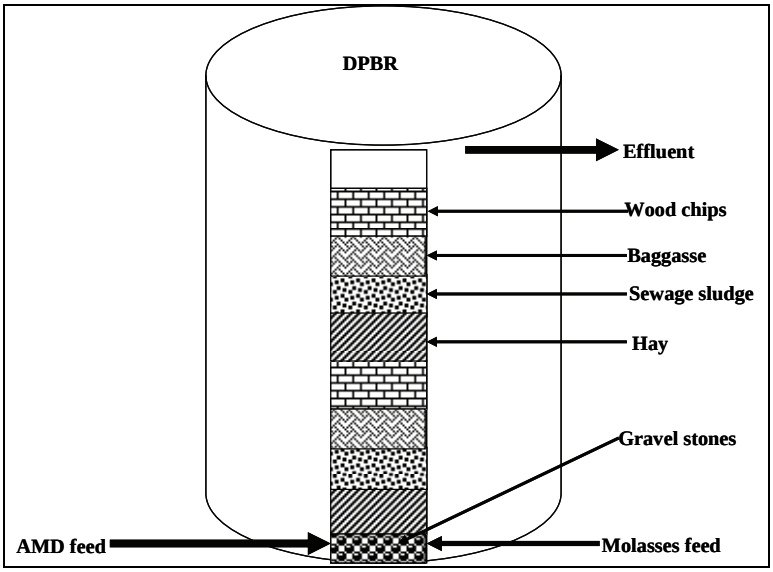

Figure 2. 5. An illustration of the degrading packed bed reactor showing various lignocellulosic carbon materials.

The DPBR was selected for this study as it had been the subject of investigation in a study on the bio-remediation of AMD utilising lignocellulose as a carbon and electron

donor source. This reactor has been patented and provides better sulphate reduction activity in passive AMD treatment compared to the conventional sulphate reduction reactors. (Coetser *et al.*, 2005) This increased activity of the DPBR is ascribed to the continuous dosing with a 0.05% (vol/vol) 'kick-start' carbon (a readily degraded carbon source such a liquid molasses) to the DPBR. This in turn results in the enhanced reduction of sulphate to sulphide and generation of high alkalinity. The high sulphide and alkalinity further contributes to the degradation of lignin in the reactor which otherwise would not have been possible. This has been reported as the major reason for the decline in performance of many passive AMD treatment reactors. The effluent from the DPBR was fed through a hose to the LFCR.

Once the LFCR was filled up with the sulphide-rich influent, it was found that biofilm formation commenced within two hours, forming a Thin and transparent layer on the surface of the water, and appeared to behave in a manner comparable to that observed in the natural environment.

Once operational, the biofilm could be harvested every eight or 24 hours depending on its thickness. This required a number of harvesting trials as the biofilm development stage at the time of harvest determined the product that sedimented to the bottom of the channel. . Initially, the effluent port was shut and the water level in the channel was allowed to rise until the biofilm could float off of the surface into a settling cone (Figure 2.2) where it could be further drained of excess water and dried. However, this resulted in a loss of most of the biofilm making it impossible to calculate a mass balance. The second method entailed disturbing the surface tension of the biofilm by spraying a fine mist of water over the biofilm surface and dislodging the biofilm from the sides of the channel and allowing it to drop to the bottom of the channel.

If harvested around eight hours (Sticky biofilm), the harvested product resembled a fine powder trickling to the bottom of the channel. However, if harvested 12 to 24 hours later, the biofilm resembled long sheaths of white material which dropped to the bottom of the channel reactor until removed manually.

2.2.2 Floating Sulphur Biofilm Formation

During operation of the LFCR it was discovered that the FSB appeared, formed and matured in three distinct stages (Figure 2.6). These were termed “Thin”, “Sticky” and “Brittle” based on the observations of the biofilm consistency.

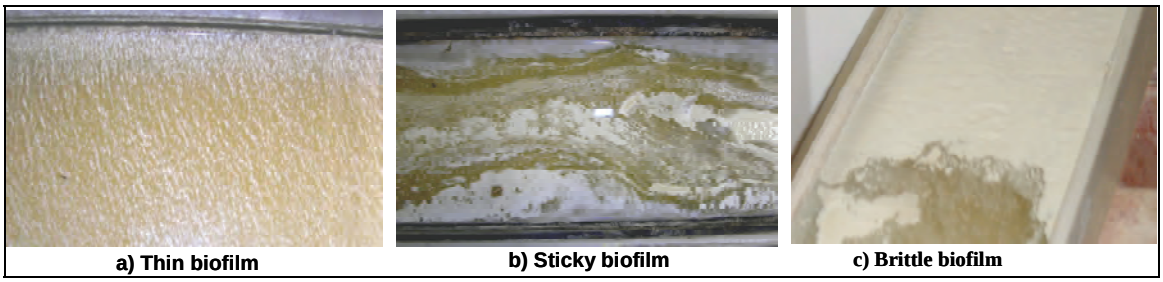

Figure 2. 6. Photographs showing the development stages of the floating sulphur biofilm through the three distinct stages: a) Thin, b) Sticky and c) Brittle.

Once the system was operational the Thin FSB formed as a transparent to slightly opaque layer on the surface of the water after two hours. Between three to eight hours later the biofilm would thicken to form a Sticky structure which was whiter and somewhat slimy and stuck to probes when they were inserted into the water. A further four hours later the Sticky FSB thickened to form a Brittle structure which breaks cleanly when disturbed.

2.2.3 Biofilm Sample Collection

For examination, the FSB was collected at each development stage by lifting on a 0.2µm nylon filter membrane. Figure 2.7 shows a side view of a Brittle biofilm following collection. Although cross-sectional measurement of the Brittle biofilm averaged 50 to 60 µm in spite of the biofilm structure collapsing once it was removed from the water surface.

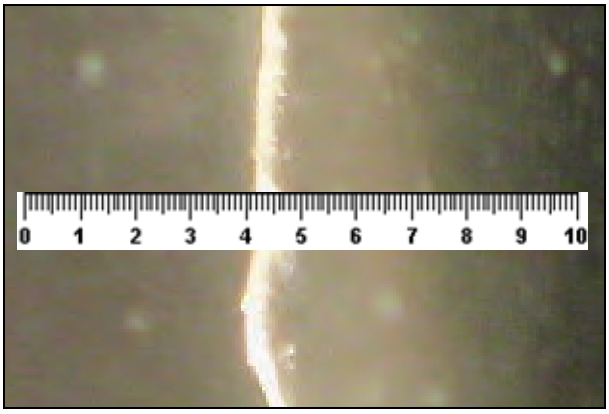

Figure 2. 7. A cross section of the Brittle biofilm viewed under a dissecting microscope (X100 magnification) showing a structure that is 50 to 60 µm thick in its collapsed form.

2.2.4 Microscopy

Samples for light microscopy were heat fixed on microscope slides before examination while those for scanning electron microscopy (SEM) were fixed in 2.5% gluteraldehyde solution in 0.1 m phosphate buffer (pH 7) overnight (Cross, 2000). The harvested biofilm was collected by settling within the reactor at the Brittle stage and at the end of a run the LFCR was drained and the precipitate removed. This was then dried for three to five days at 80^{o}C, and allowed to cool off in the dessicator and then weighed regularly until a stable dry weight was obtained (Figure 2.8). The dried precipitate was used for sulphur determination, spectroscopic analysis and mass balance calculations.

Figure 2. 8. Dried biofilm sample from the collected sediment accumulated at the bottom of the Linear Flow Channel Reactor.

2.2.4.1 Light microscopy

Light microscopy was used to examine the bacteria present in all stages of FSB formation, from Thin to Brittle. Gram staining was used in order to visualize the cells present in the film, (Brock, 1970). Samples were examined on an Olympus BX50 microscope.

2.2.4.2 Scanning electron microscopy

Due to the fragility and thinness of the FSB, a sandwich sampling technique was developed at EBRU (Gilfillan, 2000) to prepare material for SEM examination. This technique involves collecting the biofilm on the surface of a 0.2µm nylon filter and covering it with a similar filter paper. The sandwiched biofilm and filters were then stapled and compressed between copper bookends for examination (Figure 2.9). Figures 2.10 shows a SEM section of the copper bookend-nylon membrane sandwiched biofilm.

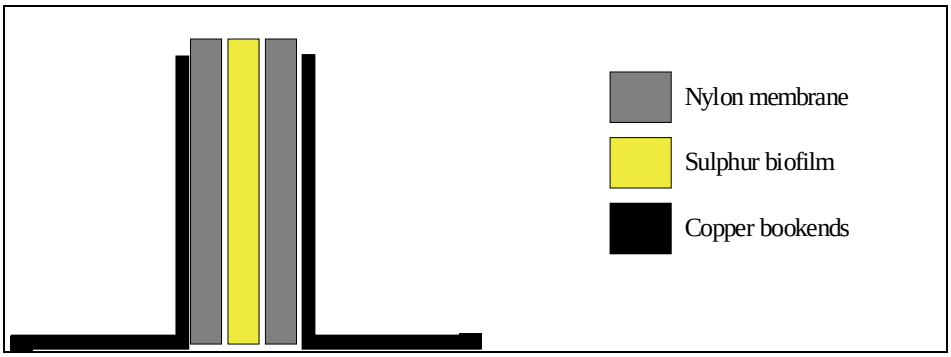

Figure 2. 9. Schematic diagram of "copper bookend" sample positioning system for sectioning samples for scanning electron microscopy studies.

The method of Cross (2000) was followed for SEM sample preparation. The samples fixed in 2.5% gluteraldehyde solution in 0.1 M phosphate buffer (pH 7.0), were washed twice in cold 0.1 M phosphate buffer for 10 minutes and then transferred through an alcohol dehydration series comprising 30, 50, 60, 80 and 90% ethanol for 10 minutes each. This was followed by two 100% ethanol washes of 10 minutes each. The samples were then dried by critical point drying in liquid CO_2 in a Polaron E3000 Critical Drying Apparatus, and sputter-coated with gold in a Polaron E5100 Sputter

Coating Unit. The sample was then inserted into a copper bookend apparatus when it was ready to view. The samples were observed in a JEOL JSM 840 SEM.

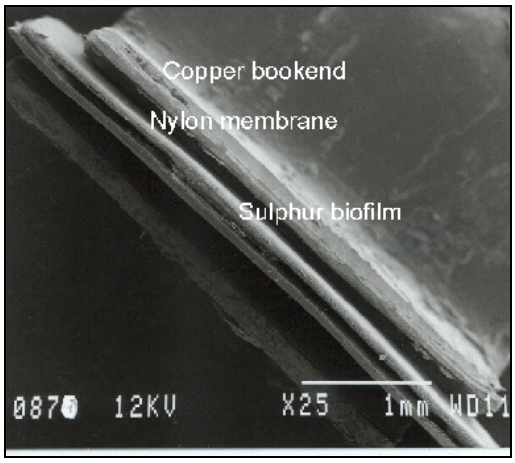

Figure 2. 10. Scanning electron microscopy micrograph of the "copper bookend" sample positioning system for sectioning samples for scanning electron microscopy studies.

2.2.5 X-ray Fluorescence Analysis

X-ray fluorescence (XRF) spectrometry analysis was undertaken using the Phillips PW 480 spectrometer at the Geology department, Rhodes University. A rhodium tube provided as the radioactive source and operated at 40kV and 70 mA. A fine collimator was used with the flow detector. The intensity of the kilo-counts per second (Kcps) at which the sulphur element is present in the sample was measured against the 2 theta degrees ($2\theta^{o}$) related to the lithium fluoride crystal (LiF 220) used.

2.2.6 Determination of Biological Sulphur

A hexadecane-water partitioning test (Janssen *et al.*, 1999) was used to determine the difference of wetting behaviour between biological sulphur and inorganic sulphur, and elemental sulphur. The yellow flowers of the sulphur standard should remain in the upper hexadecane phase while sulphur of a biological origin would become partitioned in the lower water phase. The test is based on the findings of Stuedel (1996) that inorganic elemental sulphur consists of orthorhombic S_8 crystals which have a hydrophobic surface. The hydrophilic character of the biological sulphur results from amphilic compounds covering the hydrophobic S_8 nucleus. These

compounds are long-chain polythionates (SO_3-Sn-SO_3, n=5-20), which can be detected by high pressure liquid chromatography (HPLC) (Steudel, 1989).

A 1:1 mix of water and hexadecane was made up in a test tube to which 0.2 g of the dried FSB and standard flowers of sulphur were added respectively. The test tubes were vortexed for 5 minutes and allowed to stand at room temperature until the layers separated. After separation the separated products were removed from the liquid and solvent and analysed for sulphur. A qualitative analysis of sulphur content was carried out following the modified procedure of Mockel (1984) using reverse phase HPLC.

2.2.7 X-ray Absorption Near-Edge Spectroscopy

Samples for X-ray Absorption Near-Edge (XANES) Spectrometry were sent to Bonn University Institute of Biotechnology where the examination was undertaken by Prof Alexander Prange.

2.2.8 Energy Dispersive X-ray analysis

Sample preparation was similar to SEM method used and then followed by the LEO energy dispersive X-ray (EDX) SEM analysis. Imaging of the samples and analysis of phase composition was undertaken using a LEO® 1430VP SEM (Stellenbosch University). Samples were identified with backscattered electron (BSE) and/or secondary electron images, and phase compositions quantified by EDX analysis using an Oxford Instruments 133KeV detector and Oxford INCA software. Beam conditions used during the quantitative analyses were 20 KV and approximately 1.5 nA, with a working distance of 13 mm and a specimen beam current of -3.92 nA. Despite the relatively low energy of the beam, X-ray counts with the set-up used were typically ~ 5000 cps. The counting time was 50 seconds live-time. Natural mineral standards were used for standardization and verification of the analyses. Pure Co, as well as Ti and Fe in ilmenite were used periodically to correct for detector drift. Beam conditions during semi-quantitative analyses, when used in the case of unpolished samples, were as described above and specimen beam current was not controlled and the results were normalised to100 wt%.

2.3 RESULTS AND DISCUSSION

2.3.1. Light Microscopy

The following figures show fairly typical changes as the biofilm progresses from Thin to Brittle stages. The Thin FSB showed the presence of long-chain Gram-positive streptococcal forms within large numbers of Gram-negative cocci (Figure 2.11).

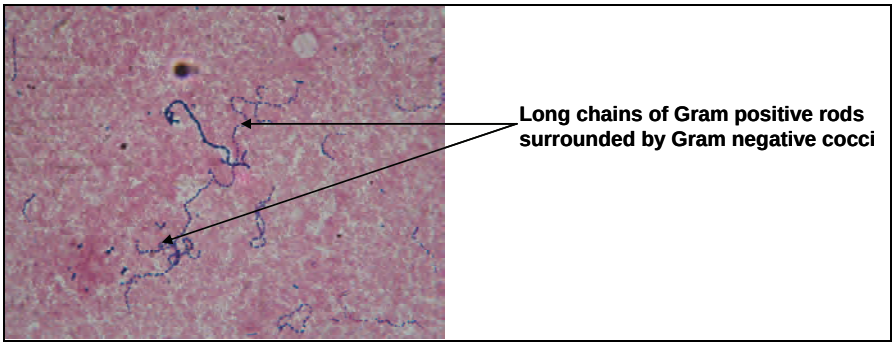

Figure 2. 11. A Gram stain of the Thin stage of the floating sulphur biofilm development showing long chains of Gram-positive streptococcal forms surrounded by Gram-negative cocci (1000X magnification).

As the biofilm developed through the Thin-Sticky form, Gram-positive streptococcal chains became less numerous and Gram-negative cocci predominated (Figure 2.12). Although repeatedly observed, no functional reason could be established for these changes.

Also present were Gram-negative inclusion bodies which could not be further examined with light microscopy (Figure 2.13).

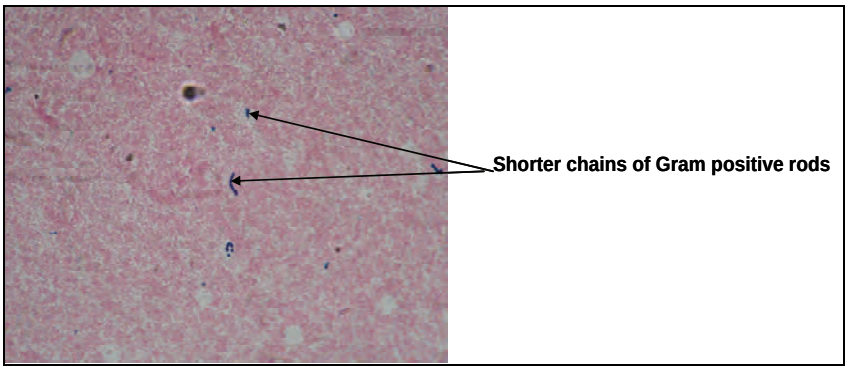

Figure 2. 12. A Gram stain of the Thin to Sticky stage of floating sulphur biofilm development showing some Gram-negative cocci and rods and numerous Gram-positive coccal forms under oil immersion (1000x magnification).

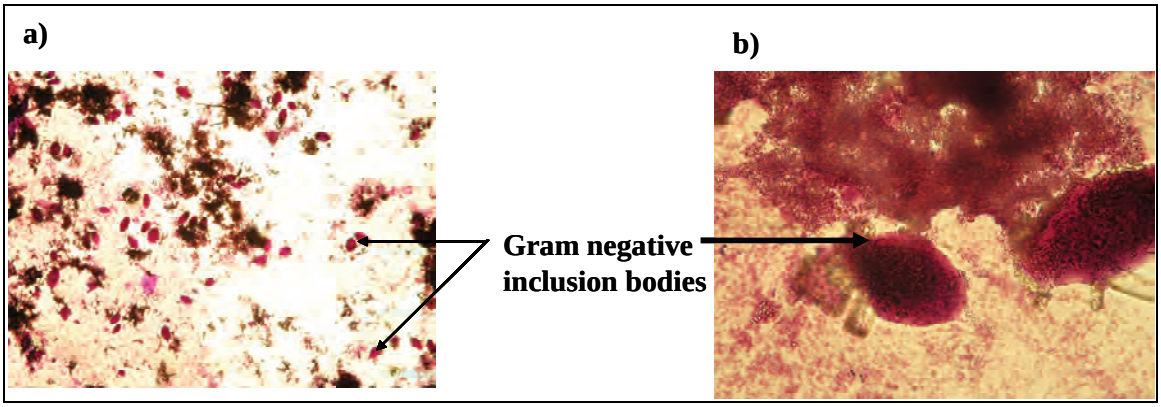

Figure 2. 13. A Gram stain of the Thin to Sticky showing the presence of Gram-negative inclusion bodies: a) 20X magnification; b) 80X magnification.

The Brittle biofilm showed the presence of inclusion bodies and refractive granules which at this stage could only be speculated to be sulphur.

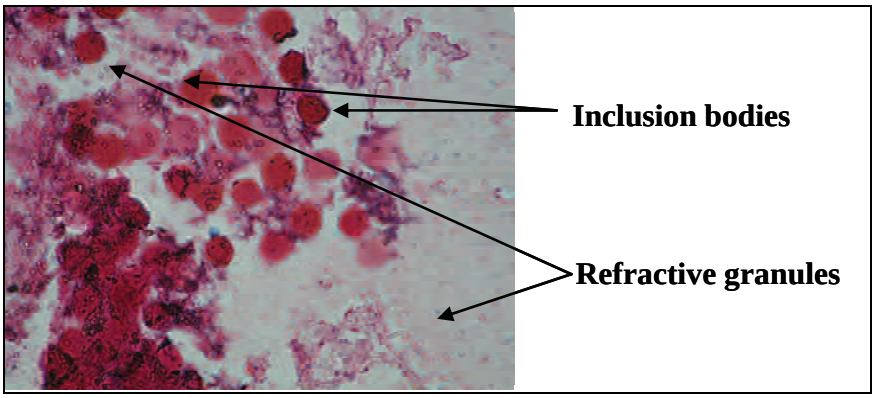

Figure 2. 14. Gram stain of Brittle biofilm showing Gram-negative inclusion bodies surrounded by refractive granules (1000X magnification under oil immersion).

2.3.2 Scanning Electron Microscopy

SEM was carried out on FSB samples from the three distinct stages in order to gain more insight into the mechanisms of formation and how the FSB development ensues. Figure 2.15 shows a mass of cocci and rods in the Thin biofilm development stage.

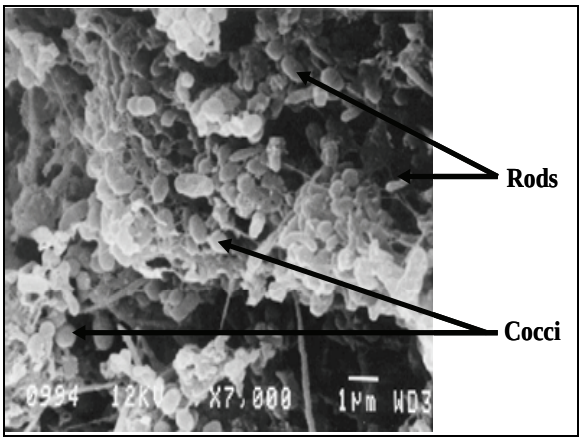

Figure 2. 15. Scanning electron microscopy micrograph of the Thin biofilm development stage showing the presence of cocci and rods.

As the biofilm progresses to Sticky, rods became far more numerous than cocci (Figure 2.16). Channels and pores for mass transfer were identified as were and refractive bodies which were speculated to be elemental sulphur.

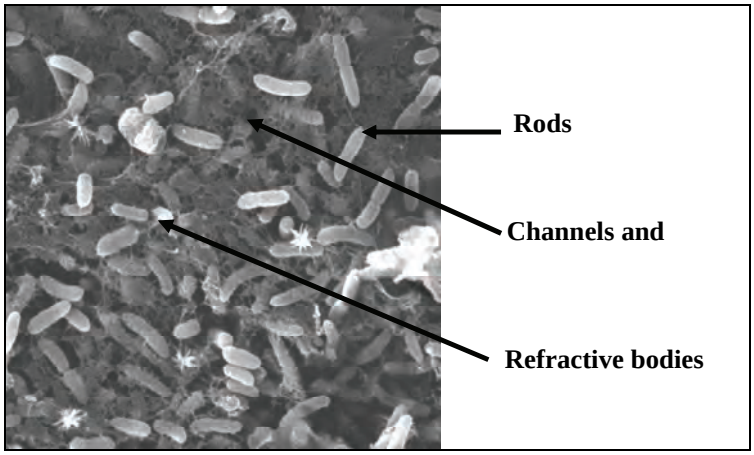

Figure 2. 16. Scanning electron microscopy micrograph of the Sticky biofilm showing the numerous rods, the appearance of refractive granules as well as channels and pores for mass transfer.

Also present in the Sticky biofilm were traces of EPS holding the bacteria and putative sulphur crystals together. A ruptured inclusion body was found to contain a mass of bacteria (Figure 2.17). A number of observations were made on the Brittle biofilm including the presence of numerous crystals which appeared to extend out of the biofilm into the bulk liquid (Figure 2.18a). At closer inspection, small, medium and large crystals were observed, possibly that of sulphur due to the almost orthorhombic shape of the large crystal (Figure 2.18b). This was later confirmed to be sulphur by EDX.

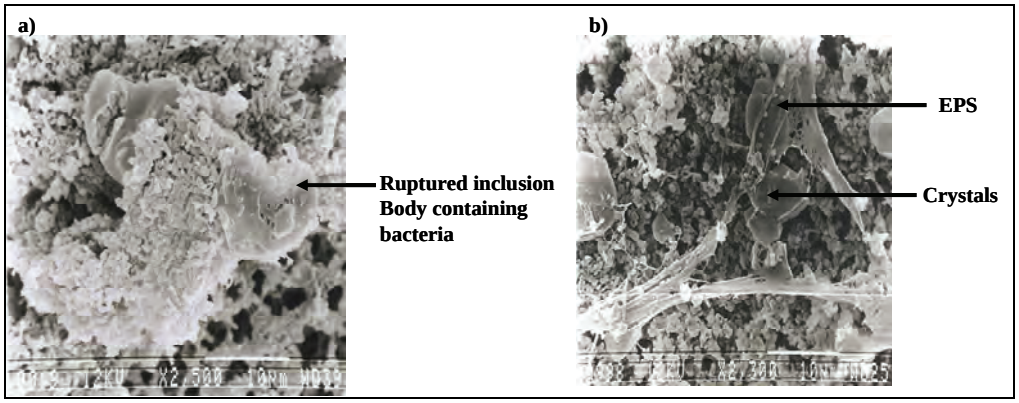

Figure 2. 17. Scanning electron microscopy micrographs of the Sticky biofilm stage showing: a) a ruptured inclusion body containing bacterial mass and b) EPS binding bacteria and crystals together.

There was evidence of EPS binding the mass of bacteria and crystals together (Figure 2.18c). Also visible in Figure 2.18c were what seemed to be a vibroid bacterium known to extrude biological sulphur on its surface (blue arrow) as well as possible

biological sulphur globule (red arrow). Closer inspection of what the latter in Figure 2.18c, revealed a refractive crystal-like material (Figure 2.18d). The small size of the globule suggested that it could not be a bacterial coccus. There were sightings of a number of protozoa (Figure 2.18e) whose roles were speculated to be that of grazers on the biofilm and/or bacteria. The ingestion of bacteria is suggested in the close up of a ruptured protozoan (Figure 2.18f). Figure 2.19 shows the presence of more bright globules thought to be biological sulphur.

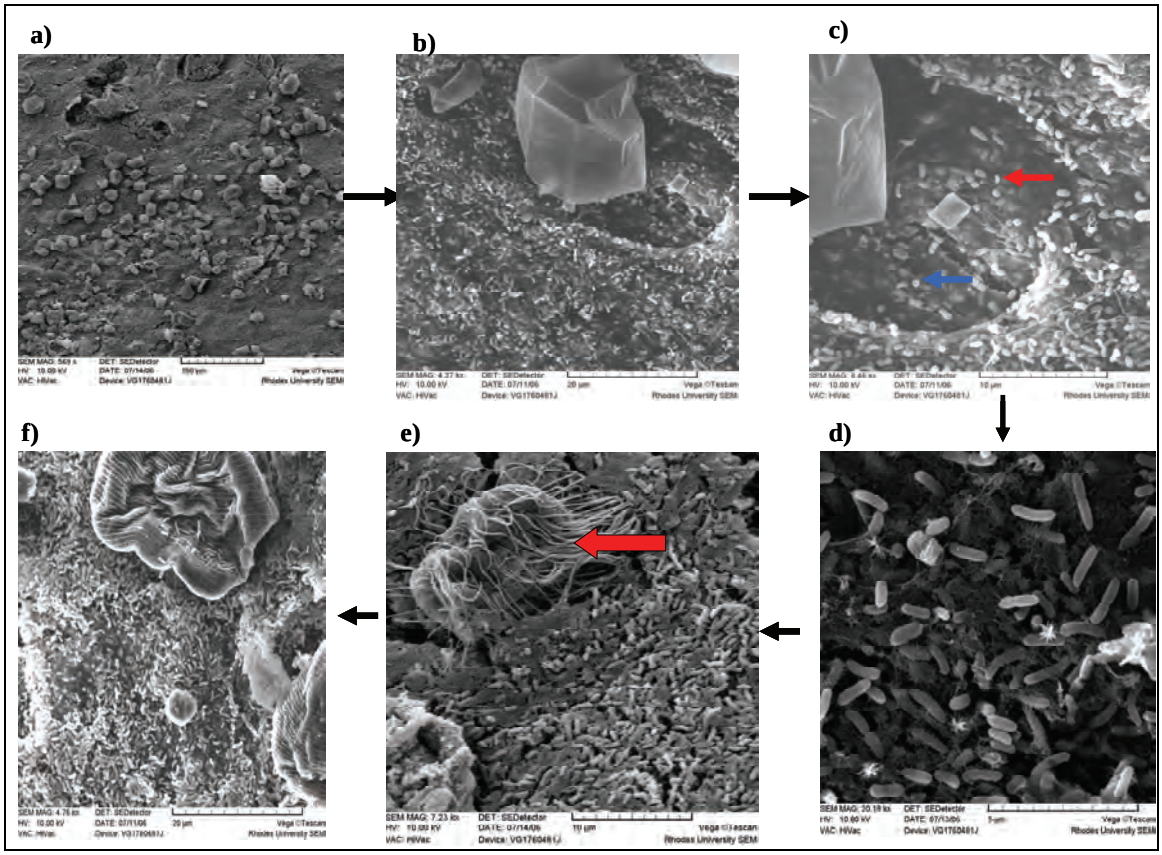

Figure 2. 18. Scanning electron microscopy micrographs of the Brittle biofilm development stage showing: a) presence of a mass of crystals; b) different sizes of crystals including large orthorhombic crystals; c) bacteria and crystals held together by mass of EPS, a possible vibroid bacterium (red arrow) and possible biological sulphur globule (blue arrow); d) a closer inspection of the possible biological sulphur globule was not possible as the structure was too small to focus on however some refractive structures were visible; e) protozoa were identified on the biofilm; f) a closer inspection at a ruptured protozoan revealed a mass of ingested bacteria.

Small crystals were observed to originate from within the bacterial EPS matrix of the biofilm while the large crystals appeared to be extruded from the biofilm and deposited on the outside of the structure (Figure 2.20).

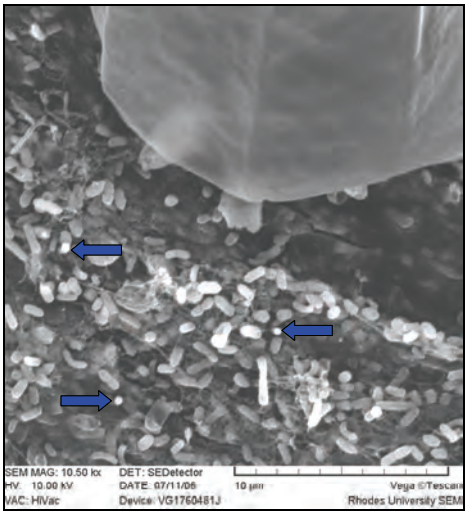

Figure 2. 19. Scanning electron microscopy micrograph of the Brittle biofilm showing a number of external globules (indicated with blue arrows) visible in close proximity to the large crystal.

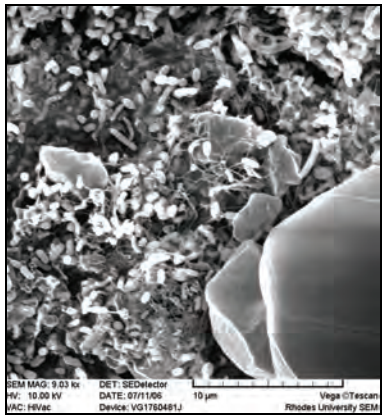

Figure 2. 20. Scanning Electron Micrograph of the Brittle biofilm showing smaller crystals firmly embedded within the EPS matrix while the bigger crystals are protruding of the biofilm.

Apart from the crystals and bacterial mass, there were large structures containing inclusion bodies which were held together by EPS Channels and pores are also clearly visible (Figure 2.21)

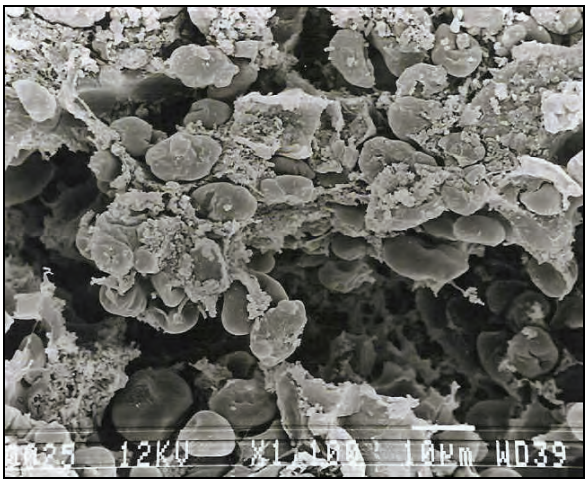

Figure 2. 21. Scanning electron microscopy micrograph of the Brittle biofilm showing a number of inclusion bodies held together by EPS as well as channels and pores for mass transfer.

2.3.3 X-Ray Fluorescence Spectroscopy

Although the SEM suggested the presence of sulphur in the biofilm, XRF was used to confirm these observations quantitatively. Figure 2.22 shows a XRF spectrum of the dried Brittle biofilm product confirming the presence of sulphur which was detected at peaks Kβ at 70.28^{o} and the Kα at 75.85^{o}. Although sulphur was detected by XRF as a dominant element in the biofilm, the form in which the sulphur occurred could not be determined using this method as it cannot differentiate between oxidation states nor distinguish biological from inorganic forms.

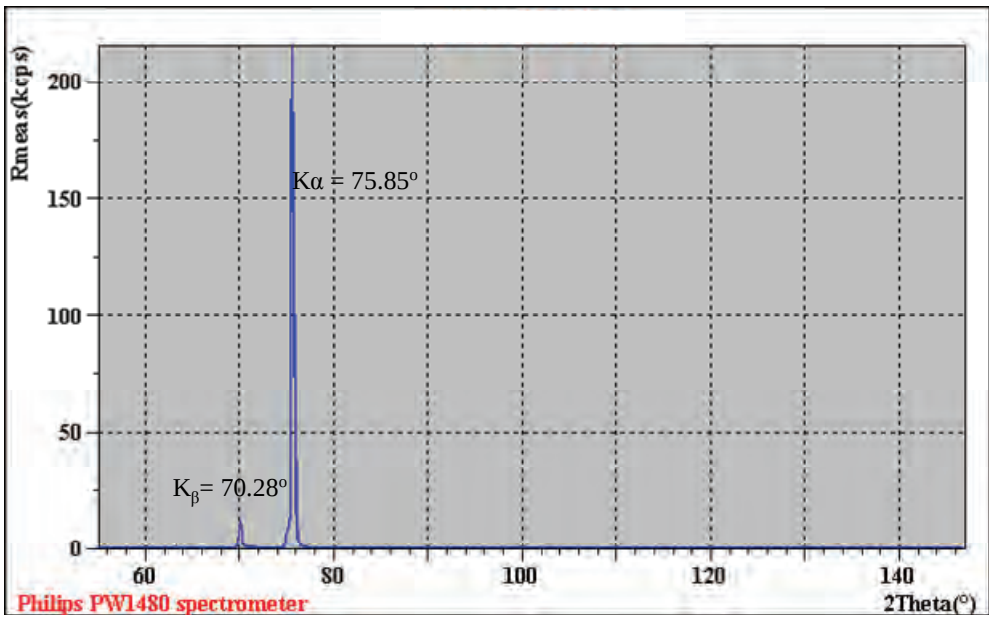

Figure 2. 22. An X-ray fluorescence spectrum of the dried Brittle stage of the floating sulphur biofilm showing the presence of the dominant sulphur peaks Kβ at 70.28° and the Kα at 75.85°.

2.3.4 Biological Sulphur Analysis

The water-hexadecane test was undertaken to determine the presence of biological and/or inorganic sulphur in the biofilm. This showed that the dried Brittle stage of the FSB contained both a standard (inorganic, S_8) form which partitioned at the meniscus in the hexadecane phase and a biological (organic) form that settled at the bottom of the test tube in the water phase (Figure 2.23). These results indicated the possible presence of more than one sulphur formation mechanism active in the biofilm. The partitioned products were further confirmed to be sulphur using reverse phase HPLC.

According to Steudel (1996) elemental sulphur produced by bacteria should be called "hydrophilic sulphur" in order to emphasize the difference between bacterial sulphur and other types of elemental sulphur. The sulphur produced by bacteria is hydrophilic and differs from elemental sulphur which is hydrophobic and has a solubility factor in water of only 5 $g.kg^{-1}$ (Hazeu *et al.*, 1988). Biological sulphur is pale yellow or white and forms spherical globules able to dissolve in organic solvents (Janssen *et al.*, 1998) and has been classified as liquid-like according to X-ray diffraction, although it does convert to crystalline S_8 when allowed to stand or when dried (Janssen *et al.*, 1998).

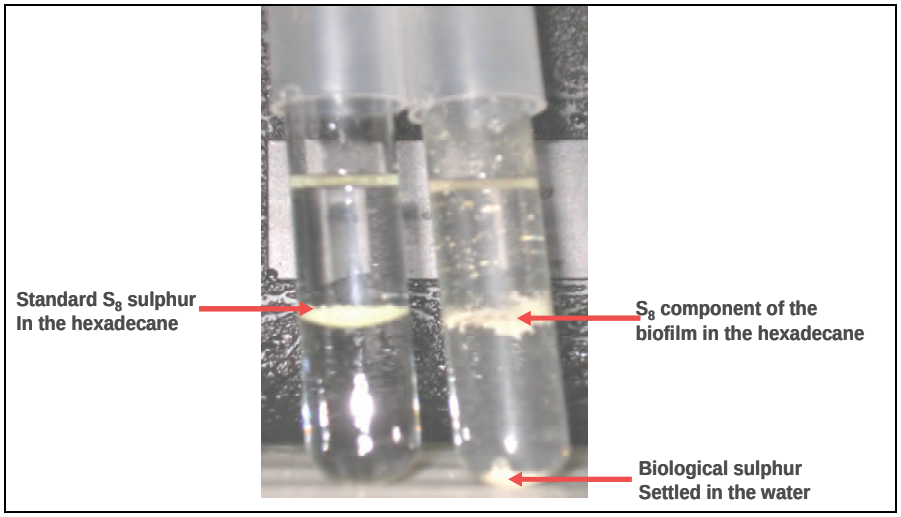

Figure 2. 23. A photograph showing a hexadecane sulphur test where the left test tube shows the standard sulphur control and on the right is the dried floating sulphur biofilm material.

2.3.5 X-Ray Absorption Near Edge Spectroscopy

The XANES results (Figure 2.24) showed that the dried samples consisted of long chain polysulphide with no S_8-rings detected while the wet sample consisted of two sulphur atoms in the zero valence, probably as polysulphide chains and not S_8-rings. There was also a component with a valence below zero, associated with H_2S and an additional presence of a higher oxidised sulphur component associated with SO_2.

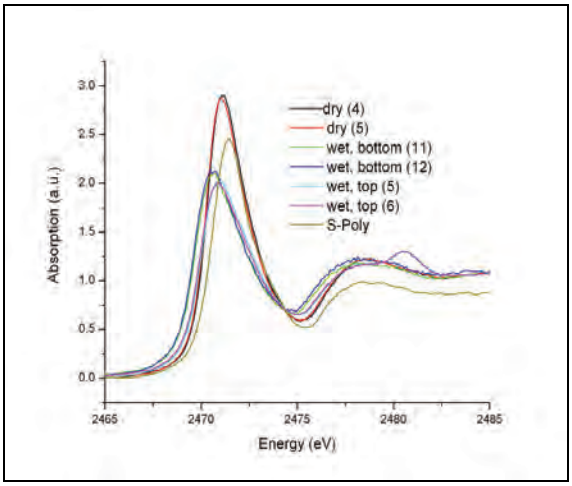

Figure 2. 24. X-ray absorption near-edge spectroscopy spectrum of floating sulphur biofilm material showing tested samples falling at the polysulphide peak.

2.3.6 Scanning Electron Microscopy – Energy Dispersive X-Ray Spectroscopy

The presence of sulphur in the biofilm was confirmed with both biological (organic) and inorganic species probably present. Although initial EM showed crystals, these could only be provisionally identified as sulphur. Further SEM-EDX studies were undertaken to confirm the identity of the crystal-like structures and to expand on an understanding of the distribution of the biological and inorganic sulphur species in the floating biofilm system.

An EDX dot scan on a small part of the outer surface of a large crystal indicated the crystal to contain 100% sulphur (Figure 2.25). There was a gold (Au) peak detected as a result of the gold coating used during SEM sample preparation.

However, scanning small crystals and large area scans of large crystals showed increasing amounts of carbon and oxygen to be present. Figure 2.26 is a dot scan on a small crystal and revealed 39% sulphur and 59% carbon.

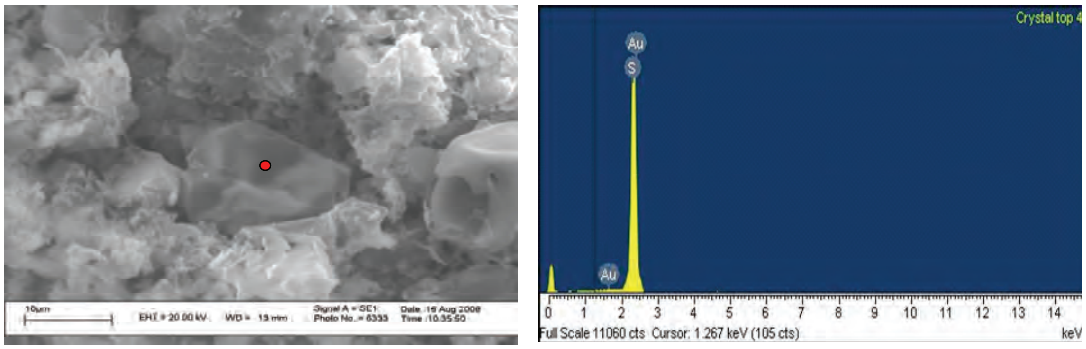

Figure 2. 25. Scanning electron microscopy micrograph and energy dispersive X-ray spectrum of a crystal from the Brittle floating sulphur biofilm (spot area indicated in red). (S=100%).

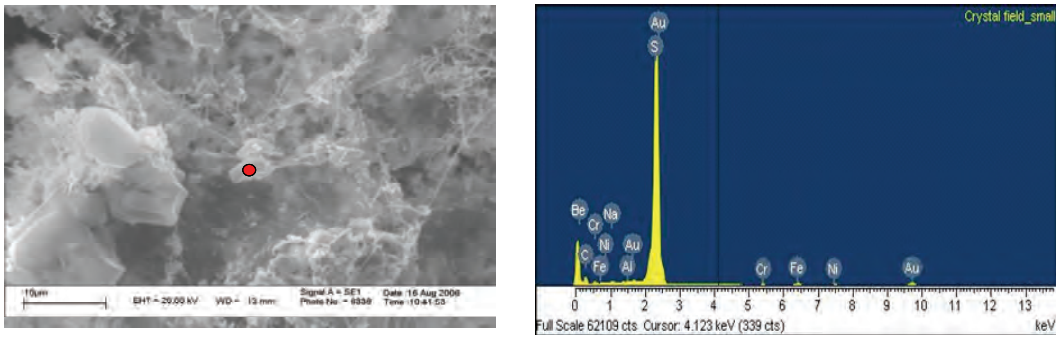

Figure 2. 26. A scanning electron microscopy micrograph and energy dispersive X-ray spectrum of the small sulphur crystal (spot area indicated in red). (C=58.6%, Na=0.342%, Al=0.106%, S=38.85%, Cr=0.124%, Fe=1.247%, Ni=0.698%).

A large scan on a large crystal (Figure 2.27) showed 68% sulphur, 26% carbon and 5% oxygen.

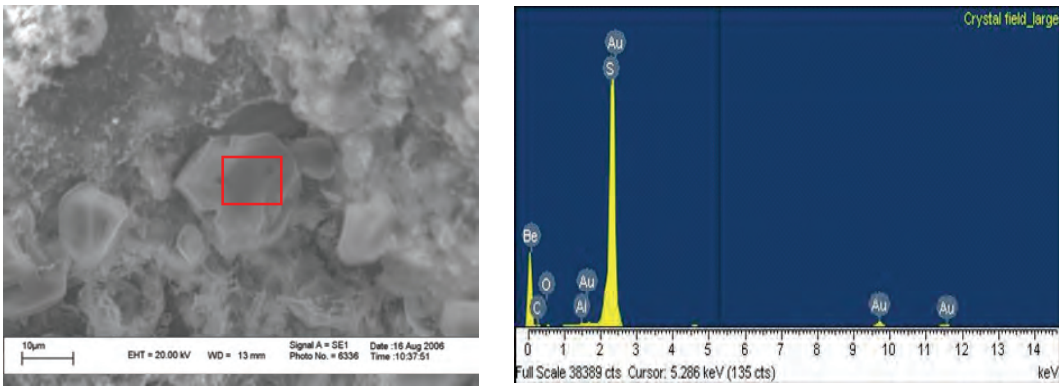

Figure 2. 27. A scanning electron microscopy micrograph and energy dispersive X-ray spectrum of a large sulphur crystal (scan area indicated in red). (C=25.8%, O=5.23%, Al=0.185%, S=67.79%).

A large scan on a small crystal (Figure 2.28) showed a 45% sulphur, 47% carbon and 7% oxygen.

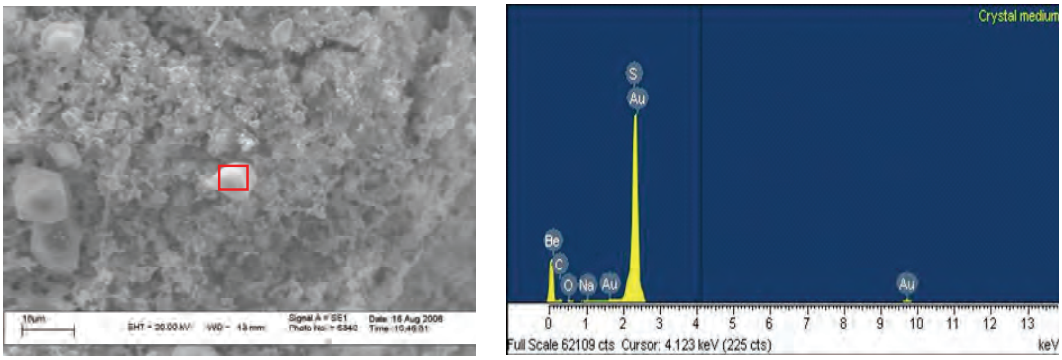

Figure 2. 28. A scanning electron microscopy micrograph and energy dispersive X-ray spectrum of the scanned area of the medium crystal. (C=47.4%, O=7.2%, Na=0.25%, S=45.16%).

The above results indicate a possibility of organic carbon sheath or film covering the surface of the crystal. This was investigated by performing a dot scan on the surface of a large crystal, then burning the same area by performing a square scan after which a second dot scan was performed on the burnt area. The results presented in Figures 2.30 to 2.32 show the results obtained for this investigation. The initial dot scan (Figure 2.29) showed 34% sulphur, 59% carbon and 6% oxygen.

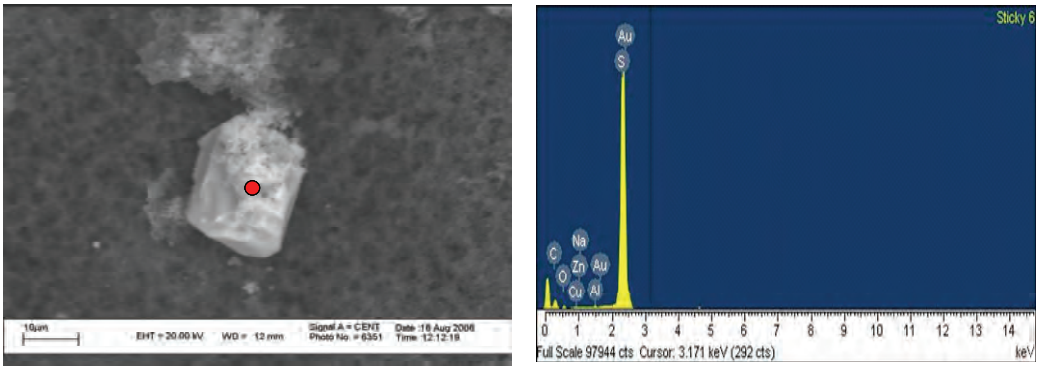

Figure 2. 29. A scanning electron microscopy micrograph and energy dispersive X-ray spectrum of a dot scan on a large sulphur crystal from the Sticky floating sulphur biofilm. (C=58.6%, O=5.311%, Na=0.076%, Al=0.042%, S=34.36%, Cu=0.378%, Zn=0.233%).

When performing a square scan to burn the outer surface of the crystal (Figure 2.30), the sulphur content increased to 44%, carbon decreased to 49% and the oxygen decreased to 5.8%.

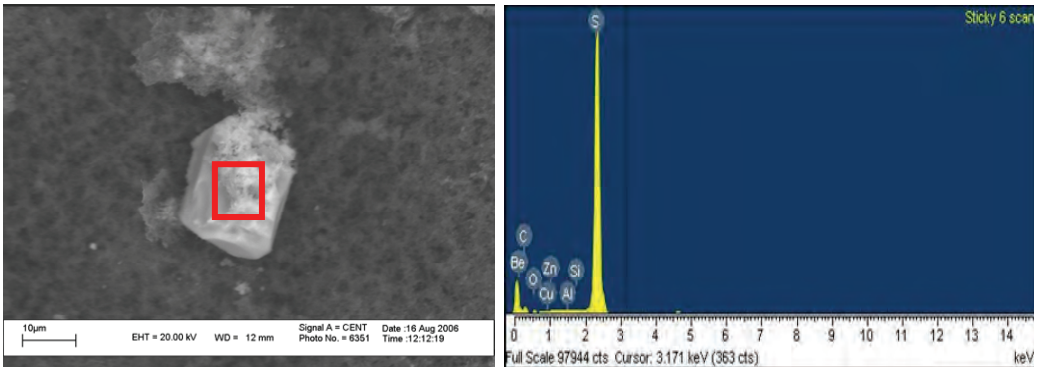

Figure 2. 30. A scanning electron microscopy micrograph and energy dispersive X-ray spectrum of a square scan used to burn off the surface of a large sulphur crystal from the Sticky floating sulphur biofilm. (C=48.9%, O=5.8%, Na=0.076%, Al=0.042%, S=44.3%, Cu=0.378%, Zn=0.233%).

A second dot scan carried out after the crystal surface was burnt off (Figure 2.31) confirmed that there was an organic sheath on the surface of the crystal as no carbon

was measured while the sulphur content measured 95% and oxygen further decreased to 3.2%

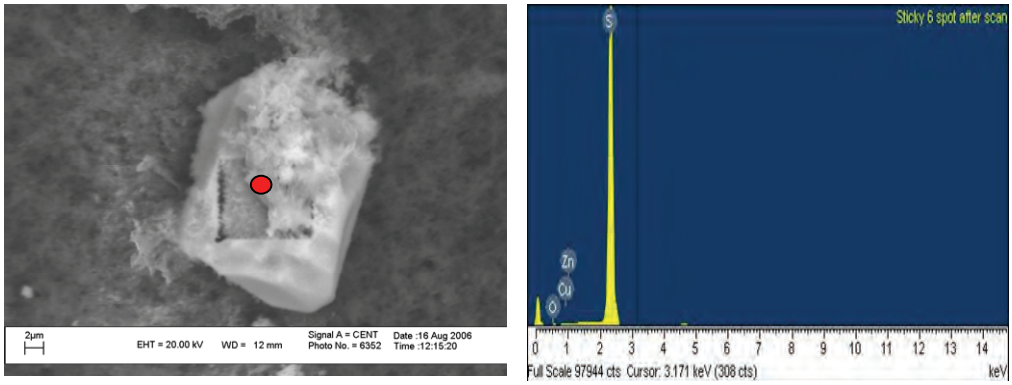

Figure 2. 31. A scanning electron microscopy micrograph and energy dispersive X-ray spectrum of a dot scan on the burnt surface of a crystal from the Sticky floating sulphur biofilm. The scan area is visibly damaged from the X-ray. (O=3.16%, S=95.2%, Cu=0.93%, Zn=0.71%; C= 0).

These results confirm that the organic film over the crystal may account for the biological/inorganic species partition results of the hexadecane extraction. However, the question remains whether the refractory globules are also sulphur and whether sulphur is present in other parts of the biofilm. SEM-EDX could not be performed on the refractive globule structures due to a size constraint. However, scanning the biofilm matrix a distance away from the crystals showed that sulphur is fairly evenly spread across the biofilm although the concentration is much lower away from the proximity of the crystals. Figure 2.32 is an EDX scan of the EPS matrix at a lower magnification with 10% sulphur, 73% carbon and 16% oxygen.

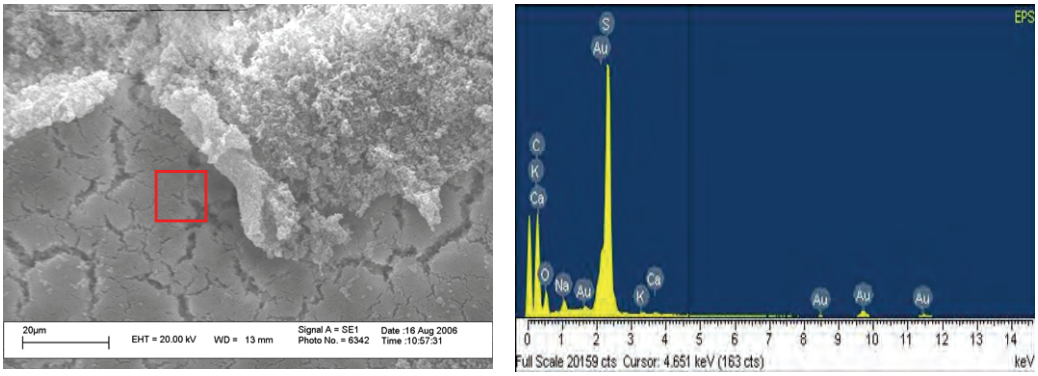

Figure 2.32. A scanning electron microscopy micrograph and energy dispersive X-ray spectrum of EPS. (C=72.8%, O=15.7%, Na=0.76%, S=9.45%, K=0.11%, Ca=0.13%).

A higher resolution EPS matrix and bacteria scan (Figure 2.33) indicated that the sulphur content was 26%, carbon 63% and oxygen 11%, indicating that there was sulphur dispersed in the biofilm outside of the crystals. Figures 2.35 and 2.36 further illustrate this observation and show fairly high resolution SEM of a protozoan (potentially mainly carbon and oxygen), nearby crystals, and in the intervening EPS/bacteria matrix.

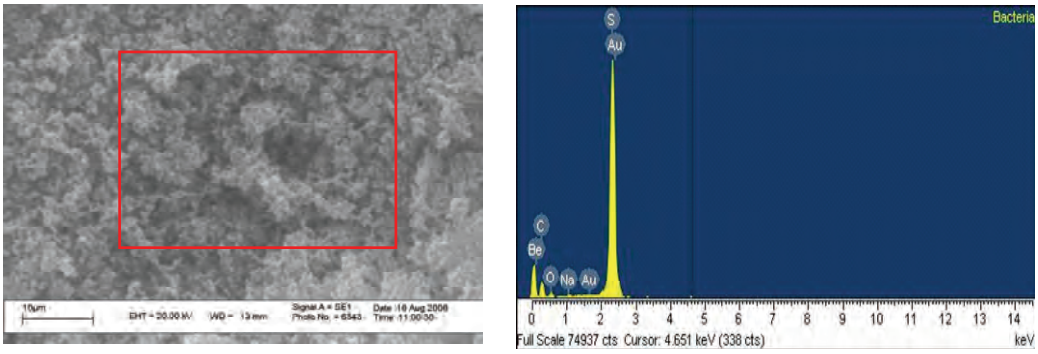

Figure 2. 32(a). Scanning electron microscopy micrograph and energy dispersive X-ray spectrum of an area of the floating sulphur biofilm containing bacteria only. (C=62.65%, O=11.2%, Na=0.3%, S=25.89%).

The EDX scan in Figure 2.34 confirms a high carbon composition around the protozoan of 78%, while sulphur and oxygen is at 14% and 8% respectively.

A carbon content of 78% and sulphur content of 13.5% was detected on a scan of the protozoan (Figure 2.34). These results indicate that there is sulphur present throughout the FSB.

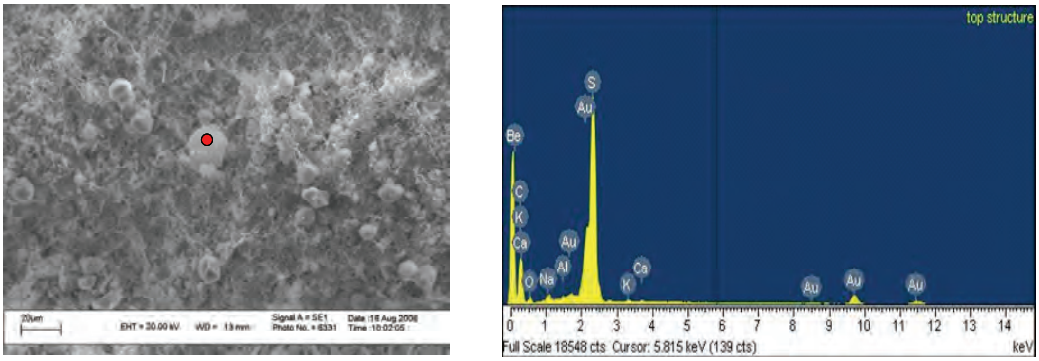

Figure 2. 33. A SEM micrograph and energy dispersive X-ray spectrum of a protozoan. (C=77.6%, O=7.9%, Na=0.58%, Al=0.10%, S=13.5%, K=0.14%, Ca=0.15%).

In Figure 2.35, an area of biofilm containing a protozoan (blue arrow), a crystal (yellow arrow), and mass of EPS/bacteria matrix (Figure 2.35a) was scanned differentially for sulphur (Figure 2.35b) and carbon (Figure 2.35c) separately. The

sulphur scan (Figure 2.35b) shows that sulphur is fairly evenly distributed across the biofilm, although richer in content in the region of a crystal in contrast to the poor sulphur content where in the region occupied by the protozoan. The carbon scan (Figure 2.35c) showed a contrasting picture to the sulphur scan where there main carbon content was observed in the region occupied by the protozoan with much less across the remainder of the biofilm. An important observation made was that there was widespread distribution of sulphur across the EPS/bacteria matrix, more than that of carbon, as would have been expected. This led to the speculation that the widespread distribution was possibly associated with the presence of small sulphur granules which account in part for the biological sulphur present in the system.

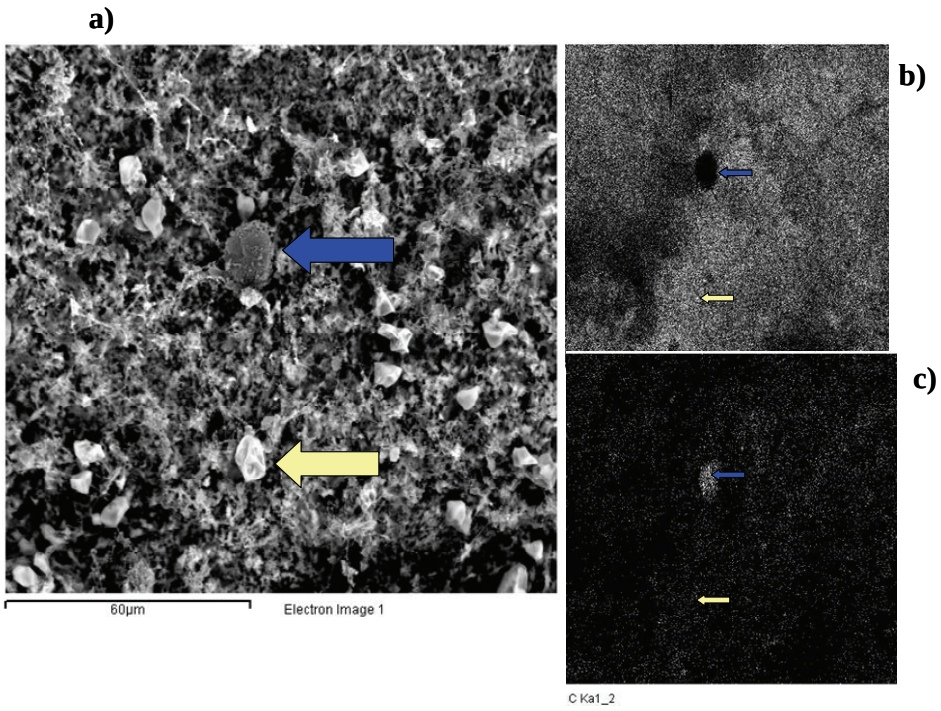

Figure 2. 34. An X-ray Spectrum Map of the area displayed in the scanning electron microscope micrograph (top) showing sulphur content (left) and carbon content (right).

2.4 CONCLUSIONS

The following conclusions were drawn from this study.

- Light microscopy investigation of the structure of the biofilm showed that it was composed, at least in part, of large numbers of bacteria.

- This was confirmed in the SEM studies with the presence of putative sulphur crystal-like structures appearing on the underside surface of the biofilm. This could account for the granular nature of the Brittle biofilm.
- The presence of sulphur in the biofilm was confirmed by XRF spectroscopy and a hexadecane: water partition experiment indicated that both biological and organic sulphur forms may be present in the biofilm.
- The EDX study confirmed that the crystal-like structures observed in the earlier SEM study were indeed sulphur in nature with some covered by a Thin film of organic matter.
- The growth of the crystals within the biofilm is indicated by the size distribution range observed, but not how this may be initiated. In any event this occurs against a background of a complex matrix of bacterial EPS.
- The question to be addressed is how the three stages of biofilm development culminate in sulphur crystal structure formation and produce the granular Brittle film.
- The role of the protozoa grazing on the bacterial/EPS matrix is undefined, but may be possible that they play an important role in the dispersion of small biological sulphur particles in the biofilm through the ingestion and excretion of bacterial extrocellular sulphur globules.

3. MICROBIAL ECOLOGY OF FLOATING SULPHUR BIOFILMS

3.1 INTRODUCTION

Identification and quantification of the members of a particular microbial community, and a clearer understanding of the functional relationships that exist between its members, is required to fully appreciate, and possibly manage, the complex processes that these communities perform in a biofilm (Davey and O'Toole, 2000).

Examination of biofilm communities is complicated by methodological problems in identifying its constituent members *in situ*, in quantifying physical, chemical and spatial distributions and in linking processes and functional activity with specific microorganisms (Hermanowicz, 2003). Therefore, to fully appreciate and understand the processes and activities within a biofilm, it is necessary to unravel the complexity of microbial consortia contributing to the biofilm life.

The application of molecular methods has revolutionized the routine identification of bacteria from environmental and industrial samples task (Amman, 1995; Head *et al.*, 1998; Santegoeds, 1998; Davey and O' Toole, 2000; Wuertz, 2003). Techniques based on the analysis of genetic material are currently used to complement the conventional microbiological approach and to determine the presence and distribution of individual bacterial species, including those in complex communities such as bacterial biofilms (Santegoeds *et al.*, 1998, Wuertz, 2003).

The study reported in the previous Chapter had provided an indication, not only of the possible complexity of the biofilm structure but also suggested that functional differentiation within the microbial population may underpin the various processes that appear to be occurring in the system and leading to biofilm formation.

The objective of the study reported in this chapter was to investigate the suggested functional differentiation by first describing the microbial ecology of the total biofilm

and then to relate the particular populations to possible functions that they may perform within the system.

3.2 MATERIALS AND METHODS

3.2.1 Reactor Development and Sampling

The channel reactor used for biofilm formation was the LFCR described in Chapter 2. The biofilm samples were collected during the three development stages (Thin, Sticky and Brittle) in sterile 1.5 mL microfuge tubes (Eppendorf) and were stored at -20^{o}C before total DNA extraction.

3.2.2 Gradient Tube Method Development

The very small cross section of the biofilm (60 to 120 µm) seemed to indicate that identification of population change distribution at different levels across the biofilm would not be possible. In this regard, method development was undertaken in an attempt to establish a spatial expansion of the biofilm based on factors of physiological distribution. A Gradient Tube system was developed in which the 60 to 120 µm of the biofilm could be spread over a 10cm agarose overlay column in a test tube (Bowker, 2002). This entailed thoroughly mixing a biofilm sample in agarose gel to form the agarose overlay column (Appendix A1), filling 10cm of a column tube, with this seeded agarose gel and thereby establishing an oxygen/sulphide gradient across the agarose column. The gradient tube method developed is shown in Figure 3.1. This was done by locating a sulphide plug (Appendix A1) at the bottom of the tube (sulphide diffusion upwards) and open to atmosphere at the top (oxygen diffusion downwards The test tubes were capped but open to atmosphere in a sterile hood, and an oxygen/sulphide gradient was allowed to establish along the length of the 10 cm agarose overlay column. While it was not possible to measure the gradients *in situ*, given its enclosure in the tube, its presence was assumed from the method that followed. The tubes were incubated for five to eight days until band formation was observed.

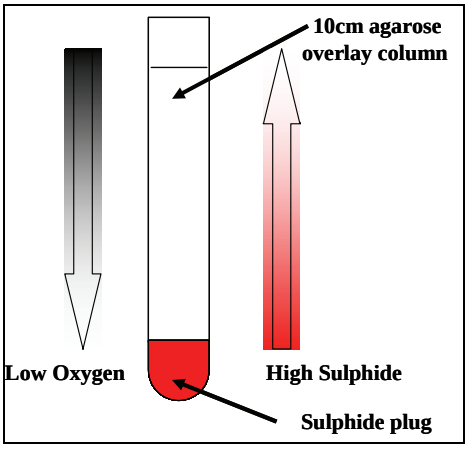

Figure 3. 1. An illustration of the Gradient Tube system in which a sample of the floating biofilm is suspended in a 10 cm agarose overlay column in a test tube. Sulphide diffuses upwards from the sulphide plug in the bottom of the tube and oxygen diffused downwards from its open top**.**

The test tubes containing the agarose and biofilm were incubated in a sterile hood at ambient temperature. Three to eight days after incubation, the formation of bands in the test tubes was observed. After five to eight days the tube was harvested by extracting the agarose overlay column onto a sterile surface and then carefully slicing into 0.5 cm sections. Agarose sections were then treated for DNA extraction, molecular typing and phylogenetic analysis using techniques described below. Once method development was completed, Gradient Tubes were prepared using floating biofilm samples collected at each of the three distinct stages of development (Thin, Sticky and Brittle). The experiment was conducted in triplicate at each stage.

3.2.3 Molecular Typing and Phylogenetic Analysis

Molecular typing was undertaken on each of the Gradient Tube sectioned samples, and on the composite biofilm sample collected at each of the three stages of biofilm development. Before harvesting, the base of the test tube was broken carefully while maintaining the integrity of the contents. The agarose overlay column was then extruded and the samples cut into 0.5 cm sections and collected in sterile 1.5 mL microfuge tubes and stored at -20 ^{o}C.

3.2.4 DNA Extraction

The total DNA extraction method according to Sambrook *et al.* (1989) was applied to the different biofilm bands formed in the Gradient Tubes and composite biofilm samples were collected at each stage of development. The first step involved placing the samples at 55^{o}C in a water bath (Labcon) to melt the agarose gel. Glass beads were added to the samples before vigorous shaking on a vortex Genie-2 (Scientific Industries). The samples were then collected in 1.5 mL microfuge tubes (Eppendorf, Merck®), concentrated by centrifugation at 13 000 rpm for five minutes in an Eppendorf 5415D desktop centrifuge. The pellet was washed with 500 µL of 2 x TE (Tris/EDTA) buffer pH 8.0 (Appendix A-3). The pellet was re-suspended in 500 µL of 2X TE buffer.

The sample was further lysed by adding 6 µL of a 50 µL/mL lysozyme (Appendix A) enzyme and a 25 µL of a 10% sodium dodecyl sulphate (SDS) detergent (Appendix A). The sample was incubated in a Labcon incubator at 37^{o}C for three hours, followed by five cycles of one minute freezing and one minute thawing in liquid nitrogen and boiling water respectively. An aliquot of 100 µl of 10% cetyltrimethylammonium bromide (CTAB) and 200 µl of 5 m sodium chloride (NaCl) were added to the samples followed by one hour shaking incubation at 55 ºC.

Each of the samples was aliquoted into 500 µL volumes in sterile 1.5 mL Eppendorf microfuge tubes and the cell lysate was extracted with an equal volume of phenol, vortexed and centrifuged at 13 000 rpm for two minutes. The upper aqueous layer was collected and extracted in an equal volume of phenol: chloroform: isoamyl alcohol (24:24:1) (Appendix A), vortexed and centrifuged at 13 000 rpm for two minutes. This was repeated until the pink colour was removed from the aqueous layer.

Nucleic acids were precipitated with 2.5 volumes of ice cold 96% rectified ethanol overnight at -20°C. The DNA was concentrated by centrifugation on an Eppendorf model 5810R desktop centrifuge at 4^{o}C for 25 minutes and re-suspended in 20 µL TE buffer. A 10 µL aliquot of each DNA was stored at 4 ºC for immediate use and short-term storage, while the remainder was stored at -20 ^{o}C. The DNA was electrophoresed

on a 0.8% agarose gel (Appendix A) containing 100 µL of ethidium bromide (Appendix A). A λ Pst1 molecular weight marker (Appendix A) was used to check the molecular weight of the product.

3.2.5 Polymerase Chain Reaction

The PCR reaction was performed using universal 16S primer GM5F (Appendix A) and a GC clamped primer 907R (Appendix A) from Inqaba biotech. The enzyme used was Taq DNA polymerase (Promega) at a concentration of 0.5µL per 25 µL reaction. A 2.5 µL aliquot of buffer containing magnesium chloride ($MgCl_2$) was added per 25 µL reaction (Appendix A). In cases where the $MgCl_2$ concentration was adjusted, 2.5 µL of buffer without $MgCl_2$ was added per 25 µL reaction and the volume of water added adjusted accordingly to give a final volume of 25 µL. Each of the four deoxynucleoside triphosphates (dNTPs) was added to a final concentration of 1 µL per 25 µL reaction. The dNTPs were from Inqaba biotech. The reaction was made up to 25 µL with a calculated volume of autoclaved pure water (Sigma).

Amplification was performed on a Hybaid PCR Sprint thermocycler using a touch-down PCR procedure (Table 3.1). The PCR product was analyzed on 1% agarose gel containing ethidium bromide and visualized on a UV transilluminator (UVP BioDoc-It™ system) fitted with a digital camera. Bands were cut out from the gel and purified using QIAprep® spin miniprep Kit (Qiagen).

3.2.6 Denaturing Gradient Gel Electrophoresis

DGGE method according to Myers *et al.,* (1987) was applied for the high probability detection of any differences between two sequences. The technique was based on the reduction in DNA fragment mobility in a dense medium when part of the double helix unravels. Strand separation was induced by using different concentrations of the denaturants formamide and urea made up to 50 mL (Appendix A).

For the purpose of this study, the DGGE gels used a 55 to 65% denaturant gradient prepared from the 100% denaturant stock. The gradient increased from the top to the bottom of the gel, parallel to the direction of electrophoresis. During electrophoresis

the chemical denaturants induced strand separation of the DNA fragments, while the high temperature 65^{o}C melted the DNA fragments for easier separation. The fragments were analysed on a 6% acrylamide gel (Appendix A) from Sigma-Aldrich. The gradient was prepared in a BIORAD Model 385 gradient former.

Table 3. 1. Touch-down programme used for PCR amplification**.**

Reaction	**Temperature**	**Duration**	**No of cycles**
Initial Denaturation	95ºC	2 minutes	1 cycle
Denaturation	94ºC	30 seconds	4 cycles
Annealing	68ºC	45 seconds	
Extension	72ºC	2 minutes	
Denaturation	94ºC	30 seconds	4 cycles
Annealing	66ºC	45 seconds	
Extension	72ºC	2 minutes	
Denaturation	94ºC	30 seconds	4 cycles
Annealing	64ºC	45 seconds	
Extension	72ºC	2 minutes	
Denaturation	94ºC	30 seconds	4 cycles
Annealing	62ºC	45 seconds	
Extension	72ºC	2 minutes	
Denaturation	94ºC	30 seconds	12 cycles
Annealing	60ºC	45 seconds	
Extension	72ºC	2 minutes	
Final extension	72ºC	5 minutes	1 cycle

The system used for electrophoresis was a 10x10 Protean 5 vertical electrophoresis unit (BioRad). A 1X TAE buffer (Appendix A) was used for electrophoresis at 65ºC and 120 V for two hours.

To obtain the different bands that had formed on the gel, a silver staining system from BIO-RAD was used as per manufacturer's instructions. The bands were visualized on a UV transilluminator (UVP BioDoc-It^{TM} system) fitted with a digital camera. After visualization, the bands were excised with sterile scalpel blades, into sterile 1.5 mL eppendorf microfuge tubes containing 200 µL TE buffer. These were kept at -20^{o}C for further use in cloning and sequencing.

3.2.7 Transformation and Cloning

The excised PCR product was extracted using phenol: chloroform: isoamyl alcohol (24:24:1), re-amplified by PCR and confirmed by subsequent DGGE that the product consisted of a single band. The re-amplified PCR product was cloned into the pGEM®-T Easy Vector system (Promega, USA) as per manufacturer's instruction, and transformed into high efficiency *E. coli* JM 109 competent cells from which extracted plasmid was prepared for sequencing.

The transformants were screened on Luria Bertani (LB) agar plates containing 100 μg/mL ampicillin (Amp). Before plating, the LB/Amp plates were spread with IPTG (Appendix A) and X-Gal (Appendix A) after which they were incubated overnight at 37°C.

Transformants with an insert in the β-glycosidase gene appeared white on the X-Gal plates as opposed to blue colonies which have a plasmid but no insert in the β-glycosidase gene. The white colonies were picked with a sterile toothpick, inoculated into 5 mL LB broth and incubated in a shaker overnight at 37 ^{o}C. The plasmid was extracted using Qiagen® plasmid extraction kit according to the manufacturer's instruction.

To confirm the presence of insert, EcoR1 digestion was performed. EcoR1 was expected to cut on either side of the 568 base pairs (bp) fragment, resulting in two bands on a gel, one a 3 018 bp plasmid fragment and the other a 586 bp insert. Plasmids with the correct insert were prepared for sequencing.

3.2.8 Sequencing

Plasmids containing inserts were sequenced using Big Dye Terminator 3 sequencing kit (Applied Bio systems) with 100 to 200 ng of template DNA according to the manufacturer's instructions. Sequences were obtained by using a universal sequencing primer T7 or SP6 (Integrated DNA Technology (IDT), USA). Cycle sequencing was performed on a Perkins Elmer (Applied Biosystems) 9700 thermocycler.

The products were purified using DNA Clean & Concentrator TM-5 columns (Zymo Research, USA) as per manufacturer's instructions. The eluted DNA was dried at 37°C and then stored at 4°C until sequenced. DNA sequence was determined on an automated ABI 3100 Prism® Genetic Analyzer at Rhodes University, South Africa.

3.2.9 Phylogenetic Analysis

Chromatograms were generated by the ABI PRISM® Genetic Analyser Data Collection system 2.0.1 by Applied Biosystems. These chromatograms were converted into text format using Gene Tools and then put into the National Centre for Biotechnology Information Basic Local Alignment Search Tool (NCBI BLAST) database. BLAST is a set of similarity search programs designed to explore all of the available sequence databases (Altschul *et al.*, 1990). The percentage similarity to an identified species was recorded, also the length of the match and the E value, which is important for determining the accuracy of the result. To obtain the phylogenetic relationship between the clones, the data was analyzed using the Neighbor Joining (N-J) algorithm.

3.3 RESULTS AND DISCUSSION

The Gradient Tube and total biofilm samples were examined for molecular typing in order to determine the microbial populations existing within the biofilm and to possibly identify their spatial distribution in the biofilm using the Gradient Tube method and to correlate the results of the tubes to the total biofilm samples examined in the same manner.

3.3.1 Gradient Tubes

The Gradient Tubes were incubated at ambient temperature for five to eight days in a sterile hood and a range of clearly identifiable bands were observed (Figure 3.2).

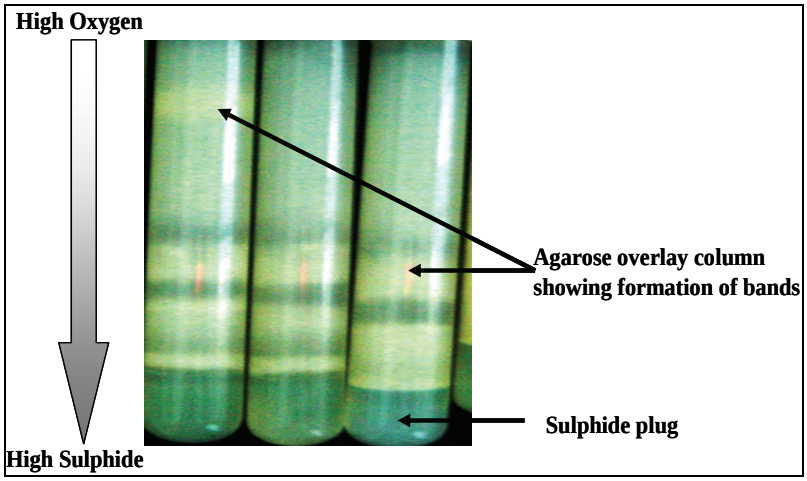

Figure 3. 2. Gradient Tubes showing the emergence of clearly define bands indicating the presence of microbial growth within the oxygen/sulphide gradient.

It was assumed that the aerobic or micro-aerophilic forms present in the innoculum would grow in the upper layers of the agarose overlay column and that the anaerobic sulphide tolerant forms in the lower layers. In this way, the microorganisms in the agar overlay were selected according to their sulphide and oxygen preference in the Gradient Tubes, with sulphide oxidizing forms establishing growth in those zones providing the appropriate physiological requirements.

3.3.2 Molecular Typing

3.3.2.1 Gradient Tubes

The agar plug in the tubes was extracted and then sectioned into 0.5 cm lengths and prepared for DNA extraction, by melting them at 37^{o}C and, following electrophoresis on 0.8% agarose gel, successful extraction of the high molecular weight DNA could be observed at the top of the gel (Figure 3.3).

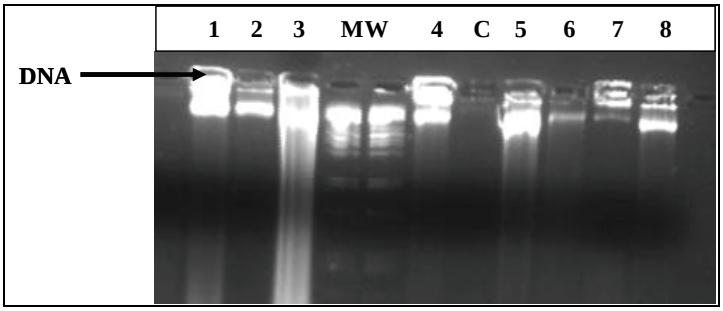

Figure 3. 3. A 0.8% agarose gel showing high molecular weight DNA. MW denotes λPst1 molecular weight marker and C the negative control.

The 16S rDNA gene was amplified using the PCR primers GM5F and 907R, and yielded a 586 bp amplification product (Figure3.4).

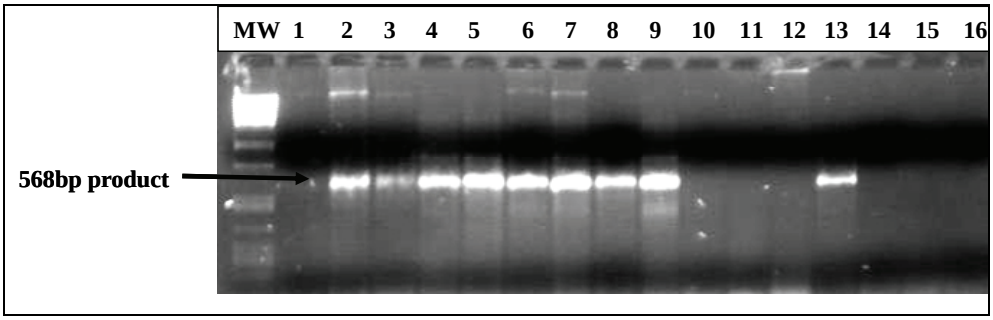

Figure 3. 4. A 1% agarose gel showing 568bp amplified polymerase chain reaction products.

The PCR product was separated by DGGE using a 55 to 65% denaturing gradient and yielded different bands on the acrylamide gel after silver staining and visualization in a ultra violet (UV) transilluminator (UVP BioDoc-It^{TM} system fitted with a digital camera) (Figure 3.5).

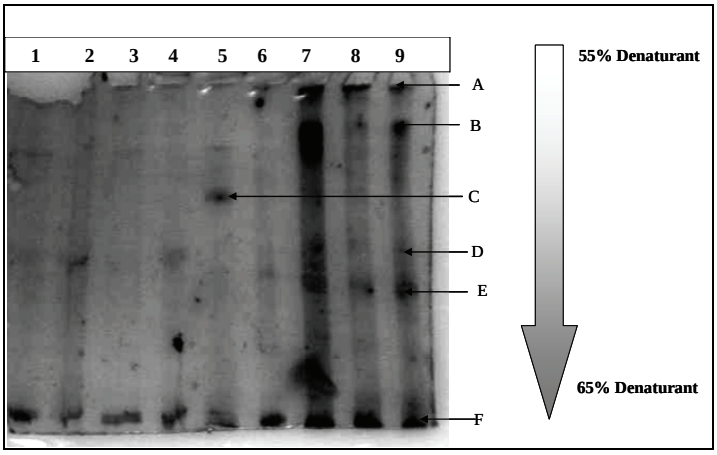

Figure 3. 5. A 55 to 65% gradient DGGE acrylamide gel showing the separation of the various bands.

A total of thirteen samples were collected from the Gradient Tubes. However, after amplification only nine PCR products were obtained. The samples one to nine (Figure 3.5) were collected at different points in the tube, with 1 denoting the first sample from the top of the tube and nine being one of the bands further down closer to the sulphide plug. The bands formed were marked A to F according to their position on the acrylamide gel. Thus samples were named with a number and letter (e.g.1A denotes the top band of PCR product 1).

The excised and amplified DGGE bands were transformed into high fidelity competent *E. coli* JM109 cells using a pGEMTM-T Easy Vector as described previously. EcoR1 digest of the extracted plasmids was performed. Figure 3.6 shows the two bands cut on either side of the 586 bp fragment. The top band represents the 3018 bp plasmid fragment and the bottom is the 586 bp insert. In some cases, three separate bands were observed, indicating one large plasmid fragment and two smaller fragments which add up to 586 bp. The samples with correct inserts were prepared for sequencing. The data obtained from the NCBI was used to obtain the description of the sequenced sample based on the percentage relationship to the sample of the bacteria in the database to the sample. This was used to formulate a phylogenetic tree (Figure 3.7).

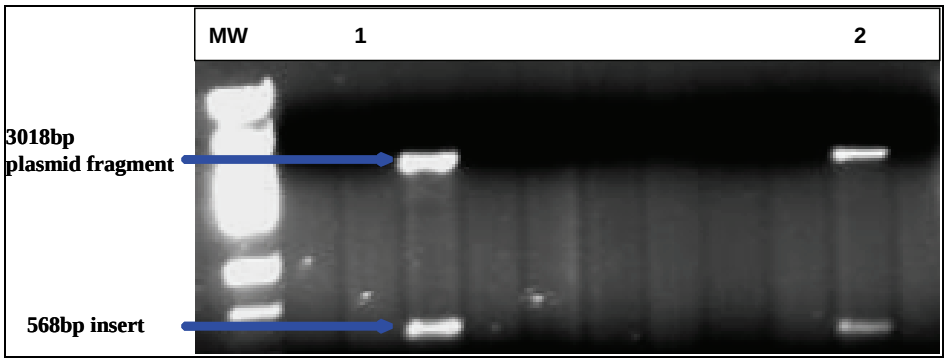

Figure 3. 6. A 1% agarose gel showing the plasmid fragment and insert after digestion with EcoR1.

3.3.2.2 Total Biofilm

The biofilm samples were also examined using DNA extraction, PCR and DGGE and cloning as above mentioned.

3.3.3 Phylogenetic Analysis

3.3.3.1 Gradient Tubes

A phylogenetic tree (Figure 3.7) and table summary (Table 3.2) samples were formulated for the Gradient Tubes samples

Table 3. 2. Summary of the Gradient Tubes species identified in the phylogenetic tree.

Name/Number	**Family**	**Isolate**
BA000001 *Pyrococcus horikoshii* OT3	Archaea; Euryarchaeota; Thermococci; Thermococcales; Thermococcaceae; *Pyrococcus*.	
Clone 8e		**Gradient tube**
AY569302 uncultured *Chryseobacterium sp.*	Bacteria; Bacteroidetes; Flavobacteria; Flavobacteriales; Flavobacteriaceae; *Chryseobacterium*; environmental samples.	Microbial diversity of the pink mat from the Spectacles Hot Spring in Rehai, Tengchong, China
Clone 9.5c		**Gradient tube**
CR933234 Uncultured bacterium partial	Bacteria; environmental samples	Novel major bacterial candidate division within a municipal anaerobic sludge digester
AY953234 uncultured anaerobic bacterium	Bacteria; environmental samples	Unique microbial diversity of anaerobic swine lagoons
AY570639 uncultured bacterium	Bacteria; environmental samples	Microbial diversity in a low-temperature, biodegraded Canadian oil reservoir
AF280841 Uncultured bacterium mLe1-2	Bacteria; Bacteroidetes; environmental samples	Phylogenetic analysis of bacterial communities in mesophilic and thermophyllic bioreactors treating pharmaceutical wastewater
AY949860 *Bacteroides* sp. strain Z4	Bacteria; Bacteroidetes; Bacteroidetes (class);	*Bacteroides* sp. strain Z4, from paper mill waste water

	Bacteroidales; Bacteroidaceae; *Bacteroides*	
Clone 11b		**Gradient tube**
Clone 13a		**Gradient tube**
AB025196 *Caulobacter* sp. MBIC3983	Bacteria; Proteobacteria; Alphaproteobacteria; Caulobacterales; Caulobacteraceae; Caulobacter.	Phylogenetic Classification of *Mycoplana* species
AJ717390 *Brevundimonas bullata* isolate AC23	Bacteria; Proteobacteria; Alphaproteobacteria; Caulobacterales; Caulobacteraceae; *Brevundimonas.*	Bacterial diversity in a non-saline alkaline environment: heterotrophic aerobic populations
AY689051 *Mycoplana* sp. 6C_11	Bacteria; Proteobacteria; Alphaproteobacteria; Rhizobiales; Brucellaceae; Mycoplana.	Annual variation phylogenetic diversity of antibiotic-resistant bacteria in the lower Lake Geumgang.
DQ177489 *Brevundimonas* sp. Tibet-IX23	Bacteria; Proteobacteria; Alphaproteobacteria; Caulobacterales; Caulobacteraceae; *Brevundimonas*.	Climate warming and tundra viable bacteria dynamics on Qinghai-Tibet Plateau
Clone 9.5b		**Gradient tube**
AF237975 *Planococcus citreus*	Bacteria; Firmicutes; Bacillales; Planococcaceae; *Planococcus*	Horizontal and Vertical Complexity of Attached and Free-Living Bacteria of the Eastern Mediterranean Sea
AF500008 *Planococcus citreus* strain TF-16	Bacteria; Firmicutes; Bacillales; Planococcaceae; *Planococcus*	Isolated from sea water of a tidal flat in Korea
AY428552 *Planococcus maritimus* strain KMM 3738	Bacteria; Firmicutes; Bacillales; Planococcaceae; *Planococcus*	*Planococcus algae* sp. nov. an unusual 'a-shaped' alkaliphilic Gram-positive bacteria isolated from degraded thallus of the brown algae
AF237975 *Planococcus citreus*	Bacteria; Firmicutes; Bacillales; Planococcaceae; *Planococcus*	Horizontal and Vertical Complexity of Attached and Free-Living Bacteria of the Eastern Mediterranean Sea, Determined by 16S rDNA and

		16S rRNA Fingerprints
AY741387 Uncultured bacterium clone Lan-37	Bacteria; environmental samples	Community Constitute and Phylogenetic Analysis on Silkworm Uncultured Intestinal Bacteria
AY735408 *Enterococcus faecium*	Bacteria; Firmicutes; Lactobacillales; Enterococcaceae; *Enterococcus*	Screening and isolation of Lactobacillus from traditional Korean fermented foods
AB009228 unidentified rumen bacterium RFN80	Bacteria; environmental samples	Predominant Bacterial Species of the Rumen
Clone5b		**Gradient tube**
AY050603 Uncultured bacterium clone GOUTA13	Bacteria; environmental samples	Microbial diversity in an *in situ* reactor system treating monochlorobenzene contaminated groundwater as revealed by 16S ribosomal DNA analysis
AY985323 Uncultured bacterium clone C233	Bacteria; environmental samples	Diversity of the human intestinal microbial flora
AY985477 Uncultured bacterium clone C437	Bacteria; environmental samples	Diversity of the human intestinal microbial flora
AY916338Uncultured bacterium clone C583	Bacteria; environmental samples	Diversity of the human intestinal microbial flora
Clone 3a		**Gradient tube**
AF011343 *Azoarcus communis*	Bacteria; Proteobacteria; Betaproteobacteria; Rhodocyclales; Rhodocyclaceae; Azoarcus	Identification of N2-fixing plant- and fungus-associated Azoarcus species by PCR-based genomic fingerprints
AJ007007*Azoarcus sp*.	Bacteria; Proteobacteria; Betaproteobacteria; Rhodocyclales; Rhodocyclaceae; Azoarcus	Analysis of the relative abundance of different types of bacteria capable of toluene degradation in a compost biofilter
AJ430348 *Comamonas kersterii*	Bacteria; Proteobacteria; Betaproteobacteria; Burkholderiales; Comamonadaceae; *Comamonas*	Description of *Comamonas aquatica* comb. nov. and *Comamonas kerstersii* sp. nov. for two subgroups of

		Comamonas terrigena and emended description of *Comamonas terrigena*
AY258065 *Acidovorax sp*. 98-63833	Bacteria; Proteobacteria; Betaproteobacteria; Burkholderiales; Comamonadaceae; *Acidovorax*	Undescribed bacterial pathogens isolated from human tissues
AY168755 *Hydrogenophaga sp*. YED6-4	Bacteria; Proteobacteria; Betaproteobacteria; Burkholderiales; Comamonadaceae; *Hydrogenophaga*	Characterization of Arsenite Oxidizing Biofilms: Molecular and Cultivation Approaches and Community Rates of Arsenite Oxidation
AY569978 *Hydrogenophaga sp*. Esa.33	Bacteria; Proteobacteria; Betaproteobacteria; Burkholderiales; Comamonadaceae; *Hydrogenophaga*	Characterization of a novel selenium methyltransferase from freshwater bacteria showing strong similarities with the calicheamicin methyltransferase

.

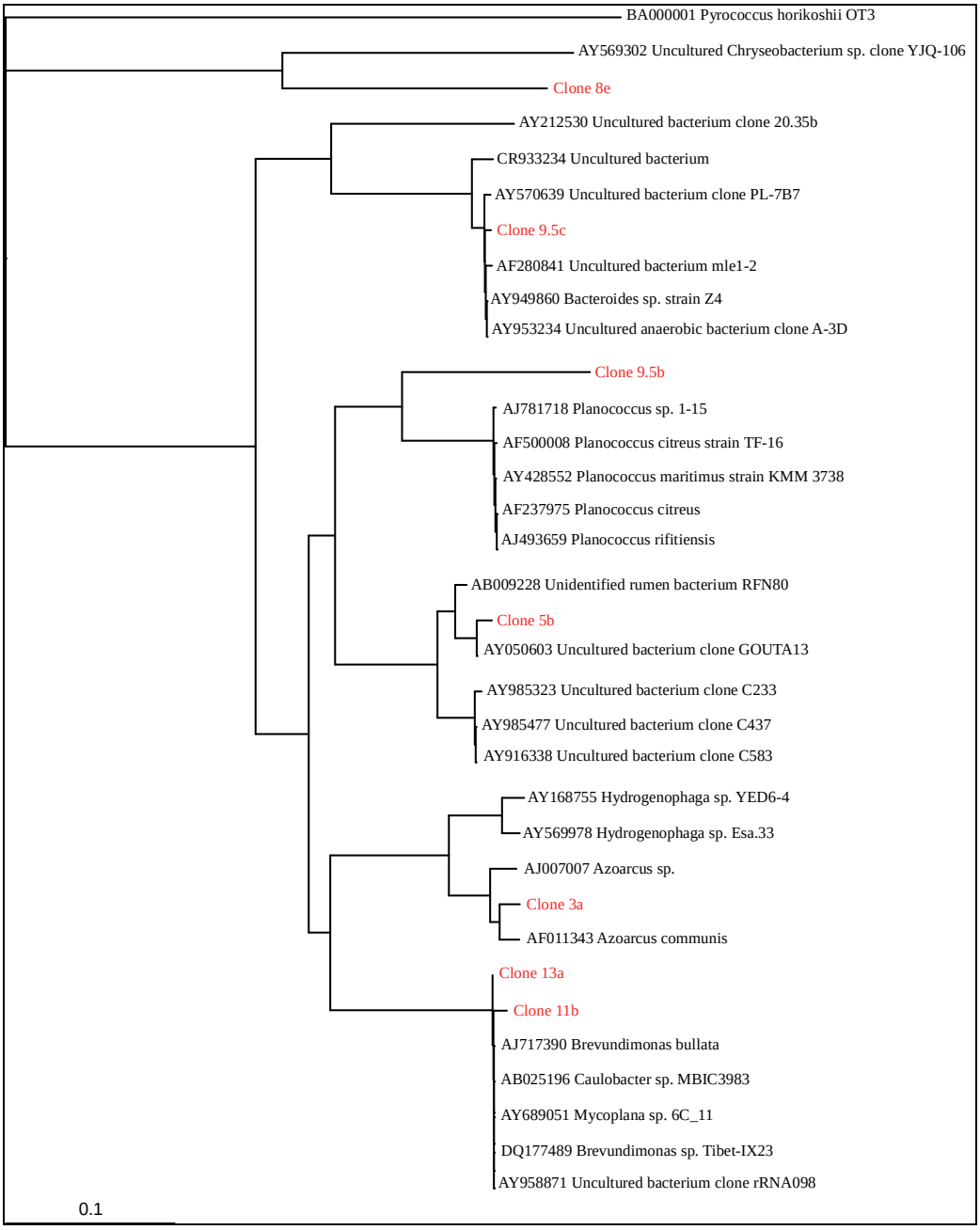

Figure 3. 7. Phylogenetic tree relating Gradient Tube section sample sequences to known species from the NCBI database.

3.3.3.2 Total biofilm

Figure 3.8 is a composite phylogenetic tree formulated for the total biofilm samples collected from the three stages of development and is summarised in Table 3.3

Table 3. 3. Summary of the total biofilm species identified in the phylogenetic tree.

Name/Number	**Family**	**Isolate**
BA000001 *Pyrococcus horikoshii* OT3	Archaea; Euryarchaeota; Thermococci; Thermococcales; Thermococcaceae; *Pyrococcus*.	
Clone 9f		**Biofilm**
DQ168844 Uncultured *Prevotella* sp. clone J28	Bacteria; Bacteroidetes; Bacteroidetes (class); Bacteroidales; Prevotellaceae; *Prevotella*; environmental samples.	Fermentative biohydrogen production using heated anaerobic sludge
AY212535 Uncultured bacterium clone 5.16	Bacteria; environmental samples	Assessment of equine fecal contamination: the search for alternative bacterial source-tracking targets
AY212542 Uncultured bacterium clone up.21	Bacteria; environmental samples	Assessment of equine fecal contamination: the search for alternative bacterial source-tracking targets
AY212521 Uncultured bacterium clone 20.16	Bacteria; environmental samples	Assessment of equine fecal contamination: the search for alternative bacterial source-tracking targets
AY212530 Uncultured bacterium clone 20.35b	Bacteria; environmental samples	Assessment of equine fecal contamination: the search for alternative bacterial source-tracking targets
AY831467 Uncultured bacterium clone 4E	Bacteria; environmental samples	Biotransformation and dissolution of petroleum hydrocarbons in natural flowing seawater at low temperature
Clone 1f		**Early Brittle film**
AF414444 *Cytophaga* sp. SA1	Bacteria; Bacteroidetes; Sphingobacteria; Sphingobacteriales; Flexibacteraceae; *Cytophaga*	Isolation and characterization of filamentous bacteria from papermill slimes

AJ634056 Cytophaga sp. 0401 852	Bacteria; Bacteroidetes; Sphingobacteria; Sphingobacteriales; Flexibacteraceae; Cytophaga	Identification based on 16S rRNA gene sequencing
AJ440996 *Flavobacterium gelidilacus*	Bacteria; Bacteroidetes; Flavobacteria; Flavobacteriales; Flavobacteriaceae; *Flavobacterium*	Diversity of 746 heterotrophic bacteria isolated from microbial mats from ten Antarctic lakes
AJ507151 *Flavobacterium gelidilacus*	Bacteria; Bacteroidetes; Flavobacteria; Flavobacteriales; Flavobacteriaceae; *Flavobacterium*	*Flavobacterium gelidilacus* sp. nov., isolated from microbial mats in Antarctic lakes
AY468484 *Chryseobacterium* sp. LDVH 3	Bacteria; Bacteroidetes; Flavobacteria; Flavobacteriales; Flavobacteriaceae; *Chryseobacterium*	Polyphasic study of *Chryseobacterium* strains isolated from diseased aquatic animals
AY468465 *Chryseobacterium* sp. FRGDSA 4580/97	Bacteria; Bacteroidetes; Flavobacteria; Flavobacteriales; Flavobacteriaceae; Chryseobacterium	Polyphasic study of *Chryseobacterium* strains isolated from diseased aquatic animals
AY468454 *Chryseobacterium* sp. UOF CR2995	Bacteria; Bacteroidetes; Flavobacteria; Flavobacteriales; Flavobacteriaceae; *Chryseobacterium*	Polyphasic study of *Chryseobacterium* strains isolated from diseased aquatic animals
AY468455 *Chryseobacterium* sp. UOF CR4395	Bacteria; Bacteroidetes; Flavobacteria; Flavobacteriales; Flavobacteriaceae; *Chryseobacterium*	Polyphasic study of *Chryseobacterium* strains isolated from diseased aquatic animals
Clone2c		**Thick Sticky Biofilm**
AY532570 Uncultured bacterium clone 1013-28-CG21	Bacteria; environmental samples	Subsurface microbial communities and geochemistry within a vertical transect of a uranium-contaminated aquifer
AF458288 Uncultured epsilon proteobacterium ML615J-7	Bacteria; Proteobacteria; Epsilonproteobacteria; environmental	Composition of bacterial assemblages from alkaline, hypersaline Mono Lake,

	samples.	California
AY532543 Uncultured bacterium clone 1013-1-CG20	Bacteria; environmental samples	Subsurface microbial communities and geochemistry within a vertical transect of a uranium-contaminated aquifer
AB197158 *Sulfurimonas* sp. Go25-1	Bacteria; Proteobacteria; Epsilonproteobacteria; Campylobacterales; Helicobacteraceae; *Sulfurimonas*	Distribution, phylogenetic diversity and physiological characteristics of epsilon-Proteobacteria in a deep-sea hydrothermal field
AF355050 Uncultured epsilon proteobacterium Arctic96B-13	Bacteria; Proteobacteria; Epsilonproteobacteria; environmental samples.	Phylogenetic composition of bacterioplankton assemblages from the Arctic Ocean
Clone 11a		**Biofilm**
Clone 10a		**Biofilm**
AF237975 *Planococcus citreus*	Bacteria; Firmicutes; Bacillales; Planococcaceae; *Planococcus*	Horizontal and Vertical Complexity of Attached and Free-Living Bacteria of the Eastern Mediterranean Sea
AF500008 *Planococcus citreus* strain TF-16	Bacteria; Firmicutes; Bacillales; Planococcaceae; *Planococcus*	Isolated from sea water of a tidal flat in Korea
AY428552 *Planococcus maritimus* strain KMM 3738	Bacteria; Firmicutes; Bacillales; Planococcaceae; *Planococcus*	*Planococcus* algae sp. nov. an unusual 'a-shaped' alkaliphilic Gram-positive bacteria isolated from degraded thallus of the brown algae
AF237975 *Planococcus citreus*	Bacteria; Firmicutes; Bacillales; Planococcaceae; *Planococcus*	Horizontal and Vertical Complexity of Attached and Free-Living Bacteria of the Eastern Mediterranean Sea, Determined by 16S rDNA and 16S rRNA Fingerprints
AY741387 Uncultured bacterium clone Lan-37	Bacteria; environmental samples	Community Constitute and Phylogenetic Analysis on Silkworm

		Uncultured Intestinal Bacteria
Clone 9.5a		**Biofilm**
Clone9.5aNQP		**Biofilm**
AY221599 Uncultured soil bacterium clone HN1-35	Bacteria; environmental samples	Microbial Community Analysis of Soils Contaminated with Lead, Chromium and Organic Solvents
AB066266 *Enterococcus mundtii*	Bacteria; Firmicutes; Lactobacillales; Enterococcaceae; *Enterococcus*	Biochemical and genetic characterization of mundticin KS, an antilisterial peptide produced by *Enterococcus mundtii* NFRI 7393
AF061013 *Enterococcus mundtii*	Bacteria; Firmicutes; Lactobacillales; Enterococcaceae; *Enterococcus*	Determination of 16S rRNA sequences of enterococci and application to species identification of nonmotile *Enterococcus gallinarum* isolates
Y18340 *Enterococcus mundtii*	Bacteria; Firmicutes; Lactobacillales; Enterococcaceae; *Enterococcus*	Direct Submission
AF539705 *Enterococcus ratti*	Bacteria; Firmicutes; Lactobacillales; Enterococcaceae; *Enterococcus*	*Enterococcus hirae* implicated as a cause of diarrhea in suckling rats
AY675247 *Enterococcus faecium*	Bacteria; Firmicutes; Lactobacillales; Enterococcaceae; *Enterococcus*	Identification of bacteria from fermented Korean traditional foods
AY653231 *Enterococcus faecium*	Bacteria; Firmicutes; Lactobacillales; Enterococcaceae; *Enterococcus*	Comparison of three PCR primer sets for identification of vanB gene carriage in feces and correlation with carriage of vancomycin-resistant enterococci: interference by vanB-containing anaerobic

		bacilli
AY735408 *Enterococcus faecium*	Bacteria; Firmicutes; Lactobacillales; Enterococcaceae; *Enterococcus*	Screening and isolation of *Lactobacillus* from traditional Korean fermented foods
AB009228unidentified rumen bacterium RFN80	Bacteria; environmental samples	Predominant Bacterial Species of the Rumen
Clone 13bQP		**Biofilm**
DQ104970 Bacterium SRMC-52-8	Bacteria	Co-selection for microbial resistance to metals and antibiotics in freshwater microcosms
AY957941 Uncultured bacterium clone B3NR69D26	Bacteria; environmental samples	Population diversity in model drinking water biofilms receiving chlorine or monochloramine residual
AY953163 Uncultured anaerobic bacterium clone B-1AW	Bacteria; environmental samples	Unique Microbial Diversity of Anaerobic Swine Lagoons
AY953184 Uncultured anaerobic bacterium clone B-1R	Bacteria; environmental samples	Unique Microbial Diversity of Anaerobic Swine Lagoons
AJ430348 *Comamonas kersterii*	Bacteria; Proteobacteria; Betaproteobacteria; Burkholderiales; Comamonadaceae; *Comamonas*	Description of *Comamonas aquatica* comb. nov. and *Comamonas kerstersii* sp. nov. for two subgroups of *Comamonas terrigena* and emended description of *Comamonas terrigena*
AY258065 *Acidovorax sp*. 98-63833	Bacteria; Proteobacteria; Betaproteobacteria; Burkholderiales; Comamonadaceae; *Acidovorax*	Undescribed bacterial pathogens isolated from human tissues
AY168755 *Hydrogenophaga* sp. YED6-4	Bacteria; Proteobacteria; Betaproteobacteria; Burkholderiales; Comamonadaceae;	Characterization of Arsenite Oxidizing Biofilms: Molecular and Cultivation Approaches and Community Rates of

	Hydrogenophaga	Arsenite Oxidation
AY569978Hydrogenophaga sp. Esa.33	Bacteria; Proteobacteria; Betaproteobacteria; Burkholderiales; Comamonadaceae; Hydrogenophaga	Characterization of a novel selenium methyltransferase from freshwater bacteria showing strong similarities with the calicheamicin methyltransferase
Clone 10aQP		**Biofilm**
AB021404 *Pseudomonas geniculata*	Bacteria; Proteobacteria; Gammaproteobacteria; Xanthomonadales; Xanthomonadaceae.	Phylogenetic affiliation of the pseudomonads based on 16S rRNA sequence
DQ192172 *Stenotrophomonas maltophilia* strain flds	Bacteria; Proteobacteria; Gammaproteobacteria; Xanthomonadales; Xanthomonadaceae; *Stenotrophomonas*	Direct Submission
AY038620 Uncultured eubacterium clone GL182.22	Bacteria; environmental samples	16S rRNA sequence analysis and phylogenetic characterization of microbial communities associated with lacustrine subsurface sediments
AY038621 Uncultured eubacterium clone GL184.24	Bacteria; environmental samples	16S rRNA sequence analysis and phylogenetic characterization of microbial communities associated with lacustrine subsurface sediments
AY038629Uncultured eubacterium clone GL178.1	Bacteria; environmental samples	16S rRNA sequence analysis and phylogenetic characterization of microbial communities associated with lacustrine subsurface sediments

AY038628 Uncultured eubacterium clone GL178.11	Bacteria; environmental samples	16S rRNA sequence analysis and phylogenetic characterization of microbial communities associated with lacustrine subsurface sediments
AF513452 Xanthomonas group bacterium LA37	Bacteria; Proteobacteria; Gammaproteobacteria; Xanthomonadales; Xanthomonadaceae.	The Hawaiian Archipelago: a microbial diversity hotspot
Clone 1d		**Early Brittle**
Clone 2d		**Thick Sticky**
AJ536782 Uncultured bacterium 16S rRNA gene, isolate cMM319-25	Bacteria; environmental samples	Molecular analysis of the microbial community in drainage water from a magnesite mine, in the Graz area, Austria
AJ536777 Uncultured bacterium 16S rRNA gene, isolate cMM319-03.	Bacteria; environmental samples	Molecular analysis of the microbial community in drainage water from a magnesite mine, in the Graz area, Austria
AJ536781 Uncultured bacterium 16S rRNA gene, isolate cMM319-21	Bacteria; environmental samples	Molecular analysis of the microbial community in drainage water from a magnesite mine, in the Graz area, Austria
AJ536792 Uncultured bacterium partial 16S rRNA gene, isolate cMM319-58	Bacteria; environmental samples	Molecular analysis of the microbial community in drainage water from a magnesite mine, in the Graz area, Austria
AJ536802 Uncultured bacterium partial 16S rRNA gene, isolate cMM319-73	Bacteria; environmental samples	Molecular analysis of the microbial community in drainage water from a magnesite mine, in the Graz area, Austria
Clone 1c		**Early Brittle**

AJ536804 Uncultured bacterium partial 16S rRNA gene, isolate cMM319-75.	Bacteria; environmental samples.	Molecular analysis of the microbial community in drainage water from a magnesite mine, in the Graz area, Austria
DQ088740 Uncultured bacterium clone BE24FW032601C18W17-4	Bacteria; environmental samples	Planktonic microbial communities associated with fracture-derived groundwater in a deep gold mine of South Africa
AJ536780 Uncultured bacterium 16S rRNA gene, isolate cMM319-18	Bacteria; environmental samples	Molecular analysis of the microbial community in drainage water from a magnesite mine, in the Graz area, Austria
AB118236 *Thiovirga sulfuroxydans*	Bacteria; Proteobacteria; Gammaproteobacteria; Chromatiales; Halothiobacillaceae; *Thiovirga*	Isolation, characterization, and in situ detection of a novel chemolithoautotrophic sulfur-oxidizing bacterium in wastewater biofilms growing under micro-aerophilic conditions
AJ536785 Uncultured bacterium 16S rRNA gene, isolate cMM319-33	Bacteria; environmental samples	Molecular analysis of the microbial community in drainage water from a magnesite mine, in the Graz area, Austria
AJ536786Uncultured bacterium 16S rRNA gene, isolate cMM319-34	Bacteria; environmental samples	Molecular analysis of the microbial community in drainage water from a magnesite mine, in the Graz area, Austria
DQ125329 Uncultured Halo*Thiobacillus* sp. clone B225FWB5	Bacteria; Proteobacteria; Gammaproteobacteria; Chromatiales; Halothiobacillaceae; *HaloThiobacillus* ;	The distribution of microbial taxa in the subsurface water of the Kalahari Shield, South Africa

	environmental samples	
AJ536787 Uncultured bacterium 16S rRNA gene, isolate cMM319-39.	Bacteria; environmental samples.	Molecular analysis of the microbial community in drainage water from a magnesite mine, in the Graz area, Austria
AJ536779 Uncultured bacterium 16S rRNA gene, isolate cMM319-14	Bacteria; environmental samples.	Molecular analysis of the microbial community in drainage water from a magnesite mine, in the Graz area, Austria
Clone S1A		**Biofilm**
Clone S2E		**Biofilm**
Clone S2A		**Biofilm**
AY096035 *HaloThiobacillus* sp. WJ18	Bacteria; Proteobacteria; Gammaproteobacteria; Chromatiales; Halothiobacillaceae; *HaloThiobacillus*	Novel acidophiles isolated from moderately acidic mine drainage waters
X97534 *Thiobacillus* sp.	Bacteria; Proteobacteria; Betaproteobacteria; Hydrogenophilales; Hydrogenophilaceae; *Thiobacillus* .	*Thiobacillus* sp. W5, the dominant autotroph oxidizing sulfide to sulfur in a reactor for aerobic treatment of sulphidic wastes
AF173169 *Thiobacillus neapolitanus* DSM 581	Bacteria; Proteobacteria; Gammaproteobacteria; Chromatiales; Halothiobacillaceae; *HaloThiobacillus* .	*HaloThiobacillus Kkellyi* sp. nov., a mesophilic, obligately chemolithoautotrophic, sulfur-oxidizing bacterium isolated from a shallow-water hydrothermal vent in the Aegean Sea
AY686547 *HaloThiobacillus neapolitanus* strain OSWA	Bacteria; Proteobacteria; Gammaproteobacteria; Chromatiales; Halothiobacillaceae; *HaloThiobacillus* .	A *HaloThiobacillus* from The Old Sulphur Well at Harrogate
L79962 *Thiothrix fructosivorans* strain Q	Bacteria; Proteobacteria; Gammaproteobacteria;	Phylogenetic relationships of filamentous sulfur bacteria

	Thiotrichales; Thiotrichaceae; Thiothrix.	isolated from wastewater-treatment plants
AJ548906 Uncultured *Thiobacillus* sp.	Bacteria; Proteobacteria; Betaproteobacteria; Hydrogenophilales; Hydrogenophilaceae; *Thiobacillus* ; environmental samples.	High-diversity biofilm for the oxidation of sulfide-containing effluents
Y09280 *Thiobacillus* baregensis	Bacteria; Proteobacteria; Betaproteobacteria; Hydrogenophilales; Hydrogenophilaceae; *Thiobacillus* .	A new sulfoxidizing bacterium from sulfurated thermal waters of Bareges

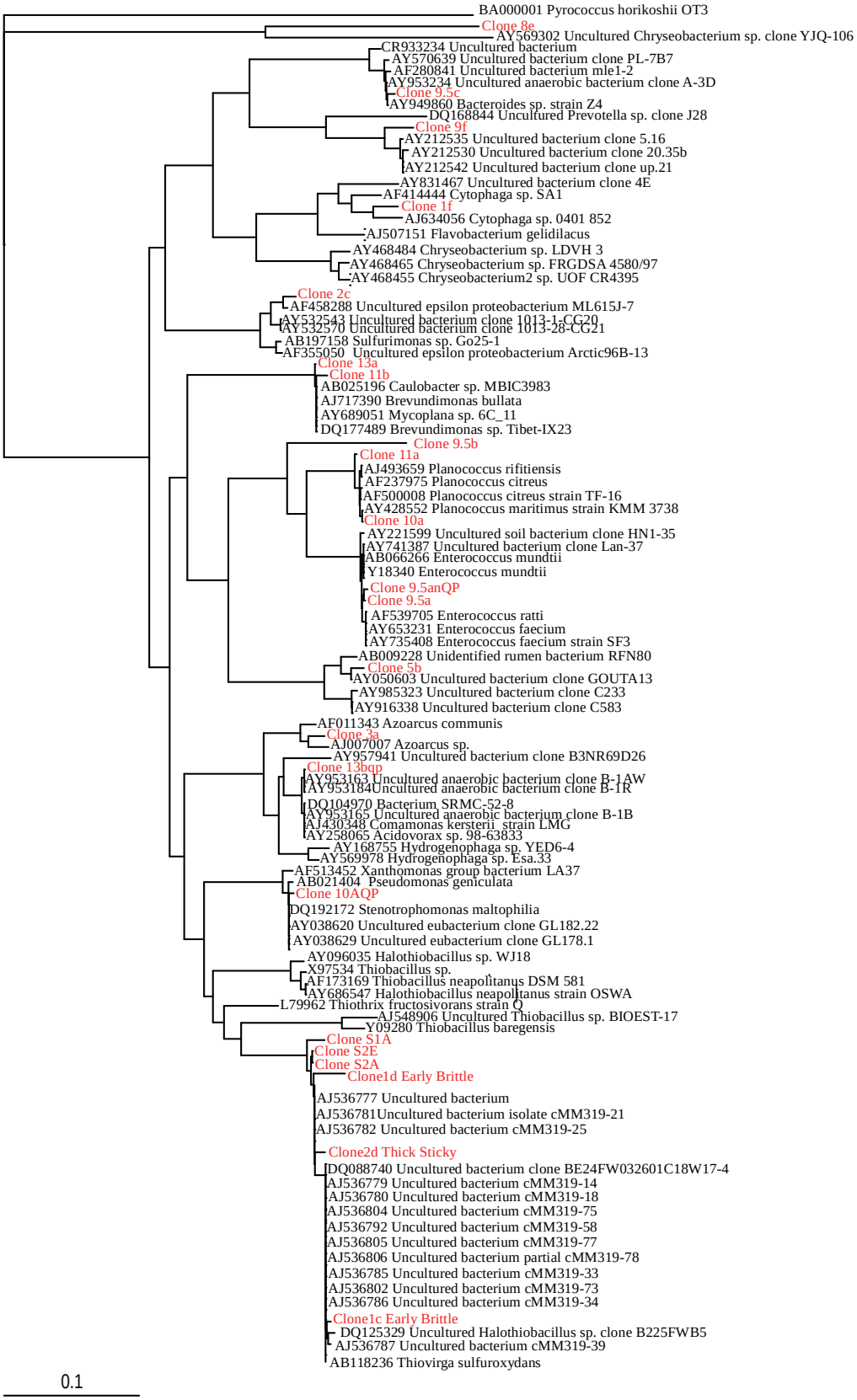

Figure 3. 8. Overall Phylogenetic tree relating total biofilm and Gradient Tube section sample sequences to known species from the NCBI database. This tree includes all isolates for the study and represents an aggregate picture of the populations present

3.3.4 Overall Biofilm Microbial Population

Species found near the top of the Gradient Tubes (aerobic zone) were found to be related to *Azoarcus* sp., which has been identified as a role player in the degradation of aromatic hydrocarbons and which also has denitrifying capabilities (Hurek *et al.*, 1997). *Azoarcus communis* has been associated with plant matter and may have originated from the sulphide generating DPBR reactor which contained grass and other ligno-cellulosic material.

Another clone appearing near the top of the Gradient Tubes was found to be related to an uncultured bacterium which has previously been isolated in an underground *in situ* ground water remediation reactor system filled with aquifer sediments (Juteau *et al.*, 1999). This reactor system contained sporulating and non-sporulating sulfate-reducing bacteria. The most commonly occurring clones obtained from the sediment samples of this reactor were related to the beta-Proteobacteria and to *Acidithiobacillus ferrooxidans* (Karavaiko *et al.*, 2003).

Halfway down the Gradient Tubes (intermediate oxygen and sulphide concentrations), a clone was isolated which was closely related to an uncultured *Chryseobactrium* (Bernadet *et al.*, 2005). *Chryseobactrium* belong to the *Flavobacteria* group which are commensal organisms and also opportunistic pathogens. *Flavobacteria* are Gram-negative aerobic rods with rounded or tapered ends and showing gliding motility (Bernadet *et al.*, 2005). They are able to decompose several polysaccharides, but not cellulose, and are widely distributed in soil and freshwater habitats. An isolate from the early Brittle biofilm growing on the Channel reactor was also found to be closely related to the *Chryseobacterium*.

Below the halfway point in the Gradient Tubes a clone closely related to *Bacteroides* spp., and other uncultured anaerobic bacteria were identified (Zhang and Chen, 2005). The *Bacteroides* are obligately anaerobic, Gram-negative and saccharolytic, producing acetate and succinate as their major metabolic end-products (Zhang and Chen, 2005). This particular *Bacteroides* type strain was documented to be growing in paper mill waste water and in our study it could have originated from the lignocellulose-packed DPBR. The uncultured bacteria closely related to this Gradient

Tube clone were isolated from mainly anaerobic sludge digesters or anaerobic swine lagoons. This indicated that the oxygen levels half way down the Gradient Tube were probably already very low – possibly from anoxic to anaerobic. *Bacteroides* related species were also identified in the biofilm samples.

Just below the halfway point in the Gradient Tube a clone closely related to *Planococcus citreus* was identified (Romano *et al.*, 2003). *Planococcus* are Gram-positive and generally aerobic to microaerophilic. Their cells are coccoid, which can occur in pairs, tetrads and aggregates, and they are motile by means of a single polar flagellum. *Planococcus* sp have previously been isolated from algal mats collected from a sulphurous spring and from seawater in a tidal flat, indicating sulphidic environments (Romano *et al.*, 2003). *Planococcus* sp related bacteria were also found in the LFCR reactor biofilm samples.

Clones identified near the bottom of the Gradient Tubes were found to be closely related to *Brevundimonas* sp. (Zhang *et al.*, 2005), *Caulobacter* sp. (Hamada and Suzuki, 1999) and *Mycoplana* sp (Bae *et al.*, 2004). *Brevundimonads* are Gram-negative, rod-shaped α-proteobacteria which are documented to produce copious exopolysaccharide capsular material (Verhoef *et al.*, 2002). The biofilm is apparently composed of large quantities of EPS which forms the matrix of the structure. This is probably bacteriological in origin (with *Brevundimonas* as a key candidate) and not only provides the appropriate micro-environment in which sulphur oxidation occurs, but also supports the sulphur crystal structures that are then formed in the system. As an EPS producer, *Brevundimonas* may play an important role within the biofilm structure. Its occurrence which was observed only near the bottom of the Gradient Tube suggests that it prefers a high sulphide and anaerobic to anoxic environment. This also suggests that *Brevundimonas* may require the presence of oxygen consuming aerobes and micro-aerophiles in the biofim zone above its location at the air/water interface to allow the Redox conditions necessary for its growth and function. *Chryseobacteria* and *Bacteroides*, which are known aerobic polysaccharide consumers, could provide this function.

Some of the sulphur bacteria are known to have very specific growth requirements in laboratory culture, and this may explain why some of these were not observed in the Gradient Tubes, which were unoptimised systems.

Samples 10A and 11A collected just above the sulphide plug were found to be closest to the *Planococcus sp*.

There was a cluster of samples collected closer to the top of the tube which were closely related to each other but had no close match on the database. In subsequent sequences, a sample from the biofilm also was found to be closely related to also *Brevundimonas. dimuta* which utilizes sulphur-containing amino acids and reduced sulphur forms for its growth (Zhang *et al.*, 1999).

A number of possibly important clones were observed in the biofilm which were not found in the Gradient Tubes. This may have been due to more rigorous growth conditions required which are present in the biofilm but were not duplicated under artificial culture conditions in the Gradient Tubes. A close match to *Thiovirga sulforoxydans* was found for one of the clones which have been reported as a novel chemolithoautotrophic sulfur-oxidizing bacterium found in wastewater biofilms growing under micro-aerophilic conditions (Ito *et al.*, 2004).

Clone 2c was closely matched to a *Sulfurimonas* species which had been isolated in a study on the distribution, phylogenetic diversity and physiological characteristics of ε-Proteobacteria in a deep-sea hydrothermal vent field (Nakagawa et al., 2005). Various clones related to sulphur-oxidizing bacteria including *Thiobacillus* (Visser et al., 1997), *Halothiobacillus* (Hallberg and Johnson, 2002) and *Thiothrix* (Howarth *et al.*, 1999), a filamentous sulphur bacterium, were identified from the biofilm samples.

Figure 3.9 summarises the relationship of the phylogenetic analysis to the position of the particular samples collected from the different levels in the Gradient Tubes.

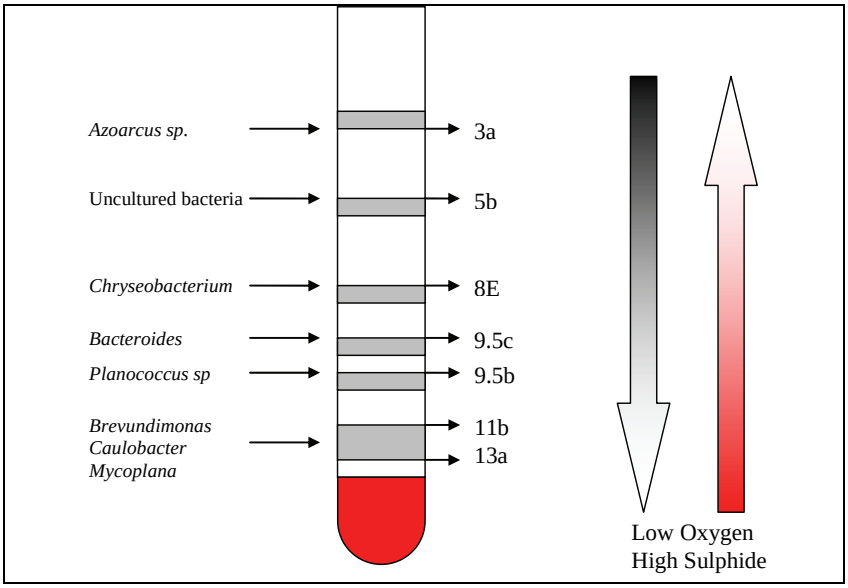

Figure 3. 9. A diagrammatic illustration of the results obtained from sequencing of the Gradient Tube samples drawn from different zones along the length of agarose overlay column.

The various bacterial species identified in the phylogenetic analysis of both the FSB and the Gradient Tube systems showed expected differences but also, importantly, some marked similarities in species composition and distribution. A comparison of the populations in the two systems and a possible extrapolation of the findings in the Gradient Tube which may be related to their location within the cross section of the floating biofilm is outlined in Table 3.4.

Although the method must, by its definition, produce only indicative results, correlations of interest were observed. This includes the presence of chemoautotrophic sulphide oxidisers in the upper layer of the biofilm closest to the air/water interface. The mid zones showed a high level of comparability between the systems and species related to oxygen consuming forms, with possible Redox poising capabilities being identified.

Lastly, the *Brevundimonas* and uncultured anaerobe may be responsible for the copious EPS production which provides the matrix of the biofilm system as it matures through Thin to Brittle form.

Table 3. 4. A comparison of populations identified at the various zones in the Gradient Tubes and the total biofilm samples.

Distribution	**Gradient Tube**	**Biofilm**
Top (aerobic)	*Azoarcus* *Acidothiobacillus*	*Thiobacillus* *Halothiobacillus* *Thiothrix* *Thiovirga* *Sulfurimonas*
Middle (anoxic to anaerobic)	*Chryseobacterium* *Bacteroides* *Planococcus*	*Chryseobacterium* *Bacteroides* *Planococcus*
Bottom (anaerobic)	*Brevundimonas*	Uncultured anaerobe

3.4 CONCLUSIONS

In this study the Gradient Tube method was developed in order to expand the size of the biofilm and thus enable sampling through its vertical profile. Results indicate the findings may be related back to physiological domains within the FSB. This may be a first report of such a methodology.

A number of conclusions may be drawn from these results:

- The complex nature of the biofilm has been confirmed and it has been shown that this is composed of a number of groups occupying physiologically defined niches.
- The formation the different bands and location of species at different levels in the Gradient Tubes, suggests that a spatial distribution of the different bacterial species across the FSB.
- The demonstration of differentiation and structural/functional relationships in the FSB further confirmed that it is indeed a true biofilm.

- These findings may present a first report that floating biofilms are structured as complex systems comparable to fixed biofilm systems. This appears to be a first report confirming the differentiation of structural relationships in FSBs.
- Having established the presence of some level of structural and physiological differentiation in the FSB system, it was then necessary to acquire more detailed insight into its physico-chemical environment in order to be able to comment on a structural/functional model describing the system.

4 ASPECTS OF FUNCTION IN THE FLOATING SULPHUR BIOFILM

4.1 INTRODUCTION

Okabe *et al.*, 1999 had noted that studies which relate microbial community structure to the function of a system, and thereby determine individual contributions to the aggregate population performance, are quite scarce in the literature. This may be attributed in part to methodological problems presented in effective *in situ* monitoring of microbial activities in small structures, such as some biofilms.

Within biofilms, the convection of compounds is hindered, and consequently limitations in mass transfer to the cells often limit conversion rates. Because of this resistance to mass transfer, biofilms develop various microenvironments, which can differ markedly from the bulk liquid. This complicates the interpretation of community structure/function analysis because extrapolation of community behaviour from that of individual cells is impossible without some knowledge of their microenvironment (Santegoeds *et al.*, 2002).

Schramm *et al.*, 1999 have noted that microsensors offer a direct and robust way to investigate these microenvironments. Microsensors may be used to measure a range of physico-chemical parameters such as Redox potential, pH, sulphide and dissolved oxygen (De Beer and Schramm, 1999). Due to their small size, microsensor measurement tends to cause minimal disturbances to the system and thus allows for micro-gradients within micro-environments to be measured with high fidelity (Santegoeds *et al.*, 2002). These gradients are a function of local transport rates (usually diffusion), and also substrate conversion rates, and thus allow for the spatial distribution of microbial activity to be derived from the substrate profiles.

An advantage of microsensor use is that the spatial gradient information acquired may be used to unravel closed cycles in a biofilm such as sulphate reduction coupled with sulphide oxidation. Santegoeds *et al.*, 2002 noted that the measurement of net substrate conversion usually underestimates the processes taking place within the biofilm as some internal metabolic cycles can be hidden. Even though these could be

playing a major role in the biofilm, they would not be reflected in the aggregate picture of the microbial community structure.

Ramsing *et al.* (1993) used microsensors and molecular techniques for the first time while investigating sulphate reduction in a trickling-filter biofilm. Schramm *et al.* (1999) combined microsensors and molecular techniques to study nitrification also using a trickling-filter biofilm. Both studies showed a good correlation between microbial conversion (sulphate reduction and nitrification) and microbial population distribution within the biofilms.

While considerable use has been made of microprobes in recent years, and these have been applied to the study of fixed biofilm systems (De Beer *et al.*, 1994), while no literature reports were found on their use in floating biofilm investigations. Thus the objective of this study was to use microprobes to explore the presence of gradients occurring across the depth of the FSB.

4.2 MATERIALS AND METHODS

The microsensors (Unisense) were set up and calibrated according to the manufacturer's instructions and used to measure sulphide, pH and Redox potential gradients present in the biofilm at the three stages of development.

4.2.1 Microsensor Set-up

Microsensors were used to measure pH, Redox potential and sulphide gradients within the FSB. The *in situ* measurements were taken at the three different stages of sulphur biofilm development (Thin, Sticky and Brittle). Prior to microprobe measurements, the inlet and outlet to the channel reactor were closed and the system was allowed 1 hour to stabilise from a continuous flow operation.

4.2.2 Microsensor Measurement

The microsensor apparatus was sourced from Unisense, Denmark and a typical set up is illustrated in Figure 4.1.

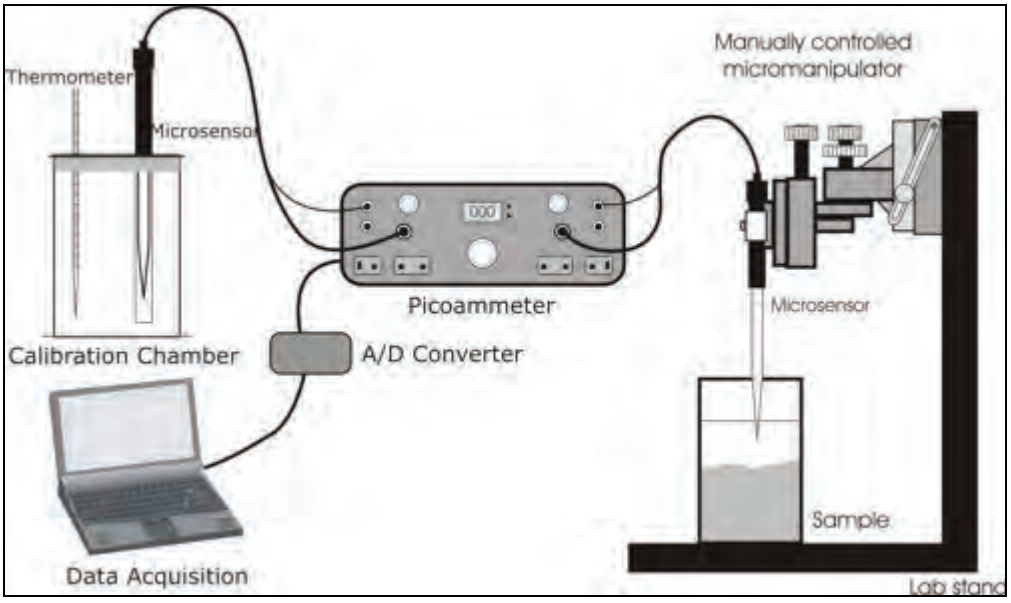

Figure 4. 1. An illustration of the microsensor system showing the component instruments used for analyzing biofilm samples. These include the microprobe, a micromanipulator and the interface and computer logger (Unisence, microsensor manual).

The system comprised of a manually controlled micromanipulator MM33. It had a precision range 10 μm in the x-axis and 100 μm in the y- and z-axes for clamping the microprobes during measurements. The picoammeter (for sulphide determination) and pH/ORP millivolt meter (for pH and Redox potential measurements) were used to detect the signal from the microsensor, after which it was converted to an analogue voltage output proportional to the microsensor signal. The output was then sent to the data acquisition device (computer) loaded with the Unisense Profix software that converts the signal reading to pH units and Redox potential millivolts. The sulphide signal measured was converted to concentration (mgL^{-1}) using a sulphide standard curve. In order to position the microsensors in the microenvironment, a laboratory stand was designed at EBRU and positioned over the reactor as shown in Figure 4.2.

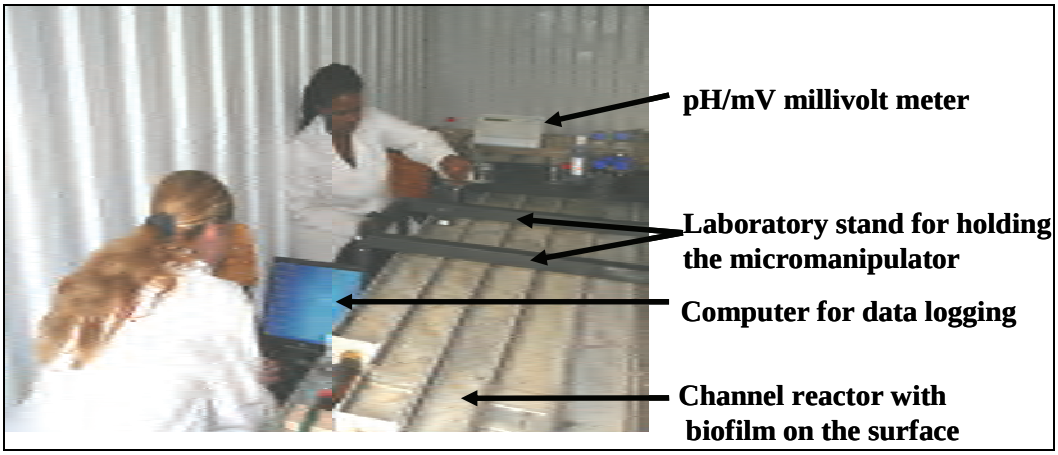

Figure 4. 2. The microsensor apparatus as set-up in the sulphur biofilm constant environment laboratory which housed the Linear Flow Channel Reactors. Measurements of Redox potential, pH and sulphide concentration were recorded.

4.2.3 Microelectrodes

pH and Redox potential electrodes were calibrated at 25^{o}C in a constant environment (CE) room using standard pH buffers (4, 7 and 10). The pH and Redox potential were measured with glass microelectrodes connected to a high-impedance pH/millivolt meter (PHM210). The pH and Redox potential electrodes used were miniaturized glass electrodes with an outer tip diameter of 20-20 µm. The reference electrode (REF 5000) used for pH and Redox potential measurements was a simple open-ended Ag-AgCl electrode with a gel-stabilized electrolyte with a tip diameter of 5000 µm. During calibration the reference and microelectrode were immersed in the same solution while connected to the millivolt meter and the same applied when the *in situ* measurements were taken.

The sulphide microelectrode was calibrated by measuring the signal in a dilution series of a standard solution (hydrogen sulphide dissolved in wastewater flushed with nitrogen to prevent sulphide oxidation). The concentration of the sulphide measured in the biofilm was calculated using the slope and intercept of the calibration curve. The sulphide electrode was found to show a linear response to sulphide concentrations between 0 and 500 mgL^{-1}.

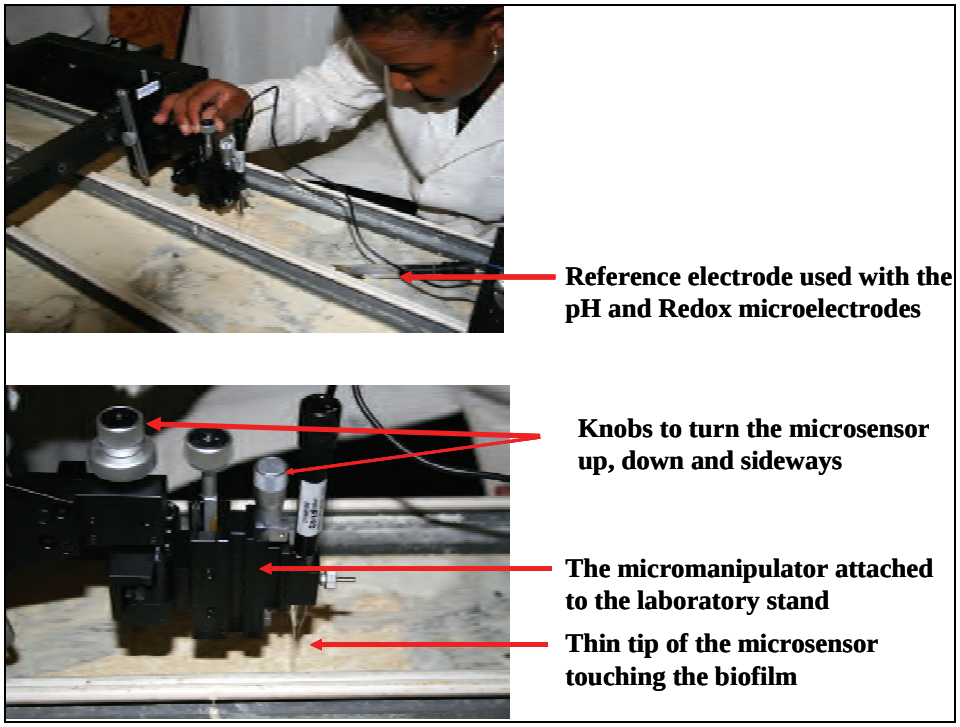

Figure 4. 3. A closer view at the micromanipulator and microsensor set up above the Linear Flow Channel Reactor while acquiring measurements across the depth of the floating sulphur biofilm.

The measurements were taken across a depth of 50 mm through the FSB and into the bulk liquid. Initial measurements were collected at 5 µm intervals from 0 to 400 µm depth after which the readings were taken at 100 µm intervals until 1 mm depth. Readings between one and ten millimeters depth were taken at 1 mm intervals into the bulk liquid. From 10 mm to 50 mm the readings were taken at 10 mm intervals. Thus, a total of five different measurement ranges were collected per microsensor for each of the different biofilm forms (Thin and Brittle) and the control (no biofilm). The results presented show a representative result of a (n = 5) set of each variable measured per biofilm stage. The results obtained for the Sticky biofilm were found to be very variable due to the Sticky biofilm adhering to the tip of the microsensor, and thus preventing free movement of the microsensor tip through the biofilm. As a result, the Sticky biofilm results have not been presented here.

4.2.4 Biofilm Thickness Measurement

The thickness of the biofilm was approximated from microprobe penetration during the measurements of sulphide, pH and Redox potential gradients at the three stages of biofilm development. However, the hydrated biofilm influences the bulk water system

underlying it and clear transitions are less easy to observe, especially for the Thin biofilm.

4.3 RESULTS AND DISCUSSION

The microsensor results have been presented for each investigation (pH, Redox potential and sulphide) in the form of depth profiles (y-axis) and measurements (x-axis). Each determination is comprised of four graphs (A to D) which detail the four different range intervals over which measurements were made (5 µm, 100 µm, 1 mm and 10 mm).

4.3.1 Sulphide

The microsensor results for the Thin, Brittle and Control samples over the depth 0 to 50 mm depth range are shown in Figures 4.4 to 4.6. Clearly defined sulphide gradients were observed to occur in the FSB system with pronounced differences seen between the control and biofilm samples as well as between the Thin and Brittle biofilm systems (Figure 4.4). From the results presented, the depth of the Thin and Brittle biofilm was observed to be 260 to 380 µm respectively which is a more accurate depth determination compared to the sandwiched biofilm micrometer measurement reported in Chapter 2. *In situ* reading of the fully expanded biofilm with its integrity intact provides an indication of the actual zone of influence of the biofilm.

The control sulphide depth profile shows a fairly constant reading at around 140 mgL^{-1} throughout the depth study down to 50 mm. The variability in results from the surface to 250 µm may reflect noise due to the increased frequency of measurement taken over this range (Figure 4.4). Both Thin and Brittle biofilms show similar trends in sulphide concentration through their vertical profile. At a depth of 50 µm, sulphides peak at around 125 mgL^{-1} and then fall again until a depth of 80 µm is reached. Thereafter, the vertical profile of sulphide in the respective biofilms differ.

In the Thin biofilm, the sulphide level shows a pronounced rise from 50 to 400 mgL^{-1} over the narrow depth range of 80 to 110 µm. It then declines gradually over the depth

range of 110 to 300 µm. From 300 µm depth sulphides gradual decline to 25 to 50 mgL^{-1} until the 50 mm depth is reached.

The Brittle biofilm shows similar trends but with a pronounced rise in sulphides starting somewhat deeper at 150 µm and then peaking at 450 mgL^{-1} at the concentration interface point. While its decline to 150 mgL^{-1} at around 300 µm is comparable to the Thin biofilm system, the concentration rises once again to 450 mgL^{-1} at around the 350 µm depth and then declines very gradually from this point until the 20 mm depth where it drops to levels comparable to that of the Thin biofilm system (Figure 4.4).

While the interpretation of these observations is dependent on the concomitant pH and Redox potential measurements, it is apparent that the biofilm has introduced profound changes in sulphide profile compared to the control system.

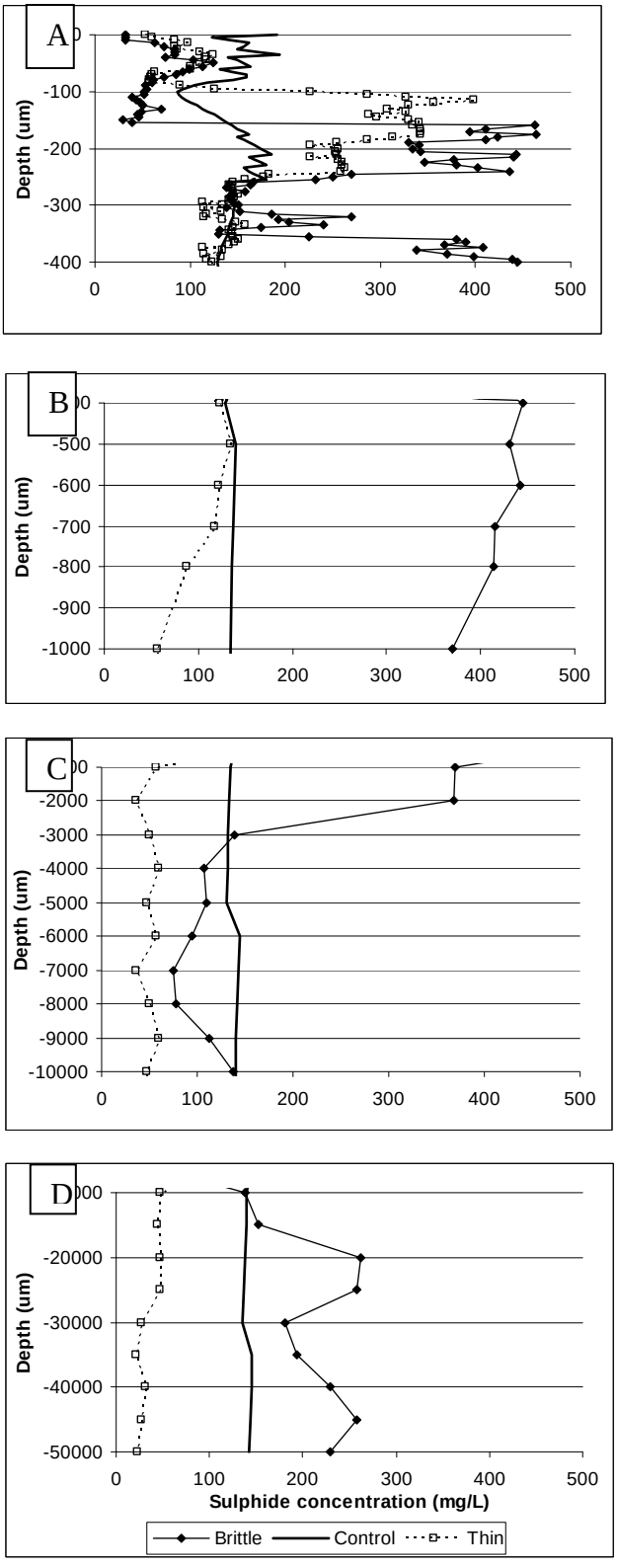

Figure 4. 4. Sulphide microsensor measurements of the Thin and Brittle biofilm compared to the control across 0 to 50 mm depth in ranges from 0 to 400 µm at 5 µm (A), 400 µm to 1 mm at100 µm intervals (B), 1 mm intervals to 10 mm at 1 mm (C) and 10 mm to 50 mm at 10 mm intervals(D).

4.3.2 pH

The result of the Thin, Brittle and control for pH measurements are shown in Figure 4.5. Both the Thin and Brittle biofilms showed a marked rise in pH immediately in the first 100 µm which was not seen in the control where the pH remained constant in the pH 7.3 to 7.8 range (Figure 4.5). The pH increase observed in the Brittle biofilm was higher than that of the Thin biofilm with the maximum pH measured being 8.9 and 10.8 for the Thin and Brittle biofilm respectively. This increase in biofilm pH could possibly be attributed to the sulphide oxidation reaction in which the production of elemental sulphur is associated with a hydroxyl ion being produced as a product according to Equation 4.1 (Steudel, 1996).

$$2HS^- + O_2 \rightarrow 2S^o + 2OH^- \qquad 4.1$$

This observation correlates with the pronounced fall of sulphide in this area. The higher reading in the Brittle biofilm may be correlated with higher sulphur production products observed in this system. The small rise in sulphide level observed within this area of increased pH (Figure 4.4) may indicate some sulphate reduction occurring here. This may occur due to some complete oxidation of sulphide taking place in addition to sulphur formation.

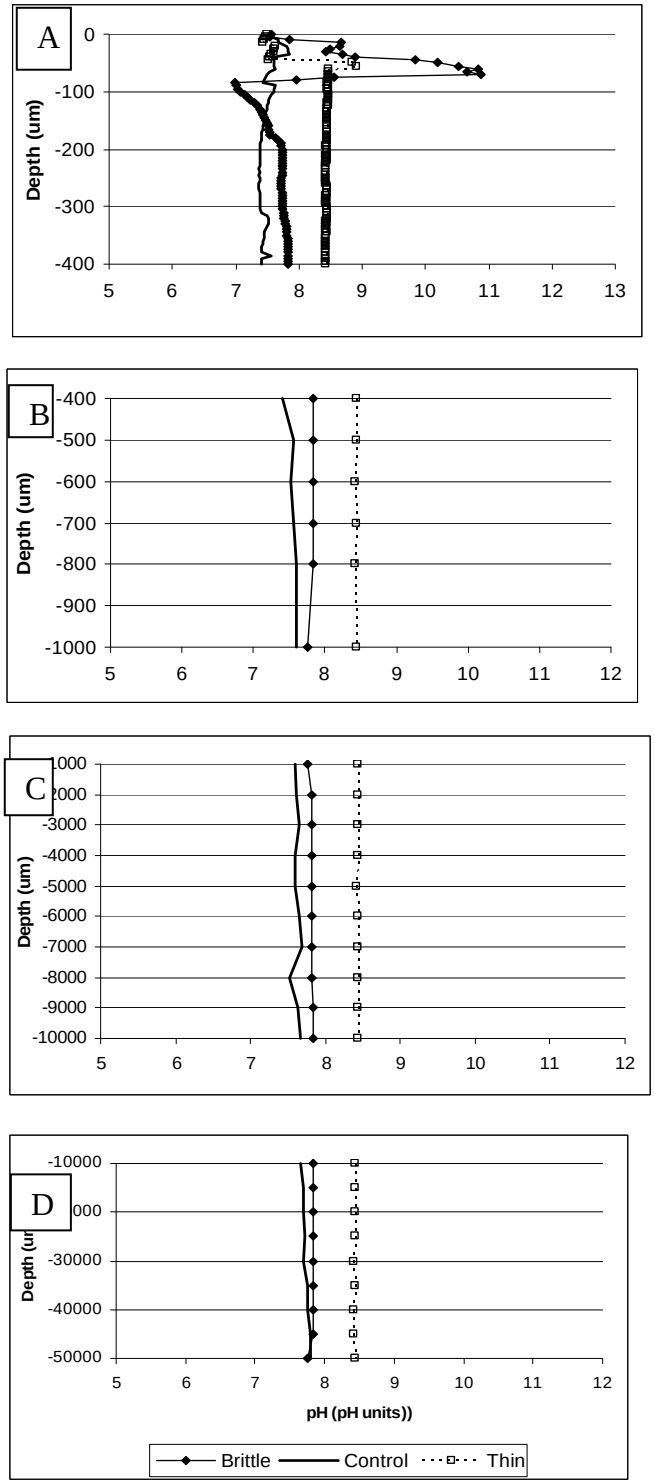

Figure 4. 5. pH microsensor measurements of the Thin and Brittle biofilm compared to the control across 0 to 50 mm depth in ranges of 0 to 400 µm at 5 µm intervals (A), 400 µm to 1 mm at 100 µm intervals (B), 1 mm to 10 mm at 1 mm intervals (C) and 10 mm to 50 mm at 10 mm intervals (D)**..**

4.3.3 Redox potential

The Redox potential readings in the three systems studied appear to correlate quite closely with the observations of sulphide and pH measurements noted above. The Redox potential falls sharply over the same range. Again the control shows little change from around 200 mV with a slight drop near to the surface.

However, in contrast to the rise in pH in the 50 µm depth range, the Redox potential falls sharply over the same range. In the case of the Thin biofilm there is a gradual decline from around 300 µm depth and in the Brittle biofilm it starts from around 280 µm depth.

Steudel (1996) had noted that the Redox window of -150 mV is required for the chemical oxidation of sulphide to elemental sulphur. This observation could also explain why sulphur crystal formation occurs readily in the Brittle biofilm compared to the Thin biofilm where the Redox potential barely reaches -80 mV.

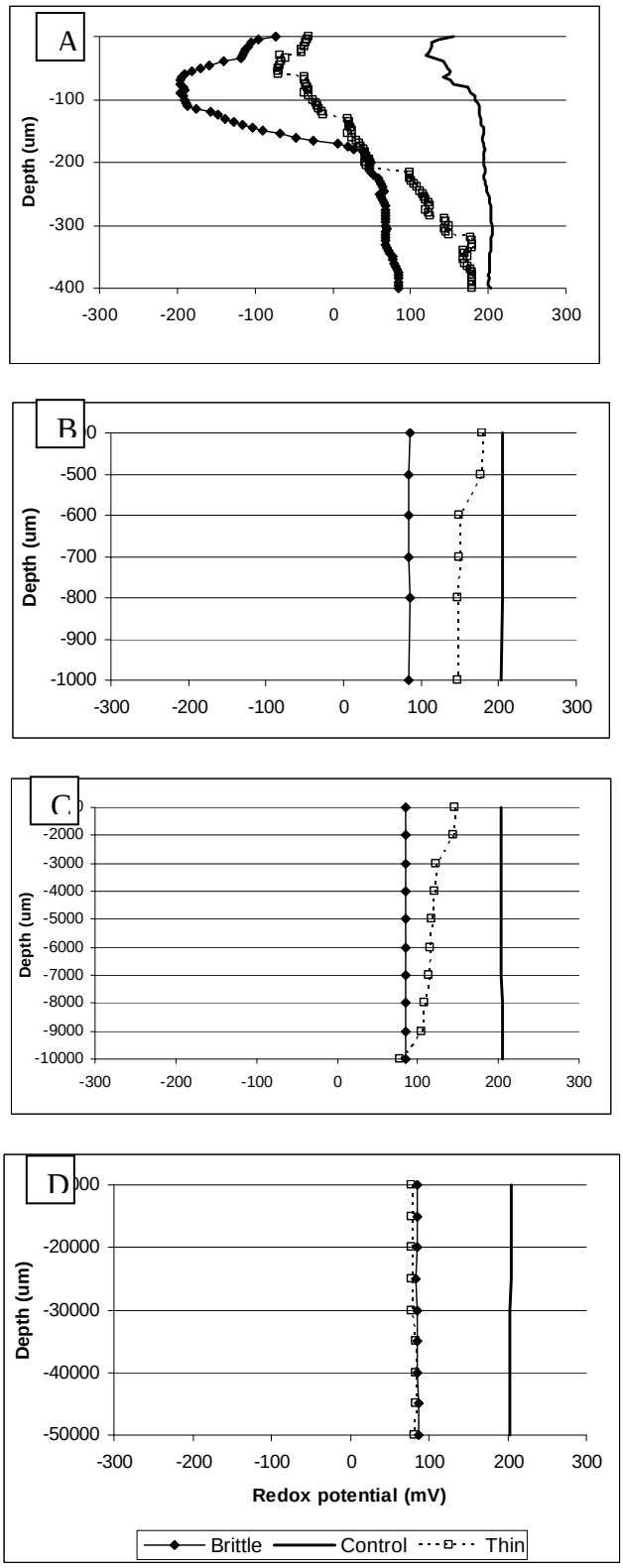

Figure 4. 6. Redox potential microsensor measurements of the Thin and Brittle biofilm compared to the control across 0 to 50 mm depth in ranges from 0 to 400 µm at 5µm intervals (A), 400 to 1 mm at100 µm intervals (B), 1 mm to 10 mm at 1 mm intervals (C) and 10 mm to 50 mm at 10 mm intervals (D).

4.4 CONCLUSIONS

The conclusions drawn from this study were as follows:

- Microsensors were used for the first time in the measurement of the characteristics of FSBs.
- Steep physico-chemical gradients were observed to be established across the system.
- An inverse relationship is observed between pH and Redox potential which correlates with sulphide removal in the biofilm. While comparable, the effect is more pronounced in the Brittle biofilm where sulphur production is also greater.
- Description of aspects of the physico-chemical environment of the FSB system provides for the integration of structural and microbial population data to propose a structural/functional account of the system. This accumulation of information enables the formulation of a descriptive model which is dealt with in the following chapter.

5. DEVELOPMENT OF A DESCRIPTIVE STRUCTURAL/ FUNCTIONAL MODEL FOR THE FLOATING SULPHUR BIOFILM SYSTEM

5.1 BACKGROUND

FSBs have not been well documented in the literature, despite their role in the natural sulphur cycle and their now apparent potential use in biotechnological process development (Rose, *et al*., 1996, Jorgensen *et al.*, 1998, Dunn, 1998). Attributes of the structure and function of the FSB have been described in the studies reported here and provide the basis, possibly for the first time, for constructing a descriptive model accounting for the performance of these systems.

The following summarises the main background information now available on these structures and provides the basic inputs that might be used in an attempt to construct a structural/functional descriptive model for the FSB phenomenon.

FSBs have been noted to occur on the surface of sulphide-rich organic wastewaters including the effluent of sulphate reducing bioreactors, sewage and tannery waste stabilisation ponds and sulphidic anaerobic lignocellulose wastes (Dunn, 1998, Jorgensen *et al.*, 1998, Rose *et al*., 1998);

In the channel reactor system developed for the study of FSB under laboratory conditions, and fed a lignocellulose-based effluent, the biofilm developed through three clearly defined stages termed here as Thin, Sticky and finally, Brittle film;

Light and electron microscopy studies revealed a complex, and apparently differentiated, biofilm structure composed of a range of bacterial morphologies, an apparent EPS architecture and putative sulphur crystals. SEM studies also showed that in addition to the crystals, small sulphur granules were also dispersed throughout the biofilm;

The sulphur composition of the crystals was confirmed in EDX, XRF and XANES studies;

Molecular microbial ecology studies of the FSB population showed the presence of aerobic sulphide oxidizing bacteria including *Thiobacillus*, *Halothiobacillus*, *Acidothiobacillus*, *Thiovirga*, *Sulfurimonas* and *Thiothrix*. Micro-aerophilic and

obligate anaerobic bacteria such as *Chryseobacterium*, *Bacteroides*, and *Planococcus* spp. and the copious EPS producer *Brevundimonas* sp. were also identified from the same structure. This suggested the establishment of both steep physico-chemical and physiological gradients within the system

The gradient tube experimental system was developed to extend the linear dimension of these gradients across an agar column and, with a mixed biofilm innoculum, to determine the selection and growth of individual members of the population at specific points across the gradient tube. This study strongly suggested that physiological gradients were, indeed, established in the system and that the various groups of bacteria identified established themselves under the specific conditions appropriate for their growth. A comparison of the molecular analysis for the gradient tubes and the whole mixed biofilm sample is summarised in Table 3.4;
Microsensor studies confirmed the presence of sulphide, pH and redox gradients across the FSB.

5.2 DESCRIPTIVE MODEL OF THE FLOATING SULPHUR

It is apparent from the experimental observations summarised above that the FSB is a true biofilm structure and shows clearly differentiated structural and functional characteristics. These data also provide an indication of how the system may function and, although possibly not yet in the correct sequence, the following steps of a descriptive model have been proposed and are outlined in Figures 5.1-5.4.

1. Aerobic and micro-aerophilic microorganisms establish at the air/liquid interface, possibly initially using liquid surface tension to maintain themselves in this zone. Given the anaerobic state of the bulk liquid, the growth of these organisms is constrained by oxygen diffusion, and an increasingly reductive environment is established across a steep gradient close to the air/liquid interface (~50 μm). The Eh is reduced from +180 mV to ~ -50 mV. The aerobic and micro-aerophilic forms include bacteria such as *Azoarcus* sp., that are able to degrade aromatics and other compounds released in the lignocellulose packed bed reactor. This may account for the Thin biofilm stage (Figure 5.1).

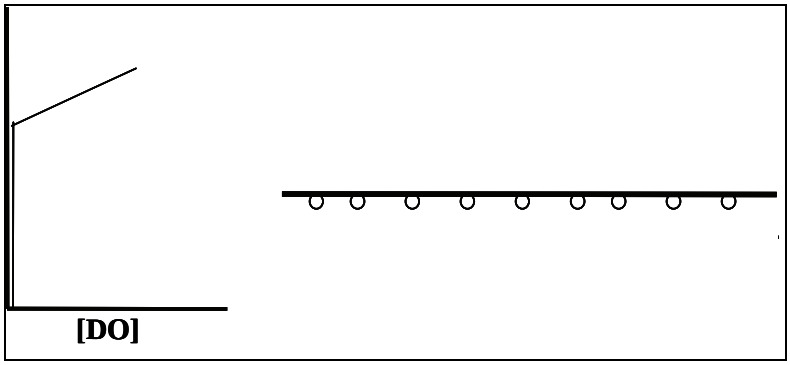

Figure 5. 1. Diagrammatic proposed account of observations in the Thin film or first stage of Floating Sulphur Biofilm formation. Here aerobic bacteria (circle) attach to the liquid surface (black line), the dissolved oxygen (DO) is rapidly reduced (assumed) and results in the establishment of the steep Redox gradients observed.

2. Once conditions have become anoxic and the Redox appropriately poised, anaerobic species such as *Brevundimonas* may start to grow within the lower reaches of the system and copious EPS production commences. The EPS could thus provide an expanding matrix and maintain a correctly poised microenvironment in which the sulphide oxidation reactions may occur. This may account for the appearance of the Sticky film as the slime producers locate underneath the initial aerobic population (Figure 5.2).
3. Once the above is in place, sulphide oxidising bacteria appear in larger numbers in the upper aerobic part of the biofilm with the production of possibly both internal and external sulphur globules. The biological sulphur may be released into the biofilm and this may be effected, to some degree, by protozoa grazing on the bacterial population in the biofilm. Sulphide oxidising bacteria which have been identified in the FSB, and are likely to occur here, include *Thiobacillus* , *Halothiobacillus, Thiothrix, Thiovirga, Sulfurimonas* and *Acidothiobacillus* spp. This may account for the first stage of sulphur formation observed in the Sticky and in the Brittle films (Figure 5.3).

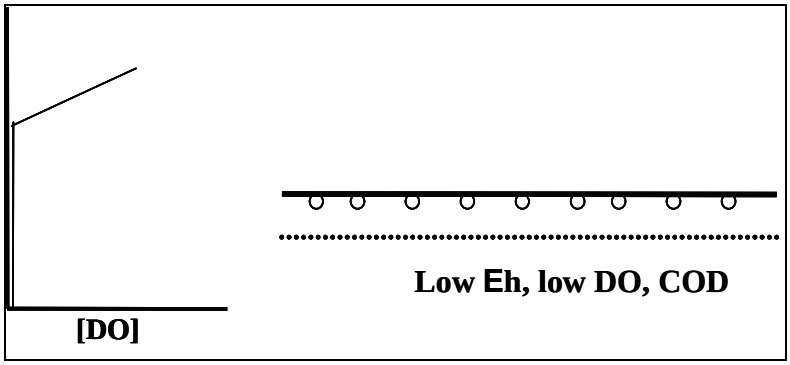

Figure 5. 2. Diagrammatic proposed account of observations in the Sticky film or second stage of Floating Sulphur Biofilm formation. Here micro-aerophilic and anaerobic bacteria establish in the system (circles) and copious EPS production commences (dotted line).

4. Where biological sulphur is released and dispersed through the biofilm, the formation of inorganic elemental sulphur may occur, based on the reaction mechanisms proposed to account for elemental sulphur formation in the presence of polysulphides (Steudel, 1996). In the initial steps, sulphide reacts with elemental sulphur and results in chain elongation to form polysulphide molecules of varying length (Sn^{2-}) until n = 9 (above n=9 the polysulphide chain is thought to be unstable).

$$HS^- + S_8 \rightarrow H\text{-}S\text{-}S_7\text{-}S \rightarrow H^+ + S_9^{2-} \quad (5)$$

Polysulphide is an unstable molecules and undergoes homolytic cleavage of the S_9^{2-} to produce a mixture of compounds including S_4^{2-} and S_5^{2-}.

$$S_9^{2-} + HS^- \rightarrow H^+ + 2S_5^{2-} \quad (6)$$

$$2S_5^{2-} \rightarrow S_4^{2-} + S_6^{2-} \text{ ….., etc.} \quad (7)$$

Once this chain elongation commences the presence of biological sulphur may no longer play a major role in the process with the sulphur/sulphide reaction resulting in the formation of elemental sulphur. Subsequently polysulphide chains may concatenate to form S_8^{2-} which in turn will aggregate to give rise to the sulphur crystals (possibly orthorhombic) observed in the EDX study.

Reaction 1 predicts the elevation of pH during sulphur production at an Eh window below ~ -150 mV. This is, indeed, observed in Figure 4.5, where the pH rises in the 0-100 μm zone from pH 7.7 to pH 11. Figure 4.6 shows the fall in Eh

from +50 mV to -200 mV in the 0 to 200 μm zone. At this point sulphide levels also plunge from 450 mgL to 25 mgL at the 150 μm depth in the biofilm, presumably due to consumption in the oxidation reaction.

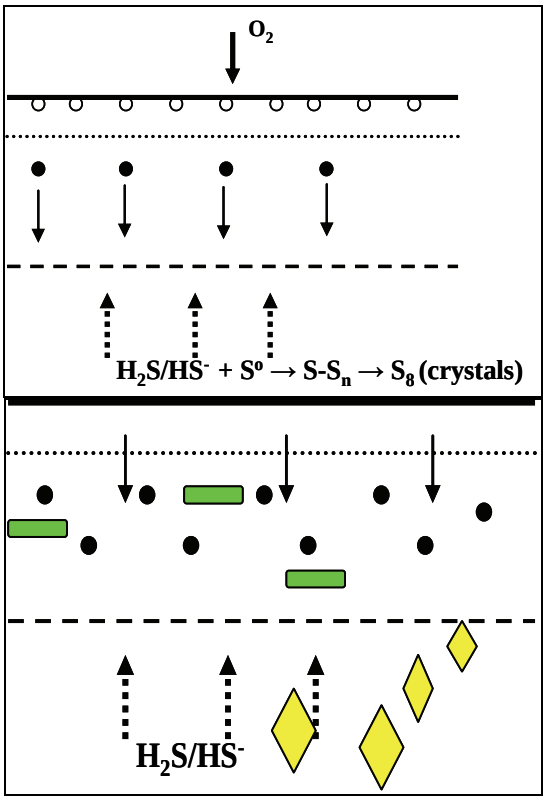

Figure 5. 3. Diagrammatic proposed account of observations in the Thick film or third stage of Floating Sulphur Biofilm formation. Here sulphide oxidising bacteria (green rectangle) establish in the upper aerobic reaches of the system and firstly small biological sulphur granules (black dot) are formed and then large sulphur crystals appear (yellow diamond).

Figure 5.4 shows a summary overview of the various process steps described above.

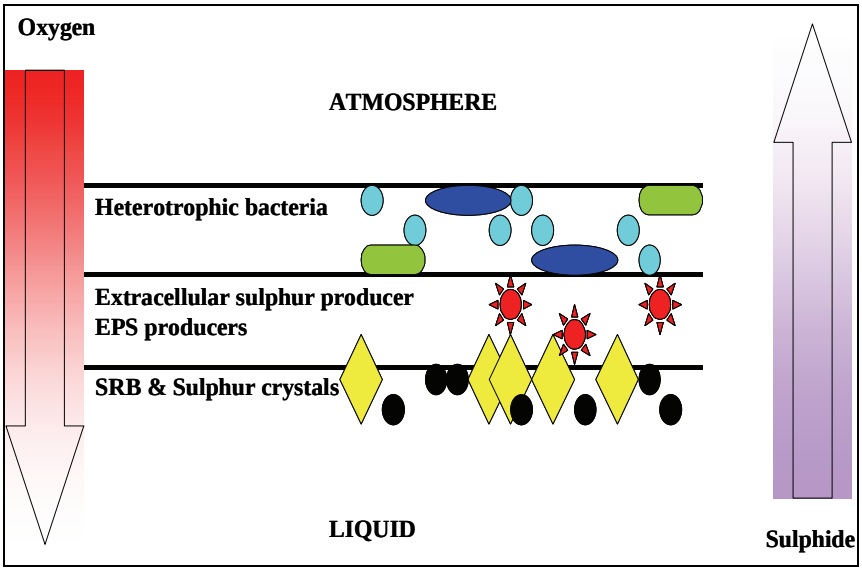

Figure 5. 4. Summary illustration of the descriptive model integrating the various processes occurring in the floating sulphur biofilm. These occur against falling DO and Redox potential gradients and sulphide migrating upwards into the biofilm. Aerobic heterotrophic bacteria (blue dots and green rectangles) establish at the air/liquid interface and, in consuming oxygen diffusing into the strongly anaerobic system, establish steep DO and Redox gradients at the surface. Below this layer, anaerobic exopolymeric substance producers generate a copious slime layer which constitutes the matrix of the biofilm (red stars). Within the correctly poised redox window, both biological (black dots) and inorganic sulphur formation occurs and gives rise to large sulphur granules which characterise the Thick film stage of the biofilm.

5.3 CONCLUSIONS

The objective of this study was to attempt to integrate the findings of the study and to develop a descriptive model accounting for structural and functional relationships in the FSB system. The principal findings were as follows:

- This study has shown that the FSB is a true biofilm which is differentiated in terms of structure, physiology and function;
- The crystals observed to form in the system were identified to be sulphur crystals;
- Steep physico-chemical and physiological gradients were identified to form within the FSB and correlated closely with predictive reactions for the system;
- The outcome of the structural/functional study may provide a basis for a rational approach in applying the FSB system in AMD treatment.

6. DEVELOPMENT OF THE LINEAR FLOW CHANNEL REACTOR AS A TREATMENT UNIT OPERATION

6.1 INTRODCUTION

Observations of the occurrence of FSBs, and the preliminary study by Gilfillan (2000) and then Bowker (2002) as well as this study, had suggested the possibility that the system may be developed and applied as a sustainable sulphide removal unit operation that could be linked to biological sulphate reducing processes. Work was initiated at EBRU in the development of a Linear Flow Channel Reactor and the following chapters outline this investigation. Bioreactor development was undertaken following laboratory scale investigation of the LFCR under controlled conditions taking the naturally occurring FSB to perform fundamental investigations.

The objective of this study was therefore to attempt possible application of the FSB phenomenon as a post treatment unit operation for the removal of sulphide generated during passive AMD treatment, particularly considering its robustness in terms of start up, and low maintenance requirement. The simplicity presented by this reactor design allows the volume to fluctuate according to the flows it is intended to treat and can be operated without the complexity of pumps. This complies with the requirements for routine but infrequent maintenance identified by Pulles (2002) as a prerequisite for passive treatment systems. The LFCR was scaled up from a two to a four and then to an eight channel reactor and investigated as a post treatment unit operation for sulphide removal from AMD treated effluent.

6.2 MATERIALS AND METHODS

6.2.1 Reactor Development and Optimisation

The Linear Flow Channel Reactor operated in the CE room and described in Chapter 2 was scaled up, through various stages (two- to four- and through to eight-Channel LFCR) in the investigation of process scale-up. This lead to the development of a sulphide removal system that produced elemental sulphur as the end product. The need for removal of residual sulphide from the effluent of the channel led to the

addition of two more channels to form a four-LFCR (Figure 6.1). The Four-Channel LFR had a surface area of 1.1 m^2 (2.5 m X 0.11 m).

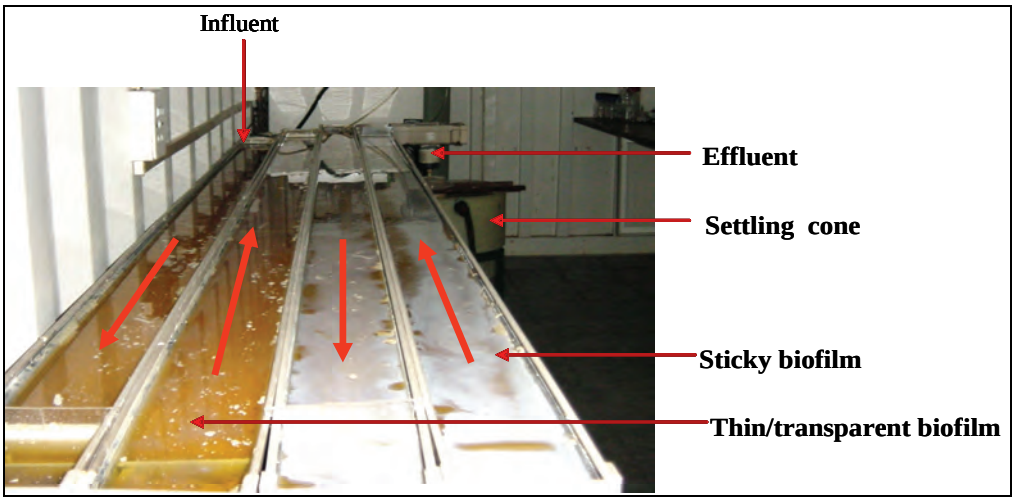

Figure 6. 1. Four-Channel Linear Flow Channel Reactor set up in the controlled environment room operating at 25^{o}C.

While monitoring the operation of the Four-Channel LFCR, further questions arose resulting in four more channels being added to form the Eight-Channel LFCR (Figure 6.2). This Eight-Cannel LFCR had a total surface area of 2.2 m^2.

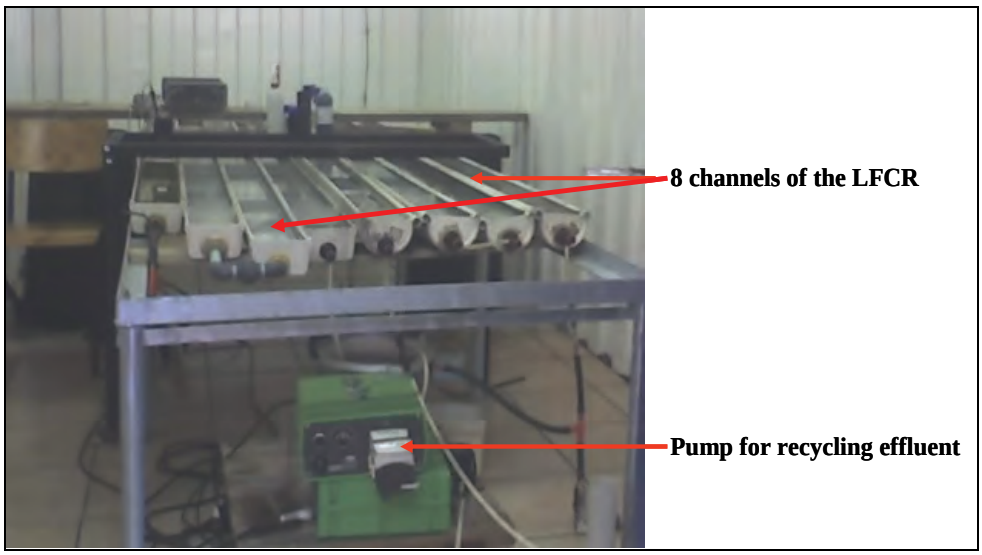

Figure 6. 2. Eight channel Linear Flow Channel Reactor operated in the controlled environment room at 25^{o}C.

6.2.2 Process Operation

The start up of the reactor involved the sourcing of feed from the DPBR described in Chapter 2 where the development of the FSB was observed. The reactor was allowed to run continuously for 24 to 48 hours until the development of the FSB from Thin through to Brittle had been observed. The biofilm was then harvested and allowed to form a sediment using the spraying technique described in Chapter 2, after which the channels were drained and cleaned of any FSB. At this stage the steady state of the reactor had been reached, and the influent and effluent measurements for mass balance calculations commenced. The reactor was then operated over a period of time ranging from 7 to 18 days at a time, and once sufficient data had been collected, the reactor would be drained.

The drained liquid from the reactor was measured and the volume calculated was used for mass balance calculations. After draining the residual water, the sediment was collected into funnels allowing further water to be drained and after which the sediment was dried in an oven at 80^{o}C for 3 to 5 days until no further weight loss could be detected. The weight was determined by placing the dried sample in the desiccator to cool off before being weighed and re-dried.

Influent and effluent samples of the LFCR were collected and analysed for different sulphur species including sulphur, sulphide, sulphate and thiosulphate. pH, Redox potential and COD were also measured.

The channel reactor was initially operated at various flow rates to determine optimum flow for biofilm formation. As a result, 2 618 L.m^{-2}.d^{-1} was chosen as the optimum flow and 1 309 L.m^{-2}.d^{-1} was used as the half flow of operation. It was also noted that the potential application of this type of technology would be in passive AMD treatment systems as a post-treatment unit for removing sulphide from the effluent of the upstream sulphate removal units. Thus the conditions under which the reactor would operate in practicality would be in conditions similar to these where the passive treatment systems are currently operating.

Temperature was regarded as an important controlling variable that needed to be understood, as previous experience had shown that biofilm formation is sensitive to temperature and flow rate. Thus, in this investigation temperature was varied over a range representing summer and winter conditions. Operation of the reactor was tested at three temperatures, namely, 25, 20 and 15^{o}C. The 20^{o}C represents the average or median while 25^{o}C and 15^{o}C represent the summer and winter season highs and lows respectively.

This study attempted to replicate the natural sulphur formation phenomenon, observed outdoors on the surface of sulphide-rich tannery ponds, under controlled environment conditions, in order to investigate the yields of sulphide removal at different temperatures and flows.

6.2.3 Analysis

Triplicate samples were drawn for each of the data sets reported and analysed for sulphide, sulphate, thiosulphate, sulphur and pH. Results were averaged and reported as the mean of three samples.

6.2.3.1 Sulphide

The Merck® Spectroquant system was used for sulphide determination (Merck®, South Africa). Samples were collected in test tubes containing 100 µL of 0.1 m zinc acetate solution. Photometric readings were made using the SQ 118 spectrophotometer (Merck).

6.2.3.2 Sulphate and Thiosulphate

Ion chromatography was used for the determination of sulphate with a model 600 Waters high pressure liquid chromatograph (HPLC) and model 432 Waters conductivity detector (Waters, South Africa) fitted with an IC-Pak^{TM} anion 4.6 X 50 mm column (Waters, South Africa). Samples were prepared using a ten-fold dilution of sample in milli-Q water and then filtered through a 0.45 µm nylon filter before passing it through two Waters Sep-Pak® light C_{18} cartridges (Waters, South Africa) to

remove contaminating organic compounds. The samples were then injected and run at 1 mL.min^{-1} and analysed using the EMPOWER software programme (Waters, South Africa). A Borate/Gluconate buffer concentrate (Appendix B) was used for eluent (Appendix B) preparation. All chemicals and filters were from Merck®, South Africa. A standard concentrate (Appendix B) containing Fe^{-}, Cl^{-}, NO^{3-}, Br^{-}, HPO_4^{2-} and SO_4^{2-} in milliQ water was prepared. The injected standard was prepared weekly by diluting 100 µL of the concentrate standard in 100 mL of milliQ water.

6.2.3.3 pH

pH was measured using a WTW pH330 meter (Merck ®, South Africa).

6.2.3.4 Sulphur

A modified Mockel (1984), reverse HPLC method was used for sulphur determination. Three 1 mL samples were collected, centrifuged for 5 minutes at 13 000 rpm on an Eppendorf, centrifuge 5415D (Merck®, South Africa), and air dried. After drying, 1 mL of acetone was added to the pellet, and left to stand for 1 hour with vigorous shaking every ten minutes. The samples were filtered through a 0.45 µm nylon filter (Merck, South Africa) and analysed using the EMPOWER software on a 600 model Waters HPLC and a 2487 model dual λ absorbance detector fitted with a Nova-Pak® C18 3.9X150 mm column (Waters, South Africa). The samples were injected into the HPLC and run at 2 mL.min^{-1} using a 5:95 ratio of water: methanol (Hypersolv for HPLC, BDH from Merck®, South Africa) as the eluent. A 20 ppm standard of elemental sulphur (Appendix B) in acetone was prepared and injected with samples for standardisation.

6.2.3.5 Chemical Oxygen Demand

Chemical oxygen demand (COD) was assayed using a digestion and titration method outlined in Standard Methods (APHA, 1998). The sample was oxidised in a boiling solution of acidic potassium dichromate ($K_2Cr_2O_7$) containing silver sulphate (Ag_2SO_4)., Glass balls, 1 g mercuric sulphate ($HgSO_4$), 25 mL of water, 10 mL sample, 40 mL digestion mixture and additional water to make up the solution to 100

mL were added to an Erlenmeyer flask attached to a condenser. The mixture was refluxed on a hot plate for two hours after which it was cooled. Four drops of ferroin indicator were added before titrating with 0.1N ferrous ammonium sulphate. A red-brown to blue endpoint was used.

The COD concentration in mgL^{-1} was calculated as: (A-B) x [N/a] x 8000

Where:

A = mL ferrous ammonium sulphate solution for blank
B = mL ferrous ammonium sulphate solution for sample
a = mL aliquot of sample
N = Normality of ferrous ammonium sulphate solution (derived from standardisation of [10 mL of potassium dichromate, 125 mL of sulphuric acid: water (1:3), 4 drops ferroin indicator in 300 mL Erlenmeyer flask] with ferrous ammonium sulphate was titrated to a red brown to blue end point).
N = [0.25/ mL titre]

6.2.3.6 Sulphur Biofilm Harvesting

After each reactor run, covering a range of operating conditions, the system was shut down and drained and the settled biofilm collected and dried at $80^{o}C$ for three to five days.

6.2.3.7 Mass Balance

Mass balances were calculated to account for influent, effluent and recovered sulphur species. Based on previously reported results for sulphur biofilm formation (Rein, 2002; Bowker, 2002), it was assumed that the major sulphur species fraction in the biofilm could be recovered as S^{o} (elemental sulphur), S_8 (orthorhombic sulphur form), Sn^{-} (polysulphide), HS^{-}(sulphide ion computed to a counter cation), $S_2O_3^{-}$ (thiosulphate ion computed to a counter cation) and SO_4^{2-} (sulphate ion also computed to a counter cation). Some of the data reported above provides a further preliminary indication of the sulphur species present in the biofilm. However, for the purposes of

the mass balance calculation, the biofilm sulphur fraction was considered to consist of elemental sulphur.
The percentage mass balance recovery was calculated as follows:

Total sulphur species IN = Total sulphur species OUT + Total sulphur RECOVERED.

$S^o + SO_4^{2-} + HS^- + S_2O_3^- = (S^o + SO_4^{2-} + HS^- + S_2O_3)_{OUT} + (S^o + SO_4^{2-} + HS^- + S_2O_3)$ RECOVERED

Mass balance loss (%) = $[(S_{IN} - S_{OUT}) + (S_{RECOVERED}) / S_{IN}] * 100$

Mass balance recovery (%) = 100 – Mass balance loss

Sulphide removal (%) = $[(\text{Sulphide}_{IN} - \text{Sulphide}_{OUT})/\text{Sulphide}_{IN}]*100$

Sulphur recovery (%) = $[(\text{Sulphur}_{OUT} - \text{Sulphur}_{IN})/\text{Sulphide}_{IN}]*100$

6.2.3.8 Statistical validation

Statistical validation of the data was performed using the software package Statistica (data analysis software system) Version 7.1 (StatSoft, Inc 2005).

6.3 RESULTS AND DISCUSSION

6.3.1 Four-Channel Linear Flow Channel Reactor Operation

Following reactor development studies in which the Four-Channel LFCR was commissioned, optimization investigations commenced. This involved operation of the LFCR over a range of temperature and loading rate conditions. These are reported below together with the mass balance data. The objective was to determine operational conditions on which a process scale-up programme could be based. In each case, the results reflect a start up to shut down period following steady state operation of the system.

6.3.1.1 Four-Channel Linear Flow Channel Reactor operated at 25^{o}C and 2 618 L.m^{-2} d^{-1} loading rate.

The four channel LFCR was operated continuously from start up for a period of 24 days at 25^{o}C and a 2 618 L.m^{-2} d^{-1} loading rate. Figure 6.3 shows the results of this study and reports data for analysis of sulphide (A), sulphate (B), sulphur (C) and thiosulphate (D) over this period. The mean of the distribution of the data is plotted in Figure 6.4 showing sulphide (A), sulphate (B), sulphur (C) and thiosulphate (D). A standard t-test was used to determine the significance of the results.

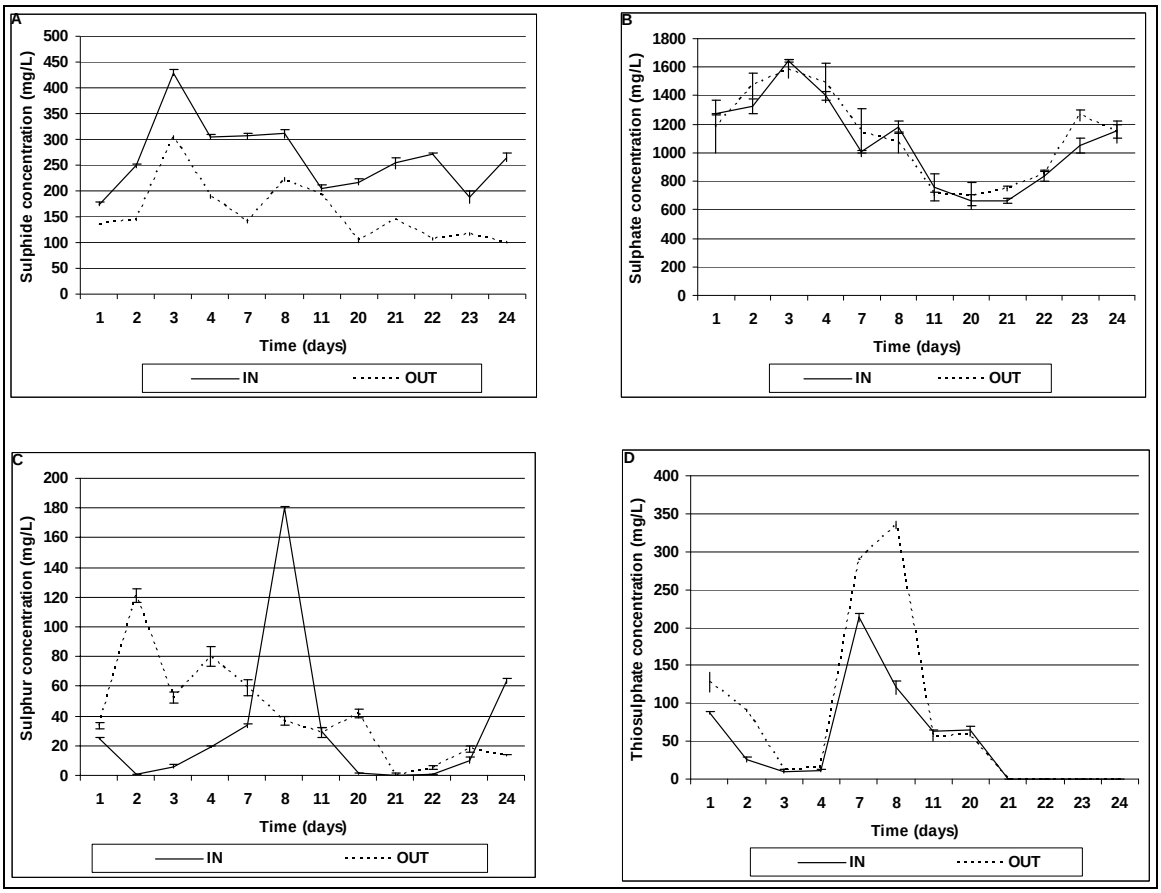

Figure 6. 3. Influent and effluent sulphur species measured in the Four-Channel Linear Flow Channel Reactor over 24 days at 25^{o}C and 2 618 L.m^{-2} d^{-1} loading rate. Sulphide (A), Sulphate (B), Sulphur (C) and Thiosulphate (D).

Fluctuations in the feed concentration of all sulphur species were observed which is consistent with use of the lignocellulose packed bed reactor system and has been reported elsewhere (Molwantwa *et al.*, 2003). The results in Figure 6.3(A) showed maximum influent sulphide concentration of 420 mgL^{-1} and a minimum of 180 mgL^{-1}

with an average influent and effluent sulphide concentration of 161 and 74.3 mgL^{-1} respectively over the 24 days

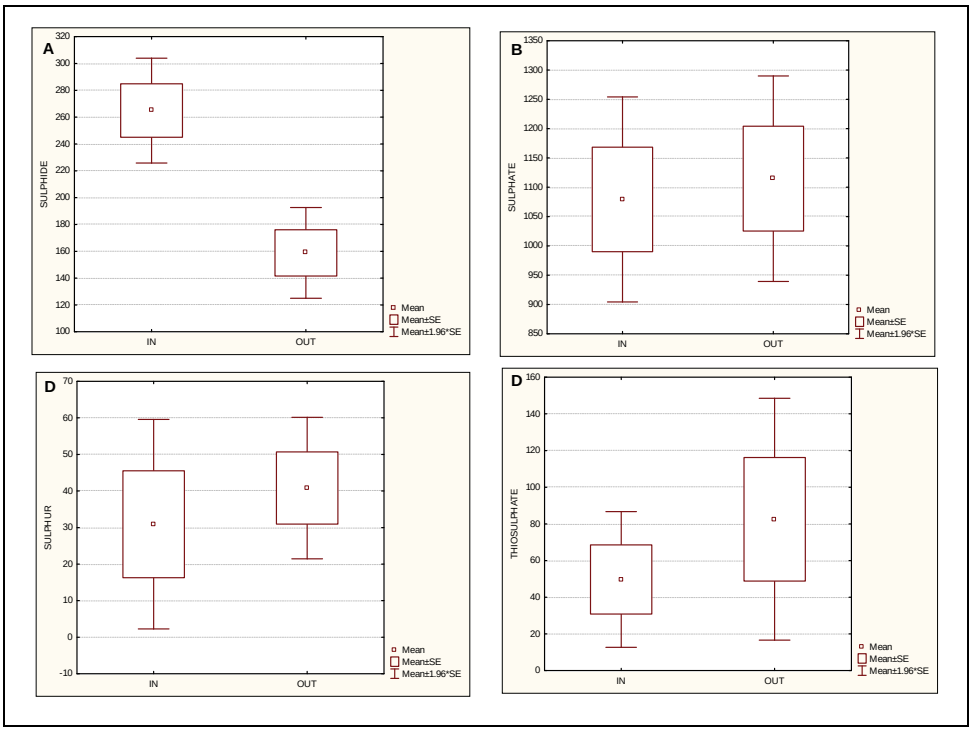

Figure 6. 4. Box and whiskers plot of the Four-Channel Linear Flow Channel Reactor operated at 25°C and 2 618 $L.m^{-2}d^{-1}$ showing the mean of distribution of influent and effluent sulphide (A), sulphate (B), sulphur (C) and Thiosulphate (D) over the 24 days operation period.

Figure 6.4 indicates a significant average percentage sulphide removal of 54% across the system ($t = 4.024$; $df = 22$; $p<0.05$). However, Figure 6.4(B) shows an average of 1203 and 1292 mgL^{-1} influent and effluent respectively which indicates that the average sulphate increase of 6.8% was not significant ($t = -0.28$; $df = 22$; $p = 0.78$). Thiosulphate removal of 37% (Figure 6.3D) was also not significant ($t = -0.85$; $df = 22$; $p = 0.401$). These results indicate partial to complete oxidation of influent sulphide beyond the intermediate sulphur step. Neither oxygen nor Redox potential is under control in this system and controlling the oxidation of sulphide beyond the sulphur step would form an important objective in the optimization of the LFCR sulphide removal process. Elemental sulphur in suspension (Figure 6.3C) shows some variability and possibly reflects sulphur that may have been formed in the feed system and also particles of the biofilm which break away and remains in suspension following biofilm harvesting. The difference between the influent sulphur concentration of 107 and 92.3 mgL^{-1} in the effluent sulphur was not significant

(t = -0.56; df = 22; p = 0.58). These changes, as well as the sulphur recovered in the biofilm harvesting operation, are taken into account in the mass balance calculation (Table 6.1).

6.3.1.2 Four-Channel Linear Flow Channel Reactor operated at 25^{o}C and 1 309 L.m^{-2} d^{-1} loading rate.

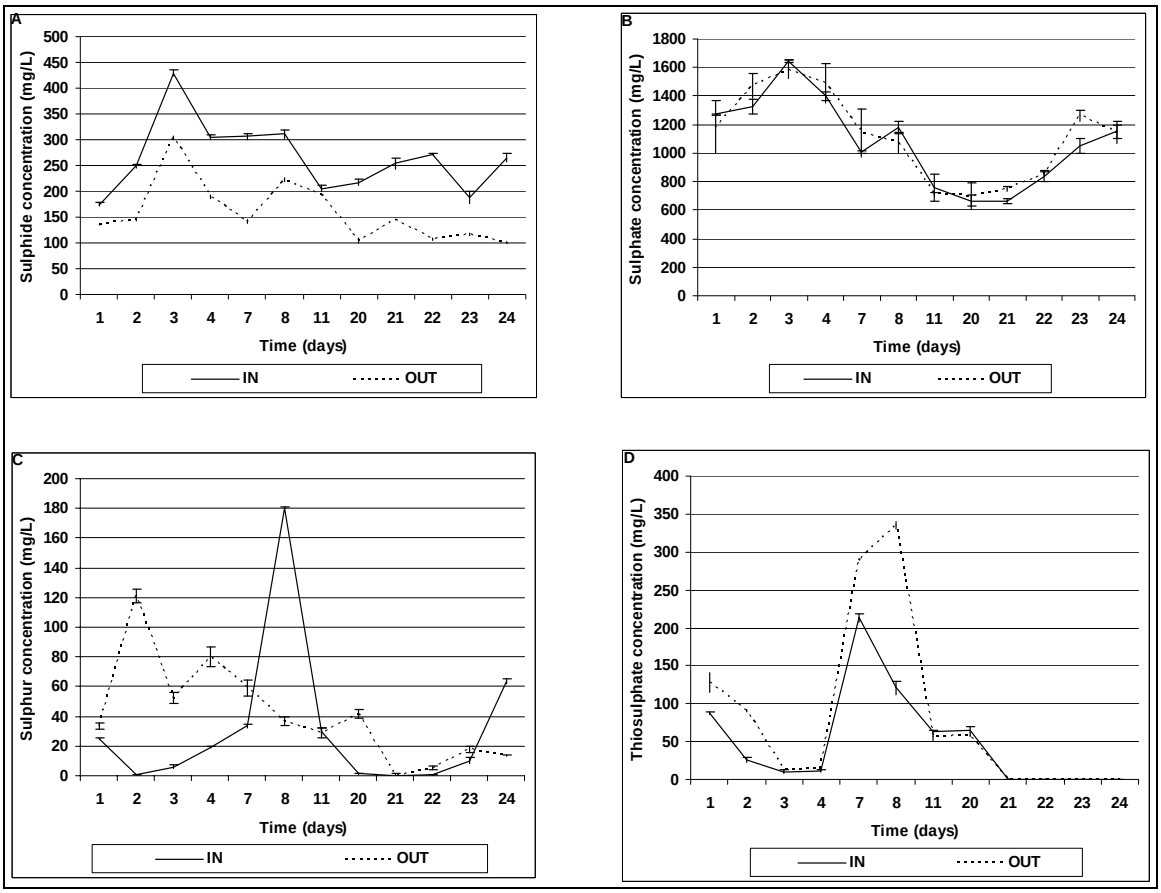

Figure 6. 5. Influent and effluent sulphur species measured in the Four Channel Linear Flow Channel Reactor over 19 days at 25^{o}C and 1 309 L.m^{-2} d^{-1} loading rate. Sulphide (A), Sulphate (B), Sulphur (C) and Thiosulphate (D).

Fluctuations in the feed were also observed when the Four-Channel LFCR was operated at 25^{o}C and 1 309 L.m^{-2} d^{-1} loading rate (Figure 6.5 and 6.6). The results in Figure 6.5(A) showed an average influent and effluent sulphide concentration of 159 and 75 mgL^{-1} respectively over the 19 days. This indicates a significant average percentage sulphide removal of 52% across the system (t = 7.49; df = 9; p < 0.05). Figure 6.5(B) shows an average 5.8% increase of sulphate across the reactor which was not statistically significant, as was the increase in thiosulphate (Figure 6.5D) (t = -1.27; df = 9; p = 0.22).

It is apparent from these observations that partial and complete sulphide oxidation in the LFCR was low. Figure 6.5 and 6.6(C) indicates that the change in sulphur across the system of 7% was not significant (t-test, t = 0.18; df = 9; p = 0.85).

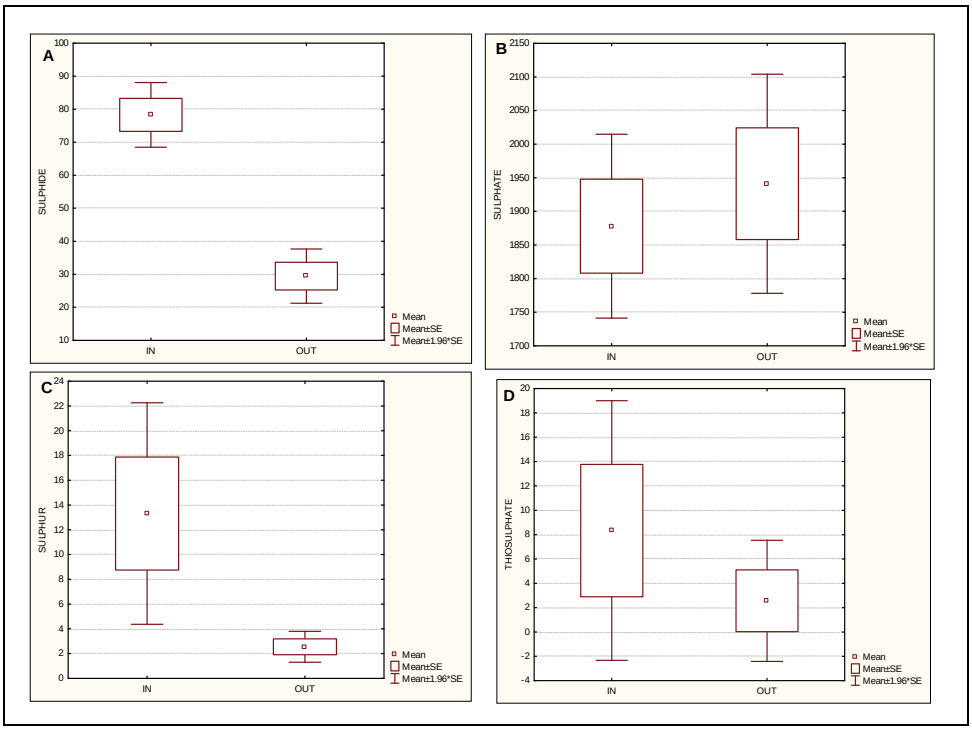

Figure 6. 6. Box and whiskers plot of the Four-Channel Linear Flow Channel Reactor operated at 25^{o}C and 1 309 L.m^{-2}d^{-1} showing the mean of distribution of influent and effluent sulphide (A), sulphate (B), sulphur (C) and thiosulphate (D) over the 19 days operation period.

6.3.1.3 Four-Channel Linear Flow Channel Reactor operated at 20^{o}C and 2 618 L.m^{-2} d^{-1} loading rate.

Figures 6.7 and 6.8 show influent and effluent data of the sulphur species for the Four-Channel LFCR operated at steady state over 8 days at 20^{o}C and 2 618 L.m^{-2} d^{-1} loading rate. The sulphide results Figure 6.7A showed an average influent and effluent sulphide concentration of 109 and 29.7 mgL^{-1} respectively indicating a highly significant average percentage sulphide removal of 72% (t = 8.07; df = 10; p = 0.001)

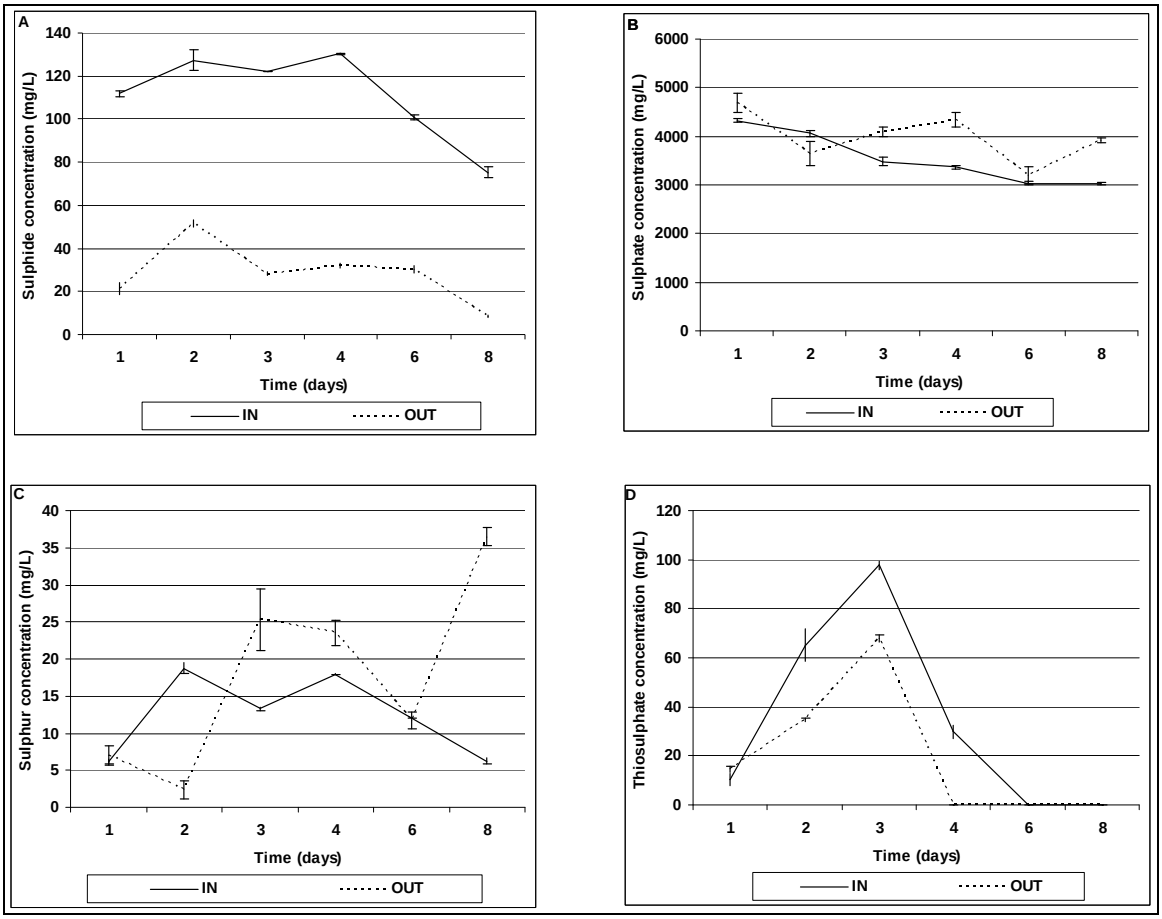

Figure 6. 7. Influent and effluent sulphur species measured in the Four Channel Linear Flow Channel Reactor over 8 days at 20°C and 2 618 $L.m^{-2}$ d^{-1} loading rate. Sulphide (A), Sulphate (B), Sulphur (C) and Thiosulphate (D).

Sulphate results (Figure 6.7 B) showed that the oxidation of sulphate to sulphide in the system was not significant with an average sulphate increase of 10% ($t = -0.97$; $df = 10$; $p = 0.36$). The increase in thiosulphate and sulphur was also not significant ($t = 0.72$; $df = 10$; $p = 0.48$).

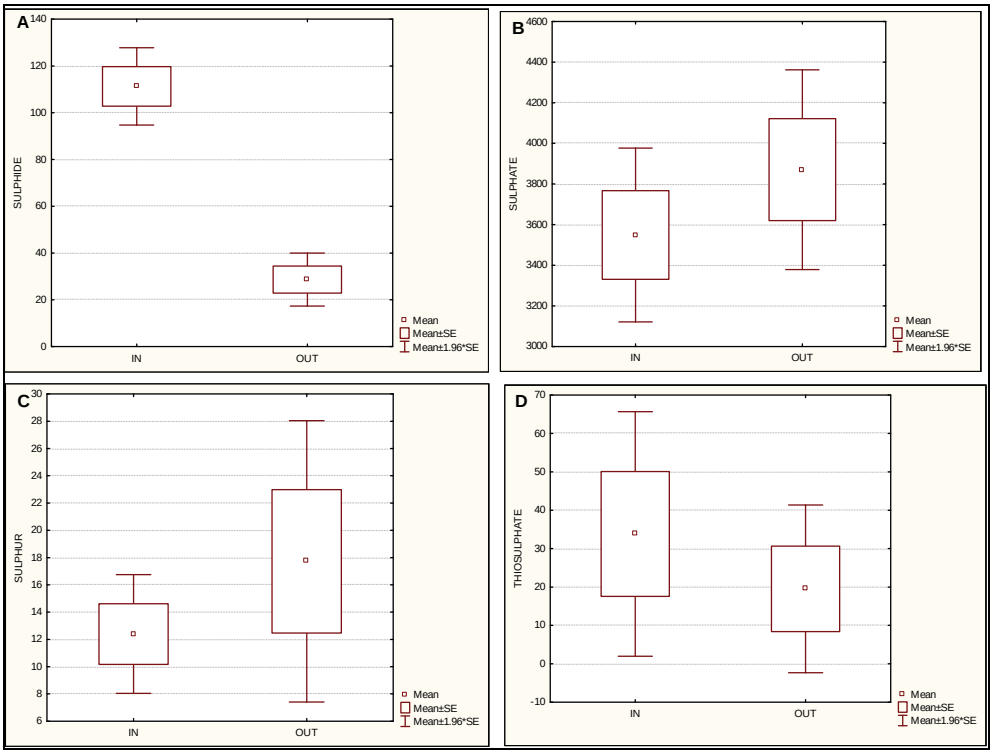

Figure 6. 8. Box and whiskers plot of the Four-Channel Linear Flow Channel Reactor operated at 20^{o}C and 2 618 L.m^{-2}d^{-1} showing the mean of distribution of influent and effluent sulphide (A), sulphate (B), sulphur (C) and thiosulphate (D) over the 8 days operation period.

6.3.1.4 Four-Channel Linear Flow Channel Reactor operated at 20^{o}C and 1 309 L.m^{-2} d^{-1} loading rate.

The Four-Channel LFCR was operated at steady state over a 9 day period at 20^{o}C and 1 309 L.m^{-2} d^{-1} loading rate (Figure 6.9&6.10). The sulphide results showed an average influent and effluent sulphide concentration of 88.1 and 36.1 mgL^{-1} respectively indicating a significant average percentage sulphide removal of 59% ($t = 7.49$; $df = 10$; $p < 0.05$). The increase in sulphate and thiosulphate were not found to be significant ($t = -058$; $df = 10$; $p = 0.57$ and $t = 0.96$; $df = 10$; $p = 0.35$ respectively). However, the increase in the sulphur concentration in the effluent of 55.4% was found to be significant ($t= 2.33$; $df = 10$; $p <0.05$).

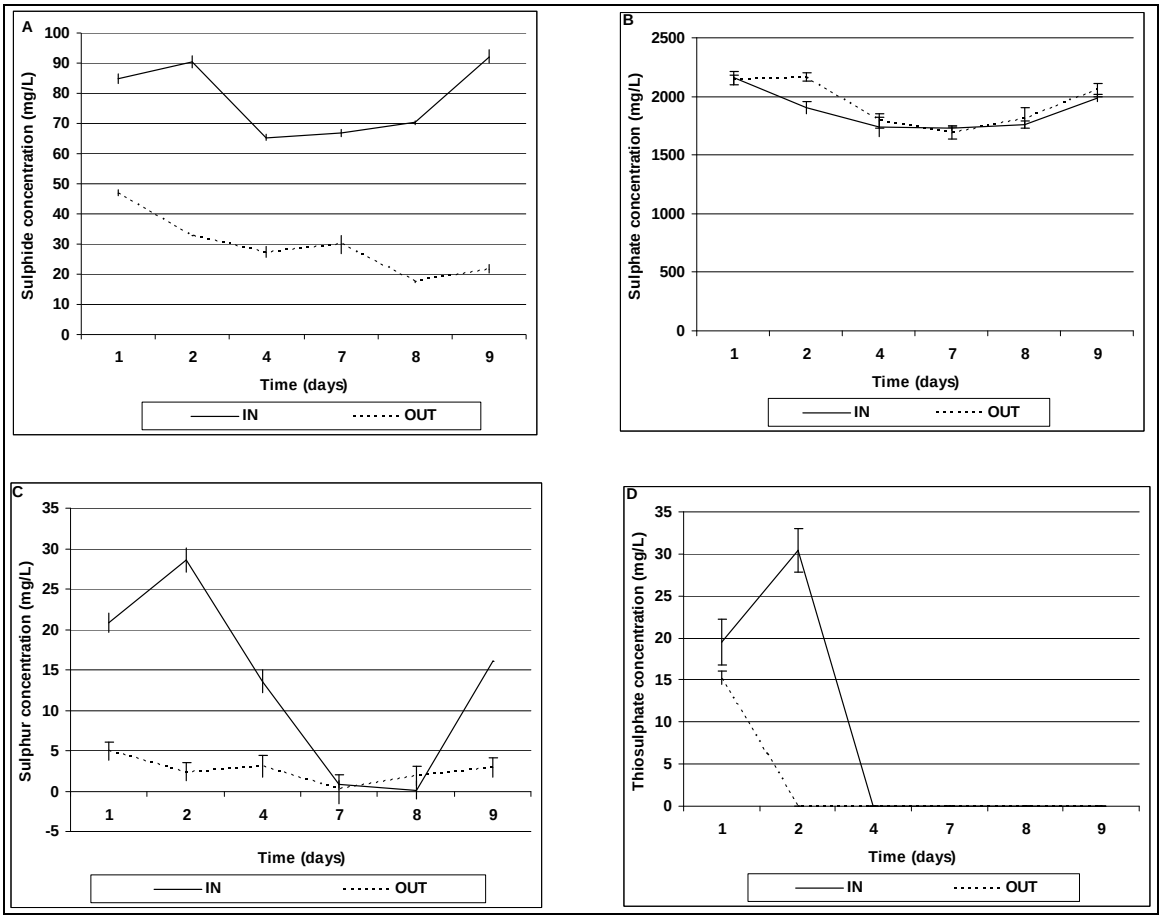

Figure 6. 9. Influent and effluent sulphur species measured in the Four Channel Linear Flow Channel Reactor over 8 days at 20^{o}C and 1 309 L.m^{-2} d^{-1} loading rate. sulphide (A), sulphate (B), sulphur (C) and thiosulphate (D).

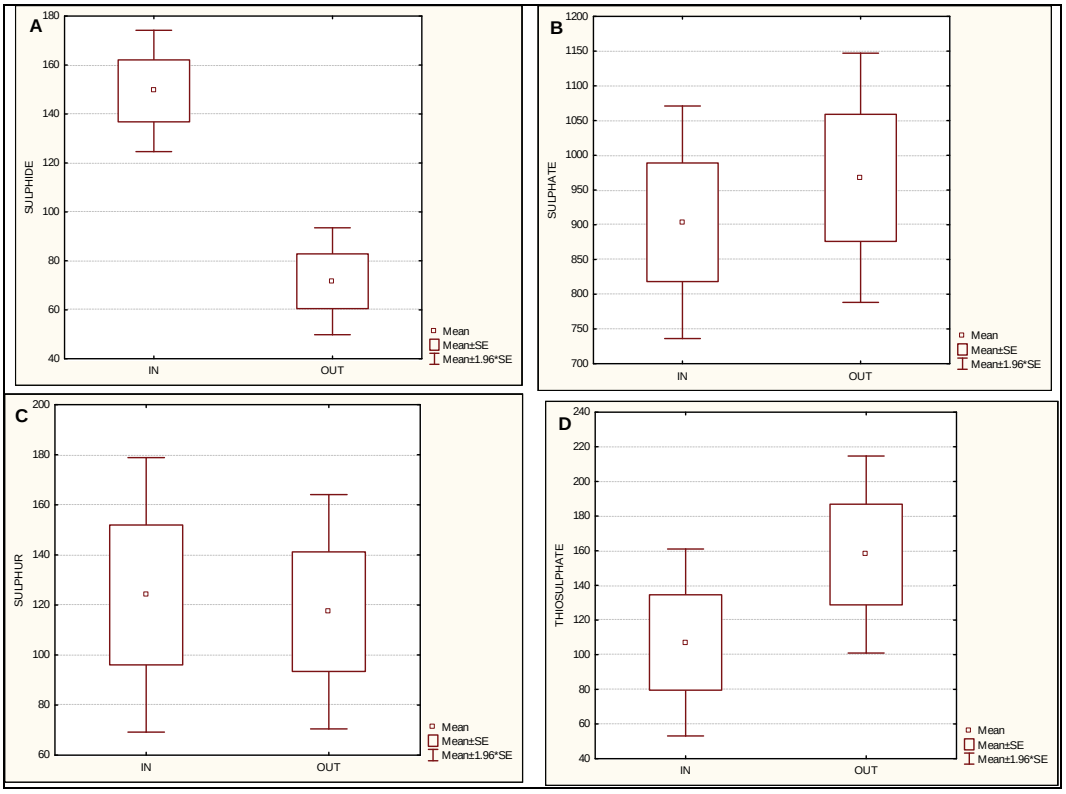

Figure 6. 10. Box and whiskers plot of the Four-Channel Linear Flow Channel Reactor operated at 20^{o}C and 1 309 L.m^{-2}d^{-1} showing the mean of distribution of influent and effluent sulphide (A), sulphate (B), sulphur (C) and thiosulphate (D) over the 8 days operation period.

6.3.1.5 Four-Channel Linear Flow Channel Reactor operated at 15^{o}C and 2 618 L.m^{-2} d^{-1} loading rate.

The Four-Channel LFCR was operated at steady state over a 7 day period at 15^{o}C and 2 618 L.m^{-2}.d^{-1} loading rate (Figure 6.11 & 6.12). The removal of sulphide across the system of 146 and 75.6 mgL^{-1} respectively indicating a significant 48% average sulphide removal ($t = 4.21$; $df = 8$; $p < 0.05$). The increases in sulphate and thiosulphate were not significant (t-test, $t = -0.91$; $df = 8$; $p = 0.39$) and (t-test, $t = 0.64$; $df = 8$; $p = 0.53$) respectively. The increase in sulphur in the effluent was not significant ($t = 0.56$; $df = 8$; $p = 0.56$).

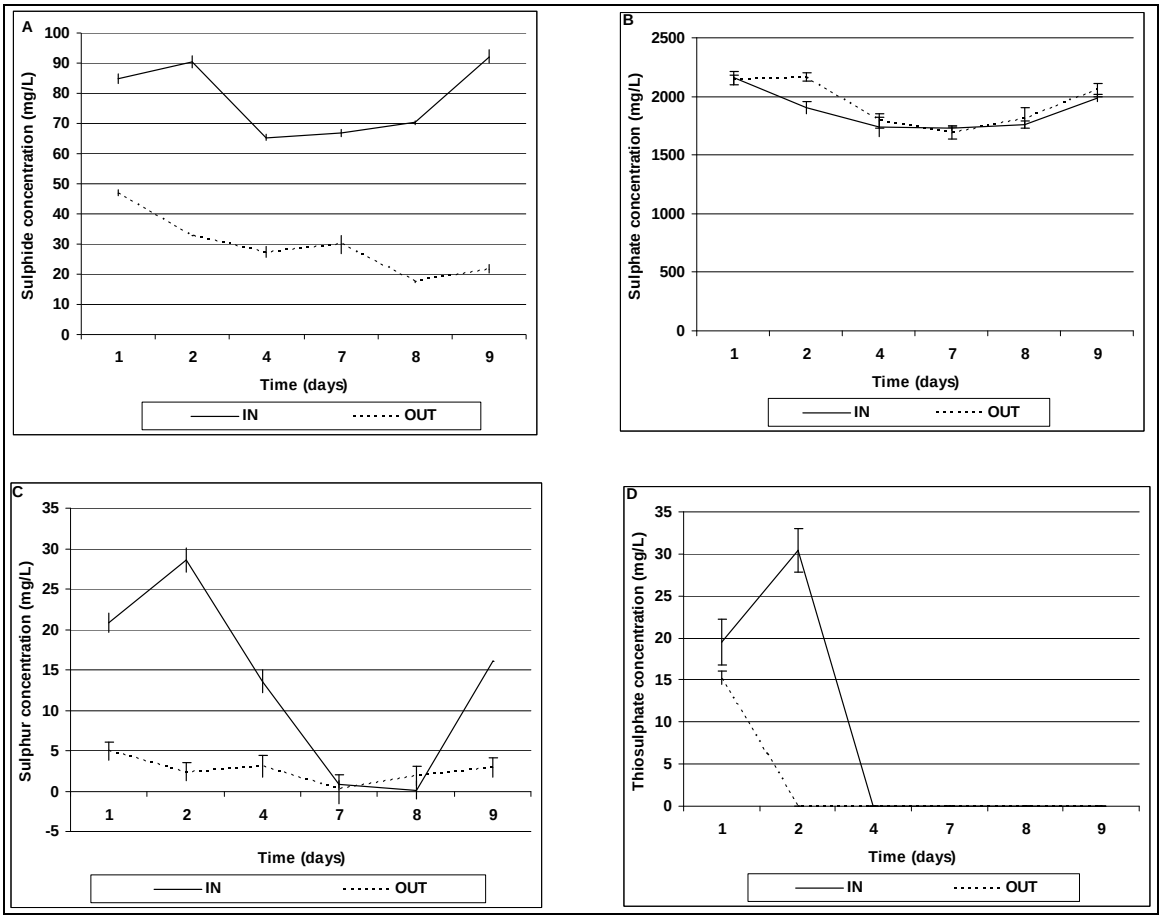

Figure 6. 6. Influent and effluent sulphur species measured in the Four Channel Linear Flow Channel Reactor over 8 days at 15^{o}C and 2 618 L.m^{-2} d^{-1} loading rate. sulphide (A), sulphate (B), sulphur (C) and thiosulphate (D).

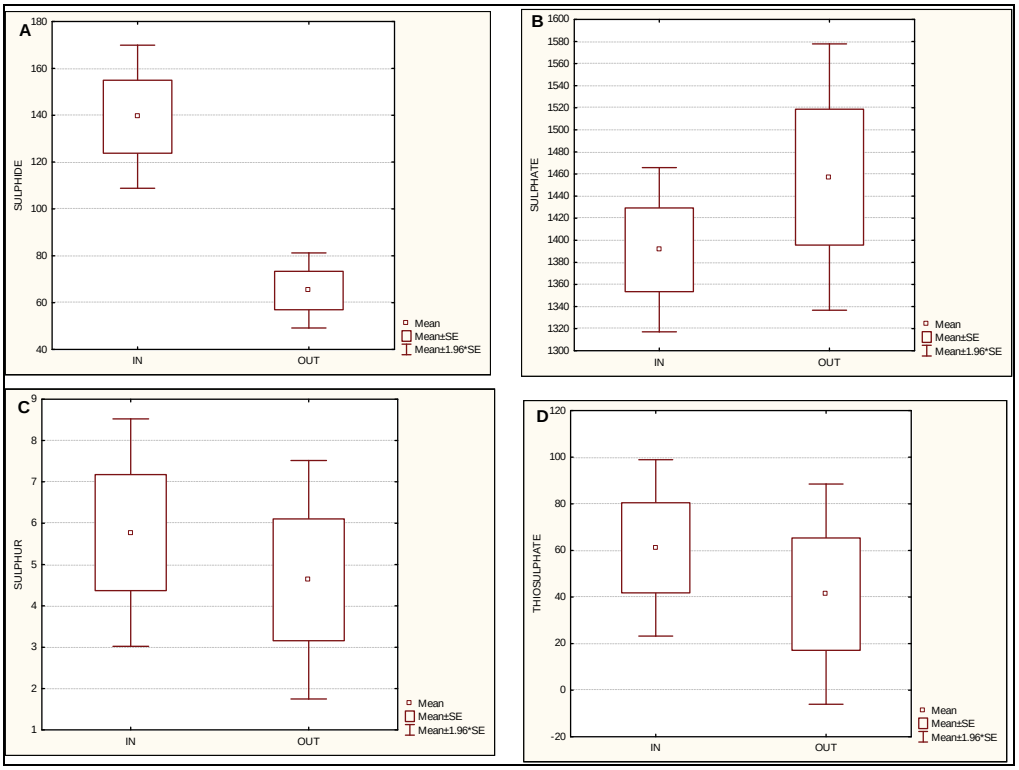

Figure 6. 7. Box and whiskers plot of the Four-Channel Linear Flow Channel Reactor operated at 15^{o}C and 2 618 L.m^{-2}d^{-1} showing the mean of distribution of influent and effluent sulphide (A), sulphate (B), sulphur (C) and thiosulphate (D) over the 8 days operation period.

6.3.1.6 Four-Channel Linear Flow Channel Reactor operated at 15^{o}C and 1309 L.m-2 d^{-1} loading rate.

The Four-Channel LFCR was operated 15^{o}C and 1 039 L.m^{-2}.L^{-1} loading rate, at steady state over a 7 day period and the results are reported in Figure 6.13 and 6.14. The 54% removal of sulphide was found to be highly significant (t = 5.92; df = 12; p = 0.001). The average percentage sulphate and thiosulphate increase was not significant (t = -0.73; df = 8; p = 0.43 and t = 1.29; df = 12; p = 0.23 respectively). Change in suspended sulphur concentration was also not significant (t = 0.87; df = 12; p = 0.40).

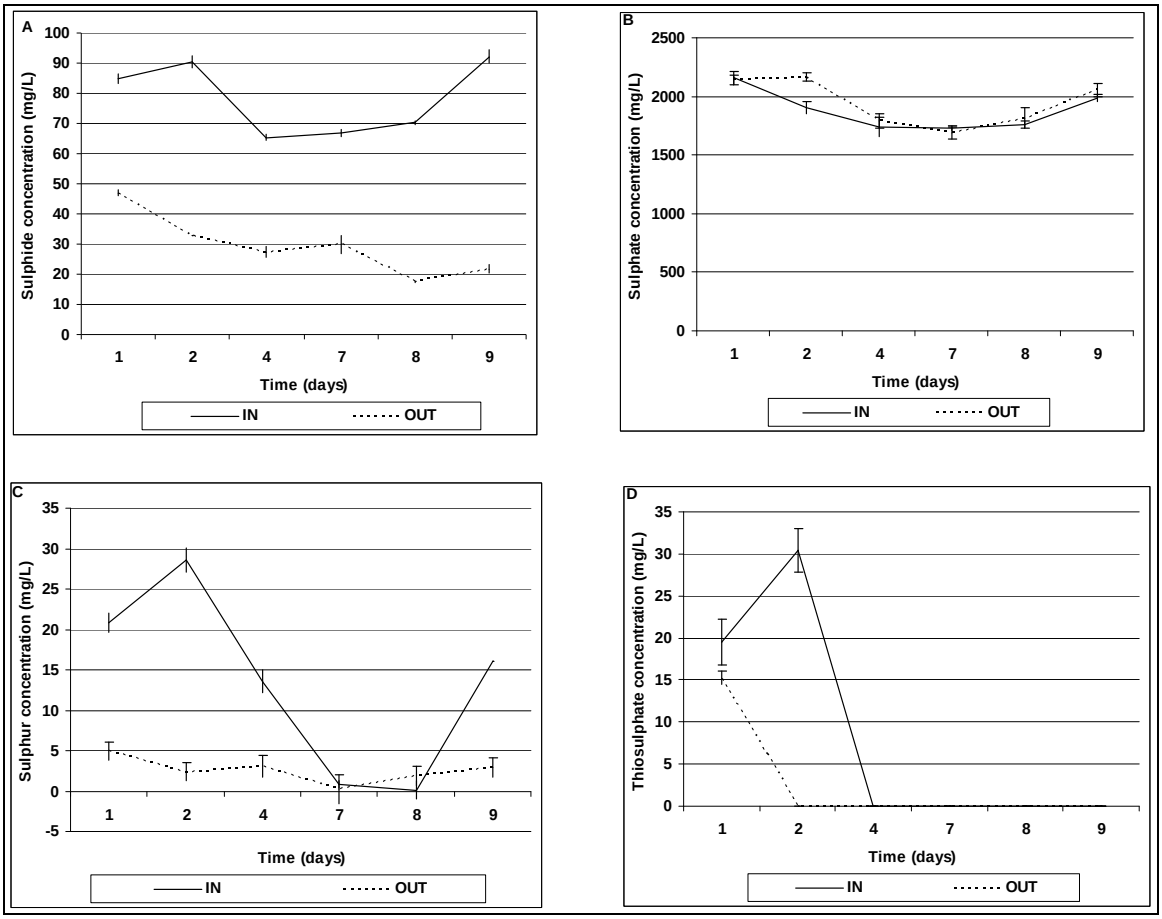

Figure 6. 8. Influent and effluent sulphur species measured in the Four Channel Linear Flow Channel Reactor over 8 days at 15°C and 1 309 L.m-2 d-1 loading rate. sulphide (A), sulphate (B), sulphur (C) and thiosulphate (D).

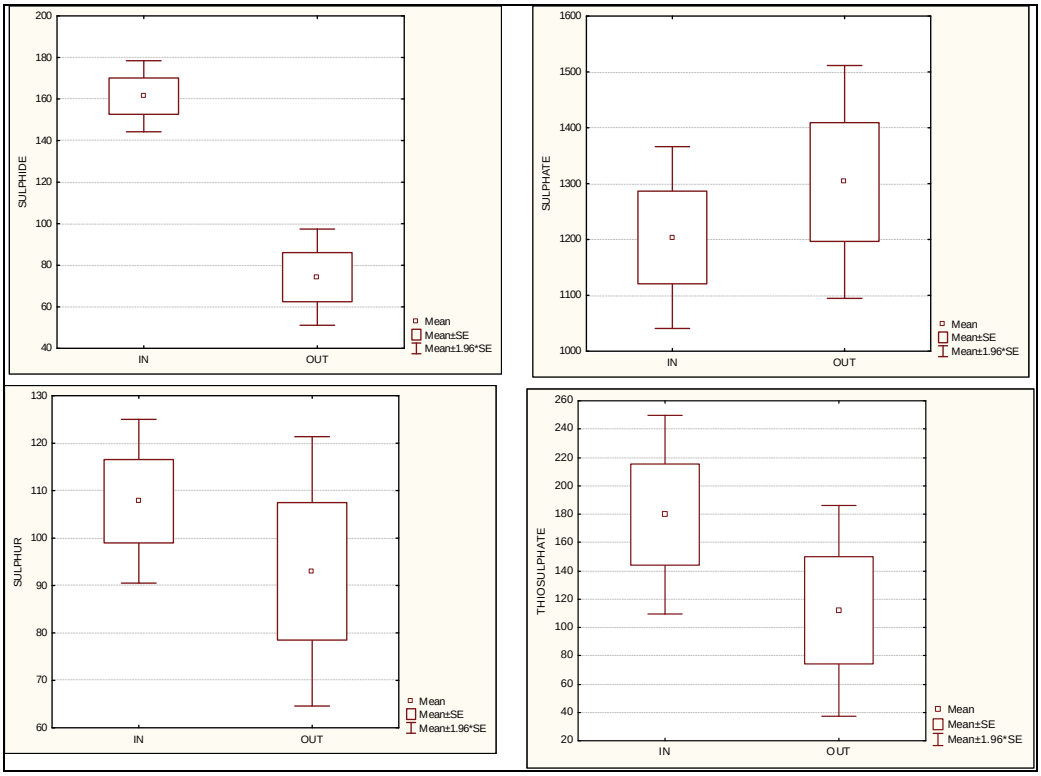

Figure 6. 9. Box and whiskers plot of the Four-Channel Linear Flow Channel Reactor operated at 15^{o}C and 1 309 L.m^{-2}d^{-1} showing the mean of distribution of influent and effluent sulphide (A), sulphate (B), sulphur (C) and thiosulphate (D) over the 8 days operation period.

The results of the LFCR process optimization studies (Figures 6.2 to 6.14) indicate that both flow rate and temperature have a significant effect on its performance. Although fluctuations in the feed sulphide concentration were observed, the relative change in sulphur species measured showed that sulphide removal was also significant. The highest percentage removal of 59% and 72% were obtained at 20^{o}C for 1 309 and 2 618 L.m^{-2}.d^{-1} loading rates respectively. While both 25^{o}C and 15^{o}C showed poorer performance than the 20^{o}C operational temperature, performance was better at 25^{o}C compared to 15^{o}C. Partial and complete oxidation of sulphide to thiosulphate and sulphate was observed throughout the investigations and, although not found to be statistically significant, it was better controlled at the lower loading rate. The complete oxidation to sulphate was, however, below 10% throughout.

Although the Four-Channel LFCR demonstrated effective sulphide removal, residual sulphide remained in the effluent which was assumed to be linked to surface area limitation. Based on this reasoning, four more channels were added to the reactor to form the Eight-Channel LFCR which is described in the following section.

6.3.1.7 Mass Balance calculations of the Four-Channel Linear Flow Channel Reactor

The mass balance at the different temperatures and flow rate operations are presented in Table 6.1.

Table 6. 1. Summary of the results obtained at different temperature and flow conditions of operation of the Four-Channel Linear Flow Channel Reactor showing system mass balance, sulphide removal and sulphur recovery presented as percentages.

Loading Rate ($L.m^{-2}$ d^{-1})	**Temperature (^oC)**	**Mass Balance %**	**Sulphide Removal %**	**Sulphur Recovery %**
2318	25	93	54	36
	20	100	72	43
	15	89	48	28
1309	25	72	52	33
	20	94	59	60
	15	86	54	22

The mass balance recovery accounts for the difference in total sulphur species (as S) entering and exiting the reactor at the different flows and temperatures measured. Mass balance of total S- species ranged between 70% and 100%. The highest sulphide removal, sulphur recovery and mass balance recovery were achieved at 20^{o}C for both loading rates. However, a trade-off between these operating conditions was observed with a higher sulphide removal at the 2 318 $L.m^{-2}$ d^{-1} loading rate, but the sulphur recovery was lower than at 1 309 $L.m^{-2}$ d^{-1}. Given that the results for complete sulphide oxidation were not significant it is possible that the sulphur crystal formation rate may be the rate limiting step here.

6.3.2 Eight-Channel Linear Flow Channel Reactor Operation

The investigation of surface area limitation on sulphide removal and sulphur formation reaction rates was carried out in the Eight-Channel LFCR (Figure 6.2). This study investigated the operation of Eight-Channel LFCR at the previously demonstrated optimal operating conditions for sulphide removal at 20^{o}C and flow rate

set at 2 618 $L.m^{-2}d^{-1}$. The reactor was commissioned and operated until steady state conditions were established and then data collected over a period of 18 days.

Figures 6.15 and 6.19 show a highly significant decrease in effluent sulphide concentration of 88% with an average influent and effluent of 133 and 15.4 mgL^{-1} measured respectively (t = 9.83; df = 24; p = 0.001). This percentage sulphide removal was higher than the highest obtained in the Four-Channel LFCR system. The sulphide measured in the effluent raged between 1.45 and 27.4 mgL^{-1} throughout the investigation which is lower than that discharged from passive AMD treatment systems. These have been found to range between 50 and 120 mgL^{-1}(Molwantwa *et al.*, 2003). This result indicates that an increase in surface area can lead to decrease in the residual sulphide in the effluent.

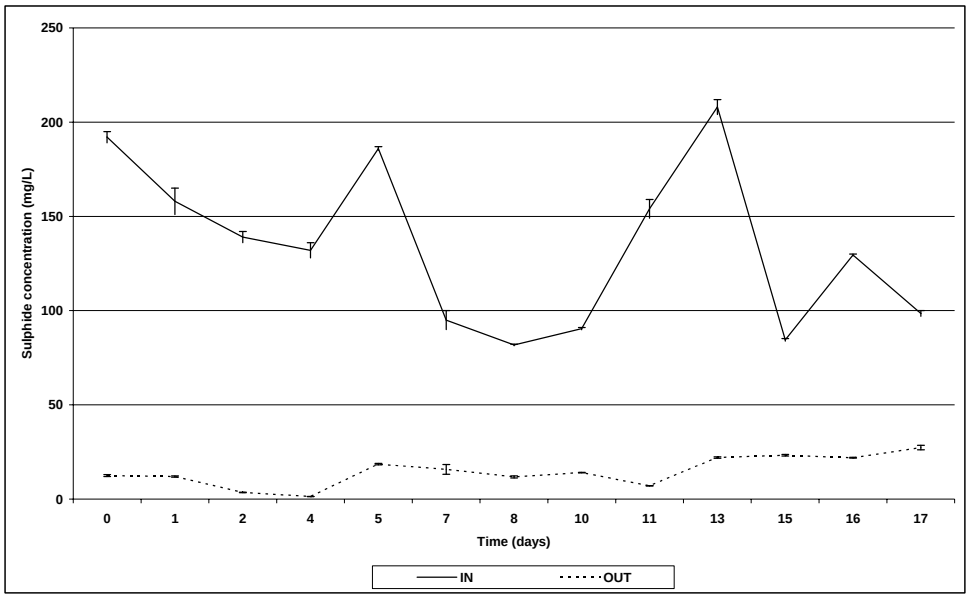

Figure 6. 10. Influent and effluent sulphide concentration of the Eight-Channel Linear Flow Channel Reactor over 18 days at 20^{o}C and 2 618 L.m-2 d^{-1} loading rate.

Figure 6.16 and 6.19 shows the influent and effluent sulphate concentration over the 18 days of operation. Variability in influent and effluent sulphate concentration was observed throughout the investigation. The average sulphate concentration measured was 1 391 and 1 456 mgL^{-1} in the influent and effluent respectively. The increase in sulphate due to complete oxidation in the system was found not to be significant (t = -0.65; df = 24; p = 0.52), and at an average percentage sulphate increase of 4.7%,

was lower than the 10% of the Four-Channel LFCR obtained under comparable operating conditions.

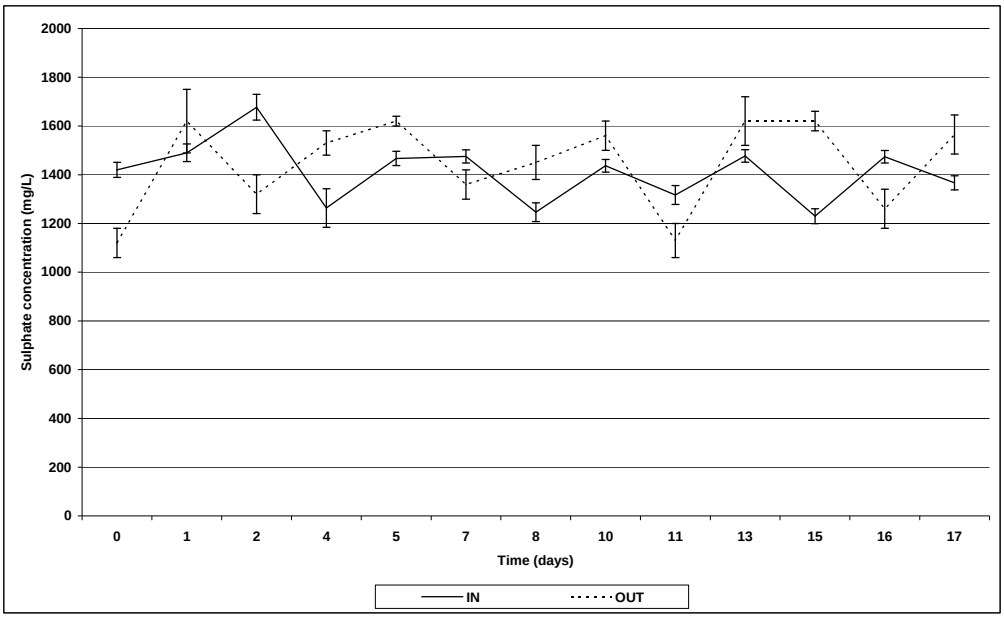

Figure 6. 11. Influent and effluent sulphate concentration of the Eight-Channel Linear Flow Channel Reactor over 18 days at 20^{o}C and 2618 L.m^{-2} d^{-1} loading rate.

Figures 6.17 and 6.19 show the fluctuations in suspended sulphur concentration. The average sulphur in the feed was 1.26 mgL^{-1} and that in the effluent was 0.34 mgL^{-1}. Although the average sulphur in the feed was lower compared to the Four-Channel LFRC, the percentage in the effluent was relatively lower. This was possibly due to the breakage of the sulphur biofilm and release of particles into suspension being limited under a larger surface area.

Figures 6.18 and 6.19 show the decrease in thiosulphate from influent to effluent of 25.7 and 1.45 mgL^{-1} respectively. This result indicates complete oxidation rather than formation of thiosulphate in the system.

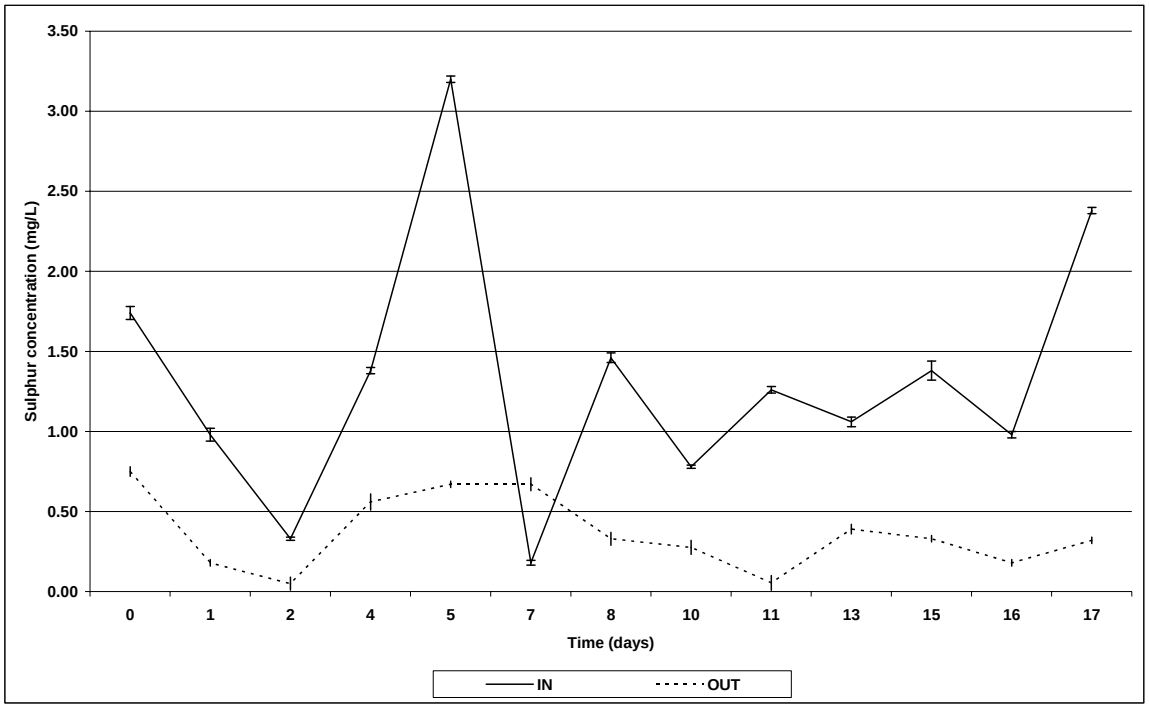

Figure 6. 12. Influent and effluent sulphur concentration of the Eight-Channel Linear Flow Channel Reactor over 18 days at 20°C and 2 618 $L.m^{-2}$ d^{-1} loading rate.

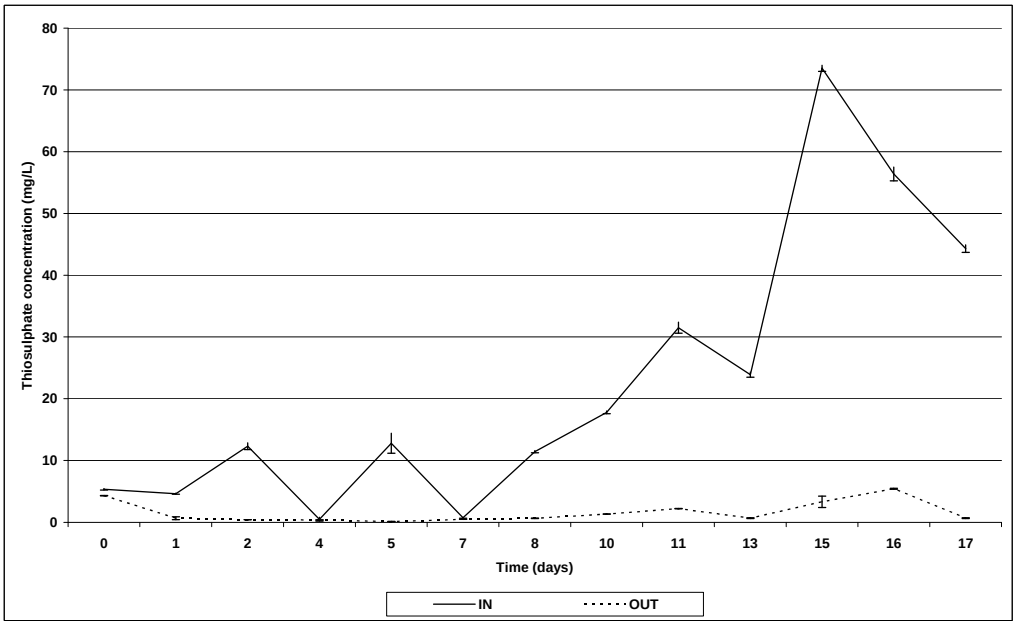

Figure 6. 13. Influent and effluent thiosulphate concentration of the Eight-Channel Linear Flow Channel Reactor over 18 days at 20°C and 2 618 $L.m^{-2}$ d^{-1} loading rate.

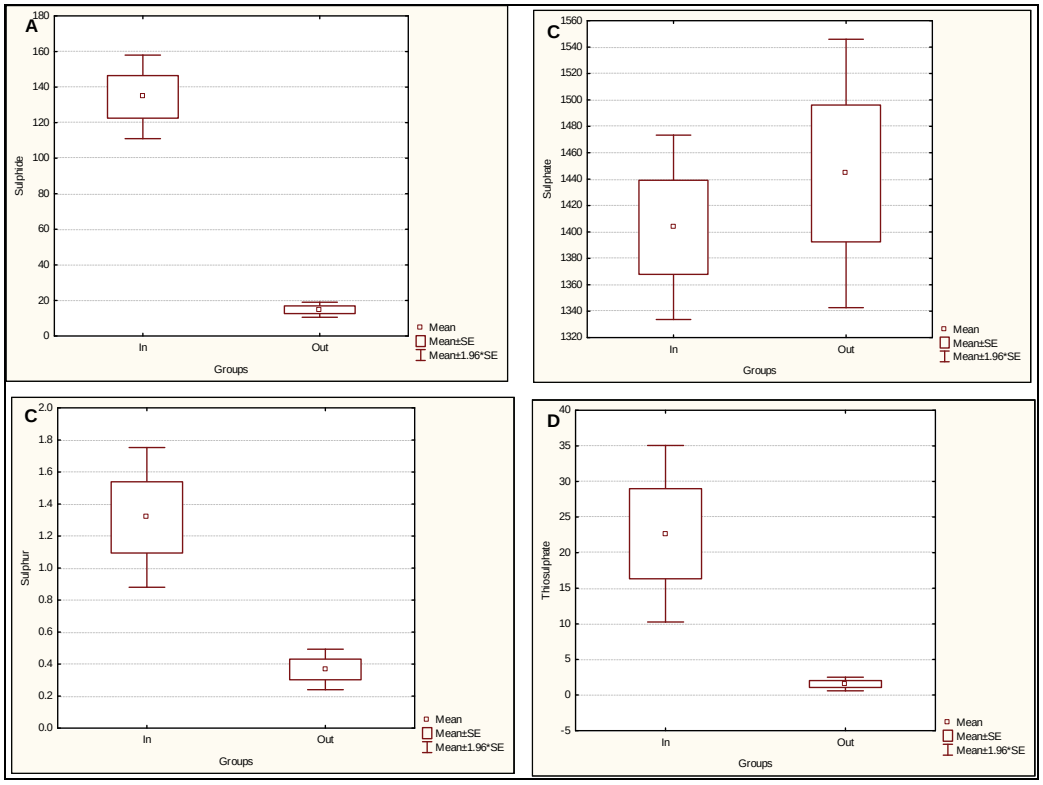

Figure 6. 14. Box and whiskers plot of the Eight-Channel Linear Flow Channel Reactor operated at 20^{o}C and 2 618 L.m^{-2}d^{-1} showing the mean of distribution of influent and effluent sulphide (A), sulphate (B), sulphur (C) and thiosulphate (D) over the 18 days operation period.

Other analyses in the Eight-Channel LFCR included the measurement of pH, Redox potential and COD. These results are shown in Figures 6.20 to 6.22 and the box and whiskers plot summarises the mean of distribution in Figure 6.23.

The increase in pH across the system from influent to effluent from pH 7.5 to pH 8 was found to be highly significant (t = -8.22; df = 24; p = 0.001) and corresponds with active sulphur formation in the reactor (Figure 6.20 & 6.23).

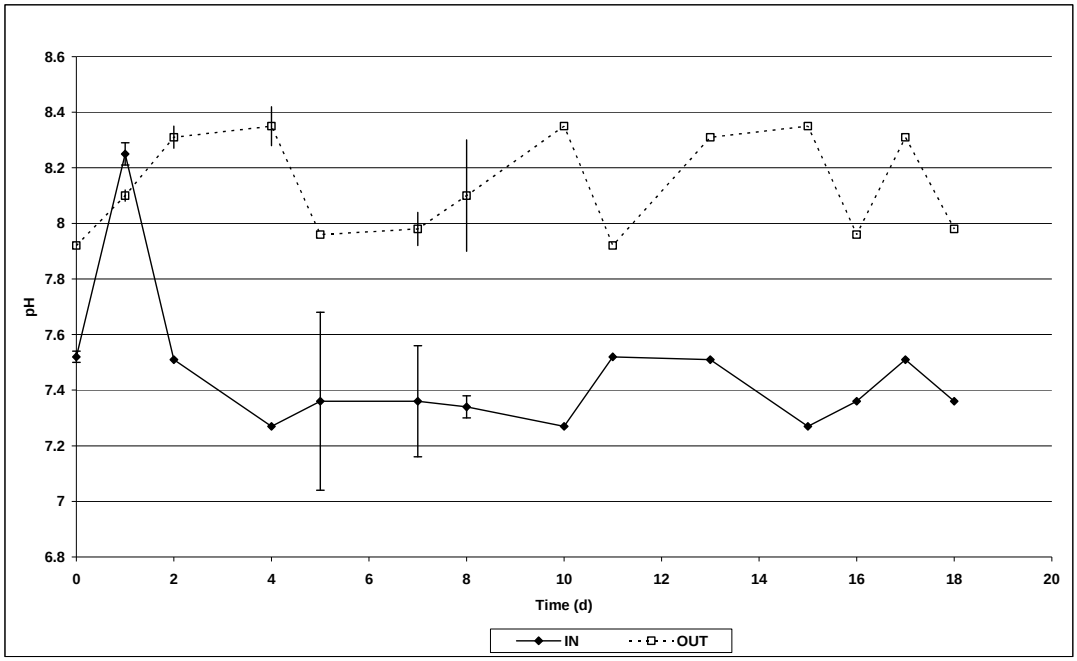

Figure 6. 20. Influent and effluent pH of the Eight-Channel Linear Flow Channel Reactor over 18 days at 20^{o}C and 2 618 L.m^{-2} d^{-1} loading rate.

The Redox potential was found to vary widely between the influent and effluent with ranges between -248 mV and +27 mV in the influent and -208 mV and -88 mV in the effluent (Figure 6.21&6.23). These differences were not found to be significant (t-test, t = -1.96; df = 24; p = 0.057). However, it is evident that for some of the time, at least, the Redox potential in the system was poised to operate around the optimal window for oxidation of sulphide to sulphur at ~ -150 mV (Steudel, 1996).

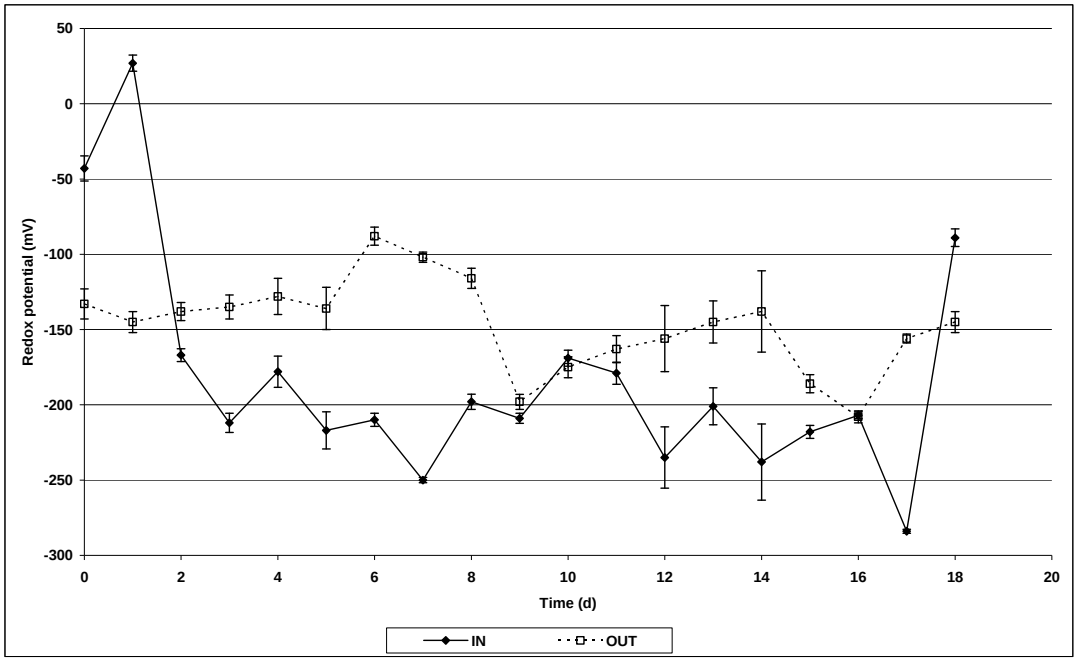

Figure 6. 15. Influent and effluent Redox potential of the Eight-Channel Linear Flow Channel Reactor over 18 days at 20^{o}C and 2 618 L.m^{-2} d^{-1} loading rate.

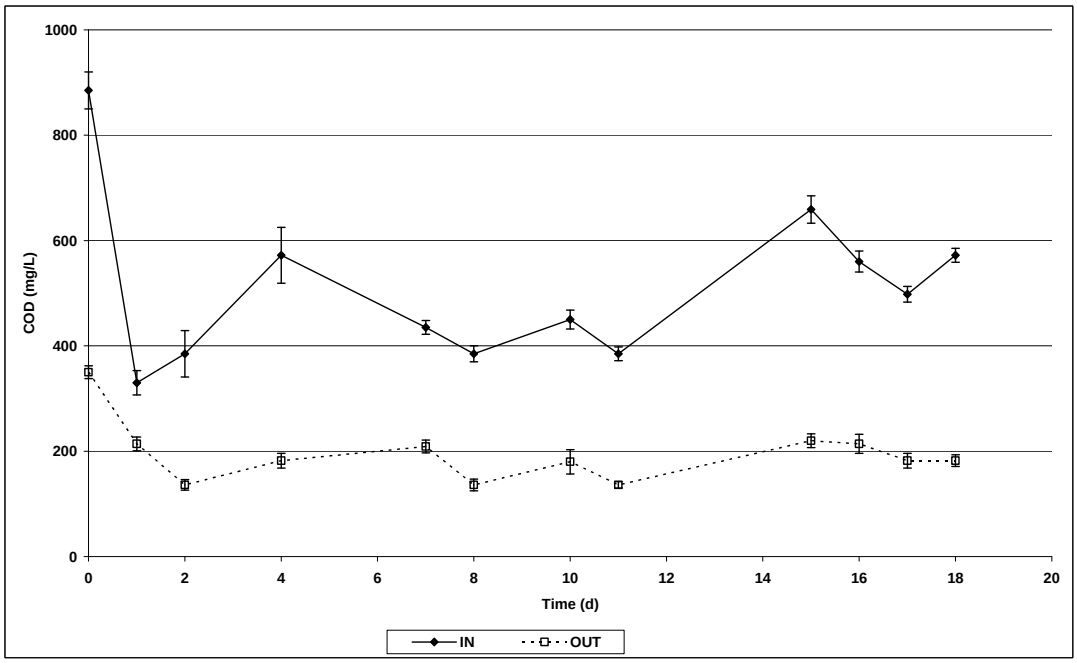

Figure 6. 16. Influent and effluent COD of the Eight-Channel LFCR over 18 days at 20^{o}C and 2 618 L.m^{-2} d^{-1} loading rate.

Influent COD concentration ranged between 330 and 885 mgL^{-1} while the effluent ranged between 136 and 350 mgL^{-1} (Figure 6.22 & 6.23). The average COD removal of 65% was found to be significant (t-test, t = 4.38; df = 24; p <0.05) indicating microbial activity within the reactor. This would be expected within the biofilm but

may also account for possible sulphate reduction occurring in the anaerobic compartment of the bulk liquid coupled with re-oxidation of sulphide in the LFCR. While difficult to prove, it is possible that the results recorded for the system represent an overall balance for the total oxidation and reduction reactions occurring in the system.

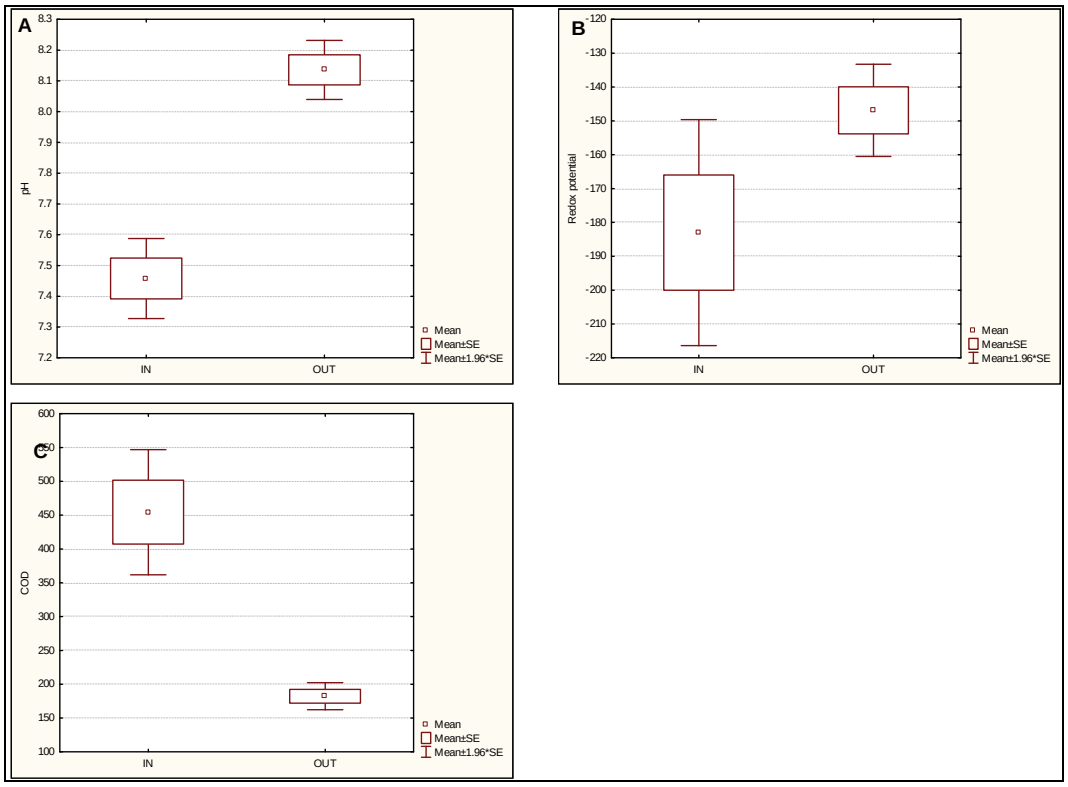

Figure 6. 17. Box and whiskers plot of the Eight-Channel Linear Flow Channel Reactor operated at 20^{o}C and 2 618 L.m^{-2}d^{-1} showing the mean of distribution of influent and effluent pH (A), Redox potential (B), and COD (C) over the 18 days operation period

6.3.2.1 Mass balance Calculations of the Eight-Channel Linear Flow Channel Reactor

The mass balance calculations for the Eight-Channel LFCR are summarised in table 6.2 showing system mass balance, sulphide removal and sulphur recovery at 20^{o}C and 2 618 L.m^{-2}.d^{-1}.

Table 6. 2. Summary of the results obtained at 20^{o}C and 2 618 L.m^{-2}.d^{-1} on the Eight-Channel Linear Flow Channel Reactor showing system mass balance, sulphide removal and sulphur recovery presented as percentages.

Mass balance (%)	Sulphide Removal (%)	Sulphur Recovery (%)
82	88	66

A higher sulphide removal (88%) and sulphur recovery (66%) was obtained from the mass balance calculations for the Eight-Channel LFCR compared to the Four-Channel LFCR operated under comparable conditions.

6.4 CONCLUSIONS

The following conclusions were drawn from the investigations on the LFCR operation and mass balance calculations.

The LFCR showed potential as a basic unit operation for sulphide removal from treated AMD wastewaters and indicated that an all-year round operation of the unit would be possible;

- The optimum operating temperature was found to be 20 ^{o}C;
- An average sulphide removal of 88%, and sulphur recovery of 66% was obtained for the Eight-Channel LFCR. This was an improvement on the performance of the Four-Channel LFCR and indicates the surface area dependence of the process at the 20^{o}C operating temperature. Increasing surface area loading thus enhances reactor performance.
- Although complete oxidation of sulphide was observed, it was found to be significantly lower in the Eight- compared to the Four-Channel LFCR under the same operating conditions.

7. DEVELOPMENT OF THE FLOATING SULPHUR BIOFILM REACTOR

7.1 INTRODUCTION

Sulphide removal in industrial-scale processes has been tackled by means of physico-chemical systems including the Stredford Process (Hammond, 1986), with high cost implications that are inappropriate for the treatment of low volumes of AMD to decant over a long period of time.. Sulphide removal by the precipitation of metal sulphides previously has been described (Van Hille *et al.*, 1999; Molipane, 2000; Rose, 2002). However, copious sludges formed in metal precipitation require sustainable removal. Biological removal has been investigated and the intensively engineered Thiopaq process has been developed (De Vegt *et al.,* 1997; Boonstra *et al.*, 1999) and applied by Paques Bio Systems B.V. at the Buldeco zinc refinery, Netherlands (Janssen, 1999). The shortcomings of this process include cost and the intensive labour and maintenance requirement, and seem inappropriate where passive treatment technologies are implemented to treat wastewater decanting from closed mines.

It is apparent that sulphide removal technologies used in AMD treatment need to be sustainable for long-term sustainable operation, especially when coupled with passive mine water treatment systems. According to Pulles (2002) “Passive treatment systems rely on the use of naturally available energy sources such as topographical gradient, microbial metabolic energy, photosynthesis and chemical energy which requires regular but infrequent maintenance to operate over its design life”. Thus the shortage of technologies involving the passive treatment of AMD and subsequent removal of sulphide are still to be addressed.

From findings reported in Chapter 6, the LFCR was successfully operated as a sulphide removal unit for AMD treated wastewaters. This study undertook to scale up the LFCR to a demonstration scale unit for operation as a post-treatment unit for sulphide removal from lignocellulose based sulphide-rich wastewater in passively treated AMD. Due to configuration changes and the need for a generic reference, the

scaled-up model of the LFCR was called the Floating Sulphur Biofilm Reactor (FSBR).

7.2 MATERIAL AND METHODS

Based on the initial studies initiated by Rein (2002) and the development of the LFCR described in Chapter 6, the system was subjected to initial scale-up investigation in the FSBR.

7.2.1 Reactor Development

Reactor development was undertaken in five successive phases.

7.2.1.1 Phase 1: The design, construction and commissioning of the Floating Sulphur Biofilm Reactor treating lignocellulosic sulphide-rich effluent

The FSBR (Figure 7.1) was constructed as a 1 m^3 bioreactor at EBRU, Grahamstown, and commissioned at the PHD research facility in Johannesburg. The reactor was fed with lignocellulosic sulphide-rich water from a passive system DPBR in order to demonstrate that lignocellulosic effluent would result in the formation of the FSB as was observed in the LFCR studies noted above and also by Bowker (2002) and Rein (2002) where sewage sludge was used for sulphide production. The FSBR was filled with the lignocellulosic sulphide-rich water connected to a silicone tubing frame to enhance oxygen diffusion through the reactor (Figure 7.2).

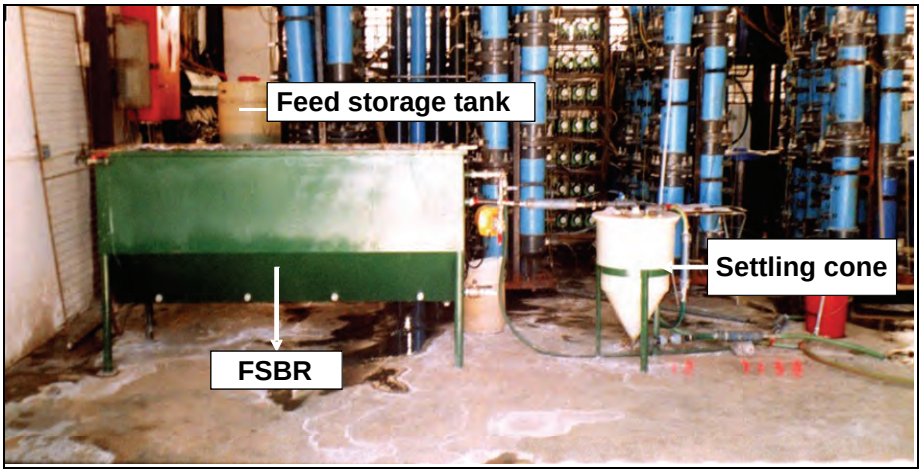

Figure 7. 1. Floating Sulphur Biofilm Reactor as initially set up at Pulles Howard and De Lange laboratories in Johannesburg.

Figure 7.2 is a diagrammatic longitudinal cross section of the FSBR configuration showing the harvesting system and the reservoir located below the linear flow zone. It was envisaged that harvested sulphur may settle and be collected here. A depth-adjustment plate was later fitted into the FSBR in order to raise and lower the depth of the reactor for maximum biofilm formation and sulphide removal.

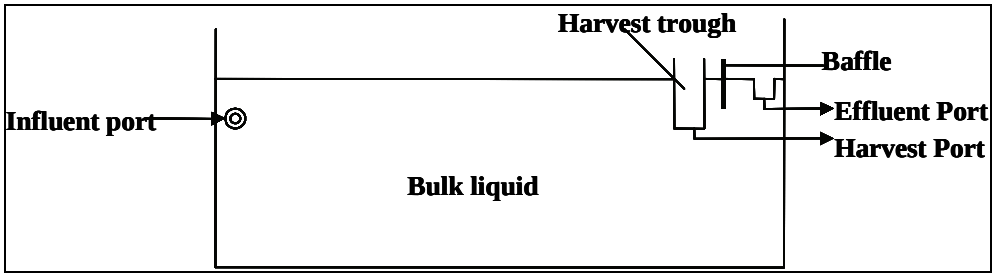

Figure 7. 2. Line diagram of the cross section of the Floating Sulphur Biofilm Reactor showing the influent and effluent ports and the harvest port.

A baffle was inserted in the FSBR between the harvest and effluent ports. Here the sulphur harvesting stage was initiated by closing the effluent port valve allowing the water level to rise until the biofilm passed into the harvest trough with a small volume of water. The harvest period lasted around five minutes depending on the degree of biofilm removal desired in the specific investigation. During harvesting, a portion of the biofilm was drawn off the water surface via the harvest port through to the settling cone. During the period when the biofilm was allowed to recover on the FSBR surface, the effluent was passed through the effluent port to waste. Alternatively,

during this stage, the entire effluent flow could be directed through the settling cone to pick up any sulphur loss occurring between harvests.

Figures 7.3 to 7.5 show details of the FSBR components and unit operations settling cone. For the collection of the biofilm, a funnel was fitted to the inlet of the settling cone to prevent airlocks.

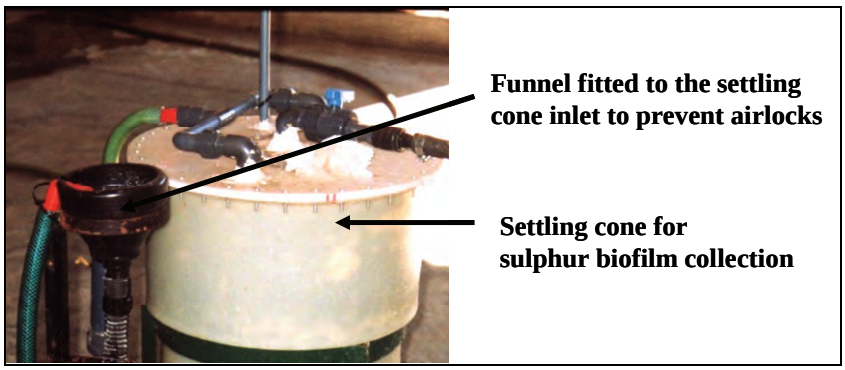

Figure 7. 3. Sulphur settling cone showing funnel installed to prevent airlocks.

To measure the flow rate through the FSBR, a tap was installed on the influent line and the valves were installed in case any regulation of flow was necessary (Figure 7.4).

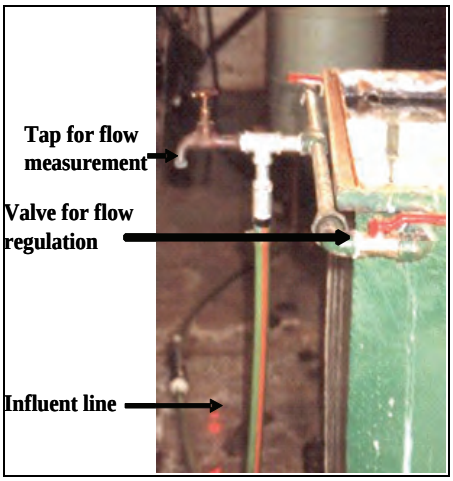

Figure 7. 4. Flow rate measurement tap and valve on the influent port.

The biofilm from the FSBR was harvested through to the settling cone where it was allowed to settle while the effluent overflows to waste (Figure 7.5).

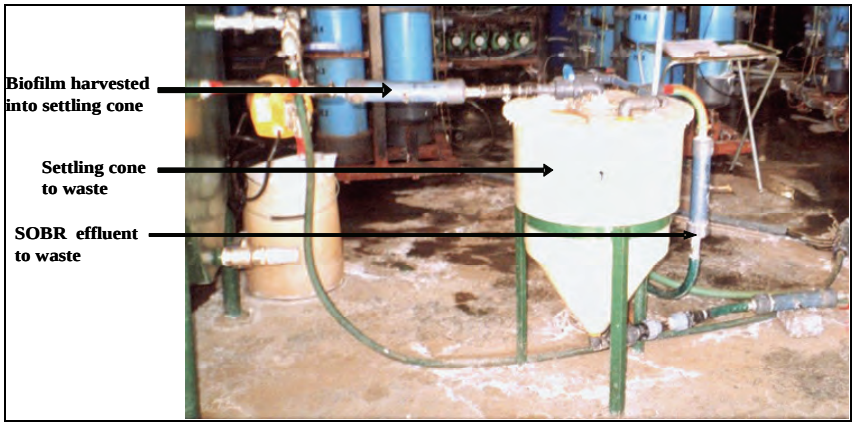

Figure 7. 5. Initial configuration showing the Floating Sulphur Biofilm Reactor connected to the cone during manual harvesting operations and passing directly to waste during inter-harvest periods.

7.2.1.2 Phase 2: Evaluation of variable sulphide loads

Sulphide-containing wastewater sourced from passive systems DPBR was supplemented with sodium sulphide (Na_2S) to investigate the effects of low and high sulphide concentration in the feed. The maximum influent sulphide concentration reached was 300 mgL^{-1}. During winter, the feed temperature was elevated by immersing the influent pipe in a 55^{o}C water bath upstream from the bioreactor.

7.2.1.3 Phase 3: Enhancing polysulphide formation by increasing oxygen transfer into the FSBR

As noted in the previous chapter polysulphide formation in the presence of sulphur particles produced by SOB such as *Thiobacillus* is a rate-limiting step in the large-scale production of elemental sulphur (Steudel, 1996). In following this line of reasoning it had been shown that biofilms including these organisms could be successfully established on air-fed silicone tubes (Rein, 2002).

Thus, a silicone tube frame (Figure 7.6) was constructed and inserted 20 to 30 mm below the water surface (Figure 7.7). Air was diffused through porous silicone tubes into the bulk liquid for enhanced polysulphide production.

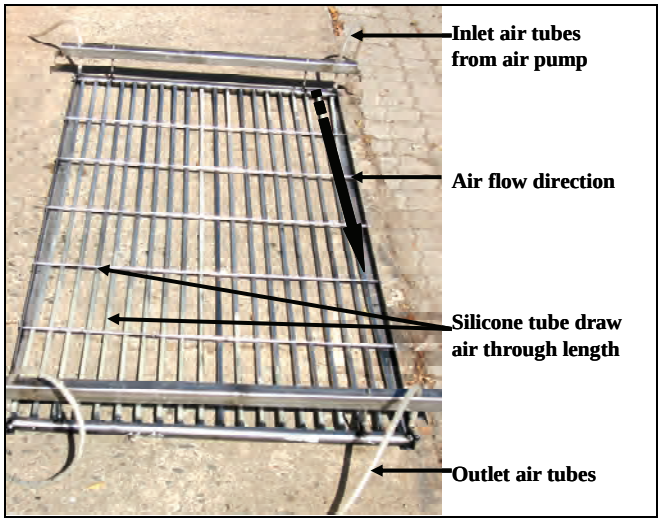

Figure 7. 6. Silicone tube frame inserted in the subsurface zone of the reactor. Air was passed through the tubes to enhance polysulphide formation.

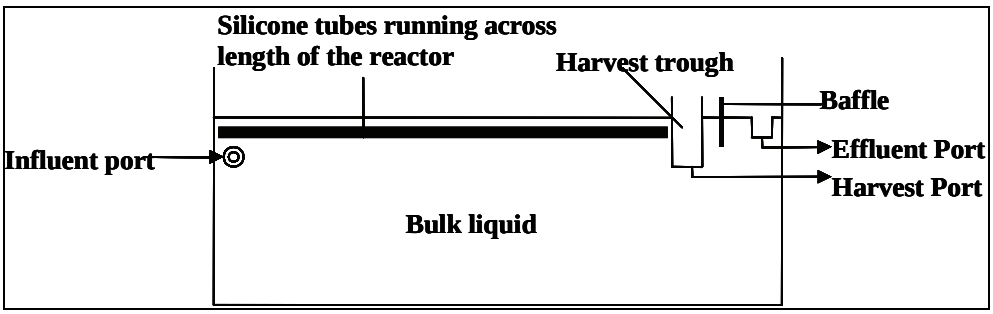

Figure 7. 7. Longitudinal cross section of the Floating Sulphur Biofilm Reactor configuration as used in the third stage of operation. The silicone tube rack (Figure 7.6) was inserted in the subsurface zone to enhance polysulphide formation.

The dedicated lignocellulose-DPBR sulphide generator (Figure 7.8) was constructed on site and linked to the FSBR.

Figure 7. 8. A lignocellulose packed sulphide generator (blue tank) providing feed to the Floating Sulphur Biofilm Reactor.

7.2.1.4 Phase 4: Optimisation of flow and dimensions of the sulphur formation zone

Given the observation of turbulent flow in the sulphur collection reservoir an adjustable plate was fitted inside the FSBR which enabled the floor of the FSBR to be lowered and raised as required (Figure 7.9).

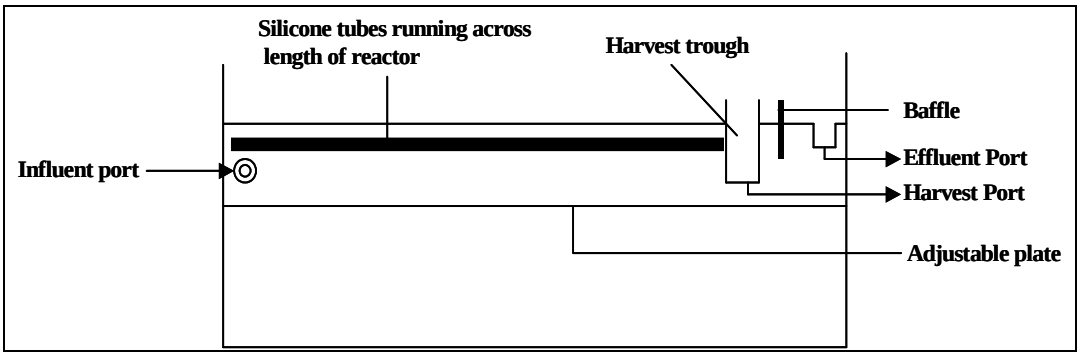

Figure 7. 9. Longitudinal cross section of the Floating Sulphur Biofilm Reactor configuration as used in Phase 4 showing the fitted adjustable plate used to lower and raise the reactor floor as required.

7.2.1.5 Phase 5: Optimisation of the harvesting procedure, installation of an automated harvesting process.

The automation of the harvesting process was introduced to allow the full optimisation of the sulphide oxidation/sulphur recovery process. Automated valves (EL-O Matic Actuator Valves) were fitted to the effluent and harvest ports facilitated the determination of optimal harvest and biofilm development periods. Figure 7.10 shows the automated valves fitted to the FSBR.

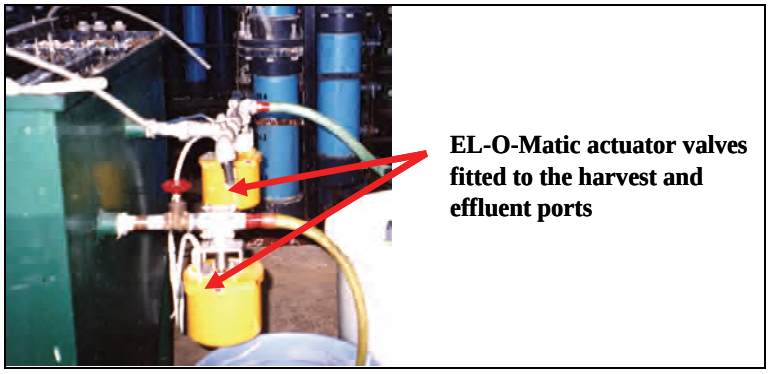

Figure 7. 10. The EL-O Matic actuator valves fitted for the automation of the flow and harvesting operations.

A summary of the five Phases of reactor development is presented in Table 7.1.

Table 7. 1. Five development phases of the FSBR during the reactor development study.

Phase	Description	Changes in operation
1	Design and construction of FSBR treating lignocellulose-based effluent	Fed FSBR with lignocellulose effluent from PHD carbon columns
2	Evaluation of sulphide loads into the FSBR	Sodium sulphide supplementation into the FSBR feed line
3	Enhancement of polysulphide formation	Installation of silicone tube frame in the subsurface of the FSBR
4	Optimisation of flow and reactor dimensions	Installation of adjustable plate to control the depth of the FSBR
5	Optimisation of the harvesting procedure	Installation of the automated EL-Omatic valves to the effluent and harvest ports

7.2.2 Analysis

7.2.2.1 Sulphide Concentration

An iodometric method was used for sulphide analysis (APHA, 1998). A volume of 200 mL sample was preserved with eight drops of 0.22 mgL^{-1} zinc acetate.

A standard iodine solution (0.05N) containing 25 g KI, 3.2 g iodine and 100 mL ddH_2O was prepared, made up to 1L with ddH_2O, and standardized against 0.025N sodium thiosulphate ($Na_2S_2O_3$), using starch solution as an indicator. An excess

volume of the iodine solution and 2 mL of 6N HCl was added into a 500 mL beaker. The sample was pipetted into the flask, until the iodine colour disappeared. More iodine was added to the flask until the colour remained. This solution was back-titrated against the sodium thiosulphate solution, adding a few drops of starch solution as the end-point approached, and continuing until the blue colour disappeared. The sulphide concentration was calculated as follows:

$$mg\ S^{-2}.L^{-1} = \frac{[(AxB) - (CxD) \times 16000}{} = mL\ sample$$

Where:
A = mL iodine solution,
B = normality of iodine solution,
C = mL $Na_2S_2O_3$ solution, and
D = normality of $Na_2S_2O_3$ solution.

7.2.2.2 Sulphate and Thiosulphate Concentration

Sulphate and thiosulphate determination was carried out as described in Chapter 6.

7.2.2.3 Sulphur

Sulphur determination was carried out using a similar method described in Chapter 6.

7.2.2.4 Redox Potential and pH

Redox potential and pH using a Zeiss 300 pH meter.

7.2.2.5 Alkalinity

Alkalinity was assayed using the two titration method (APHA, 1998). Firstly the solution was titrated with 0.02N sulphuric acid (H_2SO_4) to an orange to pink end-point with methyl orange indicator (pH 4.4) and secondly to a dark pink to clear end-point with phenolphthalein indicator (pH 8.3).

Where:

1. Water titration with H_2SO_4 (0.02N) = $\frac{mL \times 1000}{mL\ sample}$

2. Effluent titration with H_2SO_4 (0.01N) = $\frac{mL \times 5000}{mL\ sample}$

7.2.2.6 Chemical Oxygen Demand

COD was analysed as previously described in Chapter 6.

7.2.2.7 Mass Balance Calculations

Mass balance calculations were carried out as described in Chapter 6.

7.2.2.8 Statistical Validation

Statistical validation was carried out as previously described in Chapter 6.

7.3 RESULTS AND DISCUSSSION

7.3.1 Bioreactor Development

The FSBR was successfully commissioned and operated for 400 days using a lignocellulose-based sulphide-rich effluent for sulphur biofilm formation. The resulting biofilm (Figure 7.11) was Thin and speckled and had an inter-harvest period of 3 to 4 days. In the second phase, the increased sulphide concentration in the influent resulted in increased biofilm thickness (Figure 7.11) and the inter-harvest period was reduced from 3 to 4 days to 1 to 2 days. The inserted silicone air diffusion tube rack in the subsurface of the FSBR enhanced the formation of polysulphide and hence the increased thickness of the biofilm seen in Figure 7.11. The adjustable plate inserted into the FSBR allowed for variation of reactor depth in relation to sulphur

biofilm formation. The introduction of an automated harvesting process allowed for more accurate measurement of inter-harvest and biofilm recovery periods.

Figure 7.11 shows photographs of a progressive increase in the thickness and sulphur content of the sulphur biofilm harvested through the various phases of the reactor development investigations.

In phase 1, a Thin speckled biofilm formed relatively slowly and had a recovery rate of about three to four days following each harvest event (Figure 7.11A). An increase in thickness was achieved during phase 2, where sulphide supplementation was implemented (Figure 7.11B).

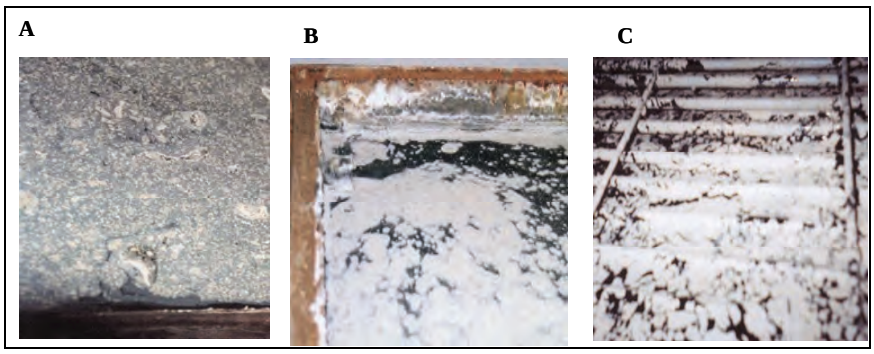

Figure 7. 11. Changes in biofilm characteristics through the various phases of reactor development investigation. (A) Phase 1: Standard FSBR design utilising lignocellulose effluent. (B) Phase 2: With sulphide supplementation. (C) Phase 3: with enhanced polysulphide formation. The sub-surface-located silicone tube frame has been lifted to indicate its attached biofilm.

The introduction of the silicone tube frame for enhancing polysulphide formation led to a further increase in biofilm thickness and substantial reduction in the harvest period from several days to around six to twelve hours (Figure 7.11C).

The results obtained for FSBR operation through the five operational phases are shown in Figures 7.12 to 7.23. The line graphs represent the actual influent and effluent variables measured over the five phases of operation, while the box and whisker plots show the significance of the differences obtained from the measured variables.

7.3.2 Sulphide

Sulphide concentration in the influent feed and the effluent from the FSBR are reported for the various phases of the study as accumulated data sets in Figure 7.12.

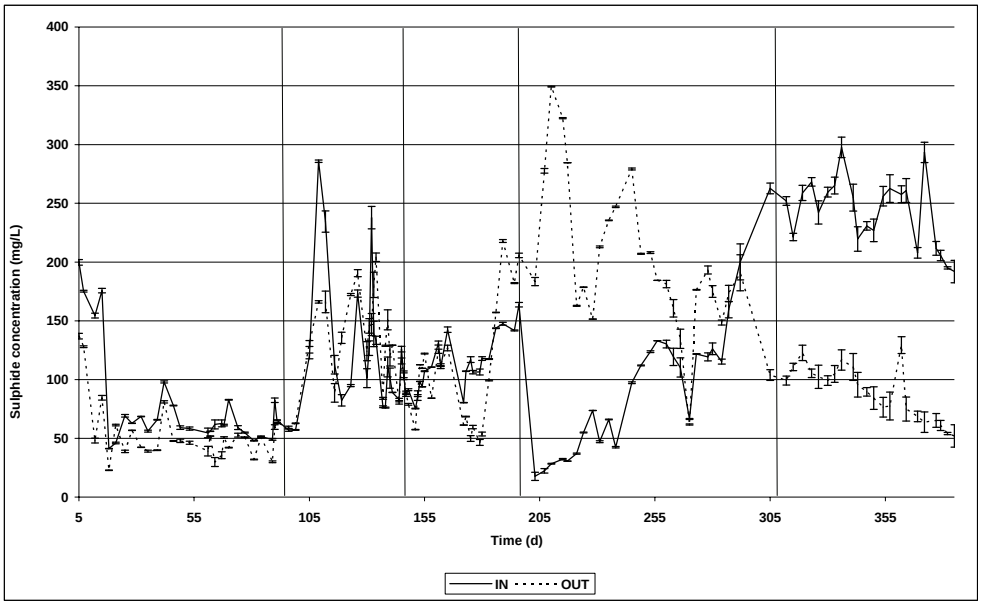

Figure 7. 12. Influent and effluent sulphide concentrations over the five phases of the reactor development study. The error bars indicate standard deviations.

The influent sulphide concentration ranged between 150 and 200 mgL^{-1} and decreased to between 50 and 80 mgL^{-1} during most part of phase 1. This decrease was attributed to the cold weather and the onset of winter. The average decrease in sulphide concentration for phase 1 was 27 mgL^{-1}. Supplementation of Na_2S into the influent line during phase 2, led to an increase in sulphide availability within the FSBR with an average feed concentration of 130 mgL^{-1}. During phase 3 about 10 mgL^{-1} sulphide removal was observed. The average influent sulphide concentration in phase 4 was 102 mgL^{-1} and the average effluent was 198 mgL^{-1} indicating an average increase in sulphide concentration of 96 mgL^{-1}. This increase in sulphide was attributed to active sulphate reduction taking place in the FSBR as a result of the readily available carbon leaching from the new sulphide generator. Once the reactor was optimized and automated during phase 5, there was an average sulphide removal of 150 mgL^{-1}.

Figure 7.13 shows means for influent and effluent sulphide concentration for each phase together with standard error and standard deviations for the data sets.

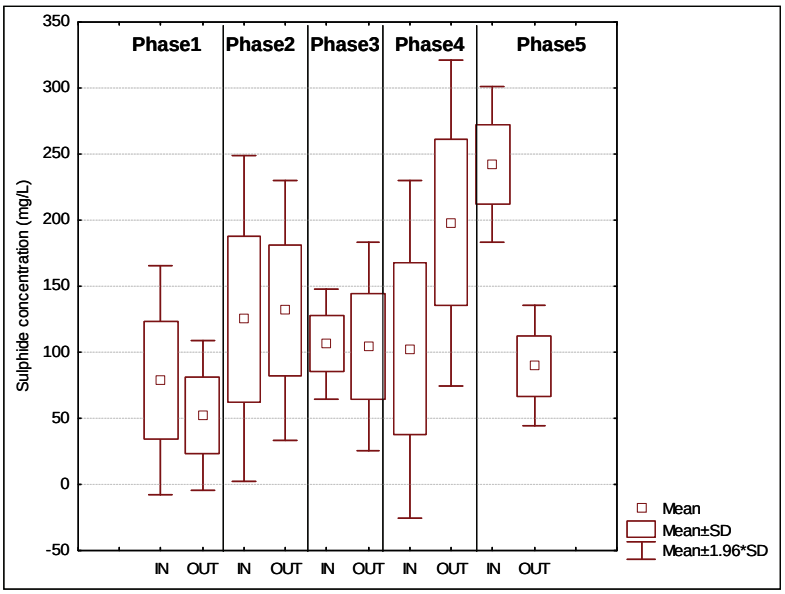

Figure 7. 13. Box and whisker plot indicating the means of influent and effluent sulphide concentration for each of the phases of the reactor development study.

No significant change in sulphide concentration was found between the influent and effluent during phase 2 (n=13; p=0.744, df =30) and phase 3 (n=21, p=0.838, df =56) of the experiment. However, the decrease in sulphide during phase 1 (n=26, $p<0.05$, df =50) and phase 5 (n=21, $p<0.01$, df=40) was found to be significant. As expected the increase in sulphide (n=21, $p<0.01$, df =56) in phase 4 was found to be significant.

7.3.3 Sulphate

Influent and effluent sulphate concentrations over the phases of FSBR operation are presented as accumulated data sets in Figures 7.14 and 7.15.

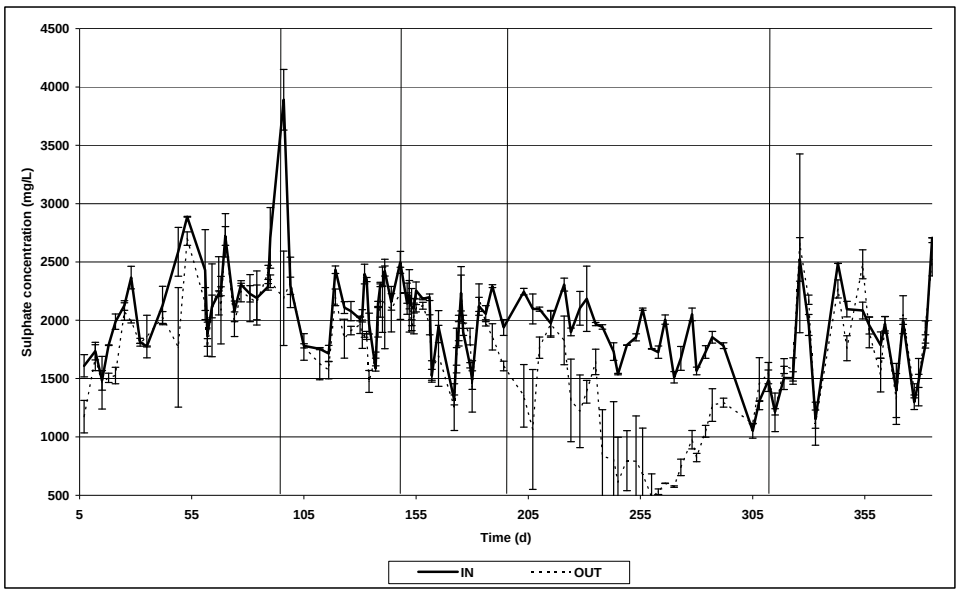

Figure 7. 14. Influent and effluent sulphate concentrations over the five phases of the reactor development study. The error bars indicate standard deviations.

Sulphate levels in both influent and effluent concentration ranged between 1 500 and 4 000 mgL^{-1} over the experimental period (Figure 7.14). An average decrease in sulphate concentration in all phases of the experiment was observed with 282 mgL^{-1} in phase 1, 116 mgL^{-1} in phase 2, 115 mgL^{-1} in phase 3 and 917 mgL^{-1} in phase 4. The decrease in sulphate observed was attributed to sulphate reduction. During phase 5, there was a slight increase in sulphate of 31 mgL^{-1} possibly due to complete oxidation of sulphide to sulphate.

Figure 7.15 reports the mean and standard errors of influent and effluent sulphate concentrations for the data sets.

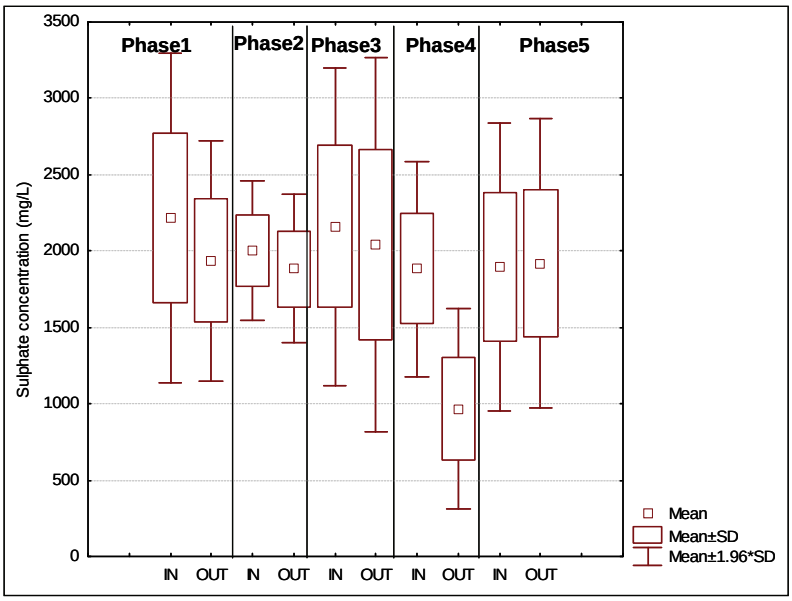

Figure 7. 15. Box and whisker plot indicating the means for influent and effluent sulphate for each phase of the reactor development study.

The statistical analysis presented in Figure 7.15 indicates that a significant decrease in sulphate occurred during phase 1 ($n=26$, $p<0.05$, $df=50$) and phase 4 ($n=21$, $p<0.01$, $df=42$) attributed to sulphate reduction taking place in the reactor. This may have been as a result of the availability of readily degradable carbon in the newly commissioned FSBR in phase 1 and the newly commissioned sulphide generator attached to the FSBR in phase 4. The decrease in sulphate in phases 2 and 3 and increase in sulphate in phase 5 were not found to be significant ($p>0.05$).

7.3.4 Redox potential

Influent and effluent Redox potential values over the phases of FSBR operation are presented as accumulated data sets in Figures 7.16 and 7.17.

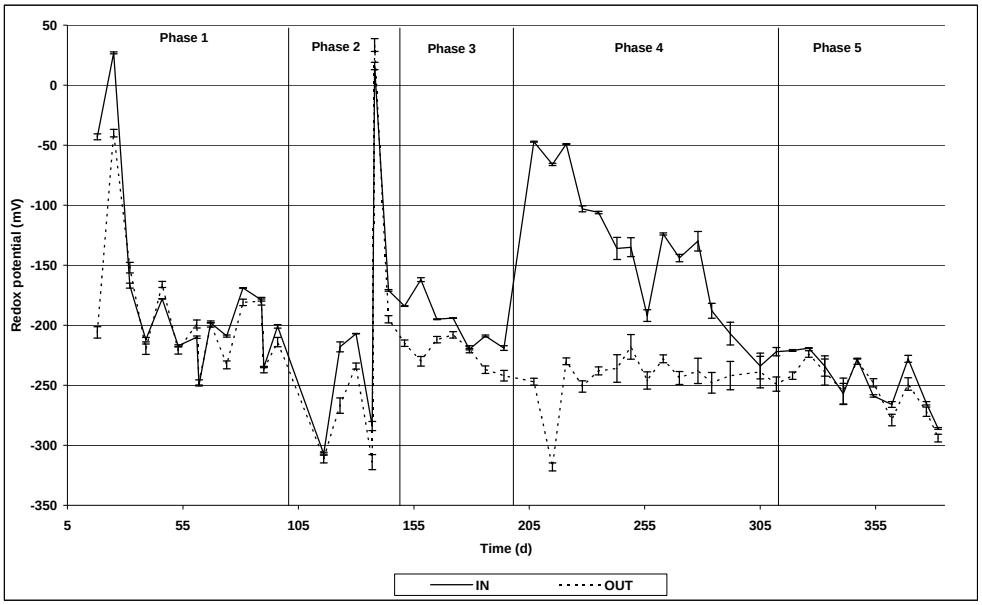

Figure 7. 16. Influent and effluent Redox potential data over the five phases of the reactor development study. The error bars indicate standard deviations.

Redox potential ranged between 50 and -350 mV over the period of reactor development investigation (Figure 7.16). The negative Redox potential values (mV) measured is generally favourable for sulphate reduction and sulphide oxidation.

Figure 7.17 reports the mean and standard errors of influent and effluent Redox potential concentrations for the data sets.

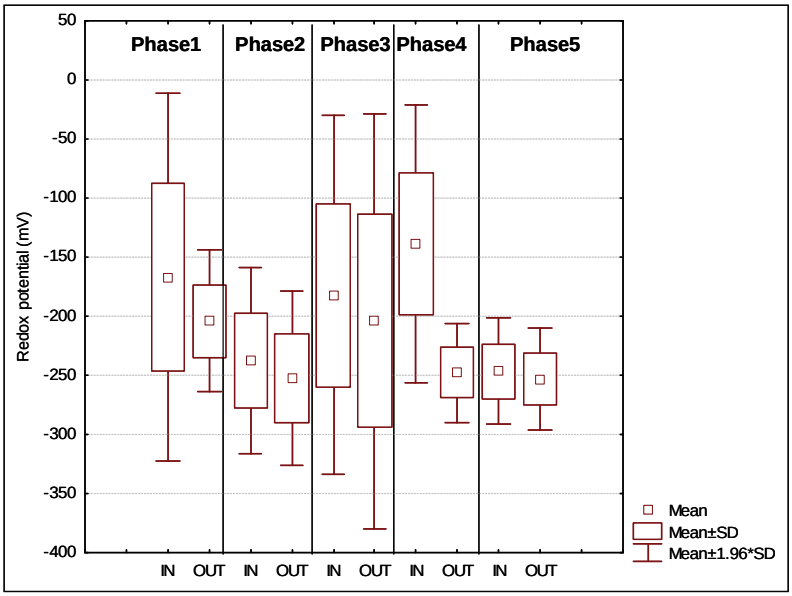

Figure 7. 17. Box and whisker plot indicating the means for influent and effluent Redox potential (mV) for the reactor development study.

The results presented in Figure 7.17 show that there was no significant increase or decrease in Redox potential in phases 1, 2, 3 and 5 ($p>0.05$), except for phase 4 ($n=21$, $p<0.001$, $df=18$) where the difference was found to be significant. This increasingly negative Redox potential is associated with active sulphate reduction occurring during phase 4 as indicated by the significant increase in sulphide and a significant decrease in sulphate.

7.3.5 pH

Influent and effluent pH results are reported in Figure 7.18 as accumulated data sets over the reactor development study.

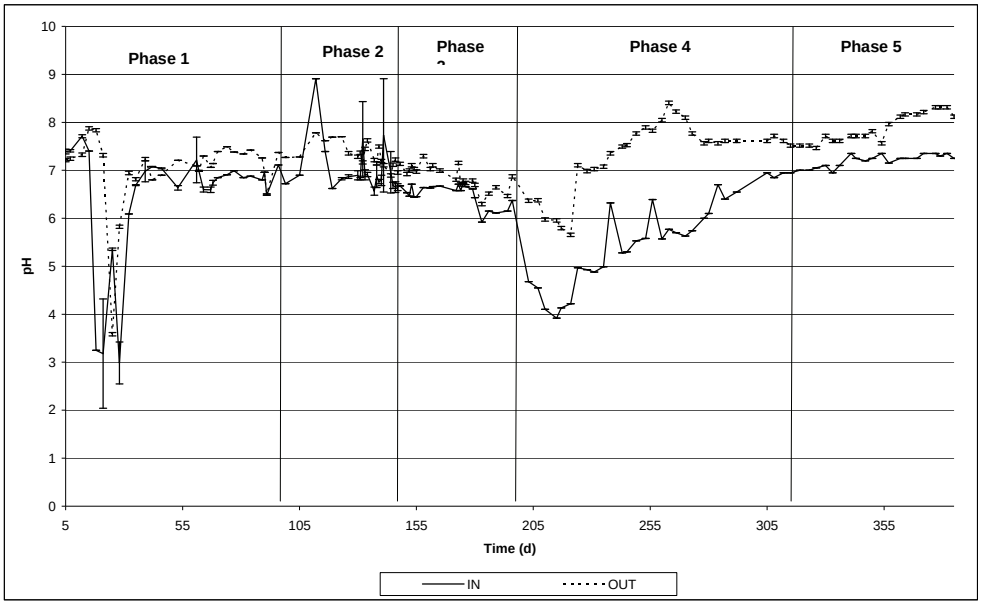

Figure 7. 18. Influent and effluent pH data over the five phases of reactor development study. The error bars indicate standard deviations.

The general trend presented in Figure 7.18 shows an increase in pH ranging between 7.6 and 7.2 in the influent to a range between 7.0 and 7.9 in the effluent. This increase in pH may be associated with an increase in the breakdown of readily available carbon during active sulphate reduction. Although the sulphate levels were reduced in all the phases except phase 5, clearly sulphur cycling must have been occurring in the system with some sulphate reduction taking place.

Figure 7.19 reports the means and standard errors of influent and effluent pH values for the phases of operation.

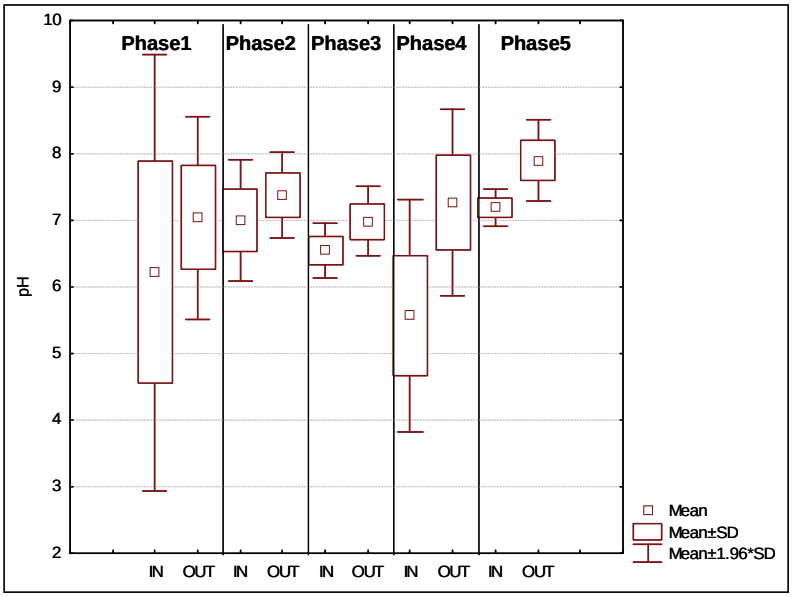

Figure 7. 19. Box and whisker plot indicating the means for influent and effluent pH for each phase of the reactor development study.

A significant increase in pH was found for all phases of the reactor development study ($p<0.05$). The average pH in the effluent after optimization during phase 5 was 7.9.

7.3.6 Alkalinity

Influent and effluent alkalinity measured as $CaCO_3$ concentration as reported in the results are shown in Figures 7.20 and 7.21.

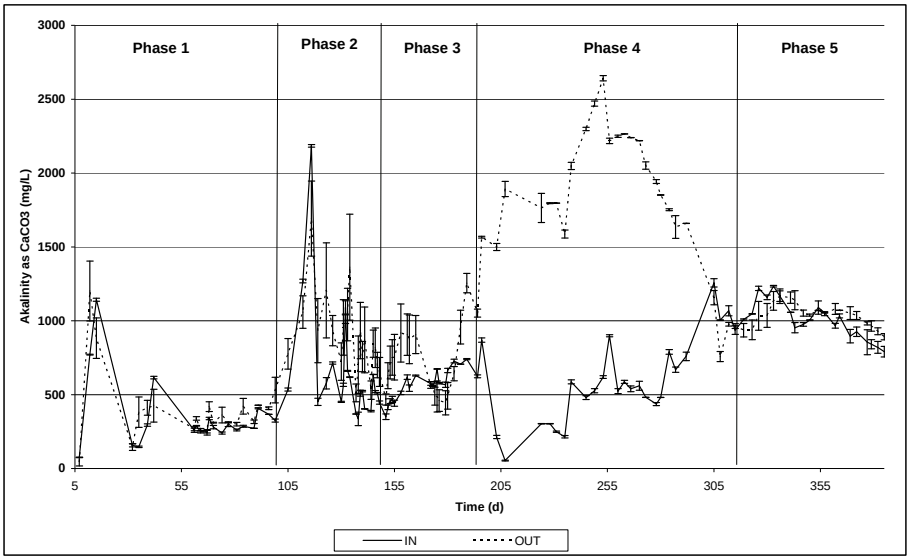

Figure 7. 20. Influent and effluent alkalinity (as $CaCO_3$) over the five phases of the reactor development study. The error bars indicate standard deviations.

The general trend presented by the alkalinity data showed an increase in alkalinity particularly in phases 2, 3 and 4. This is represented by an increase in alkalinity of 311 mgL^{-1} during phase 2, 186 mgL^{-1} in phase 3 and 1181 mgL^{-1} in phase 4. As noted above, this increase in alkalinity may be correlated with the increase in pH during the same phases of the reactor development study and could be associated with the production of bicarbonate ions during active sulphate reduction. This is further indicated by the decrease in sulphate and increase in sulphide concentration over the same period.

Figure 7.21 reports the means and standard errors of influent and effluent alkalinity as $CaCO_3$ concentration for the phases of operation.

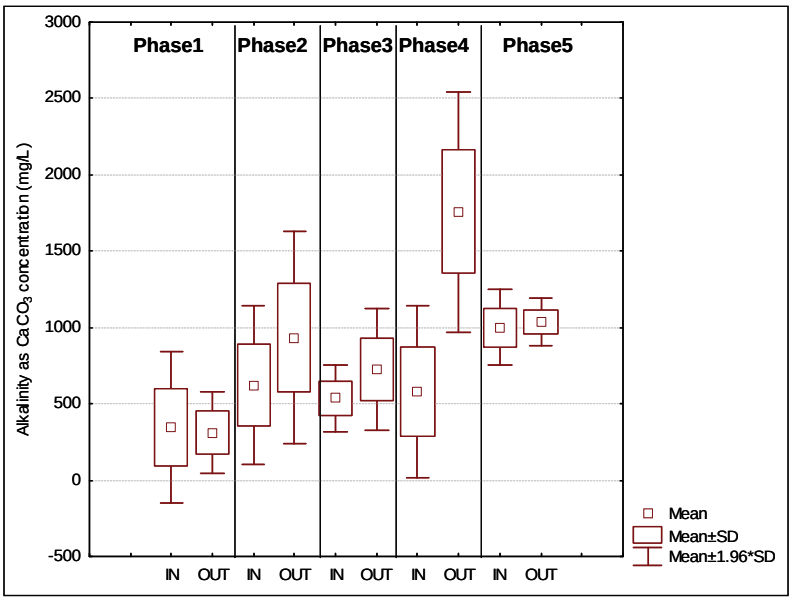

Figure 7. 21. Box and whisker plot indicating the means for influent and effluent alkalinity for each phase.

The statistical analysis of alkalinity showed a significant increase in alkalinity during phase 2 ($n=13$, $p<0.05$, $df= 26$), phase 3 ($n=42$, $p< 0.01$, $df=58$) and phase 4 ($n=21$, $p<0.01$, $df=48$) while the decrease in alkalinity during phase 1 was not significant ($p=0.62$). The increase in alkalinity measured in phase 5 was also not significant ($p=0.32$).

7.3.7 COD

Figure 7.22 reports the influent and effluent COD concentration measured as accumulated data sets over the phases of reactor development study. The general trend showed by the COD data indicates a decrease in COD during all phases of the reactor development investigation. This may be associated with carbon breakdown during active sulphate reduction and sulphur cycling for biomass sustainability during sulphide oxidation.

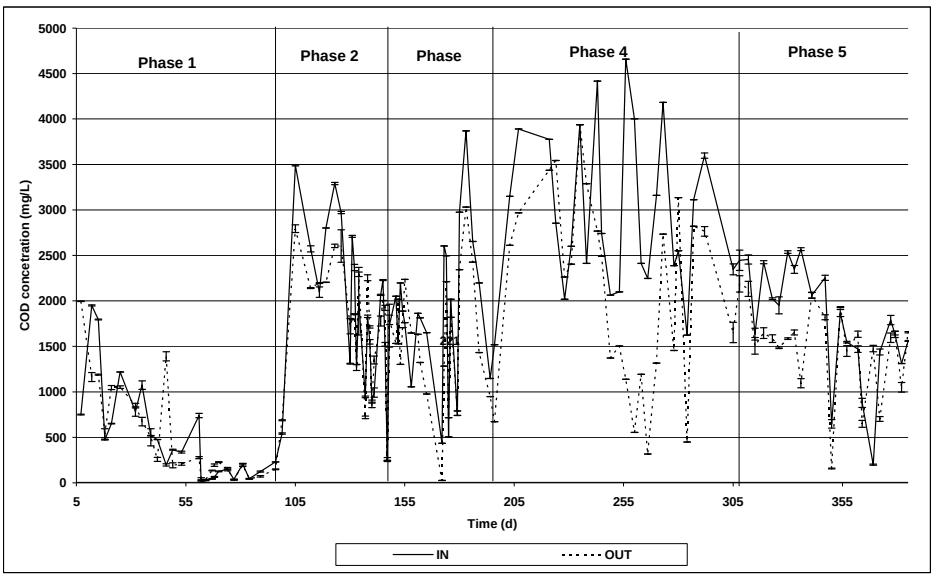

Figure 7. 22. Influent and effluent COD concentration data over the five phases of operation. The error bars indicate standard deviations.

Figure 7.23 reports the means and standard errors of influent and effluent COD concentration for the phases of operation.

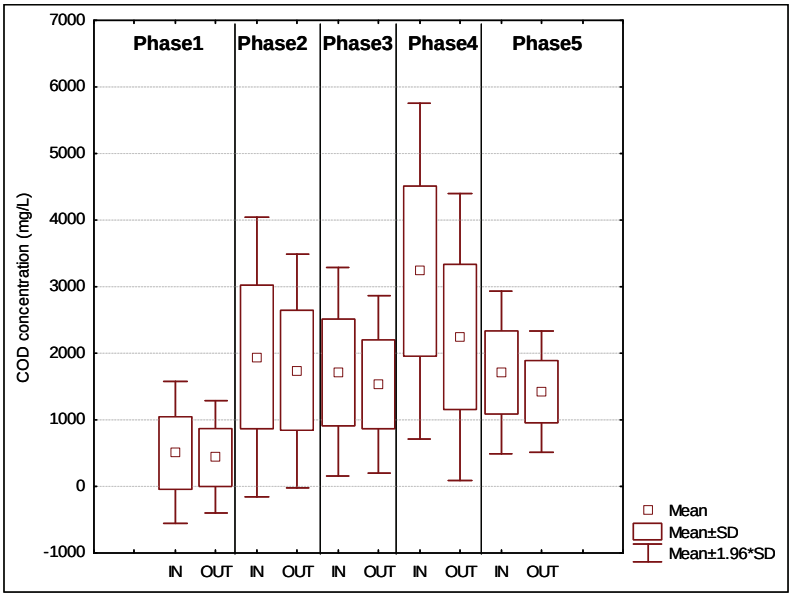

Figure 7. 23. Box and whisker plot indicating the means for influent and effluent COD for each phase of the reactor development study.

The statistical analysis indicate that although there was a general decrease in COD throughout the operational period, the decrease was only significant in Phase 4

(n=21, $p<0.05$, df =58) while in the other phases the decrease in COD was not significant ($p>0.05$).

7.3.8 Mass Balance

Table 7.2 summarises the mass balance data calculated during phase 5 of the investigation showing percentages of mass balance of the system sulphide removed and sulphur recovered. There was an average of 56% sulphur recovery, 65% sulphide removed and 15% sulphur loss recorded over the phases of operation (Table 7.2) indicating an almost 1:1 conversion ratio of the sulphide available for conversion to elemental sulphur

Table 7. 2. Mass balance summary of the reactor development study showing system mass balance, sulphide removal and sulphur recovery over the five phases of the investigation

Phase	**Mass Balance recovery (%)**	**Sulphide removal (%)**	**Sulphur recovery (%)**
5	78	65	56

7.4 CONCLUSIONS

This chapter described preliminary studies undertaken to evaluate the scale-up potential of the LFCR as a sulphide removal operation. The following conclusions were drawn from this study:

- The use of lignocellulose effluent was successfully investigated for sulphide oxidation instead of sewage sludge which had been used in previous studies as the carbon source for generating the sulphide-rich feed for the development of the FSBR.
- The reliability of the FSBR system and sustainability of the sulphur production process over the experimental period formed key objectives of the optimisation and possible scale-up potential of the sulphide oxidation technology.
- Although the data was variable during the reactor development study, optimisation was achieved with an average sulphide removal of 65% and sulphur recovery of 56%.

- Although the harvesting system had been changed from a settling to a surface skimming operation, the performance of the FSBR in terms of sulphide removed and sulphur recovered was not as efficient as the LFCR. However, the recovery rate of the biofilm was decreased from three to four days in phase 1, to six to 12 hours in phase 5. These differences require further investigation in follow-up studies.
- The complete oxidation of sulphide to sulphate and its reduction back to sulphide indicated active sulphur cycling within the system. This will need to be addressed in future optimisation studies.

8. CONCLUSIONS AND RECOMMENDATIONS

8.1 CONCLUSIONS

Floating Sulphur biofilms have been noted to occur on the surface of sulphide-enriched waste-water bodies without their structure and function in these environments, or indeed the performance of floating biofilms in general, being the subject of much comment in the literature. The occurrence of these structures on anaerobic, organic-rich sulphide ponds as observed by EBRU researchers at Rhodes University in the late 1980s, led to a number of preliminary studies in which it was suggested that they were, in fact, true biofilms composed of a diverse group of microorganisms, and having an apparently differentiated structure. Little else was known of their detailed structure or their function correlation, nor had any consideration of their potential in the treatment of sulphide wastewaters been dealt with in the literature outside of this group.

The investigations reported in this study have thus built on the observations of earlier preliminary studies carried out at EBRU. This has focused firstly on developing a structural/functional model accounting for the performance of FSBs, and then exploring the potential application of the system as a biotechnology bioprocess development in the bioremediation of sulphidic wastewaters.

A number of conclusions may be drawn from these studies:

- Light microscopy and SEM investigation of the structure of the biofilm showed that it was composed of, at least in part, large numbers of bacteria with the presence of sulphur crystal-like structures appearing on the underside surface of the biofilm. This could account for the observed granular nature of the Brittle biofilm.
- The presence of sulphur in the biofilm was confirmed provisionally by XRF spectroscopy and hexadecane: water partition which indicated that both organic and inorganic sulphur forms may be present in the biofilm.

- The EDX study confirmed that the crystal-like structures observed in the earlier SEM study were indeed crystals of elemental sulphur and at least some of these were covered by a Thin film of organic matter.
- The complex nature of the biofilm was confirmed and showed the presence of a number of groups of bacteria occupying physiologically defined niches.
- The formation of the different bands and location of species at different levels in the Gradient Tubes, suggests a spatial distribution of the different bacterial species across the FSB.
- Microsensors were used for the first time in the measurement of the characteristics of FSBs and indicated the presence of steep physico-chemical gradients established across the system.
- An inverse relationship was observed between the pH and Redox potential across the depth of the biofilm which was correlated with sulphide removal. While comparable in the Thin biofilm, the effect was more pronounced in the Brittle biofilm where sulphur production is also greater.
- The above findings present a first report that floating biofilms are true biofilms, structured as complex systems broadly comparable to fixed biofilm systems, and are differentiated in terms of structure, physiology and function.
- The study also demonstrated the potential of these systems in bio-process application for sulphide removal from treated AMD wastewaters.
- The LFCR was developed both as an experimental tool for investigating floating sulphur biofilms and as a possible reactor design in passive treatment of AMD.
- Average sulphide removal of 88% and sulphur recovery of 66% were obtained for the Eight-Channel LFCR at an operational loading of 2 618 $Lm^{-2}d^{-1}$.
- Complete oxidation of sulphide to sulphate was identified as one of the critical variables in the operation of the process, and minimizing the extent of this reaction provides the basis for process optimisation studies.
- Process scale-up studies were undertaken with the FSBR pilot plant based on the LFCR laboratory studies. In these preliminary investigations of process-scale up, sulphide removal of 65% and sulphur recovery of 56% was achieved in a 400 days operating period.

- At the end of the phase 5 FSBR study and once optimal inter-harvest periods had been set, the recovery rate of the biofilm following harvesting decreased from three to four days in phase 1 to six to 12 hours in phase 5.

8.2 FUTURE WORK

Studies reported here represent a first detailed report on the structure and function of the floating sulphur biofilm. Further development of a bioprocess application in the treatment of sulphidic wastewaters is possible, intensive study at both the fundamental and applied levels. Important items that need to be addressed include:

- Confirmation of the crystalline structure of the sulphur that is produced in the biofilm. X-ray crystallographic studies should be considered here. Having established this, the sulphur balance between the various sulphur species should confirm the mechanism by which sulphur is formed in these systems. This information would have potentially important implications in the sulphide removal bioprocess optimisation studies;
- Variability in the formation of the biofilm and the factors influencing changes observed should be characterised and possibly related to the structural/functional model accounting for the performance of the system. In this regard, ongoing fundamental studies would feed into the bioprocess development studies;
- While the system is clearly complex and difficult to manipulate by a simple reductive approach, it is evident that further progress in process development will be dependent on deriving accurate kinetic values for the unit operations involved;
- Preliminary development of the LFCR laboratory system, and the FSBR as a bioprocess reactor prototype, has shown potential for the application of the system in the treatment of sulphidic waste-waters. However, substantial room for innovation and improvement exists here and should be the focus of an intensive future study.

8.3 RECOMMENDATIONS

The removal of sulphide from AMD treatment operations that require a reduction in sulphate salinity, remains a major bottleneck in the development of waste-water treatment technology. Although these may be considered to be provisional and a first order indication, the studies reported here provide sufficient indication that the floating sulphur biofilm system may provide a useful basis for future process technology development.

Thus based on the above observations relating to the future potential of the system, the following recommendations are made regarding actions that should be undertaken:

- Reactor development and process optimisation studies be undertaken at laboratory scale to provide the basis for further innovation and technology development;
- Although still clearly a work in progress, the existing LFCR/FSBR system should be scaled up to a reactor surface of several m^2 in order to derive experience in its operation in a passive AMD treatment system application;
- Basic studies into the nature of the floating sulphur biofilm should be continued since an improved understanding of the performance of, and constraints on, the system would feed importantly to bioprocess development operation

.

REFERENCES

Altschul, S.F., Madden, T.L., Schäffe, A.A., Zhang, J., Zhang, Z., Miller, W. and Lipman, D.J. (1997). Gapped BLAST and PSI-BLAST: a New Generation of Protein Data Programs. *Nucleic Acids Res.* **25:** 3389-3402.

Amann, R. I., Binder, B. J., Olson, R. J., Chisholm, S. W., Devereux, R. and Stahl, D. A. (1990). Combination of 16S rRNA-targeted Oligonucleotide probes with Flow Cytometry for Analyzing Mixed Microbial Populations. *Appl. Environ. Microbiol.* **56:** 1919-1925.

Amann, R. I. and Kuhl, M. (1998). *In situ* Methods for Assessment of Microorganisms and their Activities. *Cur. Opin Microbiol*. **1**:352-358.

Amann, R. I., Ludwig, W. and Schleifer, K.H. (1995). Phylogenetic Identification and *in situ* Detection of Individual Microbial Cells without Cultivation. *Microbiol. Rev*. **59**: 143-169.

Amman, R.I., StromLey, J., Devereux, R., Key, R. and Stahl, D.A. (1992) Molecular and microscopic identification of sulfate-reducing bacteria in multispecies biofilms. *Appl. Environ. Microbiol*. **58**: 614-623.

American Public Health Association (APHA). (1989). Standard Methods for the Examination of Water and Wastewater, 17th Edition. *American Public Health Association, Washington, D.C.*

Barnes, H.L. and Romberg, S.B. (1986). Chemical Aspects of Acid Mine Drainage. *J. Water Pollut. Control. Fed.* **40:** 371-384.

Basu, S.K., Mino, T. and Oleszkiewicz, J.A. (1995) Novel application of sulphur metabolism in domestic wastewater treatment *Can. J. Civ. Eng*. **22**: 1217-1223.

Bechard, G., Rajan, S. and Gould, W.D. (1993). Characterization of a Microbiological Process for the Treatment of Acidic Drainage. In:

Biohydrometallurgical Technologies. Torma, A.E., Apel M.L. & Brierly, C.L. (eds). The Minerals, Metals and Materials Society, pp: 277-286**.**

Berbee, M. l. and Taylor, J. W. (1999). Fungal physiology. In: Oliver R and Schweizer M (eds). *Molecular Fungal Biology*. Cambridge, UK: Cambridge University Press, pp: 21-77.

Bond, P. L., Hugenholtz, P., Keller, J. and Blackall, L. L. (1995). Bacterial community structures of phosphate-removing and non-phosphate-removing activated sludges from sequencing batch reactors. *Appl. Environ. Microbiol.* **61**(5): 1910-1916.

Boshoff, G., Duncan, J.R. and Rose, P.D. (1996) An algal-bacterial integrated ponding system for the treatment of mine drainage waters *J. Appl. Phycol*. **8**: 442-449.

Bowker, M. (2002). The Microbial Ecology of Floating Sulphur Biofilms. MSc Thesis, Rhodes University, Grahamstown. South Africa.

Bruser, T., Lens P.N.L. and Truper, H.G. (2000). The biological sulphur cycle. In Environmental technologies to treat sulfur pollution: principles and Engineering. Lens P.N.L and Holsof Pol L. (Eds). IWA Publishing, London. pp: 47 -86.

Buisman, C.J.N, Boonstra, J., Krol, J.P and Dijkman, H. (1996). Biotechnological removal of sulfate and heavy metals from wastewater. In: *Int. conference Advanced Waste Water Treatment*, Amsterdam, 1996.

Buisman, C.J.N., Post, R., Ijspeert, P., Geraats, G. and Lettinga, G. (1989) Biotechnological process for sulphide removal with sulphur reclamation *Acta Biotechnol*. **9**: 255-267.

Campbell, R. (1983) Microbial Ecology. Blackwell Scientific, Oxford (UK).

Carpentier, B. and Cerf, O. (1993). Biofilms and their consequences, with particular reference to hygiene in the food industry. *J. Appl. Bacteriol***.75**(6): 499-511.

Chang, I. S., Shin, P. K. and Kim, B. H. (2000). Biological Treatment of Acid Mine Drainage under Sulphate – Reducing Conditions with Solid Waste Materials as Substrate. *Wat. Res.* **34**: 1269-1277.

Chauke, G. (2002). The Microbial Ecology of Sulfate Reduction in the Rhodes BioSure Process ® MSc Thesis, Rhodes University.

Chen, K.Y and Morris, J.C. 1972. Kinetics of Aqueous sulphide removal by O_2. *Env. Sci. Tech.* **6**(6): 529-531.

Chung, Y., Huang, C. and Tseng, C. (1996). Biodegradation of hydrogen sulphide by a laboratory scale immobilised *Pseudomonas putida* CH11 Biofilter. *Biotechnol. Prog.* **12**: 773-778

Christensen, B. B., Sternberg, C., Andersen, j. B., Nielsen, A. T., Giskov, M. and Molin, S. (1999). Molecular tools for study of biofilm physiology. *Methods Enzymol.***310**: 20-42.

Coetser, S.E., Heath R., Molwantwa, J.B., Rose P.D. and Pulles, W. 2005. Implementation of the degrading packed bed reactor technology and verification of the long-term performance of passive treatment plants at Vryheid coronation colliery. WRC report no.: 1348/ 1/ 05.

Coetser, S. E., Pulles, W., Heath, R. and Cloete, T.E. (2006). Chemical characterisation of organic electron donors for sulphate reduction for potential use in acid mine drainage treatment. *Biodegradation* **17**(2): 67-77.

Coetser, S. E. (2004). Microbial Sulphate Reduction in Passive Acid Mine Drainage Treatment Systems. PhD Thesis. University of Pretoria.

Cole, M.B., Arnold, D.E. and Watten, B.J. (2001). Physiological and Behavioral Responses of Stonefly Nymphs to Enhanced Limestone Treatment of Acid Mine Drainage. *Water Res.* **35**: 625-632.

Cork, D.J., Jerger, D.E. and Maka, A. (1986). A biocatalytic production of sulfur from process waste streams. *Biotechnol. Bioeng. Symp*. Ser. **16**:149-162.

Costerton, J.W. (1995) Overview of microbial biofilms. *J. Industrial Microbiol*. **15**: 137-140.

Costerton, J.W., Lewandowski, Z., De Beer, D., Caldwell, D., Korber, D. and James, G. (1994). Biofilms, the customised microniche. *J. Bacteriol*. **176**: 2137-2142.

Cytryn, E., Van Rijn, J., Schramm, A., Gieseke, A., De Beer, D. and Minz, D. (2005). Identification of bacteria potentially responsible for oxic and anoxic sulphide oxidation in biofilters of a recirculating mariculture system. *Appl. Environ. Microbiol.***71** (10): 6134-6141.

Daims, H., Nielsen, P. H., Schleifer, K-H. and Wagner, M. (2001). *In situ* characterization of *nitrospora*-like nitrite-oxidising bacteria active in wastewater treatment plants. *Appl. Environ. Microbiol.* **67** (11): 5273-5284.

Danese, P.N., Pratt, L.A. and Kolter, R. (2000). Exopolysaccharide production is required for development of *E. coli* K-12 Biofilm. *Biol. Rev.* **64:** 847-867.

Dart, R.K. and Stretton, R.J. (1980). Microbiological aspects of pollution control, Second edition. pp. 192-207. Elsevier, Amsterdam.

Davey, M.E. and O'Toole, G.A., (2000). Microbial Biofilms: From Ecology to Molecular Genetics. *Microb. Molecular Biol Rev.* 64: 847-867**.**

Davidson, W., Reynolds, C.S., Tipping, E. and Needham, R.F. (1989). Reclamation of acid waters using sewage sludge. *Environ. Pollut.,* **57**:251-274.

De Beer, D. and Muyzer, G. (1995). Multispecies biofilms: report from the discussion session. *Wat. Sci. Tech*. **32**: 269-270.

De Beer, D. and Schramm, A. (1999). Micro-environments and mass transfer phenomena in biofilms studied with microsensors. *Wat. Sci. Tech*. **39**: 173-178.

De Beer, D. and Stoodley, P. (2006). Microbial biofilms. In the prokaryotes. Vol 1: Symbiotic Associations. Dworkin, M., Falkow, S., Rosenberg, E, Schleifer, K-H. and Stackebrandt, E (Eds). Springer, New York. pp: 904-937.

De Beer, D., Stoodley, P., Roe, F. and Lewandowski, Z. (1994). Effects of biofilm structures on oxygen distribution and mass transport. *Biotechnol. Bioeng*. **43**: 1131-1138.

De Beer, D.A., Schramm, C.M., Santegoeds, C.M. and Kuhl, M. (1997). A Nitrite Microsensor for Profiling Environmental Biofilms. *Appl. Environ. Microbiol.* **63**:973-977.

Dill, S., Cloete, T.E., Coetser, L. and Zdyb, L. (2001). Determination of the Suitability of Alternative Carbon Sources for Sulphate Reduction in the Passive Treatment of Mine Water. *WRC Report No. 802/1/0* Water Research Commission, Pretoria, South Africa.

Dunn, K.M., (1988). The biotechnology of high rate algal ponding systems in the treatment of saline tannery wastewaters. PhD Thesis, Rhodes University, Grahamstown. South Africa.

Dunne, W.M. (2002). Bacterial adhesion: seen any good biofilm lately? *Clinical Microbiology reviews*. **15**: 155-166.

Dvorak, D.H., Hedin, R.S., Edenborn, H.M and McIntire, P.E. (2004). Treatment of metal-contaminated water using bacterial sulphate reduction: Results from pilot-scale reactors. *Biotech. Bioeng.* **40 (**5): 609 -616.

Elder, M.J., Stapleton, F., Evans, E. and Dart, J.K. (1995). Biofilm-related infections in ophthalmology. *Eye*. **9** (1): 102-109.

Gadre, R.V. (1989). Removal of hydrogen sulphide from biogas by a chemoautotrophic fixed-film bioreactor. *Biotech. Bioeng*. **34**: 410-414.

Gardner, M.N. (1998). A study of the chemolithoautotrophic bacterial rhodanese, and its potential contribution to cyanide wastage during cyanidation of bio-oxidized concentrates. MSc Thesis, University of Cape Town, South Africa.

Gazea, B., Adam, K. and Kontopoulos, A. (1996). A Review of Passive Systems for the Treatment of Acid Mine Drainage. *Miner. Eng.*, **9**: 23-42.

Gilbert, P., Maira-Litran, T., McBain, A.J., Rickard, A.H. and White, F. (2002). Physiology and collective recalcitrance of microbial biofilm communities. *Annual Reviews in Microbiology*. **46**:, 203- 256.

Gilbert, P., Das, J. and Foley, I. (1997). Biofilm susceptibility to antimicrobials. *Advances in Dental Research.* **11** (1): 160-167.

Gilfillan, J.C. (2000). The structure and microbiology of floating sulphide oxidizing biofilms. MSc Thesis. Rhodes University, Grahamstown. South Africa.

Goebel, B.M. and Stackebrandt, E. (1994). Cultural and phylogenetic analysis of mixed microbial populations found in natural and commercial bioleaching environments. *Appl. Environ. Microbiol*. **60**: 1614-1621.

Guoqiang, Z., Jie, P., Yi, Y., and Shimin, Z. (1994). Bacterial desulfurization of the H_2S-containing biogas. *Biotechnol. Lett*. **16**: 1087-1090.

Habets, L.H.A and De Vegt, A.L. (1991). Anaerobic treatment of bleached TMP and CTMP effluent in the Biopaq system. *Wat. Sci. Technol.* **24**(3-4): 331-345.

Hammond, C. (1986). The Dow Stredford chemical recovery process. *Environ Prof* **5** (1): 1- 4.

Hansen, L.S. and Blackburn, T.H. (1995). Amino acid degradation by sulphate-reducing bacteria: Evaluation of four methods. *Limnol. Oceanogr.* **40 (3):** 502-510.

Harmsen, H.J., Kengen, H.M., Akkermans, A.D., Stams, A.J. and De Vos, W.M. (1996). Detection and localization of syntropic propionate-oxidizing bacteria in granular sludge by *in situ* hybridisation using 16S rRNA-based Oligonucleotide probes. *Appl. Environ. Microbiol.* **62** (5): 1656-1663.

Head, I.M., Saunders, J.R. and Pickup, R.W. (1998). Microbial Evaluation, Diversity and Ecology: a Decade of Ribosomal RNA Analysis of Uncultivated Microorganisms. *Microb. Ecol.* **35:** 1-21.

Hermanowicz S.W., (2003). Biofilm architecture: interplay of models and experiments. In: Biofilms in wastewater treatment- An interdisciplinary approach. Wuetz, S., Bishop, P. and Wilderer, P. (Eds). IWA Publishing, London. pp 32-45.

Heuer, H., Hartung, K., Weiland, G., Kramer, I. and Smalla, K. (1999a). Polynucleotide probes that target a hypervariable region of 16s rRNA genes to identify bacterial isolates corresponding to bands of community fingerprints. *Appl. Environ. Microbiol*. **65**: 1045-1049.

Heuer, H., Krasek, M., Baker, P., Smalla, K. and Wellington, E.M.H. (1999b). Analysis of *Actinomycete* communities by specific amplification of genes encoding 16S rRNA and gel-electrophoretic separation in denaturing gradients. *Appl. Environ. Microbiol.* **63:** 3233-3241.

Hugenholtz, P., Goebel, B. M. and Pace, N. R. (1998). Impact of Culture independent Studies on the Emerging Phylogenetic View of Bacterial Diversity. *J. Bacteriol.* **180:** 4765-4774.

Ito, T., Sugita, K. and Okabe, S. (2004). Isolation, characterisation: An *in situ* detection of novel chemolithoautotrophic sulphur-oxidizing bacterium in wastewater biofilms growing under microaerophilic conditions. *Appl. Environ. Microbiol.* **70**: 3122-3129.

Ito, T., Okabe, S., Satoh, H. and Watanabe, Y. (2002). Successional Development of Sulphate Reducing Bacterial Populations and their Activities in a Wastewater

Biofilm Growing under Microaerophilic Conditions. *Appl. Environ. Microbiol.* **68**: 1392-1402.

Janssen, A.J.H., Dijkman, H. and Janssen, G. (2000). Novel Biological processes for the removal of H_2S and SO_2 from gas streams. In Lens and Hulsof Pol (Eds). Environmental technologies to treat sulfur pollution. IWA Publishing, London. pp: 265-280.

Janssen, A.J.H., Lettinga, G. and De Kaizer, A. (1999). Removal of hydrogen sulphide from wastewater and waste gases by biological conversion to elemental sulphur. Colloidal and interfacial aspects of biologically produced sulphur particles. *Physicochemical and Engineering Aspects* **151**: 389-397.

Janssen, A.J.H., Meijer, S., Bontsema, J. and Lettinga, G. (1998). Application of the redox potential for controlling a sulfide oxidizing bioreactor. *Biotech. Bioeng*. **60**: 147-155.

Janssen, A.J.H., Ma, S.C., Lens, P. and Lettinga, G. (1997). Performance of a sulfide-oxidising expanded-bed reactor supplied with dissolved oxygen. *Biotech. Bioeng*. **53**:32-40.

Johnson, D.B. (2000). Biological Removal of Sulphurous Compounds from Inorganic Wastewaters. In: Lens, P.N.L. & Hulsoff-Pol, L. (Eds). *Environmental Technologies to Treat Sulfur Pollution: Principles in Engineering.* IWA Publishing, London. pp: 175-193.

Johnson, D.B. (1995). Acidophilic Microbial Communities: Candidates for Bioremediation of Acidic Mine Effluent. *Int. Biodet. Biodeg* .**35**: 41-58.

Johnson, D. B. and Hallberg, K. B. (2005). Acid mine drainage remediation: A mini review. *Science of the Total Environment.*338: 3-14

Johnson, D.B. and Hallberg, K.B. (2003). The Microbiology of Acidic Mine Waters. *Research in Microbiology*. **154:** 466-473.

Johnson, D.B., Dziurla, M-A., Kolmert, A. and Hallberg, K.B. (2002). The Microbiology of Acid Mine Drainage: Genesis and Biotreatment. *SA J. Sci.*. **98:** 249-255.

Jorgensen, B.B., Teske, A., Cohen, Y. (1998). Sulphate reducing bacteria and their activities in cyanobacterial mats of a solar lake. *Appl. Environ. Microbiol.* **64** (8): 2943-2951.

Jorgensen, B.B. and Revsbech, N.P. (1985). Diffusive boundary layers and the oxygen uptake of sediments and detritus. *Limnol. Oceanogr.* **30** (1): 111 -122.

Kalin, M.M., Cairnes, J. and McCready, R. (1991). Ecological Engineering for Acid Mine Drainage Treatment of Coal Waters. *Resour. Conserv. Recycl.*, **5**: 265-275.

Kelly, D.P (1985). Physiology of the *Thiobacilli*: elucidating the sulphur oxidation pathway. *Microbiological Sciences,* **2**: 105-109.

Kelper, D. A. and McCleary, E. C. (1994). Successive Alkalinity-Producing Systems (SAPS) for Treatment of Acidic Mine Drainage. In: Proceedings of the International Land Reclamation and Mine Drainage Conference, Pittsburgh, PA. April 24-29, 1994. pp: 195-204.

Kim, B.W., Kim, I.K. and Chang, H.N. (1990). Bioconversion of hydrogen sulphide by free and immobilised cells of *Chlorobium thiosulfatophilum. Biotechnol. Lett*. **12**: 381-386.

Kloeke, F. V. O. (1999). Localization and identification of population of phosphate-active bacterial cells associated with activated sludge flocs. *Microbial Ecology*. **38**(3): 201-214.

Kolmert, A., Henrysson, T., Hallberg, R. and Mattiasson, B. (1997). Optimization of sulphide production in an anaerobic continuous biofilm process with sulphate reducing bacteria. *Biotechnol. Lett*. **19**: 971-975.

Kuenen, J.G. and Robertson, L.A. (1992). The use of natural bacterial populations for the treatment of sulphur-containing wastewater. *Biodegradation*, **3**: 239-254.

Kühl, M. and Jørgensen, B.B. (1992). Microsensor measurements of sulfate reduction and sulfide oxidation in compact microbial communities of aerobic biofilms. *Appl. Environ. Microbiol*. **58**: 1164-1174.

Lane, D.J., Harrison, A.P., Stahl, D., Pace, B., Giovannoni, S.J., Olsen, G.J. and Pace, N.R. (1992). Evolutionary relationships among sulphur- and iron-oxidizing eubacteria. *J. Bacteriol*. **174**: 269-278.

Lawrence, J.R., Wolfardt, G.M. and Korber, D.R. (1994). Determination of Diffusion Coefficients in Biofilms by Confocal Laser Microscopy. *Appl. Environ. Microbiol*.**60:** 1166-1173.

Lens, P.N.L., Omil, F., Lema, J.M. and Hulsof Pol, L.W. (2000). Biological treatment of organic sulfate-rich wastewaters. In Lens and Hulsof Pol (Eds). IWA Publishing, London. pp: 153-174.

Lewandowski Z. (1995). Microbial biofilms. *Annual Rev. Microbiol.*. **49** 711-745.

Lewandowski Z and Beyenal, H. (2003). Biofilm monitoring: a perfect solution in search of a problem. *Wat. Sci. Technol.* **47** (5): 9-18.

Liesack, W., Weyland, H. and Stackebrandt, E. (1991). Potential Risks of Gene Amplification by PCR as Determined by 16S rDNA Analysis of a Mixed-Culture of Strict Barophilic Bacteria. *Microbial* Ecology **21**(1): 191-198.

Lin, C. and Stahl, D. A. (1995). Comperative Analysis Reveal a Highly Conserved Endoglucanase in the Cellulolytic genus Fibrobacter. *J. Bacteriol.* **177:** 2543-2549.

Liu, W.T., Marsh, T.L., Cheng, H. and Forney, L.J. (1997). Characterization of Microbial Diversity by Determining Terminal Restriction Fragment Length

Polymorphism of Genes Encoding 16S rRNA. *Appl. Environ. Microbiol.* **63:** 4516-4522.

Madikane, M. (2002). Biosulphidogenic Hydrolysis of Lignin and Lignin Model Compounds. MSc. Thesis, Rhodes University, Grahamstown, South Africa.

Maree, J.P., Van Tonder G.J. and Millard, P. (1996). Underground Neutralization of Mine Water with Limestone. *Report to the Water Research Commission,* CSIR. WRC Report No. 609/1/96.

Maree, J.P., Du Plessis, P. and Van der Walt, C.J. (1992). Treatment of Acid Effluents with Limestone Instead of Lime. *Wat. Sci. Tech.,* **26**: 345-355.

Maree, J.P. and Hill, E. (1989). An integrated process for biological treatment of sulfate-containing industrial effluent. *J. Water Pollution Control Federation.* **59**: 1069-1074.

Maree, J.P., Gerber, A., McLaren, A.R. and Hill, E. (1988). Biological treatments of mining effluents. *Env. Tech. Lett*. **8:** 53-64.

Middelburg, J.J. (2000). The geochemical sulphur cycle. In: Lens and Hulsof Pol (Eds). *Environmental technologies to treat sulphur pollution: Principles and Engineering*. IWA Publishing, London. pp 33-45.

Molipane, N.P (1999). Sulphate reduction utilizing hydrolysis of complex carbon sources. MSc Thesis, Rhodes University, Grahamstown, South Africa.

Molwantwa, J.B (2002). Enhanced Hydrolysis of Sewage Sludge. MSc Thesis, Rhodes University, Grahamstown. South Africa.

Molwantwa, J., Coetser, S.E., Heath, R. and Pulles, W. (2003). The Monitoring, Evaluation and Verification of a Long-Term Performance of Passive Treatment Plants at Vryheid Coronation Colliery (VCC) Pilot Plant. *Final Report to WRC.* Project No.:K5/1348.

Muyzer, G. and Ramsing, N.B. (1995). Molecular methods to study the organisation of microbial communities. *Wat. Sci. Tech*. **32**: 1-9.

Muyzer, G., De Waal, E. C. and Uitterlindin, A. G. (1993). Profiling of complex microbial populations by denaturing gradient gel electrophoresis: Analysis of polymerase chain reaction amplified genes coding for 16S rRNA. *Appl. Environ. Microbiol.* **59**: 695-700.

Nielsen, P.H., De Muro, M.A. and Nielsen, J.L. (2000). Studies on the *in situ* physiology of *Thiothrix* spp. present in activated sludge. *Environ. Microbio. **2:*** 389-398.

Nielson, P.H., Andreasen, K., Lee, N. and Wagner, M. (1999). Use of Microautography and Fluorescent *In Situ* Hybridization for Characterization of Microbial Activity in Activated Sludge. *Wat. Sci. Tech.* **39**: 1-9.

Nivens, D.E., Palmer, R.J. and White, D.C. (1995). Continuous nondestructive monitoring of microbial biofilms: a review of analytical techniques. *J. Industrial Microbiol.* **15**: 263-276.

O'Flaherty, V. and Colleran, E. (2000). Environmental technologies to treat sulphur pollution: principles and engineering. Lens PNL and Hulsoff Pol L (eds). IWA, London

O'Flaherty, V., Colohan, S., Mulkerrins, D. and Colleran, E. (1999). Effect of sulphate addition on volatile fatty acid and ethanol degradation in an anaerobic hybrid reactor II: Microbial interactions and toxic effects. *Biores. Technol*. 68: 109-120.

O'Toole, G.A., Kaplan, H. B. and Kolter, B. (2000). Biofilm Formation as Microbial Development. *Annu. Rev. Microbiol.* **54:** 49-79.

Okabe, S., Hiratia, K., Ozawa, Y. and Watanabe, Y. (1996). Spatial microbial distributions of nitrifiers and heterotrophs in mixed-population biofilms. *Biotechnol. Bioeng.* **50**: 24-35.

Okabe, S., Itoh, T., Satoh, H. and Watanabe, Y. (1999). Analyses of Spatial Distributions of Sulphate-Reducing Bacteria and their Activity in Aerobic Wastewater Biofilms. *Appl. Environ. Microbiol.* **65**: 5107-5116.

Okabe, S., Satoh, H., Itoh, T. and Watanabe, Y. (1999). Microbial ecology of sulphate reducing bacteria in wastewater biofilms analyzed by microelectrodes and FISH (fluorescent *in situ* hybridization) technique. *Wat. Sci. Tech*. **39**:41-47.

Okabe, S., Matsuda, T., Satoh, H., Ito, T. and Watanabe, Y. (1998). Sulfate reduction and sulfide oxidation in aerobic mixed population biofilms. *Wat. Sci. Tech*. **37**: 131-138.

Okubo, K., Sugawa, H., Gojobori, T and Tateno, Y. (2006). DDBJ in preparation for overview of research activities behind data submissions. *Nucleic Acids Res.* **34**: D6-D9.

Paerl, H. W. and Pinckney, J. L. (1996). A mini-review of microbial consortia: Their role in aquatic production and bio-geochemical cycling. *Microbiol. Ecology*.**31** (3): 225-247.

Pareek, S., Kim, S. K., Matsui, S. and Shimizu, Y. (1998). Hydrolysis of Lignocellulosic Materials under Sulphidogenic and Methanogenic Conditions. *Wat. Sci. Tech.* **38**: 193-200.

Parsek, M. R. and Faqua, C. (2004). Biofilms 2003: Emerging themes and challenges in studies of surface-associated microbial life. *J. Bacteriol.* **186** (14): 4427-4440.

Poulsen, L.K., Ballard, G. and Stahl, D.A. (1993). Use of rRNA fluorescence *in situ* hybridisation for measuring the activity of single cells in young and established biofilms. *Appl. Environ. Microbiol*. **59**: 1354-1360**.**

Pulles Howard and De Lange (PHD), (2002). Development of low maintenance self-sustaining biological (passive) systems for the treatment of contaminated mine

and industrial effluents. Final report to the DACST Innovation Fund Project No.: 32130. September 2002.

Pulles, W., Howie, D., Otto, D. and Easton, J. (1995). A manual on mine water treatment and management practices in South Africa. WRC report no. TT 80/96. Water Research Commission. South Africa.

Pulles, W., Van Niekerk, A., Wood, A., Batchelor, A.,, Dill, S., du Plessis, P., Howie, D. and Casy, T. (2001). Pilot Scale Development of Integrated Passive Water Treatment Systems for Mine Effluent Streams. *WRC Report No.700/1/01*. Water Research Commission, Pretoria, South Africa.

Ramesh, A., Lee, D. J., Wang, M. L., Hsu, J. P., Juang, R. S., Hwang, K. J., Liu, J. C. and Tseng, S. J. (2006). Biofouling in membrane bioreactors. *Separation Science and Technol***41** 97): 1345-1370.

Ramsing, N. (1998). Molecular biological tools to study population dynamics of sulphur cycle bacteria in natural environments and bioreactors (16S rRNA molecular probes, PCR). *TMR Summer School Programme*, Wageningen, Netherlands.

Ramsing, N.B., Kuhl, M. and Jorgensen, B.B. (1993). Distribution of Sulphate-Reducing Bacteria, O_2 and H_2S in Photosynthetic Biofilms Determined by Oligonucleotide Probes and Microelectrodes. *Appl. Environ. Microbiol*. **59:** 3840-3849.

Raskin, L. Rittmann, B.E. and Stahl, D.A. (1996). Competition and Coexistence of Sulphate-Reducing and Methanogenic Populations in Anaerobic Biofilms. *Appl. Environ. Microbiol*. **62**: 3847-3857.

Raskin, L., Poulsen, L. K., Noguera, D. R., Rittmann, B. E. and Stahl, D.A. (1994). Quantification of Methanogenic Groups in Anaerobic Biological Reactors by Oligonucleotide Probe Hybridization. *Appl. Environ. Microbiol.* **60**: 1241-1248.

Rein, N. B. (2002). Biological Sulphide Oxidation in Heterotrophic Environments. MSc. Thesis, Rhodes University, Grahamstown, South Africa.

Reinhoudt, H.R. and Moulijn, J.A. (2000). Catalytic removal of sulfur from diesel oil by hydrotreating. In Lens and Hulsf Pol (Eds). Environmental treatment technologies to treat sulfur pollution. IWA Publishing, London. pp: 87-103.

Reysenbach, A., Giver, L.J., Wickham, G.S. and Pace, N.R. (1992). Differential amplification of rRNA by polymerase chain reaction. *Appl. Environ. Microbiol.* **58**(10): 3417-3418.

Rigler, R. J. (1966). Microfluorometric characterisation of intracellular nucleic acids and nucleoproteins by acridine orange. *Acta. Physiol. Scand. Suppl.* **267**: 1-122.

Robertson, L.A. and Kuenen, J.G. (1991). The colourless sulphur bacteria. In*:* Balows, A., Trüper, H.G., Dworkin, M., Harder, W. and Schleifer, K.H. (eds.) *The Prokaryotes, a handbook on the biology of bacteria: Ecophysiology, Isolation, Identification, Applications.*, Second edition, Vol. I, pp. 835-413. Springer-Verlag. New York.

Rose, P.D. (2002). Volume 1: Overview. In Salinity, Sanitation and Sustainability: A study in environmental biotechnology and integrated wastewater beneficiation in South Africa. WRC Report No.: TT 187/02. Water research Commission, Pretoria, South Africa.

Rose, P.D., Boshoff, G.A., Van Hille, R.P., Wallace, L.C.M., Dunn, K.M. and Duncan, J.R. (1998). An integrated algal sulphate reducing high-rate ponding process for the treatment of Acid Mine Drainage wastewaters. *Biodegradation* **9**: 247-257.

Rose, P.D., Maart, B.A., Dunn, K.M., Roswell, R.A. and Britz, P. (1996). High rate algal oxidation ponding for the treatment of tannery effluent. *Wat. Sci. Tech*. **33**: 219-227.

Ross, P., Mayer, R. and Benziman, M. (1991). Cellulose biosynthesis and function in bacteria. *Microbiol. Mol. Biol. Rev*.**55**(1): 35-38.

Santegoeds, C. M., Damgaard, C.M., Hesselink, G., Zopfl, J., Lens, P., Muyzer, G. and De Beer, D. (1999). Distribution of Sulphate-Reducing and Methanogenic Bacteria in Anaerobic Aggregates Determined by Microsensor and Molecular Analysis. *Appl. Environ. Microbiol*. **65**: 4618-4629.

Santegoeds, C.M., Ferdelman, T.G., Muyzer, G. and De Beer, D. (1998). Structural and functional dynamics of sulfate-reducing populations in bacterial biofilms. *Appl. Environ. Microbiol.* **64**: 3731-3739.

Sauer, K., Camper, A. K., Ehrlich, G. D., Costerton, J. W. and Davies, D. G. (2002). *Pseudomonad euriginosa* displays multiple phenotypes during development of a biofilm. *J. Bactriol.* **184** (4): 1440-1154.

Sazowsky, I.D., Foss, A. and Miller, C.M. (2000). Controls on the Removal of Iron and the Remediation of Acid Mine Drainage. *Water Res.* **34**: 2742-2746.

Scheerem, P.J.H., Kock, R.O. and Buisman, C.J.N. (1993). Geohydrological contaminant system and microbial water treatment plan for metal contaminated groundwater at Budelco. *International Symposium World Zinc*.pp. 373-384

Schoeman, J.J. and Steyn, A. (2001). Investigation into Alternative Water Treatment Technologies for the Treatment of Underground Mine Water Discharged by the Grootvlei Proprietary Mines Ltd into the Blesbokspruit in South Africa. *Desalination.* **133** : 13-30.

Schramm, A., De Beer, D., Gieseke, A. and Amann, R. (2000). Microenvironment and Distribution of Nitrifying Bacteria in a Membrane-Bound Biofilm. *Environ. Microbiol*. ***2***:680-686.

Schramm, A. De Beer, D., Van den Heuvel, J.C., Ottengraf, S. and Amann, R. (1999). Microscale Distribution of Populations and Activities of *Nitrospira a*nd

Nitrospira spp. Along a Microscale Gradient in a Nitrifying Bioreactor: Quantification by i*n situ* Hybridization and the Use of Microsensors. *Appl. Environ. Microbiol*. **65**: 3690-3696.

Schramm, A., Larsen, L.H., Revsbech, N.P. and Amann, R.I. (1997). Structure and function of a nitrifying biofilm as determined by microelectrodes and fluorescent oligonucleotide probes. *Wat. Sci. Tech.* **36**: 263-270.

Scott, R. (1995). Flooding of Central and East Rand Gold Mines: an Investigation into Controls over the Inflow Rate, Water Quality and the Predicted Impacts of Flooded Mines. *Water Research Commission Report.* No 486/1/95. Water Research Commission, South Africa.

Scousen, J., Sextone, A. and Ziemkiewicz, P. F. (2000). Acid Mine Drainage Treatment and Control. In: Bamhisle, R.; Daniels, W.; and Darmody, R. (eds). *Reclamation of Drastically Disturbed Lands*. pp: 131-168. American Society of Agronomy, Madison, WI.

Son, H. and Lee, J. (2004). H_2S removal with an immobilized cell hybrid reactor. *Process Biochem.***40**: 2197-2203.

StatSoft, Inc. (2005). STATISTICA (data analysis software system). Version 7.1. www.statsoft.com.

Steudel, R. (2000). The chemical sulphur cycle. In Lens and Hulsof Pol (Eds). *Environmental technologies to treat sulfur pollution: principles and Engineering. Lens* IWA Publishing, London.pp: 1 -28.

Steudel, R. (1988). On the nature of the "elemental sulphur" (S^o) produced by sulphur oxidising bacteria – a model for S^o globules. In: Schlegel, H.G. and Bowin, B. (eds.) *Biology of autotrophic bacteria*. *Science Tech.* Madison.

Steudel, R. (1996). Mechanism for the formation of elemental sulphur from aqueous sulphide in chemical and microbiological desulphurization processes. *Ind. Eng. Chem. Res.* **35**: 1417-1423.

Steudel, R. (2000). The chemical sulphur cycle. In Lens and Hulsof Pol (Eds). Environmental technologies to treat sulphur pollution: Principles and Engineering. IWA Publishing. London. pp: 1 -28.

Stewart, P.S., Murga, R., Srinivasan, R. and De Beer, D. (1995). Biofilm structural heterogeneity visualised by three microscopic methods. *Wat. Res*. **29**: 2006-2009.

Stoodley, P., Yang, S., Lappin-Scott, H. and Lewandowski, Z. (1997). Relationship between mass transfer coefficient and liquid flow velocity in heterogenous biofilms using microelectrodes and confocal microscopy. *Biotechnol. Bioeng*. **56**:681-688.

Stumm, J. and Morgan, J. J.(1995). Aquatic Chemistry – Chemical equilibria and rates in natural waters. John Wiley and Sons Inc. 3rd Edition.

Sublette, K.L., Hesketh, R.P. and Hasan, H. (1994). Microbial oxidation of hydrogen sulfide in a pilot-scale bubble column. *Biotechnol. Prog*. **10**:611-614.

Sublette, K.L (1992.) Microbial stabilisation of active-sulfide sludges. *Appl. Biochem. Biotechnol.* **34**/**35**: 811-817.

Sublette, K.L. and Sylvester, N.D. (1987) Oxidation of hydrogen sulfide by *Thiobacillus denitrificans*: desulfurization of natural gas. *Biotech. Bioeng*. **29**:249-257.

Takahashi, H, Kimura, B. Yoshikawa, M., Gotou, S., Watanabe, I. and Fujii T. (2004). Direct detection and identification of lactic acid bacteria in FPP using degrading gradient gel electrophoresis. *J Food Protection* **67** (11): 2515-2520.

Tuttle, J. H., Dugan, P. R., MacMillan, C. B. and Randles, C. I. (1969). Microbial Dissimilatory Sulphur Cycle in Acid Mine Water. *J. Bacteriol.* **97**: 594-602.

Van Hille, R.P. and Duncan, J.R. (1996). Bioremediation of heavy metal polluted acidic mine effluents by *Spirullina*. *J. Appl. Phycol*. **8**: 461-466.

Voordouw, G., Armstrong, S. M., Reiner, M. F., Fouts, B. R., Telang, A. J., Shen, Y. and Gervets, D. (1996). Characterisation of 16S rRNA genes from oil field microbial communities indicates the presence of a sulphate-reducing, fermentative and sulphide-oxidising bacteria. *Appl. Environ. Microbiol.* **62** (5): 1623-1629.

Vroom, J. M., De Graw, K. J., Garretson, H. C., Backsaw, D. J., Marsh, P. D., Watson, G. K., Birmingham, J. J. and Allison, C. (1997). Depth penetration and detection of pH gradients in biofilms by two-photon excitation microscopy. *Appl. Environ. Microbiol.* **65** (8): 3502-3511.

Wagner, M., Erhart, R., Manz, W., Amann, R., Lemmer, H., Wedi, D., Schleifer, K.H. (1994). Development of an rRNA-targeted Oligonucleotide probe specific for the genus *Acinetobacter* and its application for in situ monitoring in activated sludge. *Appl. Env. Microbiol*. **60**: 792-800.

Wagner, M., Amann, R., Lemmer, H., Schleifer, K.H. (1993). Probing activated sludge with Oligonucleotide specific for proteobacteria: inadequacy of culture-dependent methods for describing microbial community structure. *Appl. Env. Microbiol.* **59**: 1520-1525.

Ward, D. M., Ferris, M. J., Nold, S. C. and Bateson, M. M. (1998). A natural view of microbial diversity within hot spring cyanobacterial mat communities. *Microbiol. Mol. Biol. Rev.* **62** (4): 1358-1370.

Waterson K., Bejan, D. and Bunce, N.J. (2006). Electrochemical oxidation of sulphide ion at a boron-doped anode. *J Appl. Electrochem* **37**(3): 367-373.

Watnick, P. and Kolter, R. (2000). Biofilm, City of Microbes. *J. Bacteriol.* **182** (10): 2675-2679.

Weast, R. C. (1981). Handbook of chemistry and physics (62nd edition). CRC Press Inc., Boca Roton, USA.

Weller, R., Weller, J.W. and Ward, D.M. (1991). 16S rRNA sequences of uncultivated hot spring cyanobacterial mat inhabitants retrieved as randomly primed cDNA. *Appl. Environ. Microbiol*. **57**: 1146-1151.

Whittington-Jones, K. (2000). Sulphidogenic Hydrolysis of Complex Organic Carbon Substrates. PhD Thesis, Rhodes University, Grahamstown, South Africa.

Widdel, F. (1988). Microbiology and ecology of sulfate and sulphur reducing bacteria. In: Zehnder, A.J.B. (Eds.) *Biology of anaerobic microorganisms.* pp. 469-585. Willey and Sons Inc., New York.

Widdel, F. and Pfenning, N. (1984). Dissimilatory Sulphate- or Sulphur-Reducing Bacteria. In *Bergey's Manual of Systematic Bacteriology* Kreig, N.R. and Holt, J.G. (eds). pp. 663-679. Baltimore: Williams and Wilkins Co.

Williams, T. M. and Unz, R. F. (1985). Filamentous sulfur bacteria of activated sludge: Characterisation of *Thiothrix*, *Beggiatoa* and *Eikelboom* type 021N strains. *Appl. Environ. Microbiol*.**49** (4): 887-898.

Wu, C. J. and Janssen, G. R. (1996). Translation of *vph* mRNA in *Streptomyces lividans* and *Escherichia coli* after removal of the 5' untranslated leader. *Mol Microbiol* **22**, 339-355.[

Wuertz S. (2003). Architecture, population structure and function: Introduction. In Wuertz, bishop and Wilderer (Eds*). Biofilms in wastewater treatment*. Pp: 125-146.

Yao, W. and Millero, F. J. (1996). Oxidation of hydrogen sulphideby hydrous Fe (III) oxides in seawater. *Marine Chemistry*. **52**: 1-16.

Younger, P.L. (2004). The mine water pollution threat to water resources and its remediation in practice. *IDS-Water Europe* .http://www.idswater.com/

Younger, P.L., Banwart, S.A. and Hedin, R.S. (2002). Mine water: hydrology, pollution, remediation. Kluwer Academic Publishers. Dordrecht.

Younger, P. L. (2001). Mine Water Pollution in Scotland: Nature, Extent and Preventative Strategies. *Sci Total Environ.* **265**: 309-326.

Younger, P.L. (1998). Design, Construction and Initial Operation of Full-Scale Compost-Based Passive Systems for Treatment of Coal Mine Drainage and Spoil Leachate in the UK. IMWA Symposium, Johannesburg, pp: 413-424.

Younger, P.L., Curtis, T.P., Jarvis, A. and Pennell, R. (1997). Effective Passive Treatment of Aluminum-Rich Acidic Colliery Spoil Drainage Using a Compost Wetland at Quaking Houses, County Durham. *J. Chartered Inst. Water Environ. Mg.* **11**: 200-208.

Yu, T. and Bishop, P.L. (1998). Stratification of microbial metabolic processes and redox potential change in an anaerobic biofilm studied using microelectrodes. *Wat. Sci. Tech*. **37**: 195-198.

Zhang, T.C. and Bishop, P.L. (1994). Density, porosity, and pore structure of biofilms. *Wat. Res*. **28**: 2267-2277.

Zipper, C. and Jage, C. (2001). Passive Treatment of Acid-Mine Drainage with Vertical-Flow Systems. Reclamation Guidelines for Surface Mined Land in Southwest Virginia. Powell River Project. Virginia Cooperative Extension, Publication 460-133, pp:1-16.

.

.

A. APPENDIX A

A-1 MEDIA AND REAGENTS USED IN MOLECULAR MICROBIAL ECOLOGY STUDIES

A-1.1 Gradient Tubes

A-1.1.1 10cm Agarose Overlay Column

50 mL of the agarose overlay column was prepared using 0.5 g low melt agarose, 25 mL milliQ water and 25 mL double strength media.

A-1.1.2 Double Strength Media

The double strength media was prepared using 1.75 mL 60% sodium lactate, 1 g $MgSO_4.7H_2O$, 0.5 g KNO_3, 0.5 g Na_2SO_4, 0.5 g yeast extract, 0.25 g K_2HPO_4, 0.05 g $CaCl_2.6H_2O$ made up to 250 mL with milliQ water and autoclaved. The medium, water and agarose were heated until the agarose dissolved completely. The solution was then allowed to cool to 45 °C and 1 mL biofilm innoculum was added. Bacteria-free control tubes were set up as above but excluding the biofilm innoculum

A-1.1.3 Sulphide Plug

5 mL of 0.5 g HS^-Sulphide plug was prepared per tube. The sulphide plug was made from 0.05 g Agarose, 1.25 mL milliQ water, 1.25 mL quadruple strength media.

A-1.1.4 Quadruple Strength Media

The quadruple strength media was prepared with 3.5 mL 60% sodium lactate, 2 g $MgSO_4.7H_2O$, 1 g CH_4Cl, 1 g Na_2SO_4, 1 gyeast Extract, 0.5 g K_2HPO_4, 0.15 g $CaCl_2.6H_2O$ made up to 250 mL with milliQ water and autoclaved. The medium, water and agarose were heated until the agarose dissolved completely. The solution was then allowed to cool to 55 °C and 2.5 mL 1 g/l HS^- was added in to the sulphide plug, the plug was poured into the bottom of a sterile test tube and allowed to set before the agarose overlay column was poured.

A-2 MEDIA USED FOR MOLECULAR TYPING

A-2.1 DNA Extraction

A-2.1.1 tris /EDTA buffer

The tris /EDTA buffer was made up of 10 mM Tris/HCl, 1 mM EDTA and one part 50% glycerol made up to 1 L in a volumentric flask.

A-2.1.2 0.8% Agarose gel

The 0.8% agarose gel was prepared by adding 0.8 g agarose in 100 mL of 1 x TBE buffer.

A-2.1.3 TBE buffer

The TBE buffer comprised 10.78 g Tris base, 55 g Boric acid and 7.44 g di-sodium EDTA made up to 800 mL with milliQ water and pH to 8.3 with boric acid. Add milliQ water to make up to 1 L by adding before autoclaving.

A-2.1.5 Ethidium bromide

Ethidium bromide was prepared by adding 0.5 g of ethidium bromide to 1 mL of milliQ water

A-2.1.6 Molecular weight marker

The molecular weight marker was made up of 200 μL λDNA (0.25 μL/ mL) which was digested with 24 μL of 10 x buffer H and 10 μL of *Pst* 1 enzyme for three hours at 37°C, before adding 550 μL of 10 mM TE buffer (pH 8) and 150 μL of 6 x loading buffer

A-2.1.7 6 x loading buffer

The 6x loading buffer was made from 0.25% Bromophenol blue, 0.25% Xylene cyanol and 30% Glycerol.

A-3 REAGENTS AND PRIMES USED FOR PCR

A-3.1 Primers

A universal primer GM5F (5' – cct acg gga gcagc ag – 3') and 907R (5' – cgc ccg ccg cgc ccc gcg ccc gtc ccg ccg ccc ccg ccc gcc gtc aat tcc ttt gag ttt – 3') a gc clamped primer from Inqaba biotec were used for PCR preparation.

A-3.2 PCR Reaction Mixture

A 25 µL PCR reaction mixture was prepared using 2.5 µL PCR Buffer with $MgCl_{2,}$ 1.0 µL dNTPs, 1.0 µL 907R, 1.0 µL GM5F, 1.8 µL milliQ water, 0.2 µL Taq and 1.0 µL DNA (200- 500 ng/µL DNA).

A-4 REAGENTS USED FOR DGGE

A-4.1 100% denaturant

The 100% denaturant comprised of 5 mL of 10 x TAE buffer (48.4 g Tris base, 3.72 g EDTA, 11.42 mL Glacial acetic acid made up to 1L with milliQ water),

A-4.2 TAE buffer

TAE buffer was prepared with 48.4 g Tris base, 3.72 g EDTA, 11.42 mL Glacial acetic acid made up to 1 L with milliQ water

A-4.3 DGGE gel

A 50 mL solution of 100% denaturant, 7.5 mL of 40% acrylamide, 21 g urea and 20 mL formamide made up to 50 mL with milliQ water.

A-4.4 40% acrylamide

The 40% acrylamide was prepared from 100 g Acrylamide and 2.7 g Bis-acrylamide in 1 L milliQ

A-4.5 6% acrylamide gel

The 6% acrylamide gel was made up of 3.5 mL denaturant, 4 µL of 20% ammonium persulphate (APS) and 40 µL of TEMED (Sigma-Aldrich)

A-4.6 Luria Bertani (LB) agar

Luria Bertani (LB) agar was prepared from 30 g LB agar and 1L milliQ

A-4.7 X-Gal

X-gal was prepared using 20 mg of 5-Bromo-4-chloro-3-indolyl-β-o-galactoside in 1 mL dimethylformamide

A-5 PRIMERS USED FOR SEQUENCING REACTIONS

A T7 (5'-taa tac gac tca cta tag gg-3') and SP6 (5'-tat tta ggt gac act ata g-3') primes were used for sequencing reactions.

B. APPENDIX B

B-1 MEDIA USED IN HPLC ANALYSIS

B-1.1 Borate/Gluconate Concentrate for Sulphate and Thiosulphate Analyses

The borate/gluconate concentrate used for eluent preparation was made up in a 1 L volume containing 500 mL milliQ water, 16 g sodium gluconate, 18 g boric acid and 25 g sodium tetraborate decahydrate. Once dissolved 25 mL glygerine was added to the mixture. Further milliQ water was added to make up to 1 L.

B-1.2 Eluent Preparation Sulphate and Thiosulphate Analyses

The eluent was prepared by placing 500 mL of milliQ water was placed in a 1 L volumentric flask to which 20 mL of the Borate/ gluconate concentrate, 20 mL n-Butanol and 120 mL Acetonitrile were added. The flask was filled to the mark with milliQ water and mixed thoroughly. Before use, the eluent was filtered through a 0.22 µm Durapore membrane (GVWP).

A concentrate standard containing 1 000 ppm Fe^{-}, 2 000 ppm Cl^{-}, 4 000ppm NO_3^{-}, 4000 ppm Br^{-}, 4 000 ppm NO_3^{-}, 6 000 ppm HPO_4^{2-} and 4 000 ppm SO_4^{2-} in 100 mL milliQ water was prepared. A fresh working standard was prepared weekly by diluting 100 µL of the concentrate standard in 100 mL of milliQ water.

B-1.3 Chemical Oxygen Demand

B-1.3.1 Digestion mixture

A digestion mixture was prepared from 30 g silver sulphate, 12.25 g potassium dichromate made up to 1 L with deionised water to which 3 mL sulphuric acid was added.

B-1.3.2 Ferroin indicator

Ferroin indicator was made up of 1.485 g phennthroline monohydrate, 0.695 g ferrous sulphate in 100 mL of deionised water.

B-1.3.3 0.1N ferrous ammonium sulphate

The ferrous ammonium sulphate solution was prepared with 39 g ferrous ammonium sulphate, 980 mL water and 20 mL concentrated sulphuric acid

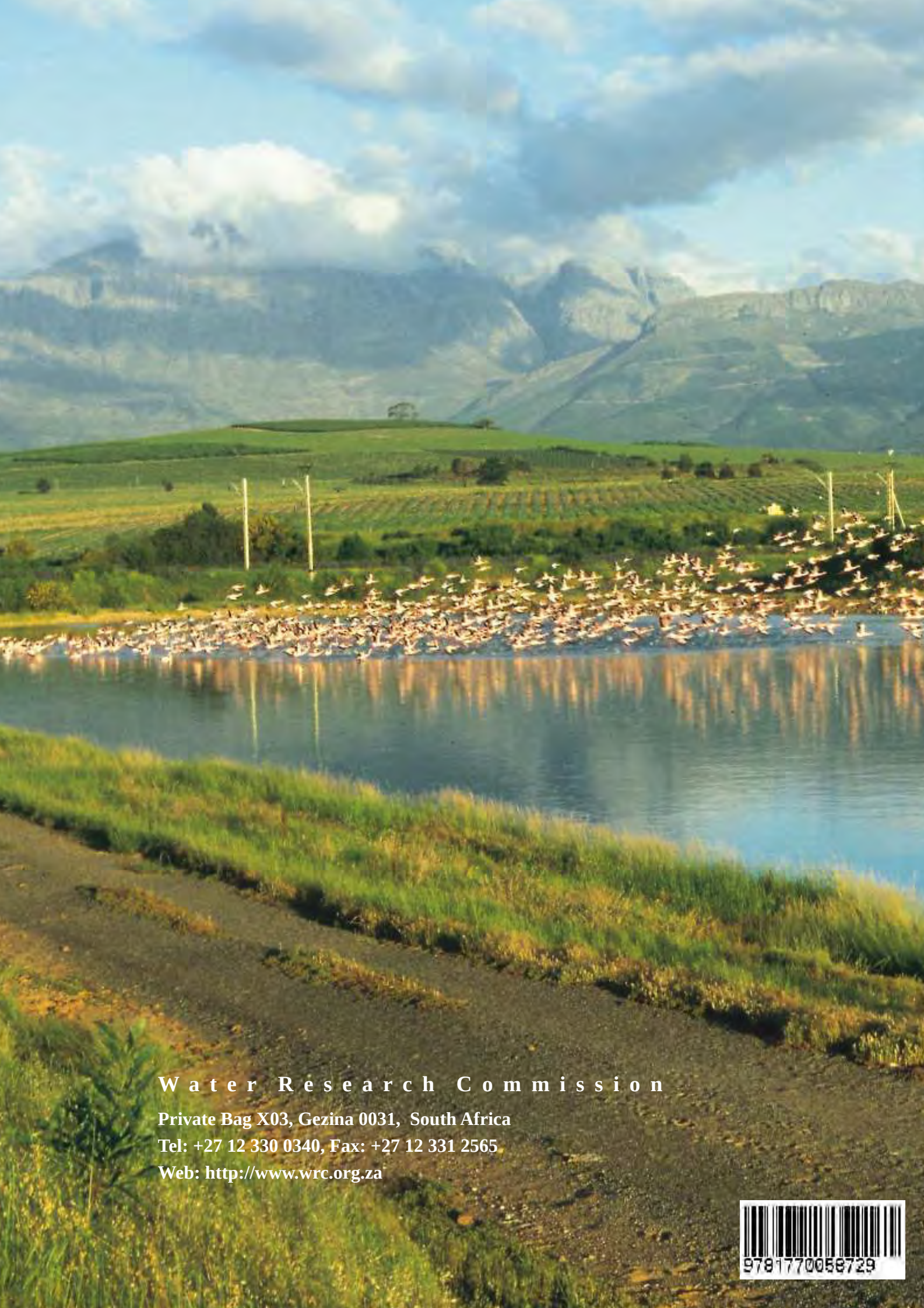

Water Research Commission

Private Bag X03, Gezina 0031, South Africa

Tel: +27 12 330 0340, Fax: +27 12 331 2565

Web: http://www.wrc.org.za

9781770058729